LONG TERM PERFORMANCE OF BACTERIA BASED SELF-HEALING CEMENTITIOUS COMPOSITES SUBJECTED TO ACCELERATED AND WEATHERING EXPOSURE

A thesis submitted for the degree of Doctor of Philosophy

By

Intisar Kadhim Gatea

Department of Civil and Environmental Engineering

Brunel University London

January 2020

Abstract

Self-healing based on bacteria is relatively new treatment strategy that focuses on cracks repairing and avoiding damage in concrete structures by using bacteria and their essential nutrients. It has been extensively studied in the past two decades in concrete applications. Many of these studies have focused on the ability of the microbiology induced calcite precipitation (MICP) to remediate the cracks or improve the mechanical properties of cementitious materials. Nevertheless, the durability of cementitious materials is considered one of the most significant problems faced in civil engineering. In order to evaluate the long term durability performance of bacteria based self-healing cementitious materials, in this study, accelerated exposure, i.e. freeze-thaw cycles, wet-dry cycles and outdoor exposure were conducted. A suitable microbial source of calcite has been investigated besides the development of a new encapsulation material that enhances bacterial releasing without affecting cement mortar properties. Effect of bacteria spores encapsulated in calcium alginate-pyrophyllite on mortar properties has also been studied. The effect of accelerated exposure on the mechanical and microstructural properties of self-healing cementitious composites has been extensively examined. The mechanical and microstructural characteristics of bacterial self-healing mortar under outdoor exposure have been investigated. The correlation between the outdoor exposure results and the accelerated test results has been checked to predict the long term performance of bacteria self-healing mortar.

It has been found that the Bacillus Sphaericus 57, Bacillus Spharicus 58 and Bacillus Megaterium 33 were suitable urease enzyme producers that capable to hydrolyse urea, generate carbonate ions, thus inducing calcium carbonate precipitation. It has also been proved that after exposing to 30 F-T cycles, the compressive strengths of SP33, SP58 and SP57 have been reduced by 19.4%, 18.37% and 21%, respectively, while the reduction in compressive strength of control mortar was 36.4% percent of the initial strength. After 30 cycles of wetting and drying, bacterial self-healing mortar samples exhibited lower compressive strength than the control. A 21% decline was observed in compressive strength for SP57, whereas for SP58 and SP33 strength dropped by 18.3% and 9.4%, respectively.

Under the same environmental conditions, the compressive strength of all bacterial mortar samples increased with the increase of exposure time. The highest compressive strength was achieved by SP33: the compressive strength value reached 53.5 MPa after 18 months of exposure with improvement of 85% comparing to control. Concerning the correlation

between the results of the accelerated exposure and those obtained under the outdoor exposure, on the basis of 18 months' time scale, it was found that the former exposure accelerated the changes in the compressive and flexural strength properties of the bacterial self-healing mortar compared with that in the latter one. Predictions of the long-term behaviour of bacterial mortar under outdoor exposure can be attempted.

Acknowledgements

I would like to express my grateful thanks to mu God for all his great bounties, particularly, health, knowledge and patience.

I wish to record my deepest appreciation to my principal supervisor, Professor Dr Mizi Fan for his advises, continuous help, interest and encouragement throughout the different stages of my study. Without his guidance and practical help, this thesis would not have been possible.

I would like to thank my Research Development Advisor, Dr Nuhu Braimah. I greatly appreciate the time and energy he gave to being my advisor, as well as his creative suggestions and comments.

I also would like to express my appreciation to Professor Nigel Saunders, Dr. Svetlana Ignatova, Dr. Carlos Pires, Dr. Antima Gupta, Dr. Arshad Khan and Jason Lombardy from the Department of Life Sciences /Synthetic Biology for their contribution, supporting and being available with invaluable suggestions during my microbiological experiments, as well as Neil Macfadyen, Simon Le Geyt and Paul Szadorski at civil engineering laboratory, for supporting all lab equipment and materials.

I would also express my gratitude to Brunel ETC's staff, Ashley Howkins and Nita Verma for your supports and great techniques on handling all equipment and machines.

Special thanks also are extended to my inspiration, my support, my encouragement- my parents. I am deeply indebted to my family, especially my sons Aymen, Ahmed and Ali and my husband Jameel who was extremely supportive during the entire study period. Their love and support provided me the energy to persevere. My heartfelt gratitude especially to my brothers and sisters who always supported me during this period.

I humbly extend my thanks to all concerned persons who co-operated with me in this regard.

Table of contents

List of tables

List of figures

List of abbreviations

$Ca(OH)_2$	Calcium hydroxide
$CaCO_3$	Calcium carbonate
MICP	Microbially induced calcium carbonate precipitation
CO_2	Carbon dioxide
YE	Yeast extract
SEM	Scanning electron microscopy
EDAX	Energy Dispersive Spectroscopy
ECC	Engineered cementitious composites
SAP	Superabsorbent polymers
PP	Polypropylene capsule
MMA	Methyl methacrylate
CSH	Calcium silicate hydrate
UFF	Urea formaldehyde formalin
UF	Urea formaldehyde
TEB	Triethylborane
PU	Polyurethane
BBSHC	Bacteria-based self-healing Concrete
BCM	Biologically Controlled Mineralization
BIM	Biologically Induced Mineralization
MCP	Microbial calcium carbonate precipitation
DIC	Dissolved inorganic carbon

CH	Calcium hydroxide
OPC	Ordinary Portland cement
LWA	Light Weight Aggregate
NH^{4+}	Ammonia
F-T	Freeze-Thaw action
PBST	Phosphate buffered saline tablet
DNA	Deoxyribonucleic acid
OD	Optical Density
FTIR	Fourier Transform Infrared Spectroscopy
TGA	Thermogravimetric analysis
FC	Filtered cement slurry
DW	De-ionized water
UTM	Instron universal testing machine
OD760	Optical Density at 760
DW	De-ionised water
TW	Tap water
CF	Cement filtrate

Chapter 1: Introduction

1.1 Background of research

Concrete is the most widely used construction material in the world nowadays as it is cheap and remarkably strong in compression. It is a composite material made up of cement, water, aggregates and other additives which help promote certain properties in the concrete. Concrete has been used in construction for thousands of years. The ancient Egyptians made bricks of mud with binding materials, such as straw, about 5000 years ago and the Chinese used a cementitious material to construct the Great Wall. However, Romans were believed by the most historical overviews to be the first who refines the concrete and its application. The Pantheon's dome is one of the famous Roman buildings constructed 2000 years ago and it is the largest unreinforced concrete dome in the world (Kırca, 2018). Modern concrete used in two major types: when Portland cement and aggregate are mixed with water, it is called ordinary plain concrete, whereas it is known as reinforced concrete when steel reinforcement is added to plain concrete. While concrete is strong, durable and commercially available, it is unfortunately vulnerable to various types of deterioration. Serious concrete deterioration is mostly initiated by concrete cracking and these cracks are often the result of a combination of factors. In some concrete, the formation of cracks is entirely acceptable and not considered to be a serious defect, while in other concrete, the strength, serviceability and appearance is adversely affected by cracks initiation. Cracks in concrete are usually an indication of the cause of the failure and not a fault in itself. Although some of these cracks may not eventually end up with structural failure, they might accelerate deterioration causing definite loss of performance of the structure leaving the structure unserviceable. Cracks can be classified into two broad categories, structural and non-structural cracks. Structural cracks may be caused by a number of factors. Some of the most significant factors are those, such as poor construction design, foundation settlement, and construction deficiency. Non-structural cracks develop due to poor quality of building materials and subjecting to fluctuating temperature and humidity (i.e. ambient conditions) (Kunal and Killemsetty, 2014). The nature of the cracks, on the other hand, can be categorised as active cracks, which appear and are likely to be progressive and to expand further even after concrete setting, and dormant cracks, which are not likely to develop further as the factor caused this deterioration is not expected to occur again. The repair of concrete damage costs a huge expense. A substantial amount of the entire budget of construction in the UK and different part of the world has been spent on the repairing, refurbishment and maintenance of concrete structures. Despite the massive

impact of this huge and intensifying market on national economies, little fundamental attention has been paid to the properties of repair materials, which affect the long-term performance of concrete structures. Inconsistencies between the repairing agent and concrete in terms of strength characteristics and modulus of elasticity, during the service life can cause durability problem. Drying shrinkage of repair material on the other hand may reduce long-term concrete efficiency and can be affected by either initial tensile strain induced in the repair, or due to cracking appeared in the interface delamination between the concrete substrate and repairing (Mangat and Limbachiya, 1995). Therefore, it is of paramount important to develop more durable building material with less regular repairs and/or advanced repairing technologies.

Cracks threaten the durability of concrete structures, as the ingress of the aggressive substances into the matrix through these cracks can cause concrete degradation. Thus, cracks may propagate and result in the exposure of the reinforcement to environments. Total or partial failure of the structure may happen after the embedded steel begins to corrode or oxidize, leading to a reduction of the in-service durability of concrete.

For that reason, different measures have been undertaken to minimize the size and number of cracks in concrete. Developing an appropriate concrete mix design, carefully selecting raw materials, choosing a proper curing regime and having an appropriate structural management of operation are among these measures. Despite the fact that it is virtually impossible to make cracks disappear, cracks can be controlled or significantly reduced. Despite of this, it is difficult to repair the invisible or inaccessible cracks. Consequently, the self-healing of cracks in concrete is indispensable and would contribute to a longer service life of concrete structures.

The phenomenon of self-healing (a crack recovery process) has been commonly known for many years. The concept of self-healing ability of concrete structure has been an area of intensive research over the past two decades and several works have been proposed to review different self-healing approaches in concrete(Van Tittelboom and De Belie, 2013). Based on the healing mechanism, approaches of self-healing in cementitious materials can be generally classified into two main categories: autogenous healing and autonomous healing. The efficiency of each approach depends on the overall condition of the material, the cementitious composite matrix and the function of the structure and etc. Autogenous healing is a natural crack recovery taking place after a period of time as a result of further cement hydration or

carbonation of calcium hydroxide (Ca (OH) $_2$). However, the ability of autogenous healing is restricted to micro cracks and depends on the presence of water. On the other hand, autonomous crack healing may be triggered with the intention of healing bigger cracks or a larger amount of cracks (VanTittelboom *et al.*, 2011c).

Introducing external agents during the autonomous healing process could be performed by two different ways: active and passive vascular systems, such as channel tubular network and cylindrical or spherical capsules. Upon cracking, the autonomous healing mechanism provokes through releasing the healing agents from their carrier stimulating the healing reaction.

Bacteria based self-healing is one approach of autonomous self-healing processes, when bacteria, deposition agents and its necessary nutrients are introduced into concrete matrix as self-healing agents. Various studies have demonstrated the efficiency of introducing of bacteria into the concrete matrix to achieve self-healing behaviour. These studies have been started in the late 2000's (Wang, De Belie and Verstraete, 2012; Jonkers and Schlangen, 2009). Briefly, it was hypothesized that upon concrete cracking and ingress of water, the bacteria present at the crack surface will be activated and expected to precipitate $CaCO_3$ to heal the cracks, obstructing the ingress of water and chemicals. For calcium carbonate ($CaCO_3$) precipitation to occur, both carbonate precipitating bacterium and their necessary nutrients are pre-added into concrete throughout mixing process. In the presence of calcium solution, bacteria releases carbonate and different bacterial species produces different $CaCO_3$ minerals.

Active microorganisms and its mineral precipitation accompanied with biological processes can be found in almost every natural habitat on the Earth (López-García *et al.*, 2005; Shen, Buick and Canfield, 2001) . It has been frequently reported that bacteria from various natural media (e.g. soil and aqueous media) are able to precipitate calcium carbonate $CaCO_3$ in laboratory and site conditions (Lian *et al.*, 2006; Rodriguez-Navarro *et al.*, 2003; Krumbein, 1979). Calcium carbonate deposition in a variety of environments seems to be attributed to different kinds of bacteria along with abiotic factors (medium constitution and salinity (Rivadeneyra *et al.*, 2004; Knorre and Krumbein, 2000).

Under favourable environments, microbial calcium carbonate precipitation is a wide spread process occurring in nature (Boquet, Boronat and Ramos-Cormenzana, 1973) and the formation of carbonate sediments and soil carbonate deposits is highly depended on this

microbial activity (Peckmann, Paul and Thiel, 1999; Rivadeneyra *et al.*, 1993; Chafetz and Folk, 1984; Morita, 1980; Krumbein and Giele, 1979).

The process of calcite precipitation from a supersaturated solution in a microenvironment that occurs due to the existence of bacterial cells and biochemical activities is known as Microbially induced calcium carbonate precipitation (MICP) (Bosak, 2011). The principle of minerals precipitation during MICP is the reaction between one or more metabolic products (CO_3^{2-}) secreted from organisms and ions (Ca^{2+}) in the environment. It has been previously proposed that the formation of calcium carbonate precipitation takes place through different mechanisms such as urea hydrolysis (Dhami, Reddy and Mukherjee, 2013; De Muynck *et al.*, 2010; Stocks-Fischer, Galinat and Bang, 1999), biofilm and extracellular polymeric substances (Arias and Fernández, 2008; Kawaguchi and Decho, 2002), sulfate reduction (Hammes *et al.*, 2003; Warthmann *et al.*, 2000; Castanier, Le Métayer-Levrel and Perthuisot, 1999), photosynthesis (McConnaughey and Whelan, 1997; Thompson and Ferris, 1990) and anaerobic sulfide oxidation (Warthmann *et al.*, 2000).

Yet, urea hydrolysis is considered as the most common method to precipitate calcium carbonate by bacteria (DeJong *et al.*, 2010; De Muynck *et al.*, 2010; Hammes and Verstraete, 2002). Urease catalyses the hydrolysis of urea into ammonium and carbonate and cementitious solution can be obtained from the mixture of urea and calcium solution. In this reaction, one mole of urea is hydrolysed to one mole of ammonia and one mole of carbonic acid which is spontaneously hydrolysed to another one mole of ammonia and carbonic acid.

The potential benefits of the bacteria-based self-healing approach include reduction in maintenance and repair costs comparing to conventional manual repair (Van Breugel, 2007). Biogenic calcium carbonate also has high compatibility with concrete compounds. Gollapudi et al. (1995) was the first to employ this new eco-friendly technique for cracks repairing to avoid leaching through permeable channels (Gollapudi *et al.*, 1995).

Other researchers have used the same method to enhance the stiffness and compressive strength of concrete (Ramakrishnan, Ramesh and Bang, 2001). It is also applied to treat water production problems during oil recovery and to consolidate sand fractures (Zhong and Islam, 1995).

Calcium carbonate was found to be the main mineral precipitated when the biomineralization process was induced by the soil bacterium Bacillus megaterium (Lian *et al.*, 2006).

The durability of fly ash-amended concrete was also improved by using Bacillus megaterium as a microbial source for calcite precipitation (Achal, Pan and Özyurt, 2011). Incorporation of Bacillus sphaericus culture for the biological treatment of concrete cracks was also found to be promising (Van Tittelboom *et al.*, 2010).

However, application of the micro-scale bacteria into the macro-scale concrete encountered different challenges. For example, concrete alkaline environment and the mixing mechanical forces, in certain extents, have the potential to cause damage of bacteria. Additionally, the surface life of the healing agents has to be extended in order to achieve an effective healing process. Spore forming bacterial strains have been used to tackle the above mentioned drawbacks as the spore (the dormant state of the cell) is the most suitable state of the bacteria that can be utilized for self-healing purposes. They can survive for a longer period of time comparing to living cells (from several years to hundreds of years) and have high resistibility to heat, radiation and various chemicals (Setlow, 1994).

For these reasons, the spores of bacteria are more preferable in the concrete as they last longer and can withstand the harsh conditions of concrete. However, concrete matrix has accentuated the problem of low density and porosity of structure (very small size pores of less than 1μm), which in turn put the bacterial spores at a risk of smash during cement hydration in addition to the shearing force facing bacterial spores during concrete mixing and handling. Researchers have devoted considerable attention to introduce self-healing agents with a physical barrier to withstand unfavourable environment. Encapsulation has been found to improve the microorganism's viability and survivability during handling and storage. In the encapsulation process, several problems are encountered and need to be balanced: the need for mechanically stable capsules, capability of being decomposed, ability to control cell release, being environmentally reactive and the need for low-cost encapsulation technique (Young *et al.*, 2006). The capsules typically should be designed with a suitable semipermeable, thin but strong carrier that will promote the long term microbial preservation and the survival during handling and storage.

Researchers introduced bacterial, self-healing agents (calcium source called precursor) and nutrients into a cement matrix for achieving self-healing by stimulating bacteria and its precursors to precipitate calcium carbonate on the crack's surface (Jonkers, 2007). The most common calcium source has been utilised as a precursor for calcium carbonete precipitation was calcium acetate (Park *et al.*, 2012; De Muynck *et al.*, 2008c; De Muynck *et al.*, 2008a;

Barabesi *et al.*, 2007). Therefore, calcium acetate and its possibility to induce calcium carbonate precipitation without harming other mortar properties has been used as deposition agents and investigated in this research.

Nutrients, on the other hand, are needed to promote the precipitation of calcium carbonate as they play an important role in bacterial spores germination and supplying the microbial cell with growth medium (Paine, 2016). Urea and yeast extract (YE) are the important constituent of nutrient feed as they include a simple and complex nitrogen sources. However, incorporating these nutrients into concrete should not have unfavourable effect on concrete properties. The heat generated by the hydration reactions and during the casting of concrete can be eliminated by an addition of a granular urea, because the endothermic reaction takes place by dissolving urea in water (Mwaluwinga, Ayano and Sakata, 1997).

Recently, bacterially induced carbonate precipitation has been used for the strength improvement, self-healing of cementitious materials and remediation of cracks in construction materials. In addition, this technique has been explored as a potential method to enhance the durability of cementitious materials. It has been demonstrated that using bacteria in concrete results in an improvement in its resistance to drying shrinkage, freeze thaw attack, and chemicals attack (Ramakrishnan *et al.*, 2005).

Bacterial concrete has also been found to have lower permeability and less water and chloride ion penetration compared to conventional concrete (Achal, Mukerjee and Reddy, 2013b; Achal, Mukherjee and Reddy, 2011). Moreover, in a study investigating the effect of bacterial carbonate deposition on the durability of mortar specimens with different porosity, it has been reported that the water absorption, carbonation rate and chloride movement decreased depending on the porosity of the samples (De Muynck *et al.*, 2008b).

1.2 Problem statement

Durability of concrete is partly and sometime significantly affected by the occurrence of cracks in the surface layer; therefore, it is necessary to develop new methods to eliminate cracks in concrete structures. Different measures have been attempted to address the environmental impact related to frequent repairs of concrete structures. Bio-mineralisation of calcium carbonate by using certain bacterial species is one of these measures toward solving this issue. Alkali-resistant spore-forming bacteria with self-healing attribute will heal the cracks by utilising its microbial activity and inorganic precursors embedded in concrete to

precipitate calcium carbonate. It will be an alternative for the other self-healing materials to improve concrete durability by decreasing the potential for the ingress of detrimental substances and enhancing strength properties.

Unavailability of test data for self-healing cementitious composites subjected to accelerated and weathering exposure observed in the existing literatures necessitates the investigation of bacteria based self-healing cementitious composites behaviour under accelerated and weathering exposure. Considering the identified gabs in the previous studies on long term performance of SHCC, the research study presented in this thesis has mainly focused on the experimental investigation of the long-term performance of SHCC under three separate environmental conditions, namely, freeze-thaw cycles, wet-dry cycles and outdoor environment up to 18 months. The outcomes of this study will help generate comprehensive data bases for long term performance of bacteria based self-healing concrete and develop an expert system to disseminate knowledge on bacterial concrete for constructing infrastructures in real life.

1.3 Objectives of research and methodology

The current research is aimed at studying the long term performance of cement mortar with different carbonate producing bacteria that can be utilized in construction applications. Three different types of bacteria have been selected and harvested depending on their urease activity, PH tolerance and spore formation. The viability of these bacterial species after encapsulation in calcium alginate-Pyrophyllite beads and effect of these beads on the properties of cement mortar were also examined. Bacteria are incorporated in cement mortar along with calcium acetate, urea and yeast extract as nutrients and investigated for their performance in inducing self-healing characteristics. Extensive experimental investigation is carried out to understand the effect of these biological agents as self-healing material on cement mortar. In order to study the performance of bacterial cement mortar under accelerated and weathering exposure, three types of exposure regimes have been applied. Bacterial mortars are subjected to the action of freezing- thawing cycles, wetting-drying cycles and outdoor weathering environment, thus, examining the long term performance of bacteria based self-healing mortar under various exposure conditions and better understanding prolong self-healing processes. To achieve the aims of the project, the following key objectives are proposed:

I. Explore the most suitable bacterial species for calcite precipitation under concrete environment by evaluating their urease activity, pH tolerance and spore formation.

II. Investigate the efficiency of calcium alginate-Pyrophyllite beads as encapsulation technique for protection of bacteria.

III. Study the effect of self-healing agents (encapsulated bacterial spores and nutrients) on mechanical properties such as compressive strength and flexural strength of mortars.

IV. Examine the microstructural changes due to self-healing action using SEM and EDAX analysis.

V. Evaluate the performance of bacterial mortar under different environmental exposure conditions in terms of strength properties and microstructural characteristics.

The entire research program is illustrated in the following diagram:

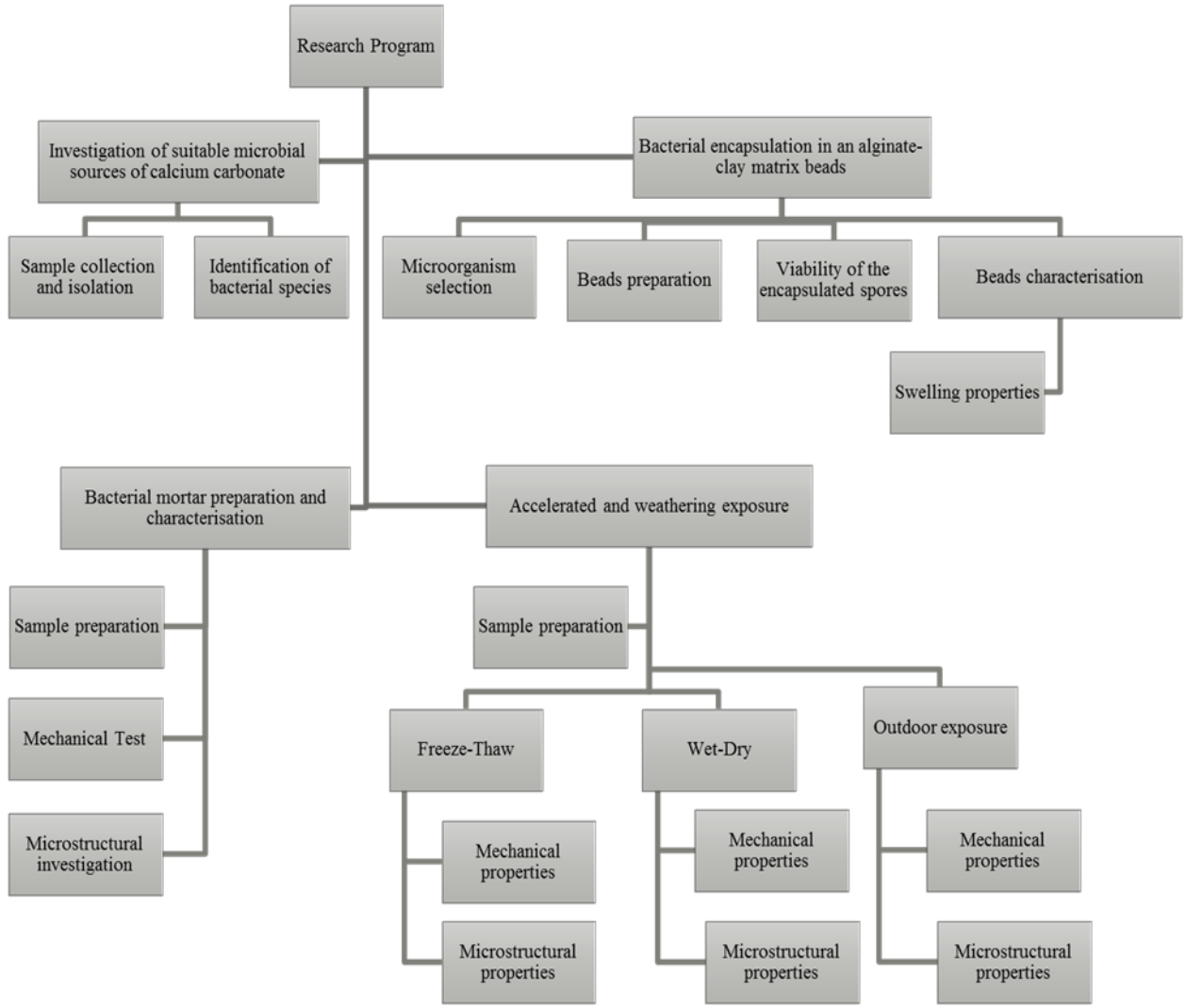

1.4 Layout of thesis

This thesis reports the experimental work undertaken to investigate the most suitable microbial source of calcium carbonate precipitation and study the long term performance of cement mortar incorporated with bacillus spores under different environmental conditions.

A review of the literature of self-healing phenomenon in construction material is detailed in Chapter 2, focusing on the mechanisms responsible for calcium carbonate precipitation and the properties of the ideal microbial source of calcite. A review of different bacterial protection and encapsulation techniques are also included, followed by the effect of bacteria, the bio deposition and nutrient material necessary for its growth on the properties of concrete investigated in previous studies. Finally, the factors affecting the durability of bio-concrete and responsible for concrete deterioration in service have been discussed in detail in this chapter.

The experimental program conducted in this study, and the materials and methods used to achieve the objectives of research are presented in Chapter 3. Bacterial isolation, identification, urease activity, the factor affecting their growth and spore preparation are explained in this chapter. The encapsulation of bacterial spores using calcium alginate–pyrophyllite bead is described. Tests on the properties of bio-mortar such as flexural strength, compressive strength, and microstructural characterisation using SEM and EDAX techniques are described. A procedure of exposing to freezing and thawing cycles, wetting and drying cycles and outside weathering exposure is discussed.

In Chapter 4, the suitable microbial source of calcite has been investigated, followed by the encapsulation efficiency and viability of spores in the calcium alginate-pyrophyllite beads in Chapter 5. The effect of bacterial spores encapsulated in calcium alginate-Pyrophyllite clay beads on mortar specimens is presented in Chapter 6. Chapter 7 includes the effect of Freeze-Thaw action on the microstructural and mechanical properties of bacterial mortar. In Chapter 8, the effect of wet-dry cycles on the microstructural and mechanical properties of bacterial mortar was studied. Furthermore, the effect of outdoor weathering exposure on the microstructural and mechanical properties of bacterial mortar has been investigated in Chapter 9.

Finally, the conclusions of the research project and recommendations for future work are given in Chapter 10, with reference to the aims and objectives of the research.

Chapter 2: Literature Review

2.1 Introduction

Since the 19th Century, and with the rapid increase in the production of Portland cement, concrete has been used extensively for the construction around the world. The advantages of concrete with a high compressive strength, easily casting and resistance to fire make it the most versatile and the most commonly used material in construction. However, its susceptibility to crack when exposed to chemical or physical attacks is one of the main drawbacks that lead to mechanical and structural failure, and shorten the operating life of the structures. In addition, the repairs and maintenance of concrete are expensive and the carbon dioxide (CO^2) emissions accompanied with cement manufacturing is high. Therefore, many studies have been conducted to improve the sustainability of this material through extending long-term durability.

In certain conditions, concrete has the potential for natural or 'autogenous' healing through a well-known phenomenon of automatic crack recovery called (self-healing). Concrete may heal its own cracks after a period of time with the continued hydration reaction of cement clinker minerals or as a result of calcium carbonate formation through the carbonation reaction between portlandite (calcium hydroxide) and Carbon dioxide (Van Tittelboom and De Belie, 2013).

2.2 Approaches to self-healing

Self-healing is the ability of the material to automatically repair any type of damage without any exterior intervention. Self-healing in cementitious materials can be broadly grouped into two main categories, autogenous healing and autonomous healing depending on the mechanisms utilised to achieve self-healing in the cracked area.

2.2.1 **Autogenous healing**

Autogenous healing refers to the partial or complete regaining of original solidity of cementations materials after exposing to a load under favourable temperature and moisture conditions (Sukhotskaya, Mazhorova and Terekhin, 1983). Concrete constituents have already by nature the ability to repair itself relying on an autogenous healing. Different factors may lead to this autogenous healing in the damaged region. Further hydration of unhydrated cement particles, carbonation to form calcium carbonate and/or calcium hydroxide are the main factors of autogenous healing. In addition to these two mechanisms,

crack sealing may be due to the sedimentation of loose particles resulting from cracking or debris existing in the ingress water, and swelling of the cement matrix (Fig 2-1)(Ter Heide, 2005).

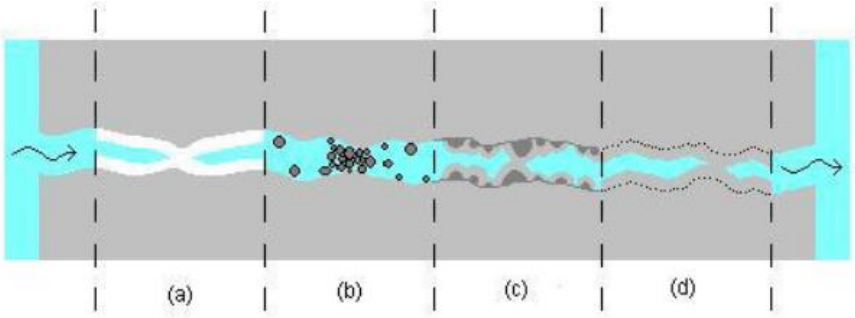

Figure 2-1 Possible causes of self-healing: (a) formation of calcium carbonate or calcium hydroxide, (b) sedimentation of particles, (c) continued hydration, (d) swelling of the cement-matrix(Ter Heide, 2005)

It has been approved that the tolerable crack width has a profound effect on autogenous healing. For completely healing, the maximum crack width has been proposed as 5 to 10µ, 100µ, 200µ, 205µ and 300µ, by Jacobsen et al. (Jacobsen, Marchand and Hornain, 1995), Reinhardt and Jooss(Reinhardt and Jooss, 2003), Edvardsen (Edvardsen, 1999), Aldea et al(Aldea et al., 2000) and Clear (Clear, 1985) respectively. As conventional concrete is a brittle material and the tensile strength is very low, the deformation potentially caused by such small cracks could be a severe challenge. As a consequence, different approaches to recuperate the weaknesses and develop the autogenous crack healing efficiency have been modified recently. Crack width control is one of these approaches applied in engineered cementitious composites (ECC) by various researchers using fibre reinforcements to improve crack width (Snoeck and De Belie, 2012; Homma, Mihashi and Nishiwaki, 2009), although external applied compressive forces were also used to restrict the crack width in cementitious composites (ter Heide and Schlangen, 2007), (Li et al., 2011) and (Li, Lim and Chan, 1998). They used polyethylene (PE) fibres in their earlier study, whereas polyvinyl alcohol (PVA) fibres were used later as cheap alternative fibre. The common characteristics of engineered cementitious composite (ECC) is high tensile ductility and fine multiple cracking with a maximum crack width under 60 µm.

Supplying water for further hydration is the second approach in this regard. Superabsorbent polymers (SAP) were firstly used as an admixture for self-healing of cracks in concrete in 2010 by Lee et. al. and further studies has been carried out later on using super absorbent

polymer in cementitious materials (Lee, Wong and Buenfeld, 2018; Lee, Wong and Buenfeld, 2016; Lee, Wong and Buenfeld, 2010). Superabsorbent polymers (SAP) were also employed as slow-release source of water (Snoeck et al., 2014; Snoeck et al., 2012; Dejonghe et al., 2011). It is cross-linked polymers which, under swelling and formation of hydrogel, are capable of absorbing large amount of water. The ionic concentration and alkalinity of the solution are the main factors that affect the swelling capacity of these polymers. Therefore, when mixed with concrete, the swelling rate of SAP is reduced. The absorbed water is later released during cement hydration and the SAP shrank generating empty macro pores. The cracks are likely to grow through the pores, so the SAP will swell again after moisture ingress into the crack. However, if the ionic concentration of the outside fluid is low compared to the inside pore solution, the swelling of SAP will increase, filling the pore space in the crack. The water is slowly released from the SAPs during dry periods to stimulate autogenous healing. Light weight aggregate is another method to stimulate self-healing process, when it used as additional water reservoir (Janssen, 2011; Qian, Zhou and Schlangen, 2010). It has been established that the water retaining capacity of clay can be used to provide additional water for further cement hydration.

The third approach to improve the autogenous crack healing capacity was crystallisation and hydration by adding different agents to activate crystals deposition in the crack. It has been found that replacing part of the cement with pozzolanic material, such as fly ash or blast furnace slag will promote autogenous healing as a result of further hydration of the remaining unhydrated binders (Van Tittelboom et al., 2012; Termkhajornkit et al., 2009). Blast furnace slag has latent hydraulic properties, this means it needs to expose to calcium-rich solutions so that the hydration reaction with water will be activated, while Portland clinker, the active component in cement is a hydraulic binder. Therefore, the particles of blast furnace slag will react with Ca(OH)2 from Portland clinker hydration. Due to the pozzolanic properties of the fly ash, the hydration reaction occurs as a result of the pozzolanic reaction between Ca(OH)2 form clinker hydration and fly ash particles. As a result, cement hydration needs to initiate first so as to activate the hydration reaction for both binder materials (fly ash and blast furnace slag). Expansive additives were also added to fill the crack by ettringite crystal formation in the presence of water, thus improving autogenous healing. Researchers used a mixture of calcium sulfo aluminate based agents and crystalline admixtures as expansive agents (Sisomphon and Copuroglu, 2011).

2.2.2 **Autonomous healing**

Autonomous self-healing system is an artificial means of crack repair which is caused by engineering additions. The principle behind autonomous self-healing is that when cracks happen, the repair mechanism can be achieved through the release of the healing agents from their containers and reaction with some stimuli such as moisture, air or heat. Autonomous crack healing is previously applied in the concrete with the aim of increasing the concrete durability and strength, reducing the water and chemical permeability, and leading to protection for the reinforcement steel against corrosion. Various mechanisms of autonomous healing have been explored based on the healing agent used, some of these mechanisms are summarised as follows:

2.2.3 **Capsule based self-healing**

Capsule based self-healing comprises all methods that use self-healing agents enclosed in capsules that are evenly distributed in concrete. The main purpose of encapsulation is to isolate the healing agent to avoid contact with concrete until crack occurrence. Upon cracking, the capsules break, leading to leak healing agents which then seal the cracks and/or form a good bond between the crack faces. Different agents can be enclosed by using this versatile encapsulation technology with capsule size in millimetre ranging down to the submicron (see Figure 2-2).

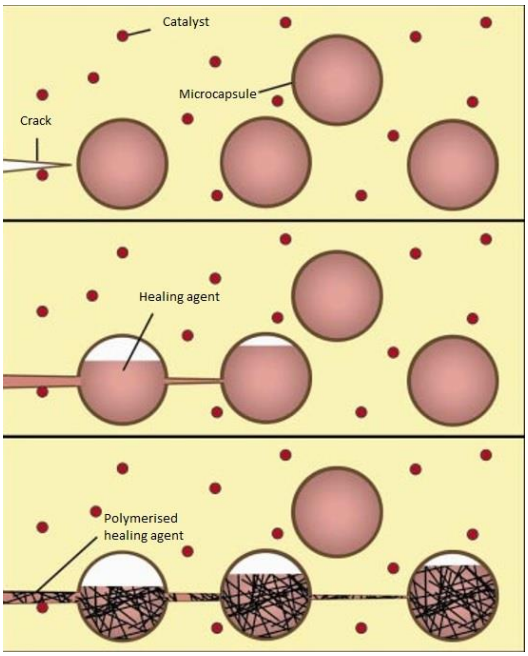

Figure 2-2 Healing agents encapsulated in microcapsules (White et al., 2001)

Sodium silicate solution, for instant, has been encapsulated in a wax capsule with diameter of 5 mm as a self-healing agent in cementitious composite. From this study, it has been established that the flexural strength and stiffness of the material recovered after inducing damage by three-point bending test (Huang et al., 2011).

Carbonate precipitating bacterium, encapsulated into a 20–100 μm modified-alginate based hydrogel demonstrated the potential of using these microcapsules for crack self-healing in concrete.

The capsule in this approach may come in spherical or cylindrical shape. The self-healing can be achieved through the release and reaction of healing agents with air or heat. An example of the self-healing upon contacting with air is the gelatin shell spherical microcapsules that contain tung oil or Ca (OH)2 used to repair cracks in cement mortar. Upon cracking, tung oil hardened when it comes in contact with air, while Ca(OH)2 leads to the formation of CaCO3 crystals as it reacted with CO2 (Cailleux and Pollet, 2009). The porous cylindrical Polypropylene capsule (PP) is an example of using heat to stimulate the reaction of healing agents. Methyl methacrylate (MMA) is inserted in the PP capsules, which are, wax coated and then mixed with concrete. When concrete starts cracking, the wax coating needs to be melted by heating the concrete in order to release the MMA throughout the capsules pores, thus curing the cracks (Dry, 2000).

In addition, some agents start reacting upon contact with cementitious matrix. For instance, sodium silicate (Na2SiO3) solution embedded in spherical capsules as a healing agent that reacts with cementitious matrix. Crack healing takes place when capsules ruptured and chemical reaction occurs between Na2SiO3 solution released from capsules and Ca(OH)2, initially exists in concrete, leading to calcium silicate hydrate (CSH) formation to seal the crack (Pelletier et al.,2011).

Another component added directly to the matrix itself or by extra capsules may react with healing agent and trigger the self-healing process. An example of a component added directly is dispersing a hardener inside the mortar matrix along with spherical capsules of bisphenol-F epoxy resin. Self-healing action occurs via polymerization reaction due to the contact between the epoxy resin leaked from the fractured capsules and the hardener inside the matrix (Cailleux and Pollet, 2009). For a study of applying bacterially precipitated $CaCO_3$ to heal cracks in concrete, diatomaceous earth was used as a carrier to protect the Bacillus sphaericus spores, whereas urea was delivered inside the cementitious matrix. It has been demonstrated

that self-healing action was based on the hydrolysis of urea by the Bacillus sphaericus strain to precipitate $CaCO_3$ (Wang, De Belie and Verstraete, 2012). Calcium lactate was also mixed directly with the cementitious matrix when it used as "food" to the Bacillus cohnii strain. The metabolic activity of this bacterium strain was directly responsible for the conversion of calcium lactate into calcium carbonate (Jonkers and Thijssen, 2010).

Extra capsules of components of the healing agent can be added separately in order to be released when capsules break and react with other agents. Two types of epoxy were embedded separately in spherical capsules with urea formaldehyde formalin (UFF) shell. However, this method was inappropriate as the two component were poorly mixed, thus delaying the epoxies hardening (Mihashi et al., 2001).

In another study, two epoxy resins were modified with a diluent chemical before embedding in spherical microcapsules with urea formaldehyde (UF) shell, so the viscosity of the resins can be adjusted to enhance mixing process(Xing et al., 2008).

The self-healing effect of Methylmethacrylate (MMA) monomer and triethylborane (TEB) encapsulated in silica gel shell dispersed subsequently in cement mortar was examined. It was found that cracks may be sealed by the contact of both components of the microcapsules after rupture (Yang et al., 2011; Yang et al., 2010).

As adding capsules to the cementitious matrix separately may not provide good self-healing results, connecting capsules to each other was tried to enhance the component contact upon rupture. Ceramic or glass cylindrical capsules filled with two-component healing agents were added to the matrix in two by two connection. The self-healing efficiency of epoxy resins, polyacrylates, polyurethane (PU) and MMA added to cementitious materials using the abovementioned technique has been evaluated, however, the PU and MMA were found to be the most suitable agents as they polymerise regardless of the mix ratio (Van Tittelboom et al., 2011b; Van Tittelboom et al., 2011a; Van Tittelboom and De Belie, 2010).

Calcium carbonate precipitating bacteria was also added along with two polyurethane components (PU) or silica gel to investigate their potential to be used for self-healing. Each agent was carried by a separate glass tube and glued together. The higher strength gained and lower water permeability coefficients have indicated the efficiency of self-healing upon using PU comparing to silica gel. However, mixing silica gel together with bacteria led to enhance

bacterial activity and precipitate more calcium carbonate comparing to only silica gel encapsulated (Wang et al., 2012a).

2.2.4 **Vascular based self-healing**

The vascular self-healing system is made up of a network of hollow tubes which carry healing agents all around the cementitious matrix. It acts as a connector between the exterior and the interior of the structure. If one healing agents used, the system called one channel vascular system, whereas multiple channel system refers to a multi-component healing agent embedded inside concrete. Upon cracking, the healing agents are drawn from the tubes into the cracked area by gravitational forces when the external suppliers are located at a higher level (see Figure 2-3).

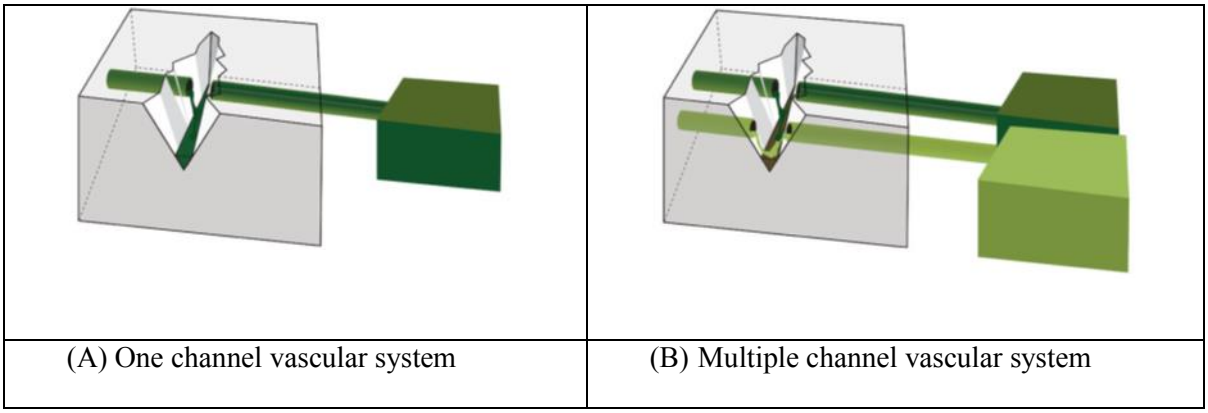

(A) One channel vascular system	(B) Multiple channel vascular system

Figure 2-3 Vascular based self-healing approaches (Van Tittelboom and De Belie, 2013)

It has been demonstrated that delivering self-healing agents by using vascular system is more practicable comparing to capsules system provided that the vascular system are hit and the healing agents are sufficiently released when crack happen. Therefore, the efficiency of this system is highly dependent on the crack depth and the distribution of the vascular system in structures (Huang and Ye, 2013). Several requirements have to be fulfilled for the material used in the vascular system, i.e. they have to be chemically inert and very brittle. Good bonding between the tubes and concrete is also important requirement besides the stability of concrete strength. Glass has been used in the manufacturing of vascular tubes, as it satisfies the requirements giving above. Yet, the destructive effect of alkali-silica reactions between glass and concrete needs to be considered (Melnyczuk and Palchoudhury, 2018).

Various structural systems have been used to assess the concept of one channel vascular self-healing system. Internal cracks in concrete beams were self-repaired using chemical adhesives released from hollow fibres (Dry and Corsaw, 2003; Dry, Corsaw and Bayer, 2003). Releasing adhesives through a vascular flow network in a concrete frame structure

subjected to dynamic loads damage led to enhance both the load carrying capability and post-yield deflection (Dry, 1996). In addition, the self-healing efficiency of released chemical sealants has been evaluated in repairing the transverse shrinkage cracking of concrete bridge decks (Dry, 1999). This approach is also applied to minimise the risk of failure of bridges and roadways (Dry, 1998) by changing the flexural, stiffness and deformation properties of the composite bridge made of self-forming polymer and concrete system (Dry, 2001). To allow continuous supply of healing agents, the tubes were connected to an exterior a tank through the open end of the tubes (Mihashi et al., 2001) or the tubes connecting to holes inside the concrete were injected with the healing agents by syringe (Pareek and Oohira, 2011).

Other researchers put porous network inside the concrete samples to mimic the self-healing process in bones. The network was made of porous concrete cylinder, which is connected to a sensor to detect the cracks formation and to a manual healing agent supplier. The cylinder was shielded by PVA film before casting the outer layer of self-compacted concrete. This film will dissolve to allow exchange between the two concrete layers. The outcomes of this study showed a regain in concrete strength and macro-crack filling (Sangadji and Schlangen, 2012; Sangadji and Schlangen, 2011).

2.2.5 **Bacteria-based self-healing Concrete (BBSHC)**

Cracking in concrete can develop at any stage of the service life of the structure due to the structural failure of concrete itself or man-made factors, such as overloading sever exposure condition, poor design and construction practice. These cracks may significantly influence the mechanical performance and durability of concrete. Therefore, it is necessary to produce concrete that is able to automatically repair the cracks and recover the damage in concrete structures. The practical phenomenon of autogenous-healing in cracks, commonly known as self-healing phenomenon has become an important research topic to study (Granger et al., 2007; Reinhardt and Jooss, 2003; Aldea et al., 2000).

The traditional repairing techniques of cracks in concrete have a number of weaknesses, such as the difference in the thermal coefficient of expansion between concrete and repairing substances along with the high cost and the impact on health and environment. Therefore, an unconventional and an eco-friendly crack remediation system have to be invented to tackle the impact of these disadvantages. Some of these systems have been accomplished using organic and inorganic filler (Yuan et al., 2008). Biotechnological applications have recently been introduced in the field of concrete and led to a new field called “bacterial concrete” or

“bacteria based self-healing concrete”, which is a strategy to remediate cracks in concrete structures based on application of bacteria to induce the precipitation of calcium carbonates (Achal, Mukherjee and Reddy, 2010a).

Bacteria based self-healing is one of autonomous self-healing mechanism that relies on biochemical process to precipitate calcium carbonate to seal the crack and improve concrete properties (i.e. durability, strength, permeability). Crack healing utilising a certain bacteria species as a self-healing agent discovered in the middle of 1990 (Gollapudi et al., 1995) . Microbes can be basically divided into three groups: bacteria, fungi, and viruses. Among these groups, some bacterial strains were found to be able to synthesize certain chemicals, such as carbonate (CaCO3) and polymorphic iron-aluminium-silicate ((Fe5AI3) (SiAl) Ol0 (OH)5). Bacteria have been used externally or added internally within the concrete mixture to remediate concrete cracks. However, different approaches can be followed when bacteria added internally. These includes adding the living cells with their broth, adding bacteria in their dormant state (spores), immobilising bacteria onto activated carbon or silica gel and using capsules or vascular system to encapsulate bacteria (Wang et al., 2012; Wu, Johannesson and Geiker, 2012; Toohey et al., 2007). In recent day, employing selective metabolic activities of particular microorganisms that precipitate calcium carbonate to enhance the general performance of concrete has taken a significant part of researcher attention. The self-healing efficiency was basically evaluated based on strength and permeability characteristics. Many researchers have attributed the improvement in properties of bacterial concrete to the precipitation of CaCO3 from bacterial activities. In a study conducted by (Bundur, Kirisits and Ferron, 2015), it was shown that calcium carbonate precipitation, mainly calcite, occurred within the cement pastes when vegetative cells of Sporosarcina pasteurii were added. Strength improvement at early age was not so pronounced due to the limited amount of CaCO3 precipitates in the pores. (Achal, Pan and Özyurt, 2011) identifies the slow growing of bacterial cells inside the alkaline concrete environment as a major cause of the limited quantity of calcite precipitates. However, increasing the incubation period will lead to precipitation of sufficient amounts of calcium carbonate. Therefore, the strength will gradually increase at later ages.

2.3 Biomineralization

Biomineralization is a process of mineral synthesis as a result of biological activities of the living organisms under favourable settings of interaction with discerning condition

(Hamilton, 2003). Generally, mineral formation process can be classified into two different mechanisms: Biologically Controlled Mineralization (BCM) and Biologically Induced Mineralization (BIM) (Lowenstein and Weiner, 1989). Nucleation and growth of the mineral particles are controlled by the organism in biologically controlled mineralization (BCM). Through this high degree of quality control process, each organism produces its unique form of minerals regardless of environmental condition. These minerals are formed at a particular position inside or on the cell and only under specific circumstances. Eukaryotic organisms or tissues mostly mineralise calcium crystals by biologically controlled mineralisation (BCM) such as teeth, bone, skeletons and sea shells (Barabesi *et al.*, 2007).

Production of calcium carbonate and formation of silica frustule in the highly productive single-celled algae and diatoms, respectively, are the most characterized example of biologically controlled mineralization. Magnetite synthesis by Magnetotactic bacteria is another example of controlled mineralization (Bazylinski, Frankel and Konhauser, 2007) and these bacteria are considered a model organism for controlled magnetic mineralization (Baeuerlein, 2004; Bäuerlein, 2003).

On the other hand, biologically induced mineralization (BIM) is considered to be unaffected by particular molecular mechanism or cell structure and carried out in an open environment. The best known example of biologically induced mineralization is calcium carbonate precipitation by bacteria which is mainly depending on the environmental factors (Brennan, Lowenstein and Horita, 2004; Ben Omar, Arias and Gonzalez-Munoz, 1997; Rivadeneyra *et al.*, 1994). Many bacteria isolated from marine or soil environments are able to induce calcium carbonate crystal formation when they cultured in different media (Boquet, Boronat and Ramos-Cormenzana, 1973). Minerals produced by biologically induced mineralization are located extracellularly. Studies have been reported that most of the minerals induced precipitation is reliant on the selective conditions (Rivadeneyra *et al.*, 1994). Among various minerals and metal oxides that formed by the use of biologically induced mineralization, carbonates are the most recognizable.

2.4 Microbial induced calcite precipitation (MICP)

Microbial Induced Calcium Carbonate Precipitation is a relatively green and sustainable phenomenon commonly found in environments, such as marine water, freshwater biofilms and soils. Through this method, organic compounds are precipitated by the combined effect of the metabolic activity of bacteria and bio mineral precursors. Calcium carbonate is a

typical precipitate of this approach formed in different polymorphs, such as calcite and vaterite (Sharma et al., 2017; De Muynck et al., 2010).

Organisms that can induce microbial calcium carbonate precipitation (MCP) through their metabolic processes can be classified into three main groups; (i) photosynthetic organisms that remove CO2 such as cyanobacteria and algae, (ii) sulphate sinking microorganisms that are responsible for sulphate reduction and (iii) a number of bacteria that are involved in the nitrogen cycle (Hammes and Verstraete, 2002; Castanier, Le Métayer-Levrel and Perthuisot, 1999). Therefore, it has been hypothesized that most of bacteria have the capability to precipitate calcium carbonate (Boquet, Boronat and Ramos-Cormenzana, 1973). Occurring of such precipitation can be attributed to the by-product of well-known metabolic process such as photosynthesis, sulphate reduction, and urea hydrolysis (Hammes et al., 2003) . However, in soil environment, the contribution of a huge amount of microorganisms in the MICP process is approved and the urease enzyme activity is found to be responsible for this phenomenon (Sarda et al., 2009).

Four key factors govern the tendency of ureolytic bacteria to produce calcite ($CaCO_3$) for microbial cementation: (1) the concentration of calcium, (2) dissolved inorganic carbon (DIC) concentration, (3) the pH value and (4) nucleation site availability (Hammes and Verstraete, 2002). However, the ability of ureolytic bacteria to release sufficient urease enzyme through their metabolic process is a crucial factor for precipitating calcium carbonate.

The mechanism of calcium carbonate precipitation is not exactly clear yet. Microbial induced calcium carbonate reaction divided into three different sequencing stages. The development of an oversaturated solution represents the starting stage, nucleation at the point of critical saturation occurs in the following stage and finally, growing of spontaneous crystal on the stable nuclei (Wong, 2015).The first reaction happened in the microbial cementation process is urea hydrolysis which is a process of decomposition of urea [$CO(NH_2)^2$] by urease enzyme as a catalyst into (NH_4^+) and carbonate (CO_3^{-2}) ions (Equation (1)).

$$CO(NH_2)^2 + 2H_2O \rightarrow 2NH_4^+ + CO_3^{-2} \quad (1)$$

The reaction between carbonates ions (CO_3^{-2}) released from Equation (1) and calcium ions (Ca^{+2}) extracted from calcium source leads to the precipitation of calcium carbonate crystals (Equation (2)).

$$Ca^{+2}+CO_3^{-2} \rightarrow CaCO_3 \quad (2)$$

Calcium ions can be derived from calcium chloride, calcium acetate and calcium nitrate that are recognized as a typical source of calcium. Apart from other metabolic activities, the ability to produce carbonates ions without a concomitant generation of protons represents the main distinctive feature of the urea hydrolysis by distributed enzyme urease. The crystallization of calcite ($CaCO_3$) precipitated from solution shows a higher solidity if the environment is rich in calcium. The rate of carbonate reaction has great effect on the binding strength of calcite crystals and the reaction that is responsible for the production of hard binding calcite cement or (biocement) can be conceivably controlled under appropriate conditions (Siddique and Chahal, 2011).

Microbially induced carbonate precipitation has encouraged scientists to employ this ability of microbes for many applications, such as Biotechnology, Geotechnology, Paleobiology and Civil Engineering (Dhami, Reddy and Mukherjee, 2013). Owing to its sustainable nature, this phenomenon has generated much attention and offers a smarter production alternative.

On the other hand, carbonate precipitation by bacteria has been stated as a potential self-healing strategy via microbiologically induced calcite precipitation (MICP) approach in cementitious material. Self-healing process via MICP can be achieved by three approaches: (i) microbial urease-catalysed urea hydrolysis (Dick *et al.*, 2006), (ii) nitrate reduction (Erşan *et al.*, 2016) and (iii) oxidation of calcium salts by aerobic bacterial metabolic activity (Wiktor and Jonkers, 2011; Jonkers *et al.*, 2010). In the third approach, instead of hydrolysis of urea, organic calcium salt is metabolically converted into calcium carbonate as the healing compound.

Calcite precipitation by bacteria is being extensively studied these days for many civil engineering applications, such as increasing stiffness and strength of sandy soil by biocementation treatment(Whiffin, 2004), protection of construction materials by surface treatment (De Muynck *et al.*, 2008), microbiological remediation of cracks in concrete (Ramachandran, Ramakrishnan and Bang, 2001), strength and durability improvement of concrete (Achal, Pan and Özyurt, 2011; De Muynck *et al.*, 2008), brick durability and sand impermeability. The small cracks of concrete could be sealed after the formation of healing products, leading to a reduction in water and dissolved ions permeability. An expensive and unsafe human intervention can therefore be avoided when self-healing approach utilised as a way to prolong the service lives of concrete structures.

2.5 Bacteria

Bacteria are a main collection of simple unicellular living organisms belong to prokaryotes. There are abundant amount of bacteria cell everywhere, around 40 million bacterial cell in each gram of soil and one million of this cell in a millilitre of fresh water; overall, there are almost five nonillion (5×10^{30}) bacteria cell on Earth (Pacheco-Torgal and Labrincha, 2013).With a few micrometres in length, bacteria cell have diversity of shapes, including the most common ones, rod (Bacillus), spherical (Coccus) and spiral (Spirillum) shaped (Wong, 2015). Bacteria are ubiquitous in soil, acidic hot spring, radioactive waste, water, and deep in Earh's crust, as well as in living substance and the live body of plants and animals.

Bacteria can cultivate and divide very quickly under favourable environment and they can quickly duplicate their populations every 9.8 min (Chahal, Siddique and Rajor, 2012a). However, the growth ability, survivability and productivity of bacteria are dependent on the purpose of using these bacteria. In research laboratory, solid and liquid media are usually used to grow bacteria. To isolate pure bacteria cultures, agar plates as a solid growth media have to be used, while, for growth evaluation or production of huge volume of cells, liquid growth media is preferred. Stirred liquid growth media is used as a cell suspension to ease the cultures division and transferring process, in spite of the difficulty of isolating a particular bacterium from liquid media. In order to easily classify definite bacteria strains, the growth media has to be selected carefully by adding specific nutrients.

The high alkalinity of concrete matrix is mainly related to the formation of portlandite (calcium hydroxide CH), the quantitatively second most important hydration product of ordinary Portland cement (OPC) after calcium-silicate-hydrate (CSH). The pH value of the matrix capillary water of fresh concrete is ranging between 11 and 13. Therefore, bacteria should have the ability to tolerate the concrete alkaline conditions for long periods as well as to endure extreme mechanical stresses caused by mixing. It has been approved the spore-forming bacteria of the genus Bacillus is be able to withstand such a high pH environment and shown to be viable for over 200 years (Schlegel and Zaborosch, 1993). One of the main reasons that enable them to remain alive for this long period of time is that these spores have remarkably thick cell walls. For the bacteria with specific characteristics, such as alkaliphilic (alkali-tolerant), spore-forming should be chosen as bio-agents for concrete matrix incorporation. It should also be more tolerant to the presence of oxygen as concrete can be penetrated, through its capillary pores, by oxygen. The Genus Bacillus is typically an aerobic

alkaliphilic spore-forming bacterium and some of them found to play the role of self-healing agents (Jonkers et al., 2010).

The principle mechanism of self-healing using bacterial spores is that after the cracks appear in the concrete, water leaks through the cracks with the food presence, activating the spores to germinate, thus producing calcium carbonate precipitates (Abo-El-Enein et al., 2013) . This mechanism reduces the pH value of this highly alkaline media to values in the range (pH 10 to 11.5) which is an ideal condition for spore's activation.

2.6 Factors affecting microbial induced calcium carbonate precipitation

The urea hydrolysis of the bacteria and the subsequent calcium carbonate precipitation are affected by many factors such as temperature, bacterial cell concentrations, type of bacteria and pH value of the medium and many more. Some of these factors were mostly assessed in relation to bacterial carbonate precipitates in sand. Thus, extra investigations are required to evaluate the effects of these factors particularly in concrete.

2.6.1 **Bacteria type**

Bacteria is one of the most influential factors affecting calcite precipitation process as it is the only living organism found in the MICP system and its activity is regarded as an important player in the precipitation of calcium carbonate. As urea hydrolysis is the more appropriate way for the production of calcium carbonate, the types of bacteria that are suitable for MICP are commonly urease positive, i.e. they have to be capable to hydrolyse urea. Many indigenous bacteria found in soils and groundwater systems have the ability to hydrolyze urea (Burbank *et al.*, 2011). The bacteria should also be alkaliphilic in order to be used for application at high pH such as the high alkaline freshly made concrete which is typically characterised by pH value between 11 and 13. Alkaliphilic bacteria refer to microorganisms that optimally grow at pH values more than 9, with some strains growing up to pH values ranging from often 10–13 (Horikoshi, 1999). The typical characteristic of alkali-resistance bacteria is their ability to sporulate under unfavourable conditions. Spore is the dormant structure of bacterial cell, i.e. no metabolic activity, with high resistant to physical and chemical stresses (Sagripanti and Bonifacino, 1996). Moreover, bacteria should not be pathogenic, i.e. they are harmless and do not cause disease. In addition, the incorporated bacteria need to be able to grow in the presence of air (aerobic) as oxygen can diffuse through the capillaries of the concrete matrix. Therefore, Bacteria genus Bacillus is found to be the

typical types of spore forming, ureolytic and alkaliphilic bacteria that can survive in the high-alkaline environment, hence used for biotechnology (Jonkers *et al.*, 2010).

Bacillus sphaericus (Wang *et al.*, 2014c; Wang *et al.*, 2014a; Wang *et al.*, 2012; Jonkers *et al.*, 2010) and Sporosarcina pasteurii (Chahal, Siddique and Rajor, 2012a; Ramachandran, Ramakrishnan and Bang, 2001; Bang, Galinat and Ramakrishnan, 2001) were the most commonly used bacteria in cementitious materials and concrete. Bacillus Megaterium was also proved as self-healing agent (Andalib *et al.*, 2016; Krishnapriya and Babu, 2015) . Based on their test observations, Paola Cacchio et all (2010) pointed out bacterial strains will affect both the size and shape of the crystals precipitated. They found out that the strain 1 from the Stiffe cave, identified as Bacillus megaterium, deposited elliptical crystals; while strain 3, a different Bacillus megaterium strain isolated from the cave, precipitated hemispheric crystals. Finally, for strain 30, a soil isolate identified as Kingella sp., they demonstrated that the calcifying bacteria were not carbonate solubilizers (Cacchio *et al.*, 2003). However, it is rather difficult to make a straight comparison between bacteria types as there are many factors affecting the $CaCO^3$ precipitation, that need careful optimization besides studying the influence of the combined factors on MICP. Microbialy induced calcite precipitation have been examined through denitrification in a minimum amount of nutrients. To enhance the MICP performance, two strains were isolated, Pseudomonas aeruginosa and Diaphorobacter nitroreducens. The results of this study indicated that the calcium carbonation precipitated in 2 days was 14.1 and 18.9 g $CaCO_3$/g NO_3-N, respectively (Erşan, De Belie and Boon, 2015).

2.6.2 **Bacteria cell concentration**

Microbially induced calcite precipitation is not only affected by the bacteria type but also the concentration of the bacteria used. Previous research has used different concentrations of Bacillus Megaterium as a bacterial healing agent in the concrete matrix (Andalib *et al.*, 2016) . The highest strength achieved due to calcification mechanism was gained by using 30×10^5 cfu/ml as an optimum bacterial concentration. In an investigation into evaluating the healing efficiency of hydrogel encapsulated spores, Wang et al. (2014) found that adding 10^9spores/ml resulted in 68% decrease in permeability and cracks less than 0.5 mm in width was sealed with calcite crystals (Wang *et al.*, 2014a). Similarly, 69% of water tightness was recovered when 10^8spores/L embedded in a Light Weight Aggregate (LWA) added to concrete mix. The results also showed that a dense, compact layer of healing products were

covering the internal crack surfaces, yet, the average sealed crack width was not measured in this study (Ducasse-Lapeyrusse *et al.*, 2017). In another study, De Muynck et al. found that the amount of calcium carbonate formed by the metabolic activity of Bacillus sphaericus was higher compared to other ureolytic strains used in this study. It was also found that treating limestone prisms with this species showed reduction in weight loss by 64% and 46% decrease in sorptivity (De Muynck *et al.*, 2013) .

It has been demonstrated that using $0.3x10^8$ or $1.2x10^8$ of B. subtilis spores/mL to examine the capacity of filling cracks during the curing time results in filling the cracks in concrete with calcite which was visualized by optical microscope (Schwantes-Cezario *et al.*, 2018) . In a study conducted by Tziviloglou et al. at Ghent University, it was found that to gain a considerable amount of calcium carbonate precipitation, the concentration of bacteria should be higher than 10^6 cells/ml (Tziviloglou *et al.*, 2016b) . To evaluate the suitability of using Bacillus sphaericus as self-healing agent for concrete cracks, Wang et al. assessed its alkaline tolerance, calcium tolerance, oxygen dependence, and low-temperature adaptability. It has been found that the bacterial ureolytic activity in the presence of 0.9M Ca^{2+} has not been affected especially at a high bacterial concentration of 10^8 cells/ml (Wang *et al.*, 2017).

Considering the theoretical assumption that each vaterite crystal is initiated by a single bacterial cell, it was anticipated that fewer but larger crystal would be formed by using less bacterial concentration. However, during their boicementation experiment, Al-Thawadi and Ruwisch (2012) reported that by increasing the concentration of bacterial cells, the average size of calcium crystal particles will be increased, leading to improving the urease activity. It would be helpful to control the size of precipitated crystals if the assumption that increasing crystal size depends on the concentration of microorganism's cells has been approved (Al-Thawadi and Cord-Ruwisch, 2012).

It has been observed that for compressive strength enhancement, the optimal bacterial concentration lies between 10^5–10^7cells/ml for all considered bacteria, while higher bacterial cell concentrations of 10^8–10^9cells/ml leads to improve the crack healing efficiency. In addition to that, the rate of precipitation of calcite depends on the type of bacteria and the bacterial concentration. However, the exact cause for reducing compressive strength at higher bacterial concentration is currently unknown. It is correct that healing the crack is the primary objective of bacterial concrete, yet it should not have a negative impact on compressive strength. Hence it is important to find the reason for the existence of the optimum

concentration for compressive strength improvement of bacterial concrete that can lead to a suitable choice of bacterial concentration as needed (Mondal and Ghosh, 2018).

Based on the literature review referred, it was found that various studies have considered 10^8spores/ml as the optimum amount of spores incorporated in concrete mixture.

2.6.3 **Temperature**

The temperature can have a direct impact on calcite formation by microbial induced calcium carbonate precipitation (MICP). The microbial enzymatic urea hydrolysis reaction is sensitive to temperature. Depending on environmental conditions and concentrations of other reactants in MICP, the temperature range of 20 °C–37 °C was found to be the optimum for most ureases used in this system (Okwadha and Li, 2010; Mitchell and Ferris, 2005). Several studies have been conducted on microbial carbonate precipitation and emphasized that temperature is the prominent factor of bio- mineralization (Ferrer *et al.*, 1988b; Ferrer *et al.*, 1988a; Novitsky, 1981) . These experiments revealed the positive effect of the temperature between 22 to 32 ^{o}C on the carbonate deposition of bacteria by developing the crystal formation ability and the amount of calcium carbonate deposed by each strain (Cacchio *et al.*, 2003). A study investigating the role of urease in calcium carbonate precipitation using Bacillus megaterium, Dhami et al. (2014) found that the enzymatic activity reduced by nearly 47% as the temperature increased to 55 °C, whereas at 35 °C, urease was entirely stable (Dhami, Reddy and Mukherjee, 2014). In another study of calcite precipitation rates generated by Bacillus pasteurii at temperatures ranging from 10 to 20 ^{o}C, Ferris (2004) reported that the hydrolysis rate of urea was five times better by increasing the temperature from 15 to 20 °C, while changing the temperature from 10 to 20 °C led to improving the urease activity by ten times (Ferris *et al.*, 2004). MICP in sand was also investigated by Van Paassen (2009) utilising the microbial urease activity of Sporosarcina pasteurii. He revealed that the urea hydrolysis rate is considerably affected by temperature. The effect of temperatures increased by 10 ^{o}C from 5 to 35 ^{o}C on urease activity was measured. At 35 ^{o}C, the urease activity factor reached 3.4(Van Paassen, 2009). Furthermore, Whiffin (2004) performed a similar series of experiments to show the urease enzyme activity of Sporosarcina pasteurii (Bacillus pasteurii) at different temperature between 15 and 80 ^{o}C. The aim of this study was to identify the optimal temperature range for biomineralisation and investigate if the changes urease rate with environmental temperature can be envisaged. It was concluded that between 15 and 25 ^{o}C, the urease enzyme activity was unchanging, while a proportional

increase was detected between 25 and 60 ^{o}C with an optimal activity at 70 ^{o}C (Whiffin, 2004). To determine the optimum conditions for calcite precipitation from microbial induced calcite precipitation (MICP), two microbial species (Staphylococcus saprophyticus and Sporosarcina pasteurii) were examined by changing specific parameters. The precipitation was observed under different temperatures (20, 30, 40 and 50 ^{o}C). It has been confirmed that both strains were sensitive to temperature and the maximum precipitation of calcite was achieved under 30 ^{o}C (Kim, Kim and Youn, 2018).

2.6.4 **PH**

The microbial urease activity is greatly influenced by the hydrogen ion concentration of the environment (Hasan, 2000). The ability of this enzyme to hydrolysis the urea is only active at specific pH levels. The ureolytic activity of bacteria could increase the pH level in the bacterial environment because of the production of ammonia NH_4^+ and bicarbonate ions that leads to the precipitation of calcium carbonate (Knoll, 2003). Previous researches have established that the ideal pH for urease is 8.0 and the enzyme activity declines beyond this level (Gorospe *et al.*, 2013; Stocks-Fischer, Galinat and Bang, 1999). Evans et al. and Arunachalam et al. provided further support for the idea that 8 is the optimal pH for urease enzyme to be active (Evans Jr *et al.*, 1991) and for the maximum $CaCO_3$ deposition (Kantha D.Arunachalam *et al.*, 2010). In a study which is set out to determine the optimum conditions for calcite precipitation from microbial induced calcite precipitation (MICP), two microbial species (Staphylococcus saprophyticus and Sporosarcina pasteurii) were examined by changing specific parameters. The hydrogen ion concentration (pH) was varied from 6 to 10. It has been demonstrated that the maximum precipitation of calcite was obtained at a pH of 7 (Kim, Kim and Youn, 2018). On the other hand, some bacteria still have the ability to breakdown the urea into ammonia and carbon dioxide at pH of 9. This is because the pH of the medium will increase by ammonia production along with the buffering action of the CO_2 produced by urea hydrolysis and cell respiration (Ng, Lee and Hii, 2012). Therefore, it is essential to choose a suitable bacterial strain in a bacteria-based self-healing system to ensure the occurrence of calcite precipitation upon cracking. Characteristics of bacterial concrete

2.6.5 **Compressive strength**

The compressive strength is common criteria used to measure the quality of concrete. It is also considered as one of the most significant properties that reflect concrete durability. Compressive strength is used as a design parameter to categorise concrete in structural

applications. The obligation of the work specifications is closely related to the test results of the concrete compressive strength (Dhami, Mukherjee and Reddy, 2012). On the other hand, the microstructure of concrete incorporated self-healing agents will change and as a consequence its compressive strength will be affected. Therefore, different researchers have studied the ability of compressive strength improvement of bacteria incorporated concrete and mortar.

The effect of Sporoscarcina pasteurii bacteria on the compressive strength has been investigated by using different cell concentrations. The optimum cell concentration of 10^5 has been reported to increase the compressive strength of the concrete sample by 22% (Chahal, Siddique and Rajor, 2012b). Other authors have studied the effect of different cell concentrations of Bacillus subtilis silica adsorbed in their cell on the compressive strength of concrete. They concluded that the compressive strength can be effectively improved by using 10^6 cell/mL (Afifudin *et al.*, 2011). Bacillus pseudofirmus and Bacillus cohnii bacteria spores have also been added to the concrete samples to study the strength characteristics of concrete. It has been reported that an increase of 10% in the compressive strength obtained from adding 10^8 spores /cm^3 of concrete (Jonkers and Schlangen, 2007). Mortar cubes were also treated with different bacteria species to study the strength characteristics. One of these studies was conducted by using Sporosarcina passteurii, the improvement in compressive strength was 17%. Another study compared the compressive strength improvement ability of Arthrobacter crystallopoietes, Sporosarcina soli, Bacillus massiliensis and Lysinibacillus fusiformis, mortar cubes treated by Arthrobacter crystallopoietes have shown 22% increase in the strength comparing to the rest of bacteria species (Park, 2010). Incorporating Bcillus sp. CT-5 into cement mortar specimens has led to an increase of 36% in compressive strength (Achal, Mukherjee and Reddy, 2010b).

It has been noticed that the compressive strength of bacterial concrete is also affected by the addition method of bacteria. In a study conducted by Ramachandran et al (2001), bacteria were embedded in a phosphate solution and directly mixed with other concrete components (cement and sand)(Ramachandran, Ramakrishnan and Bang, 2001). Like the normal water to cement ratio, phosphate solution to cement ratio was 0.49. The 28 days compressive strength recorded in this study was more than 60 MPa. In the same vein, Krishnapriya et al (2015) in their study noted down a compressive strength of 38.3MP after 28 days (Krishnapriya and Babu, 2015). However, the bacteria were mixed with potable water with a water to cement ratio of 0.55 before directly added to concrete matrix. The aggregate used in this study

consisted of a mixture of coarse and fine aggregates. The difference in compressive strength results could be attributed to the new microstructural features formed after bacterial incorporation. The higher compressive strength value recorded by Ramachandran et al (2001) could be due to the fine aggregate, which made the microstructure more compact, and using of phosphate solution instead of potable water.

Compared to Krishnapriya et al (2015), the compressive strength of concrete containing bacterial healing agent as a powder was higher (51 MPa) despite the similar mix composition used (Da Silva et al., 2015; Krishnapriya and Babu, 2015). The difference in compressive strength was due to the method of bacterial addition.

Protecting bacteria with light weight aggregate (LWA) shield is another method of incorporation of bacterial healing agent in concrete. It was found that at 28-days of concrete age, the compressive strength was lower (27MPa) using LWA with water to cement ratio of 0.5 (Tziviloglou et al., 2016a). Even though the water-to-cement ratio is nearly similar to those used for previously mentioned studies, the compressive strength decline is attributed to inclusion of LWA.

To conclude, the microstructure of concrete will be affected by the incorporation of bacteria self-healing agent which can consequently lead to the change in compressive strength. Bacterial agent addition method had a significant effect on the compressive strength. For example, shielding bacterial agent inside LWA before introducing to concrete will adversely affect the compressive strength. Yet, providing some protection for bacteria against crashing is essential to the performance of bacterial self-healing concrete. Therefore, such reduction in compressive strength can be expected in case of bacterial incorporation.

2.6.6 **Permeability**

Permeability can be defined as the simplicity of the ingression of the outside media such as liquids, gases, different harmful ions and other pollutants into the concrete (Basheer, Kropp and Cleland, 2001). The high permeable concrete fastened the ingression of fluids media leading to rapid degradation of concrete. In contrast, low concrete permeability is beneficial as it diminishes the fluids media penetration. The harmful substances ingression throughout the pores and the way potentially they penetrate into the concrete often affect the deterioration mechanisms that caused damage.

Due to these drawbacks, different studies have been conducted to determine the effect of calcium carbonate precipitation on the permeation properties of concrete. Carbonation test is used to investigate the permeability properties of cementiuous materials. The larger the pores the higher carbonation depth as it depends on the connectivity of the pores.

It has been found that incorporation of Bacillus megaterium in fly ash concrete led to reducing the absorbed water by 3.5 less than control concrete. This bacterial concrete has also exhibited lower permeability compared with the control concrete (Achal, Pan and Özyurt, 2011). Different concrete properties are related to the permeability. The reduction of permeability upon application of bacterial cells has been reported to be accompanied with the increase in alkali resistance of concrete, freeze thaw attack and drying shrinkage (Ramakrishnan, Bang and Deo, 1998).

Calcium carbonate precipitation by Sporosarcina pasteurii (Bp M-3) has brought about a remarkable reduction in water uptake, permeability, chloride penetration comparing to the control samples (Achal, Mukherjee and Reddy, 2011). Eight times and four times reduction in chloride permeability and water absorption respectively have been indicated by using S. pasteurii in fly ash concrete as calcite precipitation agents. These improvements have been achieved by adding 10^5 cells/ml (Chahal, Siddique and Rajor, 2012b).

2.6.7 **Durability**

The advancement in concrete technology is focusing on the concrete strength. However, the severity of exposure condition to which concrete is exposed over its entire life should be essentially considered along with concrete strength as both strength and durability have a profound effect on producing a more durable structure. Durability of concrete can be defined as the ability to retain initial properties, quality and serviceability over a long period of time without degradation (Shang and Yi, 2013; Shang, 2013). The compressive strength is common criteria used to measure the quality of concrete. However, compressive strength cannot precisely envisage long term concrete performance, which is relied not only on load carrying capacity, but also on concrete durability. Consequently, either connection between durability and compressive strength properties like permeability is required, or additional measurement of durability needs to be investigated (Mohr *et al.*, 2000).

As the concrete is adaptable and widely used material, the durability and long-term performance of many concrete structures should be enhanced. This performance relies on the

connectivity between concrete and its service environment, in which the ingression of harmful substances is very important (Basheer, Kropp and Cleland, 2001).

Nowadays, using ordinary Portland cement (OPC) to accomplish the high durability for structures in contact with severe environment, such as seafloor, offshore structures, tunnels, highway bridges and sewage pipes, and structures for solid and liquid wastes may not be sufficient. The heterogeneity of the concrete gives different shape and size of pores. Strength and permeability are directly or indirectly affected by the pore structure (Tanaka and Kurumisawa, 2002; Živica, 1997).

It has been agreed that the durability and mechanical strength of concrete highly depend on the characteristics of its pore structure (Khan, 2003; Poon, Wong and Lam, 1997). Therefore, it is important to study the pore structure of the concrete to understand the nature of this heterogeneous material. The permeability and chloride penetration resistance are indicators of the ingression and transportation of water, salts and other harmful substances (Mohr *et al.*, 2000). These characteristics are influenced by the porosity and the pores connectivity. In addition, open pore structure eases the ingress of substances and fluids movement thus more susceptible material (Achal, Mukherjee and Reddy, 2010b).

Recently, a biological process has been incorporated to produce a stronger and more durable concrete. This new technique named bio-concrete, employs bacteria to precipitate minerals and remediate the cracks and fissures in the concrete (Van Tittelboom *et al.*, 2010; Ramachandran, Ramakrishnan and Bang, 2001). Bacterial mineralization processes play a vital role in mineral precipitation technology to improve the properties of porous materials, such as sand consolidation (Gurbuz *et al.*, 2013), limestone monument reparation, enhancement strength of bricks (Dhami, Mukherjee and Reddy, 2012), and remediating of concrete cracks leading to produce building material with high permeability (Dhami, Reddy and Mukherjee, 2012; Wiktor and Jonkers, 2011).

Even though some investigations have been demonstrated in the application of bacteria as self-healing agent for increasing the compressive strength, a reduction in the porosity and permeability of the concrete (Jagadeesha B G Kumar, R Prabhakara and H Pushpa, 2013; Chahal, Siddique and Rajor, 2012b; Ghosh *et al.*, 2005; Ramachandran, Ramakrishnan and Bang, 2001; Ramakrishnan, Bang and Deo, 1998; Patil *et al.*,2011), there is a limited information available in the literature about the bio concrete durability.

Andalib et al. (2014) for example, reported the durability of structural bio-concrete against sulphuric acid and hydrochloric acid (Andalib *et al.*, 2014). De Muynck et al. (2008) examined the efficiency of the bio deposition treatment by assessing the degradation of mortar specimens subjected to the action of accelerated carbonation, accelerated chloride migration and Freezing and thawing cycles (De Muynck *et al.*, 2008). Truong, Kishi (Truong, Kishi and Kayondo (2013) reported the effect of crack self-healing on performance of reinforced concrete and predicted the life span of concrete member subjected to flexural loading(Truong, Kishi and Kayondo, 2013). An increase in the resistance of concrete towards drying shrinkage, sulfate, alkali and freeze thaw attack was also observed when bacteria was used to study the effect of bio-mineralisation on concrete durability. In the same study, it was found that increasing concentrations of bacterial cell makes more noticeable impact on concrete durability (Ramakrishnan *et al.*, 2005). In another study, it was reported that precipitation of a calcite layer on the surface of the bacterial specimens led to a significant reduction in chloride penetration, permeability and water uptake comparing to non-bacterial specimens (Achal, Mukherjee and Reddy, 2011). The same authors proved the efficiency of the crack sealing in the development of strength and durability of concrete structures by decreasing their permeability to water and chlorides (Achal, Mukerjee and Reddy, 2013a). In a comprehensive study of the effects of bio-deposition process on the durability of mortar samples with different porosity, De Muynck et al. (2008a) found that the water absorption reduced by 65-90% as a result of the surface deposition of $CaCO_3$ (De Muynck *et al.*, 2008).

Durability was assessed from the permeation properties and resistance towards degradation processes. Accordingly, a decrease in chloride migration and the rate of carbonation by about 25–30% and 10–40% was reported, respectively. It was also observed that the precipitation of calcite crystals layer improved the resistance of mortar samples towards freezing and thawing.

It can be concluded that the macrostructure of cement-based materials is directly related to its microstructure (Mehta and Monteiro, 2017; Korb, 2007; Diamond, 2004). Prior research has thoroughly investigated the deterioration of macroscopic properties, such as the reduction in compressive and the flexural strength, the loss in weight and dynamic elastic modulus. However, little or no research has been conducted to show the microstructure deterioration in bio concrete under exposure to environmental factors.

2.7 Bacteria encapsulation

Self-healing is relatively new treatment strategy for cracks repairing and avoiding damage in concrete structures by using bacteria and their essential nutrients. However, concrete alkaline environment and the mixing mechanical forces, in certain extents, have the potential to cause damage to bacteria. Additionally, the surface life of the healing agents has to be extended in order to achieve an effective healing process. Spore forming bacterial strains have been used to tackle the above mentioned drawbacks as the spore (the dormant state of the cell) is the most suitable state of the bacteria that can be utilized for self-healing purposes. They can survive for a longer period of time comparing to living cells (from several years to hundreds of years) and have high resistibility to heat, radiation and various chemicals (Setlow, 1994). While, the spores of bacteria are more preferable in the concrete and can withstand the harsh conditions of concrete, concrete matrix has accentuated the problem of low density and porosity of structure with very small size pores (less than 1μm) which in turn put the bacterial spores at a risk of smash during cement hydration in addition to the shearing force during concrete mixing and handling. Researchers have therefore devoted considerable attention to introduce self-healing agents with a physical barrier to withstand unfavourable environment. Encapsulation has been found to improve the microorganism's viability and survivability during handling and storage. In the encapsulation process, several problems are encountered and need to be balanced: the need for mechanically stable capsules, capable of being decomposed, able to control cell release, environmentally reactive and the need for low-cost encapsulation technique (Young *et al.*, 2006). The capsules typically should be designed with a suitable semipermeable, thin but strong carrier that will promote the long term microbial preservation and the survival during handling and storage.

Different Bacteria protection and encapsulation techniques have been used by different researchers. For quantifying concrete crack repairing potential, Wiktor and Jonkers (Wiktor and Jonkers, 2011) embedded Bacillus alkalinitrilicus and calcium lactate in porous expanded clay particles. Bio-compatible hydrogel, silica gel and polyurethane were used as a carrier to immobilize Bacillus spaericus (Wang *et al.*, 2014a; Wang *et al.*, 2012). Immobilizing bacteria with diatomaceous earth provided protection against the highly alkaline environment of concrete (Wang, De Belie and Verstraete, 2012). Self-protected enrichment culture was also used as a self-healing additive for concrete along with Ca $(NO_3)^2$ and Ca $(HCOO)^2$ as nutrients. The enrichment culture was introduced into mortar as granules (0.5–2 mm) made up of 70% biomass and 30% inorganic salts. It has been found that after 28 days of

immersion in water, the calcite precipitation was able to seal up to 0.5 mm crack width (Erşan *et al.*, 2015a).

Using polymeric gel to encapsulate microorganisms is an effective technique used in a wide extent of application (Park and Chang, 2000). Immobilizing microbial cells in a gel-like matrix not only protects them against degradation but also maintains their viability for long duration. Alginate capsule is therefore used by different researchers as it is fast and easy to obtain with adequate mechanical strength in the presence of polyvalent cations (Witter, 1996). Ability to entrap large number of bacteria is one of the main positive features of alginate beads (Zohar- Perez *et al.*, 2002; Fenice *et al.*, 2000). Sodium alginate microsphere was also successfully prepared to encapsulate the microbial spores and the living cells of Bacillus subtilis and Bacillus licheniformis (Ohadi *et al.*, 2014; Bregni *et al.*, 2000) . Soil bacterium Bacillus sp.M3 isolated from petroleum-contaminated soil was effectively immobilized in polyurethane foam (PUF) and polyvinyl alcohol (PVA)-alginate beads as a benzene removal (Kureel *et al.*, 2017). Sodium alginate, a polysaccharide occurred naturally in certain brown seaweed, has been commonly applied as an agent in the environmental decontamination for the purpose of removing the organic compounds from water. In the presence of divalent cations (e.g. calcium ion), sodium alginate mediated cation-exchange process through sol–gel transition when a calcium ion substitutes two sodium cations. This material is low cost and biocompatible, and can be easily and quickly made by encapsulation (Kittinaovarat, Kansomwan and Jiratumnukul, 2010). Agrawal, et al. defined alginate as "an unbranched binary copolymer constituted of (1, 4) linked α-l-guluronic acid and β-d-mannuronic acid" (Shilpa, Agrawal and Ray, 2003). As it is non-toxic, bio-degradable, bio-compatible and easily accessible, alginates is commonly used in industrial sectors. Because of its stability, viscosity and gelling property (hydrogels formation ability with calcium cation (Ca^{2+}) as a multivalent cations), alginate has been generally used for bio-encapsulation, e.g. synthesis of Ca-alginate microcapsules to encapsulate lipophilic drugs, chemicals, and nutrients (Liu *et al.*, 2013).

With the objective of improving the self-healing ability in asphalt, different researchers have been using calcium alginate capsules encapsulating asphalt rejuvenator (healing agent). The concept of adding encapsulated healing agent (rejuvenator) into asphalt mixture is to release the healing agent on demand (upon cracking) and healing the crack by restoring the original molecule structure of the aged binder, allowing it flow and fill the crack and repair the damage (Xu *et al.*, 2018). In a study investigating the effect of calcium-alginate capsules

containing sunflower oil on the mechanical properties and the self-healing ability of asphalt mixtures, Micaelo et al. (Micaelo, Al-Mansoori and Garcia, 2016) reported that the oil released from broken capsules will diffuse in bitumen in less than 24 h and heal the cracks. A recent study by Zhang et al. (Zhang *et al.*, 2019) involved using ca-alginate capsules containing sunflower oil as a suitable capsule for asphalt mixture. It has been found that sunflower oil can be released from the capsules to soften and improve the self-healing properties of asphalt mixtures.

Core-shell microgels consisting of an alginate core and a microgel shell was used to encapsulate Bifidobacterium longum strains to reduce their sensitivity to environmental stresses and improve their stability and efficacy in different nutritional interventions (Yeung *et al.*, 2016). Bacterial spores and magnesium acetate were also effectively encapsulated in calcium alginate beads as a bio-inspired technique to develop bacteria based self-healing concrete for application in the marine environment (Palin, Wiktor and Jonkers, 2015). In this technique, bacteria immobilized in concrete will be able to form a mineral healing precipitate preventing the ingress of aggressive chemicals.

Beads made with alginate are widely used and familiar encapsulation materials in biosciences applications, e.g. removal of cadmium ions Cd (II) from aqueous solution by encapsulating of Lentinus sajor-caju biomass (a white rot fungus species) into Ca-alginate gel beads (Bayramoglu *et al.*, 2002). The structure of these beads is three-dimensional, which is consisted of inorganic constituents and polymer with high water-absorbing capacity. As these beads are economic and have great water retention properties, they have been chosen as active adsorbents in different applications. However, when using calcium alginate in beads preparation, various problems may arise, such as gradually wearying of the beads matrix, the porous structure and poor mechanical properties (Tal, Van Rijn and Nussinovitch, 1997). A number of methods are, therefore, adopted to improve the strength of alginate-based encapsulation beads. Researchers have suggested blending various types of clay with sodium alginate. To improve stability of the beads during the encapsulation process of multi-enzymes (alpha-amylase, glucoamylase and cellulase) to hydrolyse cassava roots for glucose production, Rahim et al. blended alginate with kaolinite clay (Rahim *et al.*, 2013) . Along with alginate, which was used as a structured carrier for encapsulation of Trichoderma harzianum UPM40, Adzmi et al. (Adzmi *et al.*, 2012) added montmorillonite clay (MMT) as filler. The microencapsulation technique used in this study was aimed to improve the viability of Trichoderma harzianum UPM40 isolated from healthy groundnut

roots as effective biological control agents (BCAs). It was found that montmorillonite clay particles were homogeneously distributed throughout the alginate matrix and the resulting microcapsules were thermally stable compared with the alginate beads alone. Kaolin and bentonite have also been used as adsorbent to enhance the release of thiram, a dithiocarbamate fungicide, from starch–alginate beads and to reduce the agro-environmental pollution. It was shown that the release profile of thiram has controlled when kaolin and bentonite were incorporated in starch-alginate beads (Singh *et al.*, 2009). In a study conducted by Fravel et al. (Fravel *et al.*, 1985), microorganisms that have potential to control plant diseases were encapsulated in alginate-Pyrax beads. Calcium chloride and calcium gluconate were used as crosslinking agents. It was found that all microorganisms were viable longer when calcium gluconate used in beads formation. However, no study has used calcium-alginate-clay beads to encapsulate bacteria to be used as self-healing agents in concrete.

2.8 Effect of nutrients and precursors on bacterial self-healing concrete

Different calcium salts has been previously used as a precursor. In spite of its detrimental effect on the steel bar and durability of reinforced concrete, Calcium Chloride $CaCl_2$ is the most popular calcium source of microbial induced calcium carbonate precipitation (MICP) via urea hydrolysis approach (Zhang, Guo and Cheng, 2014). These deteriorations occur when chloride content exceeds the acceptable level, restricted by the European standard EN 206-1(0.2-0.4% chloride by weight of binder for reinforced concrete and 0.1-0.2% for pre stressed concrete) (EN,). Some of the chloride added to concrete will chemically bound by or physically adsorbed on the hydration products of the binder (Florea and Brouwers, 2012). In the literature, the term “Bound chlorides” tends to be commonly used to refer to these retained chloride ions, whereas ‘‘free chlorides’’ refers to the remaining ions which are not bound by hydration products. These free chlorides are capable to flow through the concrete matrix in solution close to reinforcement bars via the transport mechanisms (Florea and Brouwers, 2014). On account of the risk of releasing chloride ions into concrete at all ages, it is considered that the chloride content should remain below the threshold even if the addition to concrete has to be in an initially encapsulated state (Paine, 2016). Therefore, calcium nitrate as an alternative calcium source, has been used recently by many researcher to avoid the side effect of chloride ions on concrete(Wang *et al.*, 2015; Wang *et al.*, 2014c; Wang *et al.*, 2014a; Wang *et al.*, 2014b; Jagadeesha Kumar, Prabhakara and Pushpa, 2013) . It has been used in concrete for different purposes. Accelerating the initial setting time of

concrete and developing high compressive strength can be achieved by adding 6% by weight of cement of pure calcium nitrate as an antifreeze admixture. Calcium nitrate is able to react with the calcium hydroxide produced during cement hydration, and form a double and basic salt known as calcium hydroxynitrate. This salt with its needle shape crystals densifies the cement microstructure by creating an initial structural skeleton which covered by calcium hydrosilicates, leading to increasing the compressive strength (Karagöl *et al.*, 2013) . Østnor and Justnes (Østnor and Justnes, 2011) also attempted to evaluate the impact of adding calcium nitrate as an anodic inhibitor into concrete structures prone to chloride attack. It was found to be able to protect the steel reinforcement embedded in concrete from corrosion. In the urea hydrolysis pathway, when calcium nitrate is directly added to concrete, acceleration in the hydration process and increase in the degree of hydration can be observed. These changes in hydration raise concern because the Ca ions remained might not be enough to produce calcium carbonate precipitation (Wang *et al.*, 2014g). Calcium lactate is also used as a representative of organic calcium source for metabolic pathways of self-healing process. In a study set out to determine the ability of the bacteria along with calcium lactate as a two component healing agent to facilitate the calcium carbonate precipitation in cement stone, Thijssen found that abundance of minerals with size 20-80 μm formed on the cracked area (Jonkers *et al.*, 2010). Furthermore, $CaCO_3$ deposited with calcium lactate was as double as with calcium nitrate, demonstrating the positive effect of lactate on the cellular activity of the organisms, which is linked to the calcite precipitation by the production of urease enzyme (Xu *et al.*, 2015). However, the most common calcium source has been utilised as a precursor for calcium carbonete precipitation was calcium acetate (Park *et al.*, 2012; De Muynck *et al.*, 2008b; De Muynck *et al.*, 2008; Barabesi *et al.*, 2007) . Therefore, calcium acetate and its possibility to induce calcium carbonate precipitation without harming other mortar properties was used as deposition agents and investigated in this paper.

Nutrients, on the other hand, are needed to promote the precipitation of calcium carbonate as they play an important role in bacterial spores germination and supplying the microbial cell with growth medium(Paine, 2016). Urea and yeast extract (YE) are the important constituent of nutrient feed as they include a simple and complex nitrogen sources. However, incorporating these nutrients into concrete should not have unfavourable effect on concrete properties.

The heat generated by the hydration reactions and during casting of concrete can be eliminated by addition of a granular urea, because the endothermic reaction takes place by

dissolving urea in water (Mwaluwinga, Ayano and Sakata, 1997). Therefore, urea can be effectively used along with the rice husk ash in hot climates to enhance the flowability and overall durability of concrete (Makul and Sua-iam, 2018).

2.9 Microstructural test for evaluating self-healing efficiency

Microstructure tests are one of the most widely used techniques to identify and characterise the micro-texture and structure of cementitious materials. Mainly, they use some kind of microscope to observe the microstructure of the sample before and after the self-healing and increase the reliability of the obtained results (Wiktor and Jonkers, 2011; Homma, Mihashi and Nishiwaki, 2009). Therefore, different microscopic test methods have been conducted by most of the researchers such as optical microscopy along with petrographic examinations, Field Emission Scanning Electron Microscope (FESEM), Scanning Electron Microscope (SEM), environmental scanning electron microscopy (ESEM) and diffraction (X-ray XRD). Optical microscopy have been used as a tool for assessing self-healing capacity of bacterial concrete by observing the crack surface and measure the crack width before and after healing (Wiktor and Jonkers, 2011). Dimension of the precipitated crystalline products and the geometry of the crack surface have also been measured by optical microscopy (Nishiwaki et al., 2012). A scanning electron microscope (SEM) and an environmental scanning electron microscope (ESEM) are types of electron microscope that produce images and usually implemented carried out together with backscattered electron imaging (BSEI). In these methods, an electron beam is focused on a specimen to form an image. From this image, information about the crystallographic information of the sample can be obtained and the shape, size and morphology of the re-hydrated products can be determined (Van Tittelboom et al., 2012) . Petrological method, on the other hand, is a technique to study very thin slices of rock. Through this technique, light could be transmitted through mineral grains to analyse the micro-texture of the specimen and visualise the crack filled with healing agents (Sangadji and Schlangen, 2012). In term of scanning electron microscopy, calcite precipitation inside the micro-cracks of concrete by bacteria (Sporoscarcina pateurii) has been analysed by (Chahal, Siddique and Rajor, 2012a). It has been found that calcium carbonate crystals were associated with bacteria. SEM examination has also been used to investigate the self-healing capability of epoxy material in cementitious composite. The epoxy was encapsulated in the microcapsule made by urea formaldehyde resin before introducing to cementitious composite. SEM/EDX results revealed that when the crack appears in the cementitious

composite, the epoxy resin released so that development of further crack can be prevented (Dong et al., 2013).

Jonkers et al. used ESEM analysis to study the self-healing potential of bacteria to act as self-healing agent in concrete. They found that there is copious and robust precipitation of minerals, which are likely to be calcium carbonate, formed at the crack surface. The formation of these minerals is due to the presence of the bacterial cells and their metabolic conversion of the soluble calcium precursor (calcium lactate) to relatively insoluble calcium carbonate. The bacteria (B. cohnii) were added as spores to the concrete mixture with a spore concentration of 1×108 cm−3 and a calcium lactate with 0.5% of cement weight prepared with a water-to-cement weight ratio of 0.5 (Jonkers et al., 2010) . Sarkar et al. evaluated the self-bioremediation of a microbial protein-impregnated cementitious material in term of microstructure analysis using field emission scanning electron microscope (FESEM) and energy dispersive spectra (EDS). Bioremediase protein isolated from a hot spring bacterium (BKH1) was incorporated into commercial Pozzolana cement. For the bioremediase protein treated mortar specimens, each of 50 mm × 50 mm × 50 mm size, prepared at cement to sand ratio of 1:3 and water to cement ratio of 0.4, and exposed to three different concentration of bioremediase protein (2, 3 and 4 lg/g of cement); Sarkar et al. discovered the formation of irregular crystalline healing material within the cracks of the test samples. Based on this study, the structure of the crack portion of the control specimens where noticed to be amorphous when compared to the well-grown irregular crystalline structures that appear in the crack portion of bioremediase protein treated samples. Such observations are a clear indication for the formation of new materials within the cracked regions of bioremediase protein- treated mortar samples. The FESEM-EDS analysis was then performed to substantiate the formation of the newly formed healed materials. The analysis clearly illustrated peaks of Ca, Si, Al and O atoms (Sarkar et al., 2014). To investigate the effect of Ca+2 ions on self-healing of cracks in cement paste, Ca (OH)2 was added into water as a healing agent. By performing energy-dispersive spectroscopy analysis, the reaction products of self-healing were characterised. Huang and Ye found that the reaction products formed within cracks were mainly calcium hydroxide and calcium silicate hydrate and the mineralogy of these products was identical for both methods of self-healing (Huang and Ye, 2015). The effect of Ca+2 ions on self-healing was investigated experimentally Ca(OH)2 was added into water as a healing agent the reaction products of self-healing were characterized by energy-dispersive spectroscopy From the characterization, it was found that the reaction

products of self-healing mainly contain CH and C-S-H. The percentage of calcium hydroxide CH is much higher than that of calcium silicate hydrate C-S-H. The mineralogy of reaction products of self-healing induced with saturated Ca (OH)2 solution is similar to that caused by distilled water. It demonstrates that the additional Ca+2 ions do not have much influence on the mineralogy of the reaction products of self-healing.

2.10 Effects of freeze-thaw cycles on bacterial self-healing concrete

The key element for the success of concrete as a building material is its durability performance during service life. Durability of concrete can be defined as the ability to retain initial properties, quality and serviceability over a long period of time without degradation (Shang and Yi, 2013; Shang, 2013). It can also be defined as the ability to resist frost action, reinforcement corrosion, water and harmful substances penetration, carbonation, chemical attack, etc. Degradation may develop within the concrete as a result of different physical and chemical processes such as weathering action, chemical attack, abrasion or any other deterioration process (Setina, Gabrene and Juhnevica, 2013; Yun and Wu, 2011; Kong *et al.*, 2002).These processes may also include freeze-thaw cycles, acids, sulfates, alkalis attack, alkali-aggregate reactions, etc (Papadakis, Vayenas and Fardis, 1991). The abrupt temperature change in the environment is one of the most destructive actions affecting concrete. Freezing and thawing cycles in concrete structures can be defined as the temperature fluctuating above and below freezing of water (Al-Akhras, 2012). Concrete materials in the cold regions and/or under winter climate conditions are under risk of repeated freezing and thawing cycles, because the temperature alternately fluctuated. Exposing the concrete element into these conditions leads to the formation of internal micro cracks and surface spalling. The damage of concrete under freezing-thawing action may be attributed to the hydraulic pressure generated by the volume expansion associated with water transformation to ice during freezing. Concrete with inadequate tensile strength to resist hydraulic pressures develops micro-defects and consequently reduces the overall durability (Luo *et al.*, 2017).

However, the crystallization pressure of ice is also argued to be the main source of stresses during the freezing process (Scherer, 1999). The internal structure of concrete could be locally damaged after on FT cycle. However, the deterioration could considerably increase after subjecting to another FT cycle (Bowser, Krause and Tadros, 1996). The durability of bacterial concrete has been studied by many researchers, yet, there is still insufficient information about its performance under freeze-thaw attack.

Several in depth studies on the topic have been published to solve the durability problem (Zhao *et al.*, 2018; Cao *et al.*, 2018; Siline, Ghorbel and Bibi, 2017; Li, Wang and Zhao, 2017; Todak *et al.*, 2017; Girskas and Skripkiūnas, 2017; Zhu *et al.*, 2017; Zhu, Ma and Zhao, 2016; Sun *et al.*, 2002). In a study investigating the effect of sodium chloride and freeze-thaw cycling on externally loaded concrete, Sun et al. (Sun *et al.*, 2002) reported that the deterioration in the concrete was accelerated when exposed to multi-damaging processes. Zhu et al. (Zhu, Ma and Zhao, 2016) examined the behaviour of steel corrosion in reinforced concrete under freezing and thawing action. It has been found that as the freeze-thaw damage increases, especially for the concrete subjected to high freeze-thaw cycles, the bond-slip behaviour of reinforced concrete with corroded steel decreases. Another study by Siline et al. (Siline, Ghorbel and Bibi, 2017) assessed the frost resistance of pozolanic mortar by studying the physical, mechanical and thermal properties of mortars. It has been shown that porosity, water absorption and hydration progress increased, while compressive strength and thermal conductivity decreased after subjecting to freeze-thaw cycles. Whang and Zhao (Li, Wang and Zhao, 2017) researched the coupled deterioration mechanisms of frost attack and carbonation on coarse recycled concrete aggregates. The samples showed lower residual compressive strength when exposed to combined deterioration by freeze-thaw and carbonation and the depth of carbonated concrete was found to be increased with the increase of the freeze–thaw deterioration. In another study, Todak et al. (Todak *et al.*, 2017) used acoustic emissions and ultrasonic technology to detect crack development in concrete specimens subjected to thermal cycling. It was anticipated that material damage development can be quantified by observing trends in acoustic emissions throughout multiple freezing and thawing cycles. The effect of synthetic zeolite on freeze-thaw durability of concrete was investigated by Girkas and Skripkiūnas (Girskas and Skripkiūnas, 2017). Detailed examinations showed that after 28 freeze-thaw cycles, the freeze-thaw resistance of concrete increased when cement was replaced by10 wt% with synthetic zeolite. In an investigation into the effect of lightweight aggregate saturation degree on freeze–thaw resistance of light weight concrete, Zhu et al. (Zhu *et al.*, 2017) held the view that when the pre-soaked degree of this aggregates was close to saturation, the freeze-thaw resistance of the concrete would be tremendously reduced. Zhao et al. (Zhao *et al.*, 2018) examined the degree to which the bending damage of reinforced concrete was affected by exposing to freeze-thaw. It was observed that fiber incorporation reduced the effect of freeze-thaw on the damage and failure process of the sample. Cao et al. (Cao *et al.*, 2018) carried out an investigation with the aim of determining the frost resistance of fiber reinforced expansive

self-consolidating concrete. It has been demonstrated that increasing the fiber content results in a decrease in the mass change. Although mechanical properties of bacterial concrete were investigated by many researchers, there is a lack of knowledge about the freeze-thaw resistance of bacteria based self-healing concrete.

2.11 Effect of wet-dry cycling on bacterial self-healing concrete

Deterioration of concrete structure can happen due to a variety of reasons, such as corrosion of reinforcing steel, attack by acids, sulphates, and alkalis, freezing and thawing cycles, carbonization and exposing to wet/dry cycling, yet, some of concrete damage is often caused by a combination of factors.

Under wetting and drying cycles, a number of important effects could be induced. Upon drying, the resulting shrinkage that would have developed between cement paste and aggregate leads to micro-cracks formation (Kjellsen and Jennings, 1996); (Maruyama and Sasano, 2014). More micro-cracking may produce with increase the severity of drying (Wu, Wong and Buenfeld, 2015). However, some sign of swelling takes place upon concrete rewetting as the micro-cracks partially or fully closed. The effect of bacteria-based healing agent on cement mortar was examined and the assessment of the regaining of water tightness of cracked mortar samples after subjecting to wet-dry cycles or water immersion through water permeability tests was first reported by (Tziviloglou et al., 2016a). The study reveals that using of the healing agent does not affect the compressive strength of the mortar with lightweight aggregates. It was also found that the continuous immersion of the specimens with or without healing agent in water makes no big difference in their water tightness recovery. On the other hand, exposing the specimens to wet-dry cycles leads to increase the water tightness recovery of those containing the healing agent compared to specimens without it. The bacterial activity was evidenced by the calcite precipitation and oxygen concentration measurements. The self-healing capability of early age and structural cracks in concrete by using crystalline admixture as self-healing agent was studied extensively by Reddy and Ravitheja. The recovered mechanical properties of concrete were evaluated under four different exposure conditions (Water immersion, Wet-dry cycles, Water contact and Air exposure at laboratory conditions). It has been concluded that the compressive strength and split tensile strength of the tested concrete under all exposure conditions recovers after early age and structural cracks. This recovery was attributed to the calcium carbonate precipitation which confirmed by the SEM-EDS and FTIR analysis (Reddy and Ravitheja, 2018). In

addition to that, hydrogels containing B.sphaericus as a self-healing agent incorporated into mortar was demonstrated experimentally by De Belie and Wang (De Belie and Wang, 2016). In their seminal study, it was found that after four weeks incubation in wet–dry cycles of 1 h water submersion and 11 h at 60% RH, the crack was completely healed. Even though some research has been developed in related fields, such as strength recovery and crack sealing because of the formation of calcium carbonate, as mention above, research on the effect of wet-dry cycles on the durability performance of bacteria based self-healing concrete is rather limited.

Chapter 3: Materials and Methodology

3.1 Introduction

This chapter includes the detailed description of the materials used in this thesis. The mix proportions of mortar specimens, manufacturing of fresh mortar, casting, demoulding and curing of samples are also described. In the second part of this chapter are the microorganism selection, growth medium stock, and biology tests, such as the cultivation of bacteria by centrifugation and washing it. Serial dilution-tube method, spectrophotometry and alkaline agar plates, are also given. The evaluation of the mechanical and physical properties, such as flexural, compressive strength of the mortar is also given. This chapter also describes the qualitative assessment of the efficiency of self-healing using the scanning electron microscope (SEM) and Energy Dispersive Spectroscopy (EDAX).

3.2 Investigation of suitable microbial sources of calcium carbonate

3.2.1 **Sample collection**

Surface soils are a heterogeneous mixture of inorganic and organic particles that combine together to form secondary aggregates. Within and between the aggregates are voids or pores that visually contain both air and water. These conditions create an ideal ecosystem for bacteria, so all soils contain vast populations of bacteria, usually over 1 million per gram of soil. Bacteria are highly diverse in terms of the number of species that can be found in soil, in part because they are physiologically and metabolically diverse. Most natural environments represent a stunningly diverse collection of microbial species. To ensure the ecotype diversity of the bacteria used as self-healing agent, samples were collected from different environment.

To get the most diverse collection of microbial species, the samples were collected from four different natural environments. Fifty seven soil samples were collected from different locations around London, nine water samples from pond, twenty from gypsum rock and thirty five samples from concrete. To collect the soil samples, a borer was used to drill into the soil to gather 4-6 samples for each site. The site for individual samples was separated by 10 meters from each other. One gram of soil, water, gypsum rocks or concrete powder was placed in a 50mL sterile falcon tubes and kept at 4°C until assayed. Each falcon tube was labelled according to the site of isolation, and time and date of the collection. Concrete and gypsum rock samples were collected by take 3 to 6 pea-sized samples of the material. The samples were smashed with a hammer inside a sterile plastic bag then transferred the

“powder” to store in a 50 mL falcon tube. The falcon tubes were labelled with the site of isolation, time and date of collection, and type of material / source.

3.2.2 **Growth media preparation**

3.2.2.1 Recipe and steps for the preparation of Duran bottles

For any growth media used in this study, a total volume of 4L of solution in ten 500 mL Duran bottles, were prepared with 400 mL in each. These bottles were kept on the lab shelves at room temperature for up five weeks. When needed, the media was liquefied by putting the Duran bottle in a microwave at 400W for 10-15 minutes after unscrews its lid halfway through. Two specific media were used in this study for growing the microorganisms, namely; B-4 and nutrient agar media. The B-4 medium contains yeast extract which provides nitrogenous source and additional growth elements. To provide the energy source, glucose was included in this medium. This media also contains calcium acetate and agar. For each 500 mL Duran glass bottle, 1 g calcium acetate, 1.6 g yeast extract, 4 g glucose and 6 g agar were weighted and mixed with Milli-Q water up to 400 mL. Nutrient agar medium, on the other hand, were prepared using yeast extract (2 g/L), meat extract (1 g/L), peptone (5 g/L), sodium chloride (5 g/L) and agar (15 g/L). All the ingredients were purchased from Fisher Scientific, UK. For both medium, the resulting liquor was autoclaved at 121°C for 15 minutes, or according to the autoclave's specifications. The solution from the autoclave was left to cool to 50°C.

3.2.2.2 Preparation of the petri plates

To cool down the medium, the Duran bottle was placed in a 50°C water bath, as this will hold the temperature and it can be left unattended for some time. After that, the medium was poured slowly from the bottle into the centre of the petri dish until it covers about 2/3 of the dish. To spread the medium out completely, the plate may need to tilt slightly. Then, the plates were covered by placing their lids on and they were allowed cooling down for 30-60 minutes (until solidified). Later, the plates were inverted for several more hours or overnight to let them sit. Finally, the bottoms of the plates were labelled with the specific type of growth media it contains with a permanent marker.

3.2.3 **Isolation of bacterial colonies**

The samples were diluted properly in a PBST solution (PBST is prepared by dissolving 1 phosphate buffered saline tablet in 200 mL of MilliQ water in a 250 mL Duran bottle, and

adding 2 mL of Tween 20). The phosphate buffered saline tablet and the Tween 20 were purchased from Fisher Scientific, UK. Each sample was vortexed for I minute and inoculate in the first quarter of a petri dish using a sterile swab. Then, to perform a dilution, the samples were streaked on the rest ¾ of the plate through 10 µL plastic sterilized loop. The plates were labelled and incubated for 24 hrs at 30°C. The isolated colonies were further purified and periodically checked from other bacteria contamination by streaking it again in the B4 agar plates. Subsequent cultures were streaked onto medium plates with the same selective pressure to isolate single colonies. The subsequent isolates were re-grown in the same media and observed through light microscopy.

3.2.4 **Identification of bacterial species**

The Biochemical classification and morphology of vegetative cells tests were performed as described in Bergey's Manual of Systematic Bacteriology to characterize all the bacteria isolates. Shape and the position of spores were observed under microscope, using submerges 100X magnification. Gram staining, Spore staining, catalase, and oxidase test were carried out to identify the bacteria species.

3.2.4.1 Gram staining

Gram staining is a differential staining technique used in all aspects of modern microbiology, including general, medical, environmental, and industrial fields. It differentiates between the two major categories of bacteria: Gram positive and Gram negative. The gram stains reaction based on a reflection of cell wall structure of bacteria.

Cells with a thick, relatively impermeable wall that resist decolourisation and composed of peptidoglycan and secondary polymers are known to be "Gram-positive", whereas those with thin peptidoglycan layer plus an overlying lipid-protein bilayer which can be disrupted by decolourization are known to be ``Gram-negative.'' The gram-positive bacteria take up the crystal violet dye and are stained purple while Gram-negative bacteria is stained as red or pink colour with carbol-fuchsin (or safranin). However, The Gram stain is not an infallible tool for diagnosis for some bacteria with intermediate wall structure as it stains in a different manner such as, the Archaea (Beveridge, 2001).

Although the gram staining technique is remarkably simple and reproducible, it has some limitations. At least four different solutions and four staining steps are required in most gram

staining procedures. Additionally, the concentrated primary stain (crystal violet), used in this procedure are particularly messy. The staining protocol is expected to take about 3 min.

Gram staining includes three steps: staining with a water-soluble dye called crystal violet, decolorization with acetone, and counterstaining with carbol-fuchsin. The procedure for Gram-staining involves transferring a fresh bacterial colony from a petri dish onto a microscope glass slide, heat fixing the slide with the specimen by putting it on a heating plate at 70 to 80° C. The fixed smear was flooded with crystal violet solution and allowed to remain for 1 minute. The slide was rinsed gently with tap water and then flooded for one min in Gram's iodine solution (iodine and potassium iodide). The iodine solution was rinsed again and then the Gram's differentiator is applied, i.e. acetone, for one to five seconds to the point where no more stain runs off the slide. The acetone was rinsed and counterstained for 30 seconds with carbol-fuchsin then rinsed and dried the slide on absorbent paper and place in an upright position. The slide was microscopically examined for bacterial organisms using a light-microscope under oil-immersion. Gram positive bacteria stain deep violet to blue and gram negative bacteria stain pink to red (Klement, Rudolph and Sands, 1990).

3.2.4.2 Endospore staining

Endospore staining is one of the most useful diagnostic tools for detection and differentiation of bacteria in the microbiology laboratory. Bacterial ability to form endospores was tested by Schaeffer–Fulton endospore staining procedure as described by Sumbali and Mehrotra (2009) (Sumbali and Mehrotra, 2009). A bacteria colony was transferred from a petri dish onto a microscope glass slide and heat fixed. The slide with heat fixed smear was placed on wire gauze on a ring stand and covered with a piece of filter paper cut to fit the slide. The paper was soaked with malachite green and a handheld Bunsen burner was used to heat the slide till steam rising. The burner was alternately removed and the slide was reheated to maintain steaming for 3-5 minutes. To keep the paper moist, a drop or two of malachite green was added. The slide was washed thoroughly with tap water after removing the paper with a tweezer. 0.5% safranin was added for 45 seconds to counterstain the slide after draining. Finally, the slide was washed, blotted and microscopically examined under a 100X compound microscope. The spores will stain green and the most other micro organic bodies will stain red (Klement, Rudolph and Sands, 1990).

3.2.4.3 Bacterial cell morphology

The use of cell shape as a description and classification of bacterial species dates back to the advent of microbiology and has had an important role in rapid identification of bacterial. Bacteria cells are much simpler in structure than other organisms' cells due to lack of nucleus and the membrane-bound organelles. The function of cell wall is to give the cell a definite shape and structure; bacteria vary as shape, size and structure (Weidel and Pelzer, 1964; Lederberg, 1956; WEIBULL, 1953).

Bacterial cell morphology is determined with an optical microscope after Gram staining and can be classified according to three basic shapes: Coccus (spherical), Bacillus (rod-shaped), and Spiral (twisted), however pleomorphic bacteria can assume several shapes.

3.2.4.4 Endospore morphology

Endospores are tough, dormant and metabolically inert structures produced by gram positive bacteria species as a survival strategy in response to harsh environmental conditions (pH, nutrient limitations, desiccation, and temperature). They are highly resistant structures with a thick wall developed within the vegetative cells (hence the name, endo=inside) in a process called sporulation. Spore formation is useful for identifying bacteria to genus level. It is of particular importance to confirm that the isolate is endospore-former before attempting to identify to species level. Several bacterial genera can produce endospores; Bacillus and Clostridium are the two most prominent types of endospore-forming genera (Sneath *et al.*, 1986) (Endospore morphology can be seen on Fig (3-1). The morphology of endospores is determined by their location, shape and spore diameter compared with cell diameter.

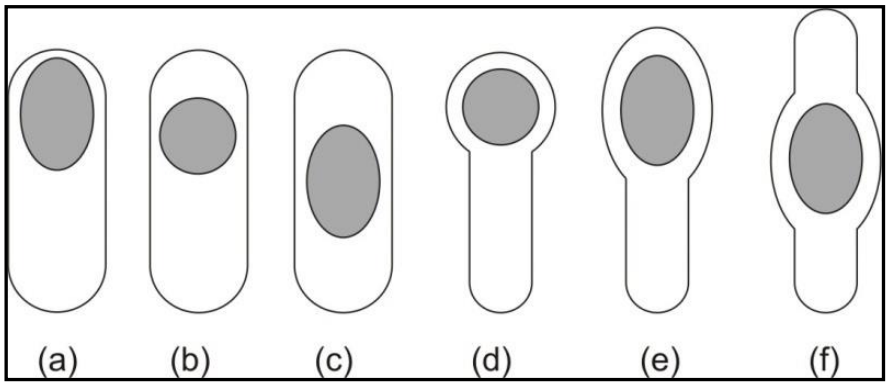

Figure 3-1 Morphology of endospores (Toth et al., 2013)

● Location: terminal (a, d, e), sub terminal (b), central (c, f).

● Shape: circular (b, d), ellipsoid (a, c, e, f).

● Spore diameter compared with cell diameter: non deforming (a, b, c), deforming (d, e, f).

3.2.4.5 Catalase test

The catalase test has been used for many years as one of the well-known techniques to differentiate the gram-positive organisms. It demonstrates the presence of catalase, an enzyme that capable of decomposing hydrogen peroxide to water and oxygen. Hydrogen peroxide (H_2O_2) is a reactive molecule, often used as a topical antiseptic to disinfect wound and the bubbles that is formed is caused by the evolution of Oxygen gas as shown in the reaction below(Taylor and Achanzar, 1972).

$2H_2O_2 \rightarrow 2H_2O+O_2$ (gas bubbles)

Organisms that use O^2 or can live in the presence of oxygen must have a way to dispose of the peroxide, because it is an oxidizing agent that can wreak devastation in cells. Producing catalase enzyme is one of those ways.

To perform the catalase test, a small amount of bacterial colony was added to a drop of 3% H_2O_2 on a dry glass slide by using a 1µL plastic loop and mixed. The rapid elaboration of oxygen (within 5-10 seconds) as evidenced by bubbling indicates the presence of the enzyme in a bacterial isolate, whereas the lack of catalase is evident by a lack of or weak bubble production. The catalase test should only perform on cultures that are no more than 24 hours old (Klement, Rudolph and Sands, 1990).

3.2.4.6 Oxidase test

Oxidase test is used in microbiology to determine the presence of bacterial cytochrome c oxidase enzyme. Oxidizing the substrate “tetramethyl-p- phenylenediamine dihydrochloride” to “indophenol” a dark purple coloured end product indicates the presence of the cytochrome c oxidase, while remaining the substrate colourless means the enzyme absence.

The Oxidase test was prepared by smearing a freshly grown colony in a filter paper soaked with a fresh aqueous solution of N,N,N’,N’tetramethyl-p-phenylenediamine dihydrochloride (Sigma). A colour change to deep blue or purple within 10-30 seconds is positive reaction, a delayed reaction or no reaction is negative. Bacterial genera characterized as oxidase positive

include Neisseria and Pseudomonas. Genera of the Enterobacteriaceae family are characterized as oxidase negative (ibid).

3.2.4.7 Selective isolation of spore forming microorganisms by the use of ethanol

The most effective techniques used for spore selection and eliminating vegetative cells were heat and ethanol treatment. Heat treatment or pasteurisation involves heating the bacteria suspension for specific times at temperatures that eliminate vegetative cells. A culture from the heated sample were streaked on a petri dish and incubated to observe potential growth of organisms. This technique is effective for isolating spore-forming bacterial and is very active for obtaining efficient spore germination. Several studies have confirmed the effectiveness of heat treatment in isolating the spore-forming species. The physio-chemical and physical conditions required to professionally isolate Bacillus species was generally studied by Emberger (1970) (Emberger, 1970). Heating treatment was the most appropriate method at a temperature ranged from 65 to 70 ^{o}C for 15 min. Another widely reported technique in the literature was to heat samples at 80^{o}C for 10 min (Claus and Berkeley, 1986). One of the limitations with this treatment is that it might be not suitable for all types of spore-formers, because of the dissimilarity of spore heat resistance among different bacteria strains. Different authors have utilised the endospores tolerance to other stress to isolate a spore-forming bacteria. It has been found concluded that Ethyl alcohol (ethanol) is toxic for vegetative cells but has a slight effect on bacterial spores. Comparing to heat treatment of 80 ^{o}C for 15 min, using 50% ethanol treatment for 1 h have shown similar effectiveness to isolate spore-forming bacteria from a mixed culture (Koransky, Allen and Dowell, 1978).

An aliquot of 10 mL of ready prepared Thioglycollate Broth and 10 mL of ethanol absolute were placed in falcon tubes, inoculate heavily with organisms, and rotated at 30-50 rpm for 1 hour at room temperature. The potential growth of spore-forming bacteria was observed by incubate a streaked Petri dish in appropriate conditions.

3.2.5 **Urease activity**

Urease activity is the microbial process of urea hydrolysis catalysed by urease enzymes, which can be obtained from a wide variety of microorganisms (Mobley and Hausinger, 1989). Urease (urea amidolydrolase: EC3.5.1.5) hydrolyses one mole of urea into one mole of carbon dioxide and two moles of ammonia as shown in the following reaction:

Reaction 1: $(NH_2)_2CO + H_2O \rightarrow CO_2 + 2NH$

The isolates were tested for their urease activity on a rapid test medium containing 364mg of KH_2PO_4, 380 mg of Na_2HPO_4, 8 g of urea, 40 gm of yeast extract and 20 ml of 0.02% phenol red added to 380 ml of distilled water, and the final pH was adjusted to 6.8 (Stuart, Van Stratum and Rustigian, 1945). This medium was filter to sterilise. 1.5 ml volumes of medium were pipette into small tubes and inoculate heavily with growth from a solid medium and the tubes were incubated at 37^{o}C in a water bath. Urease positive species produce a pink colour in 5-60 minutes as an indication for resolving the urease activity on the media. This reaction specifically represents the alkalising effect of ammonia produced upon urease activity on urea.

3.2.6 **Molecular identification of bacterial isolate**

Further identification of the isolate was performed using 16SrRNA gene sequencing. The DNA was isolated and the analysis of sequences was performed at Wellcome Trust Centre for Human Genetics, University of Oxford and the sequences were assembled using the SPAdes software at Brunel University London.

Genomic DNA was extracted and purified from overnight grown bacterial cultures with FastDNA Kit and the FastPrep Instrument. Marked orange-cap tubes containing Lysing Matrix A (from the kit) was filled with 1 ml of CLS-TC solution (from the kit) and inoculated with 200 ML of bacteria from the plate. The tubes were incubated at 37 ^{o}C incubator for 1 hour. After incubation, the red-cap tubes were processed in the FasrPrep Instrument at speed 6.0m/s for 40 sec and then centrifuged at 13000 rpm for 15 min at room temperature. Binding Matrix was thoroughly mixed to completely resuspend silics particles, and 750 Ml of Binding Matrix was dispensed in a fresh marked 2 ml tubes. 750 Ml from the resulting supernatant were carefully transferred to the Binding Matrix tubes and the content was thoroughly mixed by inverting several times and then incubated with agitation on rotating wheel for 5 minutes at room temperature. To pellet the Binding Matrix, the contents were centrifuged again at 13000 rpm for 10 sec at room temperature and the supernatant were discarded to preserve the pellet. The pellet was completely resuspended with 500 Ml of SEWS-M solution by tapping the tubes. The final solution was transferred to a SPIN Module (SPIN filter and Catch Tube). Twice 13000 rpm centrifugation for 1 minute was applied before discarding contents of Catch tube and replacing it with a recovery tube (1.5 ml Eppendorf). The DNA was eluted by gently resuspending Binding Matrix above the SPIN Filter in 100 Ml of DES or TE and the incubated for 5 minutes at 55 ^{o}C in a heat block. To bring eluted DNA into the Recovery

Tube, it was centrifuged at 13000 rpm for 1 minute and then the SPIN Filter was discarded. The next important steps of DNA extraction were RNAse treatment; it was begin by adding 2 Ml of RNase A (10mg/ml) and incubating at 37 ^{o}C for 30-45 minutes then adding 1/10 (10 Ml) volume of 3M Na-Ac pH 5.2 (20-25 Ml) and mixing thoroughly. 2.5 volumes (300Ml) of cold 100% ethanol was added and inverted several times to mix and stored at -20 ^{o}C for about 30 minutes and centrifuged at 13000 rpm for 30 min at room temperature. Pellets presence was inspected and the supernatant was carefully removed from the tubes and the pellets were washed by adding 500 Ml of cold 70% ethanol and inverting the tubes several times. The tubes were centrifuged again at 13000 rpm for 5 min at room temperature and the ethanol was removed carefully to avoid losing the pellets and left to dry at room temperature for 5 min. Finally, the DAN pellets were completely dissolved in 50-100 Ml TE buffer by gently tapping the tube and incubated in heat block at 55 ^{o}C for 5 min or room temperature for 1 hour. The DNA solution was stored at 4 ^{o}C for QA/AC and downstream applications, then -20 ^{o}C for long term storage before sending them to sequencing. In this experiment, however, it was difficult to obtain DNA from most of the strains. Out of 132 strains only 40 strains were sent to sequence and the rest were removed and discarded.

3.2.7 **Effect of pH on bacterial growth**

PH is a unit refers to negative logarithm of hydrogen ion concentration used to specify the acidity or alkalinity of a solution. Its measured value lies mostly in the range 0 to 14. In addition to its strong effects on microbial growth, environmental pH can also influence other activities and survival of the microorganisms because enzymes system of an organism function in a different pH ranges. Most of bacteria don't grow below pH 4 and generally prefer media of pH close to neutral (Dubey and Maheshwari, 2012). The most favourable pH for the growth of an organism is known as the optimum growth pH. The minimum growth pH is the lowest pH value that an organism can tolerate and the maximum growth pH is the highest pH.

This test was conducted to determine the optimum pH for bacteria growth. The pH of the growth medium (nutrient broth) was adjusted using either HCl or NaOH as appropriate from 4 to 12 at an interval of 1. A pH meter was used for pH measurements, in which the glass electrode was thoroughly rinsed with deionised water to avoid contamination and calibrated between measurements (Figure 3-2). The medium was prepared in a Duran glass bottles and sterilized in an autoclave at 121^{o}C for 15 minutes. Into each bottle, one ml of bacterial

suspension was inoculated and incubated at 37^{o}C in an incubator for 24hrs as shown in Figure 3-3. Growth was monitored by turbidity measurements (760nm) by a spectrophotometer and control bottle was used to calibrate the Optical Density (OD) to zero. The cell growth assay was performed with 3 replicates and a graph has been plotted between incubation time and pH.

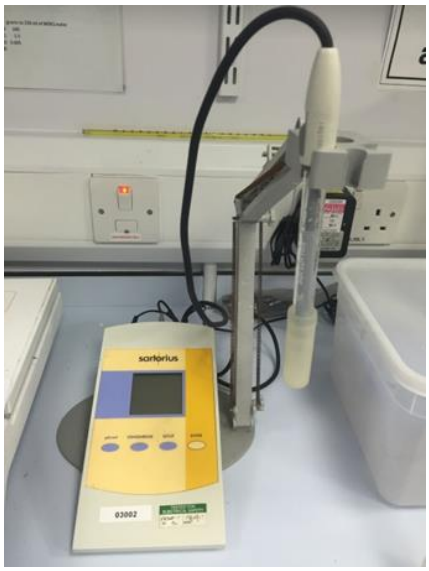

Figure 3-2 pH meter

Figure 3-3 pH Test of bacterial strains in Nutrient broth with different pH value from 4-12

3.2.8 **Spore preparation**

To obtain spores, bacterial colony was inoculated into modified sporulation nutrient agar media containing (per litre) 14g nutrient agar powder and grew at 37^{o}C for 48 hrs. The culture was observed occasionally during growth by phase-contrast microscopy. Cultures were harvested when the ratio of vegetative cells to spores became static (about 4 days). For all strains used in this study, cultures reached >99% spore content as determined by

microscopic visual approximation. The spore suspensions were centrifuged at 10,000xg for 10 min and the supernatant were carefully discarded then the pellet was washed several times with 200 ml of ice-cold distilled sterile water by centrifugation under the same conditions. These steps were repeated three to four times until more than 90% free spores were obtained under phase contrast microscopy examination. The spore suspension were kept at 4^{o}C and protected from light.

3.3 Preparation, characterization and viability of Bacillus Sphaericus embedded in an alginate-clay matrix beads

3.3.1 **Microorganism**

Bacillus sphearicus 57 and 58 were inoculated into modified sporulation nutrient agar medium and incubated at 37^{o}C. The culture was observed occasionally during growth by phase-contrast microscopy. Cultures were harvested when the ratio of vegetative cells to spores became static (about 4 days). Spores cultivation was done by collecting the culture from the petri plates (Figure 3-4 and 3-5) and suspending in a saline solution. The spore suspensions were centrifuged at 10,000xg for 10 min and the supernatant were carefully discarded then the pellet was washed several times with 200ml of ice-cold distilled sterile water by centrifugation under the same conditions. These steps were repeated three to four time until more than 90% of culture was free spores under phase contrast microscopy examination. The spore suspension were kept at 4^{o}C and protected from light.

Figure 3-4 Bacillus Sphearicus 57 inoculated into modified sporulation nutrient agar medium

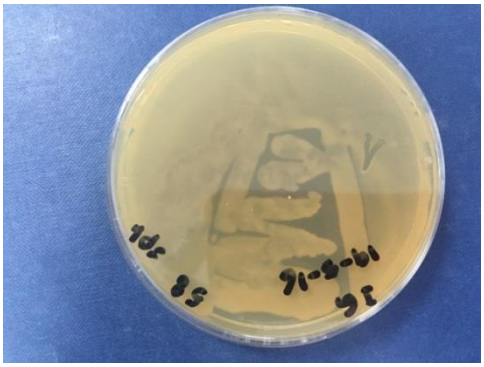

Figure 3-5 Bacillus Sphearicus 58 inoculated into modified sporulation nutrient agar medium

3.3.2 **Pyrophyllite**

Pyrophyllite is an alumino-silicate with 2:1 layered dioctahedral structure. It is a crystalline structure with chemical composition of Al_2O_3 28.35%, SiO_2 66.65%, and H_2O 5.0% and its theoretical formula as Al_2 $[Si_4O_{10}]$ $(OH)_2$ (Li *et al.*, 2014). Its layered structure consists of an octahedrally coordinated Al ions sandwiched between two linked sheets of SiO_4 tetrahedra.

Pyrophyllite clay has been widely used in various industries, particularly in the manufacture of refractories, ceramics, fiber glasses, paints, rubbers, paper, porous materials and insulating materials. And most of these applications are due to its good technological properties following thermal treatment (Virta, 2005; Robertson, 1973). Characterization and chemical structure of the pyrophyllite were done by FTIR and TGA analysis.

3.3.3 **Sodium alginates**

Sodium alginate is the sodium salt form that derived from alginic acid. It is a natural polysaccharide extracted from brown seaweeds. The linear polymers of β-(1→4)-D-mannuronic (M) and α-L-guluronic (G) acids are the main components of alginate which different from each other by their amount and linear arrangements (Nadeem and Datta, 2014). With the existence of the most divalent cations such as Ca^{2+}, Sr^{2+} or Zn^{2+}, thermally irreversible gel can be obtained as a result of the mechanical and gelling properties of sodium alginates. Therefore, it is extensively used as a carrier matrix for many controlled release dosage and the preparation of beads. Encapsulation of living organisms is another use of alginate as it is biocompatibile, biodegradabile, non-toxic and hydrophilic polymer.

3.3.4 **Beads preparation**

Production of Alginate-fly ash composite beads as a bacterial spore's capsules was carried using a two-step. Sodium alginate and pyrophyllite clay were added in the first step; into 1 Liter of sterilised distilled water as 10 to100 gm (Fravel *et al.*, 1985).

In order to mix well, 180 mililiters of the mixture was transferred into sterile deep dish based on a coupling (Figure 3-7). To incorporate the bacterial spores, 20ml of biocontrol agent was added to the mixture containing a spore suspension of either Bacillus Sphaericus 57 or Sphaericus 58 in 1.5×10^{-1} M KH_2PO_4 + 8.2×10^{-2} M K_2HPO^4 buffered 0.1 % saline (pH 6.8). In the second step, the final suspension was drop wise while stirring in a constant rate through pasture pippette with a 1 mm diameter orifice into a solution of 0.25 M $CaCl_2$. As soon as sodium alginate-pyrophylite hits the calcium chloride solution, beads are formed because the sodium ions (Na^+) are exchanged with calcium ions (Ca^{2+}) and the polymers become crosslinked (Figure 3-6). The final concentration of added spores was 10^8/ml. A laminar air flow hood was used to dry the pellets overnight.

Figure 3-6 Calcium alginate-Pyrax clay beads

Figure 3-7 Calcium alginate-Pyrax clay beads preparation apparatus

3.3.5 **Viability of the encapsulated spores**

The viability of spores' populations in the encapsulated formulation was determined in seven stages; before introducing the organism to the calcium alginate salt, immediately after

exposure to the calcium salt (pellet formation), at 24 hours (pellets first dry), and at 2, 4, 8, and 12 weeks after pellet formation. This test was taken place in order to investigate whether the spores inside the capsules were still viable. Pellets were stored under 4^{o}C in screw-capped jars. A mixture of 8.7×10^{-2} M KH_2PO_4 and 3.0×10^{-2} M Na_2HPO_4 (pH 7.7) were used to disintegrate the pellet as it is insoluble in water and then tested by dilution plating. Serial dilutions of Bacillus suspension were made, and 0.1 ml aliquots were plated on a Nutrient media and incubated at 30± 2^{o}C. Treatment of Bacillus were replicated once and repeated with five plates each at 10^{-1}, 10^{-2}, 10^{-3}, and 10^{-4} dilutions. The experimentation was done four times (Fravel *et al.*, 1985). In different spheres of microbiology, the most widely used and accepted method for estimation of colony forming units (cfu) is the serial dilution plating on a nutrient medium to monitor cultivable bacteria and yeasts (Thomas *et al.*, 2015).

3.3.6 **Swelling properties**

The ability to imbibe water and rehydrate when exposed to an aqueous fluid is one of the main characteristics of alginate beads in the dry state. These properties help alginate undergo primarily due to the hydration of the hydrophilic groups of polymers. If alginate beads exposed to water, an important swelling takes place as a result of water molecules penetration into the particles blocking the pores among the polymeric chains without causing disintegration. However, subjecting to other fluid with different pH could change the swelling performance of the alginate beads (Segale *et al.*, 2016).

Therefore, the swelling characteristics of Ca-alginate-Pyrax clay beads were studied and performed in filtered cement slurry (FC) with pH 12.2, tab water with a pH of 8.2 and in de-ionized water (DW) with pH of 7.

The experiments were repeated three times (n = 3). A suspension with a concentration of 1/10 cement/water was prepared as cement slurry in this experiment. The cement slurry was filtered after 1h of mixing to remove the undissolved particles and the pH of the suspension was around 12.5 to simulate the severe condition of concrete. Three grams of beads were weighted in a plastic beaker as the dry weight W_p. Three different solutions were made from adding tab water, de-ionize water and cement filtrate into alginate beads and weighed again as W_0. To prevent water evaporation, the beaker has to be securely sealed until beads moisture equilibrium is reached after 16hrs. A pre saturated filter paper in tab, de-ionized water and cement slurry was used to separate beads from its suspension. The solution drained through the filter paper was weighed as W_1. The swelling capacity of beads was determined

by divided the amount of water absorbed (g) by the dry weight of the beads (g); as the following equation

$S = (W_0 - W_1)/W_h$

Where

S is the swelling ratio [g/g],

W_0 is the initial weight of tab water, di-ionized water or filtered cement slurry [g],

W_1 is the weight of water or cement filtrate [g] drainainging into the burette and

W_h is the weight of dry alginate beads.

To study the re-swelling properties, the wet beads from the first swelling test were left to dry naturally at room temperature before subjecting to the second and third swelling (Wang *et al.*, 2014a).

3.3.7 **Characterization of the beads**

3.3.7.1 The fourier transforms infrared spectroscopy analysis (FTIR):

Fourier Transform Infrared Spectroscopy (FTIR) is an effective analytical technique to identify the presence of certain functional groups in a molecule. It produces a unique collection of absorption bands to detect the presence of specific impurities or to confirm the identity of a pure compound. Also, it offers a profile of the sample that can be used to screen and scan samples for many different constituents. Among all other analytical techniques, quantitative infrared spectroscopy can provide certain advantages. The benefit of this approach is that it can be used to analyse one component of a mixture, particularly when the components in the mixture are very similar in chemical structure or have nearly identical physical properties. In addition, the FT-IR requires a small amount of sample for the analysis and it can be non-destructive method of investigation. In the context of infrared spectroscopy, wavelength is measured in "wavenumbers", which have the unit cm^{-1} and the electromagnetic radiation covers the wavenumbers between 13,300 cm^{-1} and 3.3 cm^{-1}. The infrared spectrum can be approximately divided into three regions, mid-infrared spectrum (4000–400 cm^{-1}), the near-infrared region (13000–4000 cm^{-1}), and the far-infrared region which is defined as the region between 400 and 100 cm^{-1}. In general it may determine the nature of the group frequency depending on the region where it is located.

3.3.7.2 Thermogravimetric analysis

Recently, thermal analysis has become predominant, especially for polymers, plastics and fibres. Details about the temperature dependent physical properties of materials can be obtained by thermal analysis methods. Yet, the chemical changes associated with changes in temperature have not always been given by using standard thermal analysis techniques (Meurens and Yan, 2002; McClure and Stanfield, 2002). Therefore, the sodium alginate, Pyrophyllite, calcium alginate beads and calcium alginate-pyrax beads were thermally analysed using the Thermogravimetric analysis method. DSC-TGA Standard /SDT Q600 V8.3 Build 101 instrument was used in this analysis in a temperature from 24.28- 895.14^{o}C using DSC Heatflow method, in Air.

3.3.7.3 Scanning electron microscopy analysis

The surface morphology of calcium alginate beads obtained from sodium alginate, pyrophyllite clay and calcium chloride were studied by using a scanning electron microscope (an ultra-high performance field emission scanning electron microscope Zeiss Supra 35VP 20kV). To observe the beads under scanning electron microscope, beads were mounted onto specimen holders, called stubs that appropriate for the particular scanning. The stub was then gold coated with sputter module in a vacuum evaporator in an argon atmosphere included in a cathode gas.

3.4 Bacterial mortar preparation and characterisation

3.4.1 **Ordinary Portland cement (OPC)**

General purposes Ordinary Portland Cement (OPC) CEM I 42.5 N (CEMEX, Rugby, UK) complying with BS EN 197-1:2011 was used in preparation of cement mortar specimens. The chemical composition of this cement is presented in Table 3-1.

Table 3-1 Chemical composition of cement

Oxide	Oxide Composition (wt %)
SiO_2	19.7
Al_2O_3	4.8
Fe_2O_3	3.1
CaO	63.6
MgO	1.2
SO_3	3.6
Cl^-	0.1
Free CaO	2.3
Na2Oeq [1]	0.7
LOI [2]	2.7

[1] Na2O equivalent; [2] Loss on ignition.

3.4.2 **Sand**

Locally available sharp sand was purchased from Crescent supplier, Uxbridge, used in preparation of test specimens. The maximum size of sand was 1mm.

3.4.3 **Nutrient and deposition agents**

Yeast extract and urea were added as nutrients for bacteria. The total dosage of nutrients and deposition agents added to mortar mixture prepared in Chapter 7-9 was 3% of cement weight. Therefore, the dosage of urea added to the mortar mixture was 1.08% by weight of cement, while yeast extract was added with only 0.48% of cement weight. Additionally, calcium acetate hydrate ($Ca(C_2H_3O_2)_2$) were used as deposition agents in this study with addition ratio of 1.44 % of cement weight.

3.4.4 **Sample preparation**

A standard mortar mixer with a speed of 140 ± 5 rpm was used to synthesize each mixture at room temperature of 20 ± 2°C. All mixed mortars were casted in the 40mm x 40mm x 160mm oiled-moulds. The moulds were half-filled and then compacted on vibration table for

30 seconds. The mortar was filled up to the full level of the mould and vibrated for another 30 seconds.

3.4.5 **Experimental equipment**

It is noted that all of testing procedures and equipment used were verified under safety control, as well as laboratory and workshop areas. As the mortar mixtures were prepared in a small batch, a small mixer was used in the mixing process. An even film of releasing oil was applied in the steel moulds before the mortar was poured to avoid sticking and to facilitate demoulding the specimen without damage. After that, the mixtures were casted in polystyrene 40mmx40mmx160mm prismatic mould. A vibration table was also used to vibrate the casted specimen to ensure that the extra water and air bubbles trapped in the mortar are forced away to the surface. A digital scale (min. 600 g. and max. 12 kg.) was used to weigh the basic mortar components (cement and sand) and the chemical reagents were weighed on an analytical balance (0.01g precision). Plastic sheets were used to cover the samples before setting to reduce evaporation. All mortar specimens were placed in water curing tank at 20 ^{o}C before testing or applying the exposure regimes. An electrical convection oven (ELE) was employed for drying the samples in the wet-dry exposure. Freezer was also used to conduct freezing at a temperature of -15 ^{o}C for 7 hrs during the freeze-thaw exposure. A wire shelving unit was placed outside the lab with the mortar specimens to provide full weathering exposure.

3.4.6 **Testing**

3.4.6.1 Flexural strength

To determine the flexural strength of the cement mortar, a prismatic sample (40mm x 40mm x 160mm) was used. The samples were placed centrally between the two steel supporting rollers of the flexure device of Instron universal testing machine (UTM) and the third steel loading roller with a constant rate of (50 ± 10) kN/minute as shown in Figure 3-8. The test was carried out according to British Standard BS EN 196-1:2016 and results were plotted in a stress-strain diagram and automatically calculated and saved by Instron software.

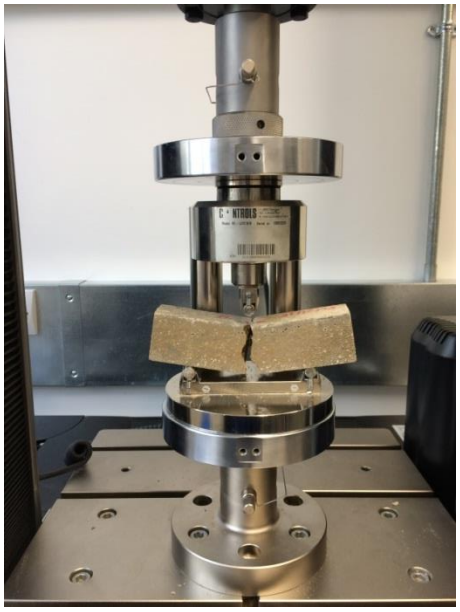

Figure 3-8 Instron Universal Machine (UTM) for flexural strength test

3.4.6.2 Compressive strength

The two cubic halves from the broken prismatic specimen of the flexural strength test were used to determine the compressive strength of the cement mortar. According to BS EN 196-1:2016, the specimens were positioned on the compressive test rig of Instron universal testing machine (UTM) using 144 kN/minute loading rate as shown in Figure 3-9. Each sample is centred between the two parallel discs. A report of calculated test results was automatically saved by Instron software. Split pieces were reserved for mechanism test of EDAX and SEM analysis later.

Figure 3-9 Instron Universal Machine (UTM) for compressive strength test

3.4.7 **Microstructural characterization (SEM and EDAX)**

SEM is fundamentally a higher magnification imaging using to view fine structural details in cross-section of sample which uses an absorbed scanned electron beam to create images of the sample, both top-down and cross-sections.

The samples were observed under an ultra-high performance field emission scanning electron microscope Zeiss Supra 35VP 20kV to investigate its microstructure. Fragmented pieces kept from the compressive test were used for microstructural characterization. In order to discuss and interpret the mechanical properties that can change due to bacterial incorporation or exposure conditions based on consistent results, SEM analysis was performed with the fragments obtained from the compressive strength test. To prepare the samples, a small piece was kept in a vacuum chamber for 24 hours to dry prior to test. Sample preparation for SEM investigation was kept to minimum because it has been stated that at some specific cases, such as examination of some deposits or specific areas of interest in a sample, which could be lost by subsequent sample preparation, minimum sample preparation may be preferable (Jana, 2006). It has been proved that the fractured surfaces and the sawn unpolished samples is the best for many SEM investigations compared to other sample preparation process. Fine crystal formations and the cracking patterns that cannot be seen on thin sections can be disclosed in the surfaces of such samples. In addition to that, incorrect diagnosis of the damage mechanism may have caused by introducing new elements to the studied material from the impregnation materials and concrete constituents soluble in the preparation media can be removed by the preparation procedures (Marusin, 1995).

As the cement mortar sample is non-conductive, the SEM observation will be a complicated process. Therefore, the samples have to be coated with a thin layer of gold to avoid problems of charging. Special glue was used to fix the samples on small cylinders. The elemental composition of the analysed samples was characterised using an Energy Dispersive X-ray Analysis (EDXA) equipped with SEM. The compositions of the elements and oxides in the sample were expressed in terms of weight percentage.

Chapter 4: Investigation of Suitable Microbial Sources of Calcium Carbonate

4.1 Introduction

Biomineralization is a dynamic biological process in which mineral precipitation takes place as a consequence of the reaction between metabolic products discharged by microbes and ions or compounds in the environment (Frankel and Bazylinski, 2003). Two different pathways, namely: biologically controlled or induced, through which bio mineral, chiefly calcium carbonate precipitated, have been characterized (Lowenstein and Weiner, 1989).

In recent times, microbiologically induced calcite precipitation has been recommended as an unconventional repairing method for micro-cracks healing in concrete. This microbial self-healing technique is more durable, environmentally-friendly and cost effective compared to other techniques. It has been established that urease positive bacteria is the most suitable microorganism to induce the precipitation of calcium carbonate ($CaCO_3$) throughout its urease activity. Urease is an enzyme produced by many different bacteria, which are able to catalyse the hydrolysis of urea into CO_2 and ammonia. During this reaction, both the pH and calcite precipitation will increase in the bacterial medium (Stocks-Fischer, Galinat and Bang, 1999).

The objective of this chapter is to select an organism with best calcite production capacity for potential source of calcite to be used in the bacteria based self-healing concrete. The isolation and identification of calcite precipitating bacteria have been carried out and the suitability of these bacteria for use in concrete has been investigated.

4.2 Materials and methods

4.2.1 **Sample collection**

The 132 different bacterial samples were collected from four natural environments: 57 from soils, 9 from pond water, 20 from gypsum rocks 7 from sharp sand, 2 air contamination and 37 from concrete. Soil samples were drilled from different locations around London using a borer to gather 4-6 samples for each site. The site for individual samples was separated by 10 meters from each other. One gram of soil, water, gypsum rocks or concrete powder was placed in a 50mL sterile falcon tubes and kept at 4° C until assayed. Each falcon tube was labelled according to the site of isolation, and time and date of the collection. Concrete and

gypsum rock samples were collected by take 3 to 6 pea-sized samples of the material. The samples were smashed with a hammer inside a sterile plastic bag, then transferred to the "powder" and stored in a 50 mL falcon tube. The falcon tubes were labelled with the site of isolation, time and date of collection and type of material / source.

4.2.2 **Cultivation media and bacteria culturing**

Two types of cultivation media were used in this study, B4 media and nutrient agar medium. B4 is a growth media used for isolation of bacterial species. To prepare a 500 mL of this media, 1g calcium acetate, 1.6g yeast extract, 4g glucose and 6g agar were added to Milli-Q water and autoclaved for 121°C for 15 minutes, or according to the autoclave's specifications. After removing the solution from the autoclave, the agar solution was allowed to cool to 50°C. Nutrient agar medium was used for supporting growth of the organisms. This media was prepared using yeast extract (2 g/L), meat extract (1 g/L), peptone (5 g/L), sodium chloride (5 g/L) and agar (15 g/L) following the same steps used to prepare the B4 media. All the ingredients of both media were purchased from Fisher Scientific; UK. Subsequent cultures were streaked onto agar plates with the same selective pressure to isolate single colonies. The subsequent isolates were re-grown in the same media and observed through light microscopy. Growth was checked regularly and quantified by light microscopic analysis.

4.2.3 **Isolation**

The samples were diluted properly in a PBST solution (PBST is prepared by dissolving 1 phosphate buffered saline tablet in 200 mL of MilliQ water in a 250 mL Duran bottle, and adding 2 mL of Tween 20). B4 media was used for the growth of cultures. The cultures were streaked in the medium through sterilized loop. The plates were incubated for 24 hrs at 30°C. The isolated colonies were further purified and periodically checked from other bacteria contamination by streaking it again in the B4 agar plates.

4.2.4 **Identification of bacterial species**

4.2.4.1 Gram staining

To perform a gram stain, a fresh bacterial colony was transferred from a petri dish onto a microscope glass slide. The slide with bacterial smear was heat fix on a heating plate at 70 to 80° C. The smear was stained by flooding the slide with crystal violet dye and letting it stand for 1 minute. The slide was slightly tilted and gently rinsed with tap water using a wash bottle. Then, the smear was gently flooded with Gram's iodine solution for one min. This

solution was added as a mordant to form a complex between the crystal violet and iodine in order to fix the dye. After rinsing the slide with a tap water, the smear will turn into a purple circle. To decolourise the smear, acetone were applied drop by drop for 1 to 5 seconds until the stain runs almost clear. The acetone was rinsed immediately with water and then counterstained for 30 seconds with carbol-fuchsin. Finally, the slide was gently rinsed with tap water and dried with absorbent paper and place in an upright position. The smear was examined using a light-microscope under oil-immersion.

4.2.4.2 Endospore staining

Endospore stain is a differential stain mainly used to distinguish between vegetative cells and endospores. The first step in the endospore staining procedure is to smear the bacterial sample at the centre of a clean microscope slide and to allow the slide to dry and heat fix. After that, the slide was covered with a piece of filter paper cut to fit the slide and saturated with malachite green solution as a primary stain. This solution will stain both vegetative cells and endospores. To help the malachite green penetrate the endospore, the slide was gently heated until it starts evaporating and reheated to maintain steaming for 3-5 minutes. The slide was then allowed to cool for 1 minute and then washed with tap water to decolorize the cells. As malachite green does not stick well to the cell wall, it washes out of cells, but not out of the endospores. The cells which have been decolorized were counterstained with a 0.5% safranin for 45 seconds. As a final step, the slide was washed, dried and observed under microscope. The vegetative cells will stain red and the endospores will be dark green.

4.2.4.3 Bacterial cell morphology

Bacterial cell morphology was used to describe the shape of an individual cell of bacteria. As a single-cell organism, bacteria come in a variety of morphologies, from spherical to spiral to rod shaped. The cell wall is the main element responsible for bacterial cell shape. An optical microscope was used to determine the bacterial cell morphology after gram staining test. Cells that have a spherical shape are called cocci (singular coccus) while, the small rods-shaped bacteria are called bacilli (singular bacillus).

4.2.4.4 Catalase test

Microorganisms that live in oxygenated environments usually have an enzyme called catalase. The function of this enzyme is to counteract the hydrogen peroxide (the toxic forms of oxygen metabolites). The response to hydrogen peroxide was observed with concentration

of 3%. A fresh dilution of H_2O_2 was made with deionised water. To test the ability of certain bacteria to produce catalase enzyme, a small amount of bacterial colony was mixed into hydrogen peroxide solution on a dry glass slide by using 1 µL plastic loop. The appearance of the bubbles elaborated over the slide indicated the presence of the enzyme in a bacterial isolates (i.e., catalase-positive). The absence or presence of trapped bubbles is an indication of lack of catalase enzyme (catalase-negative). The catalase test in this study performed on cultures that were recently isolated from different samples, less than 24 hours old at the time of testing.

4.2.4.5 Oxidase test

The test has been performed on a total of 132 strains. The organisms were grown in agar medium at 30^{o}C for 24 hours or until individual colonies were obtained. A freshly grown colony was harvested from the medium with a sterile plastic loop and smeared in a filter-paper saturated with aqueous solution of N, N, N', N' tetramethyl-p-phenylenediamine dihydrochloride solution (purchased from Sigma-Aldrich UK). If the colour of the paper changes to deep blue or purple within 10-30 seconds, this indicates a positive oxidase result. The negative reaction is indicated by the lack of colouration or by late colour development. All bacterial colonies used in this test were prepared from cultures grown under the same growing and nutritional conditions and collected at the same time. The test was performed in triplicate.

4.2.4.6 Selective isolation of spore forming microorganisms by the use of ethanol

An aliquot of 10 mL of ready prepared Thioglycollate Broth and 10 mL of ethanol absolute were placed in falcon tubes, inoculate heavily with organisms, and rotated at 30-50 rpm for 1 hour at room temperature. The potential growth of spore-forming bacteria was observed by incubate a streaked Petri dish in appropriate conditions.

4.2.5 **Urease activity**

The urease activity test is used to determine the ability of an organism to hydrolysed urea to ammonia and carbon dioxide, through the production of urease enzyme. The test medium was prepared by dissolving 364mg of KH_2PO_4, 380mg of Na_2HPO_4, 8g of urea, 40gm of yeast extract and 20ml of 0.02% phenol red in 380ml of distilled water. The resulting medium was filter-sterilised and the final pH was adjusted to 6.8. The medium was distributed into small tubes (1.5ml) and inoculated with colonies from an overnight culture. One tube was left

without inoculation as a control to check the test. The tubes were incubated at 37^{o}C in a water bath and examined for colour change. Urease positive organisms produce an intense magenta to bright pink colour in 5-60 minutes as an indication for resolving the urease activity on the media. Some organism may take several days to produce urease, therefore, it consider as weakly positive. If the organism does not produce urease, no change in the original colour of the medium can be detected and the organism known as urease negative.

4.2.6 **Molecular identification of bacterial isolate**

The DNA was isolated from bacterial cell using the FastDNA Kit and the FastPrep Instrument. Genomic DNA was extracted and purified from overnight grown bacterial cultures. 1 mL of CLS-TC solution (from the kit) was added to a tube containing Lysing Matrix A (from the kit) and inoculated with 200 mL of bacteria that were collected from the petri. The components of Lysis buffer CLS-TC are listed in the Table 4-1. The tubes were incubated at 37^{o}C incubator for 1 hour, processed in the FasrPrep Instrument at speed 6.0m/s for 40sec and centrifuged at 13000 rpm for 15min at room temperature. 750 mL from the resulting supernatant were carefully transferred to a fresh marked 2 mL tubes filled with750 mL of Binding Matrix. The components of the Binding Matrix are listed in Table 4-2. The tube contents were centrifuged at 13000 rpm for 10sec at room temperature to pellet the Binding Matrix. The pellet was completely resuspended with 500ml of SEWS-M solution. Table 4-3 includes the constituents of the concentrated SEWS-M solution. The final suspension was centrifuged two times after transferring to a SPIN Module (SPIN filter and Catch Tube). The contents of the Catch tube were discarded and the tube was replaced with a recovery tube (1.5ml Eppendorf). To elute the DNA, a Binding Matrix was gently resuspended in 100ml of DES solution and then incubated for 5 minutes at 55^{o}C in a heat block. The content of the SPIN Filter was centrifuged at 13000 rpm for 1minute to bring the eluted DNA into the recovery tube. The DES solution components are listed in Table 4-4.

To finally extract the DNA, the RNAse treatment needs to be applied. This treatment starts with adding 2ml of RNase A (10mg/ml) to the recovery tubes and incubating them at 37^{o}C for 30-45 minutes then adding 1/10 (10ml) volume of 3M Na-Ac pH 5.2 (20-25ml) and mixing thoroughly. After that, 2.5 volumes (300ml) of cold 100% ethanol was added and stored at -20^{o}C for about 30 minutes and centrifuged at 13000 rpm for 30 min at room temperature. The resulting pellets were washed by adding 500ml of cold 70% ethanol and inverting the tubes several times. The tubes were centrifuged again at 13000 rpm for 5 min at room temperature

and the ethanol was removed carefully to avoid losing the pellets and left to dry at room temperature for 5 min. Finally, the DAN pellets were completely dissolved in 50-100ml TE buffer by gently tapping the tube and incubated in heat block at 55^{o}C for 5 min or room temperature for 1 hour. The DNA solution was stored at 4^{o}C for QA/AC and downstream applications, then -20^{o}C for long term storage before sending them to sequencing. In this experiment, however, it was difficult to obtain DNA from most of the strains. Out of 132 strains only 40 strains were sent to sequence and the rest were removed and discarded. The analysis of sequences was performed at Wellcome Trust Centre for Human Genetics, University of Oxford and the sequences were assembled using the SPAdes software at Brunel University London.

Table 4-1 Lysis buffer CLS-TC components

Lysis buffer CLS-TC components	PERCENT
Urea	50%
Water, Ultra-pure	40-50%
Sodium Phosphate Monobasic Anhydrous	5-10%
Sodium Dodecyl Sulfate	1-5%
DL-Dithiothreitol	1-5%

Table 4-2 Binding matrix components

Binding Matrix Components	%
Guanidine Thiocyanate	60-70
Water	10-20
MP Silica	10-20

Table 4-3 Concentrated SEWS-M components

Concentrated SEWS-M components	%
Water, Ultra-pure	80-90
Tris Hydrochloride	10-20
Tris Base	<1.0

Table 4-4 DES solution components

DES solution components	%
Water, Ultra-pure	90-100

4.2.7 **Effect of pH on bacterial growth**

Growth curve for each bacterial species at different pH level was generated based on the changes in the OD due to bacterial growth over 24hrs. The pH of the growth medium (nutrient broth) was adjusted using either HCl or NaOH from 4 to 12 at an interval of 1. The medium was prepared in a Duran glass bottles and sterilized in an autoclave at 121^{o}C for 15 minutes. The medium in each bottle was inoculated with 1ml of bacterial suspension and incubated at 37^{o}C for 24hrs. Growth was monitored by turbidity measurements (760nm) by a spectrophotometer. A control medium bottle was used to calibrate the Optical Density (OD) to zero. The cell growth assay was performed with 3 replicates and a graph has been plotted between incubation time and pH.

4.2.8 **Spore preparation**

A modified sporulation nutrient agar medium containing (per 1 litre) 14g nutrient agar powder was used to obtain spores. Bacterial colony was inoculated into medium and cultivated at 37^{o}C for 48 hrs. The plates were monitored from time to time for spore formation under microscope. The ratio of vegetative cells to spores was static after 4 days. All spore preparations were purified by repeated centrifugation and water washing. First, bacterial cultures were suspended in a saline solution and centrifuged at 10,000xg for 10 min and then the supernatant were carefully discarded. Under the same centrifugation conditions, the resulting pellets were washed several times with 200ml of ice-cold distilled sterile water. This procedure was repeated until more than 90% free spores were obtained under phase-contrast microscopy examination. The spore suspension were stored at 4^{o}C and well protected from light until use.

4.3 Results and discussion

4.3.1 **Bacterial morphology**

Based on the appearance of the colony on cellular morphological traits (shape and presence of spherical bodies), 132 bacterial strains were selected (Table 4-5). Cultures growing on B4 media showed that some of the strains gave faster growth (within 24 h), while others

developed colonies within 72h of incubation at 30^{o}C. It is evident that after incubation, two different types of colonies were observed on B4 media. The strains that developed roundish white to beige colonies, and possessed a shiny and smooth surface with even edges that tend to spread even further (>2 mm) over time, are more likely to be Bacillus. Therefore, the rounds, light yellow colonies with rough surfaces were discarded. Morphology, microscopic features and growth characters of 132 strains of bacillus spp. are presented in Table 4-5. Under light microscope, the appearance of the organisms varied from short to long rods arranged in single, diplobacilli (in V or L shape) or short or long chains. Based on the morphological and physiological characteristics, these strains belonged to the Bacillus genus. Microscopic observations show that micro-organisms were gram positive rods and some of them were spore forming.

Table 4-5 Bacterial Cell Morphology[1]

Strain Name	Site of Isolation	Date of Isolation	Cell Morphology	Endospore Morphology	Oxidase Test	Catalase reaction to 3.0% H2O2
IG1	Brunel forest 1(soil)*	04/08/2015	Bacillus	Terminal, Circular	-	++
IG2	Brunel forest1(soil)*	04/08/2015	Bacillus	Terminal, Circular	-	++
IG3	Brunel forest 1(soil)*	04/08/2015	Bacillus	Terminal, Circular	-	++
IG4	Cowley, Uxbridge (soil)	12/08/2015	Coccus	No spore	-	++
IG5	Brunel pond(water)	11/08/2015	Bacillus	Sub-terminal, circular	-	-
IG6	Brunel pond(water)	11/08/2015	Coccus	no spore	-	++
IG7	Brunel pond(water)	11/08/2015	Coccus	no spore	-	++
IG8	Cowley, Uxbridge (soil)	12/08/2015	Coccus	no spore	-	-
IG9	Cowley, Uxbridge (soil)	12/08/2015	Bacillus	Sub-terminal, circular	-	++
IG10	Cowley,Uxbridge (soil)	12/08/2015	Coccus	no spore	-	-
IG11	Cowley, Uxbridge (soil)	12/08/2015	Coccus	not sure	-	+
IG12	Cowley,Uxbridge	12/08/2015	Coccus	no spore	-	+

	(soil)					
IG13	Cowley, Uxbridge (soil)	12/08/2015	Bacillus	Non deforming spore	-	++
IG14	Cowley,Uxbridge (soil)	12/08/2015	Bacillus	not sure	-	++
IG15	Cowley,Uxbridge (soil)	12/08/2015	Bacillus	not sure	+	++
IG16	Brunel pond(water)	11/08/2015	Bacillus	Terminal, Circular	Uncertain	++
IG17	Brunel pond(water)	11/08/2015	Bacillus	Terminal, Circular	-	++
IG18	Brunel pond(water)	11/08/2015	Bacillus	Terminal, Circular	-	++
IG19	Brunel pond(water)	11/08/2015	Bacillus	Terminal, Circular	+	++
IG20	Brunel pond(water)	11/08/2015	Bacillus	Terminal, Circular	Uncertain	++
IG21	Brunel pond(water)	11/08/2015	Bacillus	Terminal, Circular	-	++
IG22	Cambridge (soil)	20/10/2015	Bacillus	No spore	-	++
IG23	Cambridge (soil)	20/10/2015	Bacillus	No spore	Uncertain	+
IG24	Cambridge (soil)	20/10/2015	Bacillus	Terminal, Circular	-	++
IG25	Cambridge (soil)	15/10/2015	Coccus	No spore	-	++
IG26	Cambridge (soil)	12/10/2015	Coccus	No spore	-	++
IG27	Cambridge (soil)	15/10/2015	Coccus	No spore	-	++
IG28	Cambridge (soil)	12/10/2015	Bacillus	Terminal, Circular	-	++
IG29	Acton (soil)	15/10/2015	Bacillus	Terminal, Circular	+	++
IG30	Acton (soil)	12/10/2015	Coccus	Non deforming spore	+	++
IG31	Old concrete**	15/10/2015	Bacillus	Terminal, Circular	-	-
IG32	Acton (soil)	15/10/2015	Coccus	Non deforming spore	-	+
IG33	Acton (soil)	12/10/2015	Bacillus	Terminal,	-	+

				Circular		
IG34	Acton (soil)	15/10/2015	Coccus	Non deforming spore	-	++
IG35	Acton (soil)	12/10/2015	Coccus	Non deforming spore	-	++
IG36	Acton (soil)	14/10/2015	Coccus	No spore	-	++
IG37	Cambridge (soil)	14/10/2015	Bacillus	Terminal, Circular	+	++
IG38	Cambridge (soil)	20/10/2015	Coccus	No spore	-	++
IG39	Old concrete**	16/10/2015	Bacillus	Sub-terminal, circular	+	++
IG40	Old concrete**	16/10/2015	Coccus	Non deforming spore	+	++
IG41	Old concrete**	16/10/2015	Bacillus	Terminal, Circular	+	++
IG42	Old concrete**	16/10/2015	Bacillus	Non deforming spore	-	++
IG43	Old concrete**	16/10/2015	Bacillus	Non deforming spore	+	++
IG44	Old concrete**	16/10/2015	Bacillus	Non deforming spore	+	++
IG45	Old concrete**	16/10/2015	Bacillus	Non deforming spore	-	++
IG46	Old concrete**	16/10/2015	Bacillus	no spore	-	-
IG47	Old concrete**	16/10/2015	Bacillus	no spore	+	++
IG48	Old concrete**	16/10/2015	Bacillus	no spore	+	++
IG49	Old concrete**	16/10/2015	Bacillus	Non deforming spore	+	++
IG50	Old concrete**	16/10/2015	Bacillus	Non deforming spore	+	++
IG51	Old concrete**	16/10/2015	Coccus	Non deforming spore	+	++
IG52	Old concrete**	16/10/2015	Coccus	Non deforming spore	+	++
IG53	Old concrete**	16/10/2015	Bacillus	Terminal, Circular	+	++
IG54	Old concrete**	16/10/2015	Bacillus	Non deforming spore	+	++

IG55	Old concrete**	16/10/2015	Bacillus	hard to recognize	-	++
IG56	Old concrete**	16/10/2015	Bacillus	no spore	-	++
IG57	Old concrete**	16/10/2015	Bacillus	no spore	-	-
IG58	Sharped sand	19/10/2015	Bacillus	Non deforming spore	+	++
IG59	Sharped sand	19/10/2015	Bacillus	Non deforming spore	+	++
IG60	Sharped sand	19/10/2015	Bacillus	Non deforming spore	+	++
IG61	Sharped sand	19/10/2015	Bacillus	Non deforming spore	+	++
IG62	Sharped sand	19/10/2015	Bacillus	Non deforming spore	+	++
IG63	Sharped sand	19/10/2015	Bacillus	Non deforming spore	+	++
IG64	Sharped sand	19/10/2015	Bacillus	Non deforming spore	-	++
IG65	Old concrete**	20/10/2015	Bacillus	Non deforming spore	-	++
IG66	Old concrete**	20/10/2015	Bacillus	Non deforming spore	-	++
IG67	Old concrete**	20/10/2015	Bacillus	Non deforming spore	-	++
IG68	Calcium sulfate	21/10/2015	Bacillus	Terminal, Circular	+	-
IG69	Cambridge (soil)	20/10/2015	Bacillus	Non deforming spore	-	++
IG70	Calcium sulfate	5/11/2015	Coccus	No spore	+	++
IG71	Gypsim	06/11/2015	Coccus	No spore	+	++
IG72	Calcium sulfate	05/11/2015	Coccus	No spore	-	-
IG73	Old concrete**	06/11/2015	Coccus	No spore	+	++
IG74	Gypsim	09/11/2015	Coccus	No spore	+	++
IG75	Gypsim	09/11/2015	Coccus	No spore	+	++
IG76	Gypsim	09/11/2015	Coccus	No spore	+	++
IG77	Gypsim	09/11/2015	Bacillus	Non deforming spore	+	++

IG78	Gypsim	09/11/2015	Bacillus	No spore	+	++
IG79	Gypsim	09/11/2015	Bacillus	Non deforming spore	+	++
IG80	Gypsim	09/11/2015	Bacillus	Non deforming spore	+	++
IG81	Old concrete**	09/11/2015	Bacillus	No spore	+	++
IG82	Old concrete**	09/11/2015	Bacillus	No spore	+	++
IG83	Old concrete**	10/11/2015	Bacillus	No spore	+	-
IG84	Old concrete**	10/11/2015	Bacillus	No spore	+	++
IG85	Old concrete**	10/11/2015	Bacillus	Non deforming spore	+	++
IG86	Old concrete**	10/11/2015	Bacillus	No spore	+	-
IG87	Calcium sulfate	10/11/2015	Bacillus	No spore	+	++
IG88	Old concrete**	10/11/2015	Bacillus	No spore	+	++
IG89	Old concrete**	10/11/2015	Bacillus	No spore	+	++
IG90	Old concrete**	10/11/2015	Bacillus	No spore	+	++
IG91	Old concrete**	10/11/2015	Bacillus	Not sure	+	++
IG92	Old concrete**	10/11/2015	Bacillus	Not sure	+	++
IG93	Old concrete**	10/11/2015	Bacillus	No spore	+	++
IG94	Gypsim	11/11/2015	Bacillus	No spore	+	++
IG95	Gypsim	11/11/2015	Bacillus	Non deforming spore	+	++
IG96	Gypsim	11/11/2015	Bacillus	No spore	+	++
IG97	Gypsim	11/11/2015	Bacillus	Sub-terminal, circular	+	++
IG98	Gypsim	11/11/2015	Coccus	No spore	+	++
IG99	Gypsim	11/11/2015	Coccus	No spore	+	++
IG100	Calcium sulfate	13/11/2015	Bacillus	Terminal, Circular	+	++
IG101	Calcium sulfate	13/11/2015	Coccus	Non deforming spore	+	++
IG102	Queensbury(soil)	24/11/2015	Bacillus	Terminal, Circular	+	++
IG103	Baron court(soil)	19/11/2015	Bacillus	Terminal,	+	++

				Circular		
IG104	Baron court(soil)	24/11/2015	Bacillus	Terminal, Circular	+	++
IG105	Harrified (soil)	27/11/2015	Bacillus	Sub-terminal, circular	+	++
IG106	Baroun court(soil)	20/11/2015	Bacillus	Terminal, Circular	+	-
IG107	Harrified(soil)	27/11/2015	Bacillus	Sub-terminal, circular	+	-
IG108	Brunel forest 2(soil)***	24/11/2015	Bacillus	Terminal, Circular	+	++
IG109	Brunel forest 2(soil)***	20/11/2015	Bacillus	Non deforming spore	+	++
IG110	Old concrete**	19/11/2015	Coccus	Non deforming spore	+	++
IG111	Air contamination	30/11/2015	Coccus	Non deforming spore	+	++
IG112	Slough(soil)	03/12/2015	Bacillus	Terminal, Circular	+	++
IG113	Crank Garden(soil)	04/12/2015	Bacillus	Sub-terminal, circular	+	++
IG114	Air contamination	30/11/2015	Bacillus	Terminal, Circular	+	++
IG115	Slough(soil)	30/11/2015	Bacillus	Terminal, Circular	+	-
IG116	Streatham 1 (soil)	03/12/2015	Bacillus	Non deforming spore	+	++
IG117	Slough (soil)	03/12/2015	Bacillus	Terminal, Circular	+	++
IG118	Slough (soil)	03/12/2015	Bacillus	Terminal, Circular	+	-
IG119	Streatham 1(soil)	30/11/2015	Bacillus	Sub-terminal, circular	+	-
IG120	West Drayton(soil)	03/12/2015	Bacillus	Sub-terminal, circular	+	-
IG121	Streatham 2(soil)	30/11/2015	Bacillus	Sub-terminal, circular	+	-
IG122	Brunel forest 2(soil)***	24/11/2015	Coccus	No spore	+	++
IG123	Behind business	24/11/2015	Bacillus	Terminal,	+	-

	school(soil)			Circular		
IG124	Brunel forest 2(soil)***	24/11/2015	Bacillus	Terminal, Circular	+	++
IG125	Behind business school(soil)	24/11/2015	Bacillus	Terminal, Circular	+	++
IG126	West Drayton(soil)	24/11/2015	Bacillus	Sub-terminal, circular	+	-
IG127	Brunel river side(soil)	24/11/2015	Bacillus	Terminal, Circular	+	++
IG128	Queensbury(soil)	20/11/2015	Bacillus	Terminal, Circular	+	-
IG129	Streatham 1(soil)	09/12/2015	Coccus	No spore	+	++
IG130	Slough(soil)	09/12/2015	Bacillus	Sub-terminal, circular	+	++
IG131	Streatham 2 (soil)	30/11/2015	Bacillus	Terminal, Circular	+	-
IG132	Acton (soil)	03/12/2015	Bacillus	Terminal, Circular	+	-

[1]All the strains were ethanol washed and incubated aerobically at 30^{o}C.

*The forest behind Isambard Complex (North Hall and Meadow Hall) at Brunel University London.

** The concrete path in the back of Tower D building (the oldest building that was constructed at 1966) at Brunel University London.

*** The forest behind the Distribution Centre at Brunel University London.

Catalase test: Negative (-), weak or delayed (+), and Positive (+ +)

Oxidase test: + = positive reaction and - = negative reaction

4.3.2 **Gram staining**

Among 132 strains tested, 85 were diagnosed as gram negative and 40 were gram positive. Results for the gram stain test of forty strains revealed dark purple stained bacteria cells due to retaining the primary dye called the crystal violet-iodine complex in the cell wall. During decolourisation step of this test and after washing away the crystal violet-iodine complex, gram positive bacteria will retain the purple stain, because the peptidoglycan layer of the bacterial cell dehydrate, shrink and tighten. Therefore, in gram positive cell, the crystal violet-iodine complex is not able to penetrate this tightened peptidoglycan layer, rather is stuck in the cell. For this type of bacterial cells, 50-90% of the cell wall is made up of

peptidoglycan, a polysaccharide composed of two subunits called N-acetyl glucosamine and N-acetyl muramic acid (BARTHOLOMEW and FINKELSTEIN, 1958).

On the contrary, the peptidoglycan layer of the gram negative cell is thin (10% of the cell wall) and the cells have an extra outer membrane. This membrane is made of lipids, and separated from the cell wall by means of the periplasmic space (Seltmann and Holst, 2013). During the decolourisation process, the outer membrane is degraded and the purple stain is lost as the cells are unable to keep the crystal violet-iodine complex. Compared to the original crystal violet stain and iodine, the crystal violet-iodine complex has a larger molecule and is not capable of being dissolved in water.

It was observed from the test that the decolorized gram negative cells were stained red in the step of counterstaining using the water soluble safranin. However, the purple stain in gram positive cells was not disrupted by the safranin because it is lighter than crystal violet

During the examination, seven strains were undefined. These bacterial strains were characterised by longer and thicker shape compared to gram-negative bacteria, often form long chains which are characteristic for gram-positive bacteria. The possible reason of the existence of these transitional forms may be the contamination of the soil or water sample. All gram positive were sub cultured and used for further studies.

4.3.3 **Endospore staining**

Presence of endospores can be indicated by the rounded or swollen part of bacterial cell. Endospore formation is a character of an organism which has enabled a species to survive under unfavourable conditions. The vegetative cells are visible as light coloured rods in the results obtained from endospore staining test. A total of 76 bacillus strains were identified among 132 isolates, indicating the bacterial isolates capability of producing endospores. Small sub-terminal or central spores were noted in these strains that were circular or cylindrical in shape and capable of distending cells. In the other strains, spores were either free or absent. The amount of endospores was different when compared between bacterial isolates.

4.3.4 **Biochemical tests**

For identification of bacterial isolates, various biochemical tests were performed. Results for the biochemical characters (oxidase and catalase) of 132 strains are presented in Table 4-6.

4.3.4.1 Oxidase test

The oxidase test was applied to 132 strains, of which 87 gave positive results, whereas 42 were oxidase-negative (Table 4-6). The samples that showed negative oxidase activity reflect the lack of cytochrome in these microorganisms. However, 3 strains displayed uncertain results and may therefore require further tests to confirm identification. The struggle was faced in determining the oxidase activity of these three strains was because of the little pigment (violet) that absorbed into the filter paper. The failure to show definite oxidase activity may be due to young or non-well developed cultures used in this test. In this study, 15 oxidase-positive strains were catalase-negative. With the exception of four Bacillus species, oxidase activity was found among all the gram-positive organisms (36 strains). Thus, these strains have noted as uncertain in the Table 4-6, although using different test method could offer a way to detect the oxidase activity.

The principle behind the oxidase test is the visual interpretation of a colour change that result from the oxidation of the reagent (N, N, N', N' tetramethyl-p-phenylenediamine dihydrochloride) caused by a cytochorm-dependent bacterial oxidase reaction. The oxidase reaction is therefore assumed to be owing to the existence of a cytochrome oxidase, the enzyme which catalyses the oxidation of reduced cytochrome by molecular oxygen which represents the final acceptor of electrons in the electron transport chain.

4.3.4.2 Catalase Test

Table 4-5 compares the catalase reactions of 132 strains. It can be seen from the results that the majority of cultures were positive to the catalase test as they tended to produce vigorous volume of gas. Out of 132, 105 bacterial strains showed positive reactions, while 22 strains were totally nonreactive. Another 5 strains were uncertain since the response was quite delayed and the strains produced only weak evolution of gas. All the strains were able to grow in aerobic condition at 30^{o}C. Although the catalase test is rapid, simple and inexpensive, it needs to be more accurate and applicable as bacterial identification system. One of the limitations of this test was the sensitivity to the killing effect of H_2O_2. A number of studies have recommended using 10% H_2O_2 (Davidsohn, Henry and Todd, 1969; Levinson and MacFate, 1969; Cruickshank, 1968), while others suggested 3% (Montgomerie, Kalmanson and Guze, 1966; Braude and Berkowitz, 1961). However, some organisms are still reactive at a low concentration of hydrogen peroxide (0.5%) such as Serratia and Pseudomonas aeruginosa strains. Therefore, it has been suggested that there is no benefits from using concentration greater than 3% (Taylor and Achanzar, 1972). Another limitation of

this test is that some bacterial colonies are principally quickly growing organisms and many of them were in their death phase, even before 48hrs. Therefore, before recording a negative result, some care is needed.

4.3.5 **Urease activity**

Hydrolysis of urea by bacteria yields ammonia, which alkalinizes the medium and results in a pH shift which is recognised by the colour gradual transition of phenol red from yellow to magenta (pink) (Brink, 2010).

Eight isolates have been chosen to perform a urea hydrolysis assay and 7 of them were found to hydrolyse urea. Isolates with slow and no hydrolysis reaction were eliminated from consideration based on colour range created by phenol red after urea hydrolysis. Urease positive organisms that can decompose urea rapidly change the medium pH over a short time span and turn the colour of medium from yellow to pink more quickly.

Figure 4-1A shows that the urea hydrolysis for Bacillus sphearicus 57 and 58 was faster than that for most of the other isolates where the hydrolysis took place in the first 5hrs. After 16hrs, the colour change for Bacillus Megaterium 33 was clear and starts to increase with time (Figure 4-1 B). It can also be seen that in the period between 20 and 24hrs, the rate of colour change in the media for Bacillus Megaterium 31, 114 and 126 was considerably slow and almost equal for the three isolates.

The rate of urea hydrolysis for isolate 108 was substantially less than that of the other isolate (light pink after 28hrs). No colour change was observed for isolate 127 and this indicates the lack of ability to urea hydrolysis.

It was observed that the isolates are significantly different from each other in the urea hydrolyse rate. Carbonate concentration and hence calcium carbonate saturation would be increased as the urea hydrolysis increase (Verma *et al.*, 2015).

Therefore, microorganisms that have the ability to hydrolyse urea at comparatively much faster rate leading to calcium carbonate precipitation should be recommended and well-thought-out for the best option of concrete crack remediation (Nonakaran *et al.*, 2015).

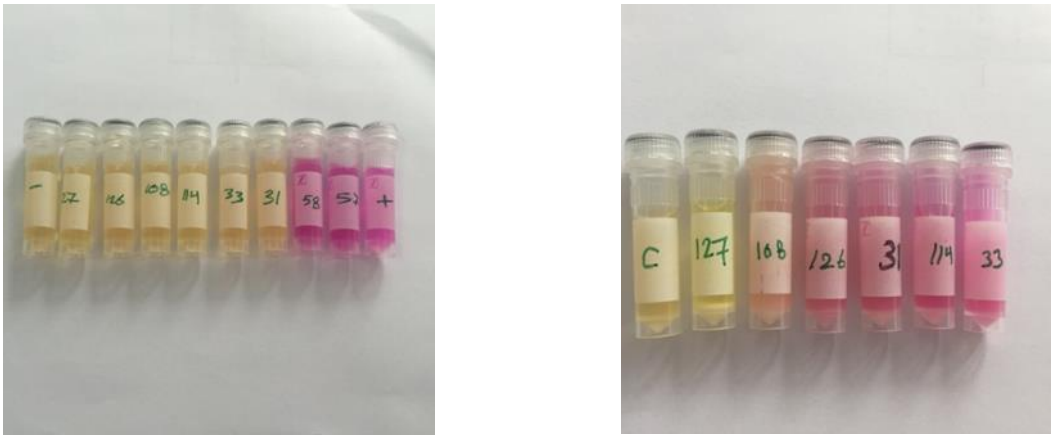

(A) Urease test results after 5hrs (B)Urease test results after 28hrs

Figure 4-1 Urease test results after 5hrs and 28 hrs.

4.3.6 **Effect of pH on bacterial growth**

The extent of alkalinisation or acidity of environmental surroundings typical for microbe growth and reproduction are unique for each species. Hydrogen ion concentration has a great effect on the bacterial growth and survival. The influence of different pH level on seven isolates grown in nutrient broth was investigated in the pH range of 4 to 12. The growth of each bacillus strain under different pH conditions are shown in Figures 4-2, 4-3, 4-4, 4-5, 4-6, 4-7 and 4-8.

The data of the effect of pH of the nutrient medium on the growth of Bacillus Sphaericus 57 are presented in Figure 4-2.The optical density was increased 128% when the pH increased from 4 to 8. When pH increased from 8 to12, OD760 was reduced 3.5 times. The results showed that pH has a significant effect on growth in Bacillus Sphaericus 57. It is evident that the optimum growth was obtained at pH 8 and it retained relatively high growth activity in the pH range 8-10. For example, at pH 10, the strain retained about 98% of its maximum growth. However, there is a steep reduction in growth activity in alkaline media (pH 11 and 12). The growth is 32% at pH 11 and 28.45% at pH 12.

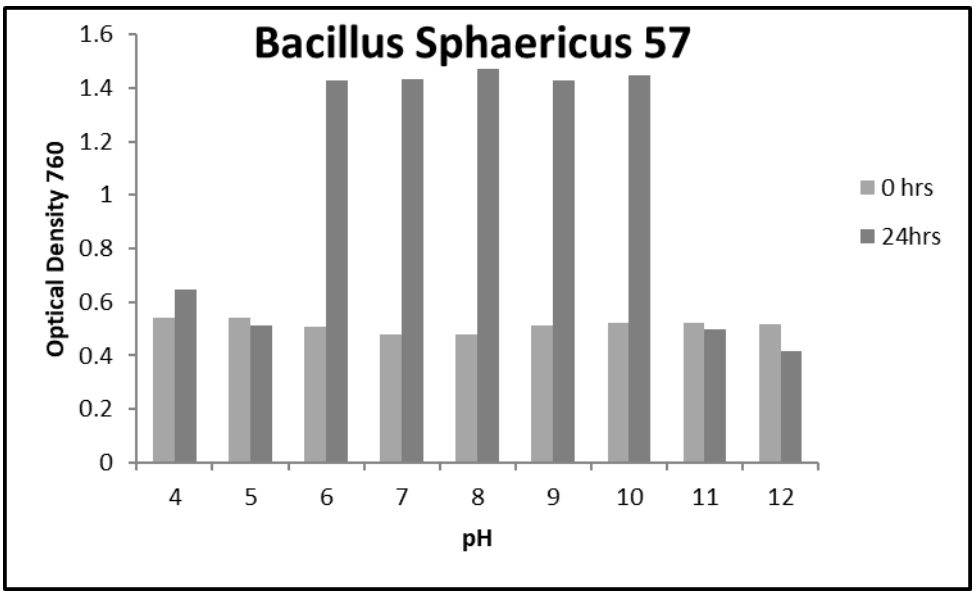

Figure 4-2 Effect of pH on Bacillus Sphearicus 57 growth

The highest optical density of Bacillus Sphaericus 58 was detected with pH 8 and the lowest was with pH 12 as shown in Figure 4-3. Its growth was fastest at pH 8 compared to Bacillus Sphaericus 57, after which it dropped steadily with increasing pH from about 1.585 at pH 9 to about 0.432 at pH 12.

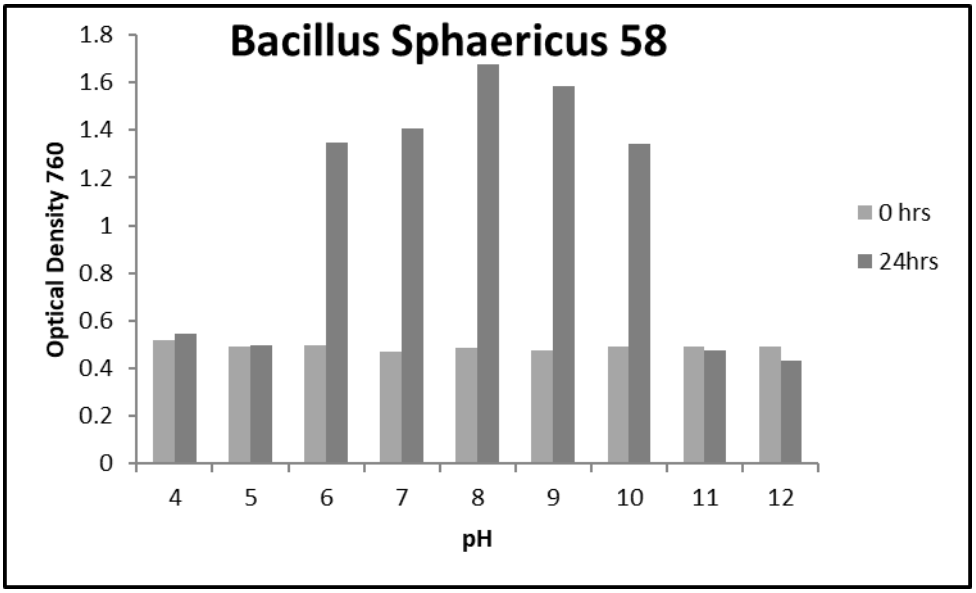

Figure 4-3 Effect of pH on Bacillus Sphearicus 58 growth

Figure 4-4 presented that the growth of isolate Bacillus Megaterium 33 was optimal at pH 8; this is in line with the maximum OD760. It was also shown that the OD760 reached 29% of maximum growth when pH increased up to 12. This isolate recorded fairly high OD 760nm values at pH ranges of between 7 and 9. However, at pH 10, the optical density reached about

31.5% of its maximum growth and decreased further when pH increased to 11. A sharp decrease in maximum optical density occurred at pH 12.

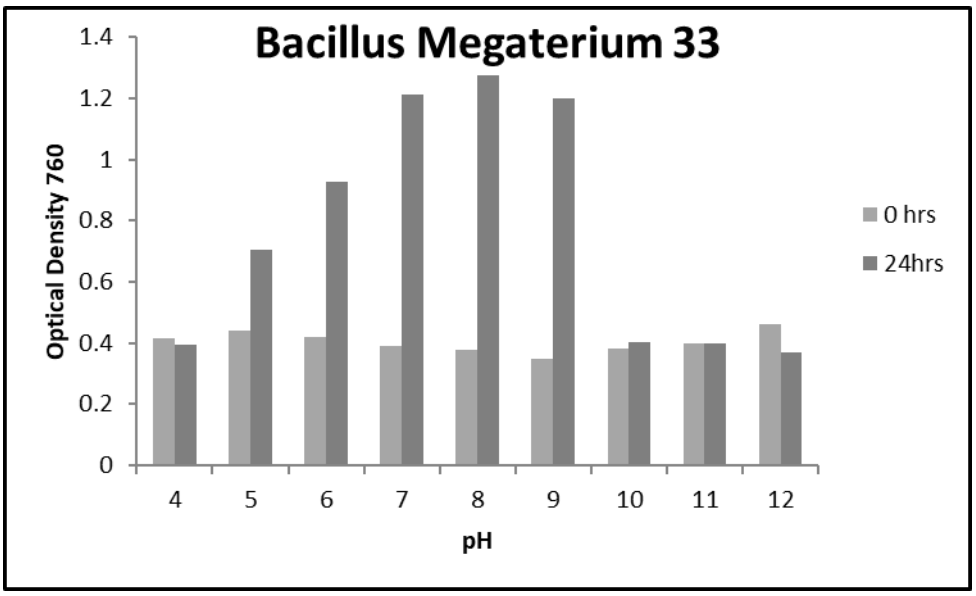

Figure 4-4 Effect of pH on Bacillus Megaterium 33 growth

Bacillus Megaterium 126 showed higher optical density at all pH levels as presented in Figure 4-5. Its highest growth was achieved at pH 8 with an OD 760nm value of 1.277. At pH 9.0, the bacterial strain also grew adequately, the growth was only 1% inhibited, while at pH 10 and 11, the growth was inhibited by about 32%. When pH level of the growth medium was below 6.0, the same trend of decreased growth was observed. However, the growth of Bacillus Megaterium 126 was less affected at pH 6.0 and 7.0.

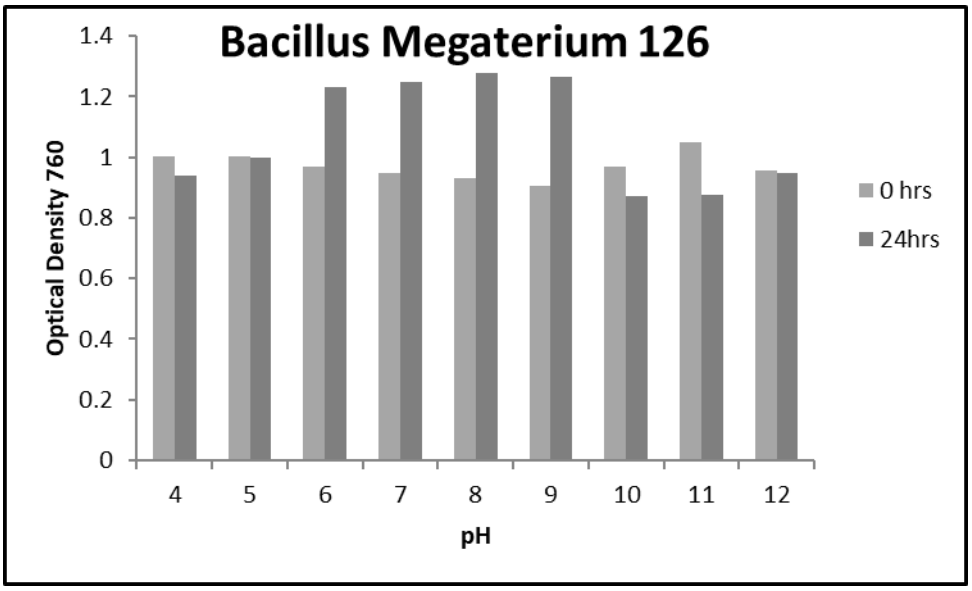

Figure 4-5 Effect of Bacilus Megaterium 126 growth

Although it grew well at all pH values, Bacillus Megaterium 31 recorded the highest OD 760 value at pH 6. However, its growth was less after 24 hrs at pH levels lower than 6.0. In the meantime, less growth inhibition was seen when the pH value of the growth medium was increased from 7.0 to 9.0. The highest level of growth inhibition found in Bacillus Megaterium 31 was 27.7% of the maximum growth at pH 12. At pH 10 and 11, the inhibition of growth was considerably less when compared with pH 12 (Figure 4-6).

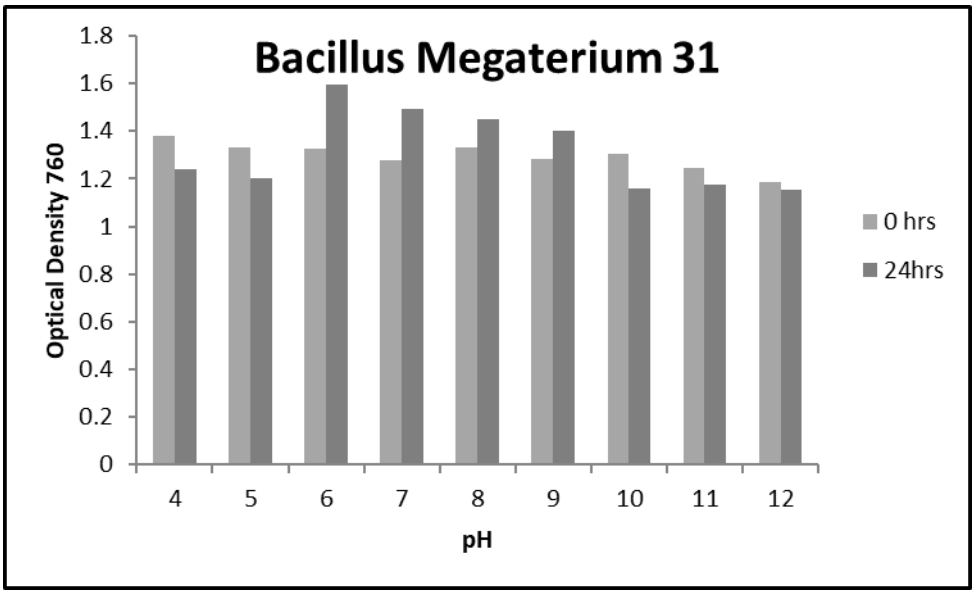

Figure 4-6 Effect of pH on Bacillus Megaterium 31 growth

Maximum growth was observed between pH 6-9 for the Bacillus Megaterium 114 (Figure 4-7). However, OD 760 was highest at pH 9 for the isolate tested. This level considered to be optimum for a good growth in Bacillus Megaterium 114. Above this level, the growth rate tended to decrease gradually. The optical density at pH 6, 7, 8 and 9 were similar to those determined for Bacillus Megaterium 126, but at pH 9 an optical density of 1.214 was found, which was slightly lower than the corresponding value for Bacillus Megaterium 126 (1.264). At pH 10, 11 and 12, Bacillus Megaterium 114 grown for 24hrs gave slightly less OD 760 nm values than Bacillus Megaterium 126 grown for the same time (Figure 4-7).

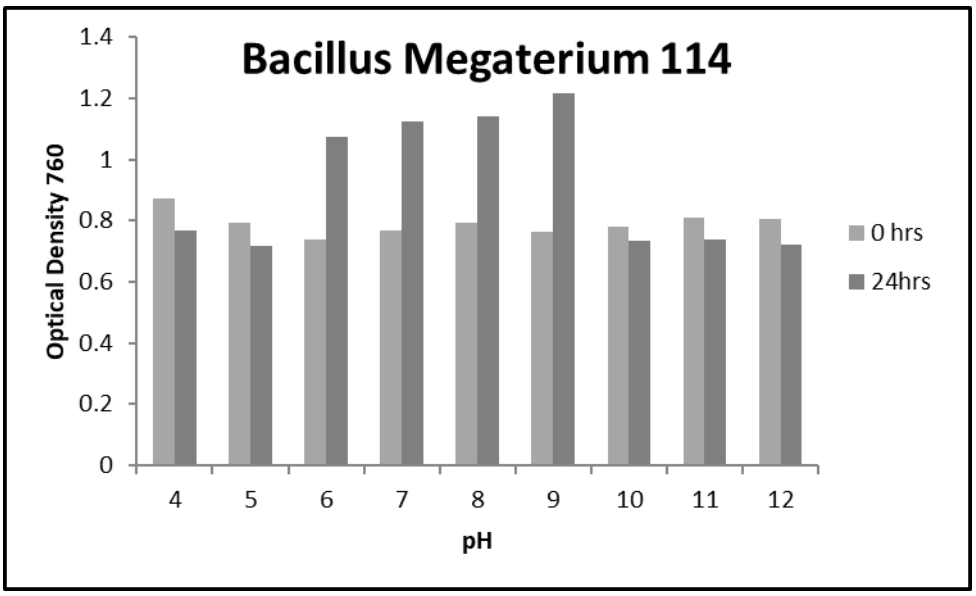

Figure 4-7 Effect of pH on Bacillus Megaterium 114 growth

In Bacillus Megaterium 108 grown under different pH levels, the optical density was gradually increased at pH values up to and including 7 (1.466). At pH values above 7, however, the growth was decreased by 6.8% with no significant difference at pH 8 and 9. Bacillus Megaterium 108 also recorded low OD7690nm values at pH 4 and 5 indicating its less tolerance to acidic environment when tested after 24hrs. Significant difference in the growth of Bacillus Megaterium 108 was detected between the pH range of 6-9 compared to the pH 4, 5, 10, 11 and 12 indicating Bacillus Megaterium 108 was more active in neutral to slightly alkaline pH environment (Figure 4-8). Lastly, at pH 10, 11 and 12, the OD760 nm of this strain was reduced to approximately 60% of the optical density that was observed at pH 7.

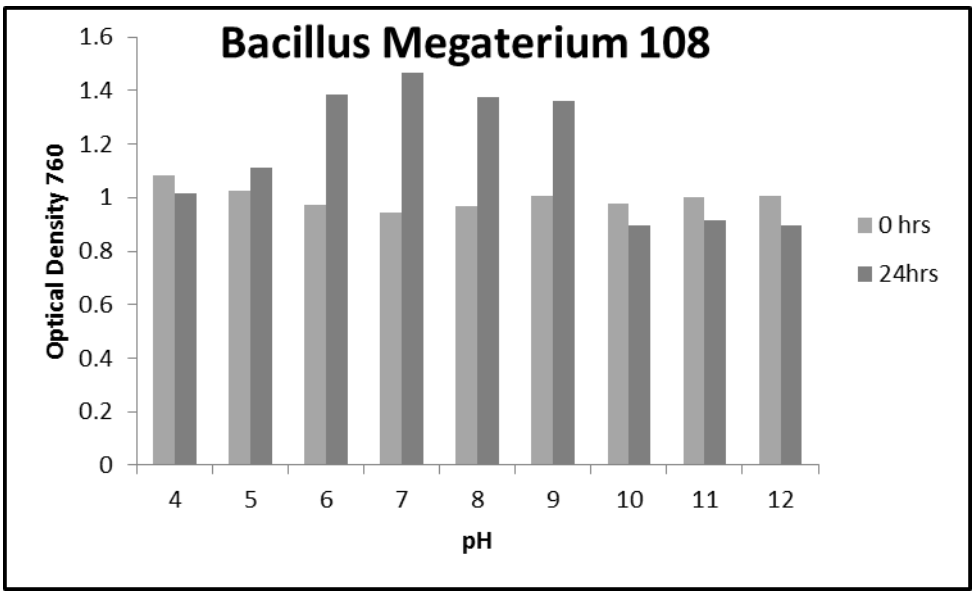

Figure 4-8 Effect of pH on Bacillus Megaterium 108 growth

In general, the highest levels of growth rates were obtained at pH 8 for Bacillus Sphaericus 57 (1.47), Bacillus Sphaericus 58 (1.679), Bacillus Megaterium 33 (1.273) and Bacillus Megaterium 126 (1.277), while pH of 9 was optimal for Bacillus Megaterium 114 (1.214), indicating that the former four bacterial species may prefer less alkaline environments for their maximum growth compared to the latter Bacillus species. It was also found that at pH 6, Bacillus Megaterium 31 showed a significant higher OD 760nm value (1.596) than other bacterial species. The optimum pH required for the growth of Bacillus Megaterium 108 was found at pH 7 with a maximum optical density of 1.466.

The overall trend of bacillus Megaterium 126, 31, 114 and 108 growths was slower compared to Megaterium 33 and sphaericus 57 and 58. All Bacillus Megaterium grew adequately at pH ranging from 6 to 9. Cell yields of some Bacillus isolates appeared to be affected by low pH as shown in the growth figures of Bacillus Meagterium 31, 108, 114, 126 at pH 4. The inhibition of growth at this pH level was substantially less when compared with pH 12, though some strains showed growth increase at this pH level such as Bacillus Sphaericus 57 and 58. The effect of pH on bacterial growth has been examined previously. It has been reported that the bacterial growth increased fivefold when the pH changed from 4 to 7(Bååth and Arnebrant, 1994). Therefore, Bacillus strains, as alkalophiles, have the ability to survive in high pH surroundings. This may attribute to the cell wall that contains certain structural components like teichuronopeptide which contributes to alkaliphily (Aono, Ito and Machida, 1999).

None of the isolates were able to grow at pH 11 and 12; however, their ability to reproduce at pH level up to 10 proposes their efficiency to be used as self-healing agent to promote calcite precipitation in highly alkaline building material (Achal *et al.*, 2009).

It has to be noted that freshly casted concrete is an alkaline environment (pH of 12 to 13). However, due to carbonation which depend on the relative humidity of concrete and exposure time, the pH value in the crack zone decreases from around 13 to as low as 8. Therefore, in order for bacterial species to be able to perform MICP and to be consistent with the alkaline environment of concrete, they need to be able to survive and grow at these pH values. The soil bacterial species are known to be alkali-tolerance and alkaliphilic strains which induce condition favourable for $CaCO_3$ formation (Boquet, Boronat and Ramos-Cormenzana, 1973). Another study conducted by Wang, et al. to evaluate the suitability of using Bacillus Sphaericus for self-healing of concrete cracks, showed that the living cells and spores of this strain can grow and germinate in a wide range of alkaline pH values from 8 to 11. However, bacterial growth and spore germination were optimum between 7~9, and retarded under higher pH values (10~11). It has also been shown, in the same study, that the bacteria had a significant ureolytic activity that responsible for calcium carbonate precipitation in the pH range of 8~11. This means that the spores embedded in concrete can germinate when a crack occurs due to the fact that the pH in concrete drops from 12.8 to 9-10 depending on the carbonation rate in the cracked area (Wang *et al.*, 2017).

Wang et al. have argued that the spores could therefore theoretically germinate in about three days in the crack zone once the conditions become favourable; when there is an adequate nutrient, water and oxygen present (Wang *et al.*, 2015) . This suggests that after introducing these spores into concrete matrix (pH > 12), they will keep dormant and only start to become metabolically active after cracks appear and the pH level at the crack surface drops.

4.3.7 **Molecular identification of bacterial isolate**

Fast DNA Kit and the FastPrep Instrument were used to extract and purify the Genomic DNA from overnight grown bacterial cultures. The DNA solution was stored at 4oC for QA/AC and downstream applications. Before sending the DNA with the readings from the FastPrep Instrument to sequencing, it was kept at -20oC for long term storage. Out of 132 strains only 40 strains were sent to sequence because it was difficult to extract the DNA from most of the strains which were removed and discarded. The characterisations of these selected strains are listed in Table 4-5. After analysing and assembling the sequences, it was indicated that six out

of all isolate were recognised as a member of the Bacillus genus. All the isolates were rode shaped and able to form endospores as typical phenotypic features of Bacillus genus (Ash et al., 1991) . The bacterial isolates 31, 33, 108, 114, 126 and 127 were identified as Bacillus Megaterium and named as Bacillus Megaterium followed by their sequence number.

4.4 Interim conclusion

The following main conclusions are derived from this chapter:

1) Based on the phenotypic characteristics such as its cell morphology and biochemical properties, the isolates were found to be Bacilli as they were all gram positive and had short to long rod shape. They were all able to grow under aerobic conditions at 30^{o}C.
2) It was found that almost half of the strains were able to sporulate when exposed to adverse environmental conditions (starvation). Oxidase and catalase tests were also performed as part of biochemical identification.
3) Genotypic characteristics revealed that six isolates were recognized as Bacillus Megaterium.
4) A very fast urease activity was noticed with Bacillus Sphaericus 57 and 58 taken from Brunel University microbiological bank for comparison. Bacillus Megaterium 33 started its urease activity after 16 h, whereas the other Megaterium isolates showed very slow or negative activity.
5) Bacillus Sphaericus 57 and 58 grew well in the environmental surroundings between pH (6-10) and Bacillus Megaterium 33 grew well in the (7-9).
6) These three isolates were therefore selected for further application in self-healing concrete to evaluate their ability to precipitate calcium carbonate crystal.

Chapter 5: Preparation, characterization and viability of Bacillus Sphaericus embedded in an alginate-clay matrix beads

5.1 Introduction

Different strategies of self-healing have been used in concrete. Encapsulation of healing agents is one of these strategies which rely on the capsules ability to deliver the healing agent after being induced by cracks. The wall of the capsules should be carefully designed so that it keeps the healing agent safe and at the same time allows the capsule to automatically break when damage occurs. Application of expansive agent mixed with other mineral admixtures into cementitious materials was also used with principle of sealing the cracks by the expansive hydration products generated after contact with water when damage happens. Self-healing based on shape memory material concept was demonstrated experimentally by different researchers. Shape memory polymer could be activated by electrical heating to repair cracks in concrete (Teall, 2016). Similarly, smart reinforced concrete beams can be produced by adding shape memory alloy during concrete casting (Kuang and Ou, 2008). It has conclusively been shown that the crack closure is nearly completed, ability to self-heal is improved and when subjecting to very large deflection, beams almost fully recovered.

Sodium alginate, a polysaccharide occurred naturally in certain brown seaweed, has been commonly applied as an agent in the environmental decontamination for the purpose of removing the organic compounds from water. In the presence of divalent cations (e.g. calcium ion), sodium alginate mediated cation-exchange process through sol–gel transition when a calcium ion substitutes two sodium cations. This material is low cost, biocompatible, and can be easy and quickly made by encapsulation (Kittinaovarat, Kansomwan and Jiratumnukul, 2010). Bead made with alginate are widely used and familiar encapsulation materials in biosciences applications (Bayramoglu *et al.*, 2002).

The structure of these beads is three-dimensional which consisted of inorganic constituents and polymer with high water-absorbing capacity. As these beads are economic and have great water retention properties, they have been chosen as active adsorbents in different applications. The thermal stability and mechanical strength of the calcium alginate beads have been found to be enhanced when supported with clays (Cavallaro *et al.*, 2013).

In this study, characterisation studies were undertaken onto alginate and alginate–pyrophyllite beads highlighting the effect of pyrophyllite on beads stability. Moreover, viability studies were carried out in order to assess the spore's survivability in the calcium-alginate-clay

matrix. The swelling properties of the beads were also examined. The characterisation of the beads was performed using Fourier transform infrared spectroscopy (FTIR), Scanning Electron Microscopy (SEM) and Energy Dispersive X-Ray (EDX).

5.2 Materials and methods

5.2.1 **Microorganism**

Bacterial spores and viable cells of model microorganism (Bacillus Sphaericus, strains 57 and 58 taken from Brunel University microbiological bank) were used as bacterial source. The reason behind choosing only two bacterial strains to be encapsulated using calcium alginate-clay beads is that it takes long time to get the beads. Therefore, it was difficult to scale up the process despite the simplicity of this method. These two bacterial species have been chosen based on their urease activity and ability to grow in relatively high alkaline environment compared to other bacterial species tested in Chapter 4. Samples were cultivated on modified sporulation nutrient agar medium at 37°C. The other chemicals used are of analytical grade. To obtain spores, cultures were examined occasionally during growth by phase-contrast microscopy. After that, cultures were collected from the petri plates when the ratio of vegetative cells to spores became static (about 4 days) and suspended in a saline solution. In order to separate vegetative cells from spores, the suspensions were centrifuged at 10,000xg for 10 min and the entire supernatant was carefully removed. After that, the pellet was washed several times with 200 ml of ice-cold distilled sterile water by centrifugation under the same conditions. This procedure was repeated three to four time until more than 90% of culture was free spores under phase contrast microscopy examination. The spore suspension were kept at 4^{o}C and protected from light.

5.2.2 **Pyrophyllite**

Pyrophyllite clay (Pyrax) is a hydrated aluminium silicate which has the appearance of talc with a density equal to 2.8 mg/m^3. It was purchased from the Ceramic Shop, USA. The chemical composition of pyrophyllite is Al_2O_3 28.35%, SiO_2 66.65%, and H_2O 5.0%.

5.2.3 **Chemicals**

Sodium alginate ($NaC_6H_7O_6$), Calcium chloride ($CaCl_2$), potassium dihydrogen phosphate (KH_2PO_4), dipotassium phosphate (K_2HPO_4) and disodium phosphate (Na_2HPO_4) were all purchased from Fisher Scientific, UK.

5.2.4 **Beads preparation**

Alginate-pyrophyllite clay beads are prepared according to the procedure reported in literature (Fravel et al., 1985) . Pyrophyllite clay (100g) was dispersed in 1 litre of sterilised distilled water under continuous stirring. Sodium-alginate suspension was prepared by dissolving 10 g of sodium alginate in sterilised distilled water. The alginate suspension was added to the pyrophyllite solution and the mixture was stirred for 1 h. Once the mixture looked homogeneous, 180 ml of the resulting suspension was transferred into sterile deep dish based on a coupling. The resulting solution was dripped while stirring in a constant rate into the 0.25 M $CaCl_2$ solution with the help of pasture pippette with a 1 mm diameter orifice. To incorporate the bacterial spores, 20 ml of biocontrol agent was added to the mixture containing a spore suspension of either Bacillus Sphaericus 57 or Sphaericus 58 in 1.5×10-1M KH_2PO_4 + 8.2×10-2M K_2HPO_4 buffered 0.1 % saline (pH 6.8). Alginate bead formation was driven by a cooperative binding of calcium ions (divalent cation) and the G-block regions of the alginate structure (Badwan et al., 1985) that form the so-called egg-box structures (Roger, Talbot and Bee, 2006; Rendevski and Andonovski, 2005). Next, the beads were sieved through mesh dry- sieves and washed with sterilised water. A laminar air flow hood was used to dry the pellets overnight.

5.2.5 **Viability of the encapsulated spores**

The viability (survival rate) of microorganisms in the calcium alginate-pyrophyllite beads was determined before introducing the organism to the calcium alginate salt, directly after encapsulation process and after 24hrs of pellet formation. The viability of bacteria was also analysed after 2, 4, 8, and 12 weeks after beads formation. The experiment was performed in four replications. To evaluate the microorganism viability, 1 g of beads were dissolved in mixture of 8.7×10^{-2} M KH_2PO_4 and 3.0×10^{-2} M Na_2HPO_4 (pH 7.7) and incubated at 30 °C for 2 h. The resulting suspension was vortexed vigorously for 30 s to release the cells from the alginate beads. After that, standard serial dilution method was used to determine the number of bacteria. This was done by plating 0.1 ml aliquots on a nutrient agar media and incubated at 30± 2^{o}C. The number of viable cells was expressed as colony forming units per gram of the dry weight of beads ($cfu\cdot g^{-1)}$.

5.2.6 **Swelling properties**

The swelling properties of the beads in different solution were monitored. This conventional method of drying and weighing offers an appropriate and fast method to study the response of

the alginate beads to the external stimuli such as pH and so on. Weighed beads (3 g) were immersed in three different solutions. The first solution (cement slurry) was prepared with a concentration of 1/10 cement to water. The cement solution was mixed and filtered after 1h to remove the undissolved particles and the pH of the suspension was around 12.5 to simulate the alkali condition of concrete. Tab water and de-ionize water were also used in this test. After 16 hrs, the swollen beads were taken out by draining the solution through a filter paper and weighted again. Then the swelling ratio of these beads was calculated with the following equation and noted as S:

$$S\ (\%) = (W_0 - W_1)/W_h$$

Where W0 and W1 denote the initial weights of water, or filtered cement slurry (g), and the weight of water or filtered cement slurry (g) flowing into the burette, respectively. Wh is the weight of dry alginate beads (Wang et al., 2014a). In this test, each swelling test was performed in three replicates, and then the swelling ratio was obtained as an average of these values. To study the re-swelling properties, the wet beads from the first swelling test were left to dry naturally at room temperature before subjecting to the second and third swelling.

5.2.7 **Characterization of the beads**

5.2.7.1 The Fourier transforms infrared spectroscopy analysis (FTIR):

FTIR spectra of the samples were obtained with a Perkin Elmer Spectrum One Fourier Transform Infrared (FTIR) spectrometer in the range of 4000–400 cm-1. In this experiment, infrared spectra of the functional groups of Pyrophyllite clay (Pyrax), sodium alginate powder and calcium alginate-Pyrophyllite beads were measured using Perkin Elmer Spectrum One Fourier Transform Infrared (FTIR) spectrometer in the range of 4000–400 cm-1. This spectroscopy characterisation was used to confirm the presence of functional groups in samples of Pyrophyllite clay (Pyrax), sodium alginate powder and calcium alginate-Pyrophyllite beads. Calcium alginate-pyrophyllite beads were dried at room temperature for 24 h prior to the analysis due to the high absorption of water which strongly dominates the spectrum. The principle of this test is that the samples placed in the path of an infrared beam will absorb and transmit light and then the light signal will penetrate the sample to the detector. The detector measures the intensity of the radiation moving into a sample and the intensity of the radiation transmitting through a sample. Its output as a function of time is converted into a plot of transmission against wavenumber by a computer using a Fourier transform method.

5.2.7.2 Thermogravimetric analysis

The decomposition behaviour of sodium alginate, pyriphyllite clay, calcium alginate-clay beads were investigated using thermogravimetric analysis (TGA). The analysis was conducted using was a themorgravimetrical analyser (DSC-TGA Standard /SDT Q600 V8.3 Build 101 instrument) operated at DSC Heatflow method. The apparatus is built to measure the weight change in a sample as the temperature changes. Weight loss graphs were produced for each sample and illustrate the percentage of weight loss as a temperature function.

5.2.7.3 Scanning electron microscopy analysis SEM and EDAX

Dried sample of calcium alginate-Pyrophyllite beads was subjected to Scanning Electron Microscopy observation (SEM, Zeiss Supra 35VP, 20kV). An Energy Dispersive Spectrometer (EDAX TEAM system) connected with SEM was used simultaneously to detect the components of beads. The bead was placed in a carbon tape, and the sample was coated with a gold layer using a sputter module in a vacuum evaporator in an argon atmosphere included in a cathode gas.

5.3 Results and discussion

5.3.1 Spores viability

The viability of Bacillus Sphaericus in the calcium alginate-clay matrix was determined before adding to the calcium alginate-clay suspension , directly after pellet formation, at 24 hours, and at 2, 4, 8, and 12 weeks after pellet formation. After serial dilutions, the number of colonies that had formed after three days of incubation at 30^{o}C was noted as colony form units per grams (cfu/g).

It can be seen that spores were still viable after being encapsulated into calcium alginate-clay matrix (Table 5-1), the spores of both Bacillus sphaericus used in this study (57 and 58) survived the calcium alginate-clay beads formation. It has been revealed that the spores during the whole process of beads preparation, from suspension state to drying state (beads drying), maintained the same viability (Table 5-1).The results also indicated that the number of viable spores decreased steadily during the period of 12 weeks.

However, the number of bacterial spores gradually drops with time; consistent decreases in microbial viability. When the Bacillus Sphaericus 57 spores entrapped in beads were tested for their viability, the number of cells declined proportionally with time (after 24 hours, 2weeks, 4weeks and 8 weeks). Interestingly, the viability of Bacillus Sphaericus 57 was

enhanced after 12 weeks as the bacterial cells were found to have multiplied even when viability was very low compared to the original. This could be a consequence of the metabolic activity of Bacillus Sphaericus 57 in the appropriate media (Nutrient agar media) which led to develop new colonies.

The fluctuated results of viability of Bacillus Sphaericus 57 spores could be due to the method of disintegration of beads to release the spores, which affected the colony form units (CFU) and the number of spores that were released was much less than the number of spores added to the calcium alginate-clay suspensions.

It is evident that the survivability of Bacillus Sphaericus 57 in beads was better than Bacillus Sphaericus 58 after 12 weeks of beads formation. Over half of Bacillus Sphaericus 57 was still viable, while only 15% of Bacillus Sphaericus 58 were survived. This behaviour was supported by other characteristics of Sphaericus 57 examined in another part of this work, such as its high pH tolerance and urease activity.

It has been found that colonies developed when spores were placed on appropriate media, even when viability was only11% of the original. Even though viability of both strains decreased appreciably (up to 89% loss) in 8 weeks, spores encapsulated in beads remained viable for at least 12wk: hence, the beads could still function as point sources of living cells as indicated by the production of colonies from beads containing spores that showed low, but measurable, viability when placed directly on culture media.

The observed decreases in viability could be due to the calcium chloride that was used as a gelling agent for sodium alginate. It has been indicated that in most cases half of the original population of most organisms dead within first 2-3 weeks after beads formation with $CaCl_2$ (Fravel *et al.*, 1985). The lack of essential nutrients could be another reason for the low spore viability after encapsulation. Precursors and nutrients were not included in the encapsulation process, because the presence of these materials can disrupt the beads formation process. Therefore, the absence of essential nutrients would result in diminished survival of the germinating spore. Although the numbers of the viable spores retrieved from beads, i.e. after 12 weeks, were low compared to the number of viable spores present in the original suspension used for the beads formation, these numbers are still substantial. The numbers of viable spores are still high, i.e. between 0.24 and 0.96×10^8 spore/ml, considering that, under suitable environmental conditions, a single viable microbial cell is theoretically enough to induce calcite precipitation (Jonkers and Schlangen, 2007).

The biocompatibility of calcium alginate-clay beads with Bacillus Sphaericus spores could be the reason behind spores' survival. Hence the matrix is sufficient to provide some protection for spores from mechanical stress and limit viability loss occurred during extended storage. Therefore, the encapsulation method detailed in this work may be effectively applied to preserve the viability of Bacillus Sphaericus against hostile concrete environmental. The alginate formulations have several advantages. The process is inexpensive and very versatile in size and composition.

Table 5-1 Viability of Bacillus sphaericus 57 and 58 encapsulated in calcium alginate-pyrophyllite clay beads

Isolate	Concentration before beads formation(spore/ml)	Survival during beads formation %	After 24h	After 2 weeks	After 4weeks	After 8 weeks	After 12 weeks
Sphaericus 57	1.6×10^{8}	100	1.37×10^{8}	0.8×10^{8}	0.34×10^{8}	0.17×10^{8}	0.96×10^{8}
Sphaericus 58	1.6×10^{8}	100	1.23×10^{8}	0.77×10^{8}	0.68×10^{8}	0.56×10^{8}	0.24×10^{8}

5.3.2 **Swelling properties**

Swelling behaviours is a very important property for alginate when it used in the form of hydrogel because their practical applications are greatly affected by this property. Therefore, the effects of pyrophyllite clay on swelling behaviours of the calcium alginate- clay beads were investigated in this section. Table 5-2 shows the swelling capacity of the beads with clay soaked in different media. Swelling capacity of beads sample in the three media was found to follow this order: cement filtrate > tab water> de-ionized water. The average swelling capacity in cement filtrate was 4.17 g/g beads. However, when the swelling test performed in a tap water, the beads exhibit a total swelling of around 2.6 (g/g). The lowest swelling capacity the beads achieved was during soaking sample in de-ionized water (2.05g/g). In the 1st test, the swelling capacity of beads in TW, DW and CF were lower than that in the 2nd and 3rd test. These results reflect those of (Wang *et al.*, 2014a) who also found that the blended hydrogels have more swelling capacity in the 2nd and 3rd than the 1st swelling test.

Performing swelling capacity test in cement filtrate showed higher results in the three tests comparing to tab water and de-ionized water. The amount of water absorbed was about 4.33 g/g in the 2nd test and 4.4 g/g in the 3rd test. This behaviour attributed to the polymeric

network nature of the calcium alginate-clay beads with many negatively charged –COO- groups that resist each other because of the electrostatic interaction in the swelling media with high pH level. Then the swelling of the beads occurs due to the osmotic pressure generation between the beads matrix and the media (Zhang *et al.*, 2010) . However, the difference between the swelling capacity values of the beads embedded in tab water and cement filtrate in not big even though the pH values of the two medias are completely different (8.2 for tab water and 12.2 for cement filtrate). This is probably owing to the extra interaction between negative charged groups form polymeric network and Ca/Mg ions in cement filtrate that can act as additional physical cross-linker (Wang *et al.*, 2015c) . Presence of many anions and cations in the de-ionized water accounts for the low swelling capacity value in de-ionized water. It is evident, then the changes in pH of swelling media affect swelling ratio of the beads. Figure 5-1 and Table 5-2 represent the mean values of the swelling properties of calcium alginate-clay beads in tab water, de-ionized water and cement filtrate.

Testing the swelling properties of the sodium alginate beads under the same condition of the alginate-clay beads was impossible because of its weak structure. It has been noticed from this study and confirmed by (Zhang *et al.*, 2010), that soaking sodium alginate beads in distilled water for 6 h, will destroyed and dissolve the beads entirely.

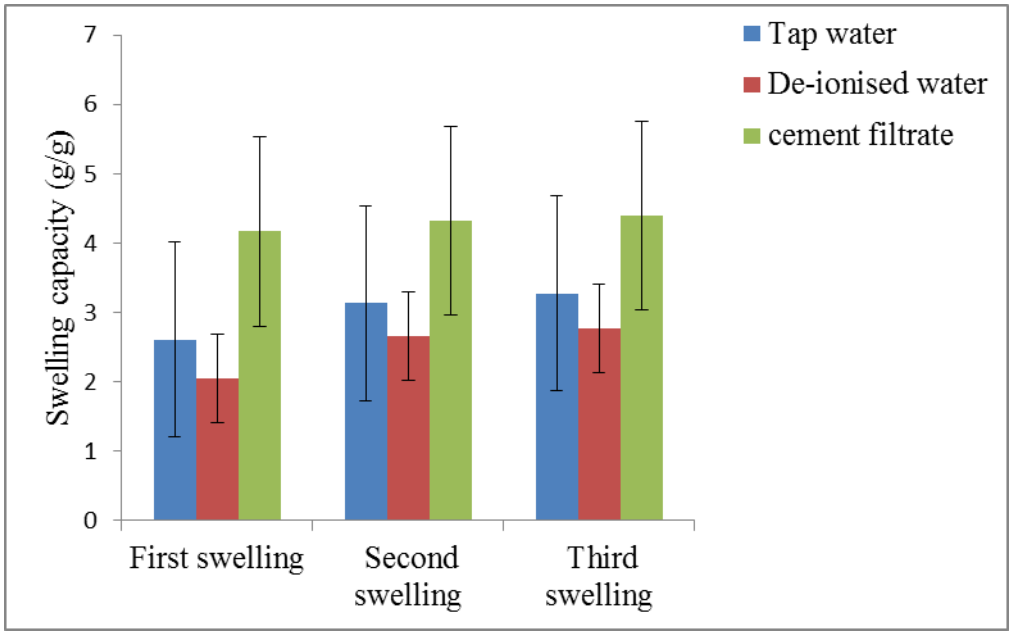

Figure 5-1 Swelling behaviour of the calcium alginate-clay beads in tab water, de-ionized water and filtered cement slurry

Table 5-2 Results of swelling behaviour of calcium-alginate beads in three different swelling media

Swelling media	First swelling			Second swelling			Third swelling		
	Swelling (g/g)	SD	CoV%	Swelling (g/g)	SD	CoV%	Swelling (g/g)	SD	CoV%
Tap water	2.61	0.21	8.06	3.13	0.22	6.97	3.28	1.40	42.80
De-ionised water	2.05	0.21	10.41	2.67	1.20	44.88	2.77	0.64	23.13
cement filtrate	4.17	0.93	22.24	4.33	0.98	22.72	4.39	1.36	31.03

The possible explanation for the low water absorption capacity of the calcium alginate-pyrophyllite clay beads is due to the presence of many negatively charged –COO- groups on the polymer chains of sodium alginate and the positive charge of the clay particles. As a result, the multiple-point electrostatic interaction between the two components of the beads makes the clay perform as inorganic multifunctional cross linkers in the alginate-clay beads. Thus, the mobility of the negatively charged sodium alginate polymer chains could be restricted by clay incorporation leading to decrease the water absorption capacity. Swelling property of the alginate-clay beads will therefore be discussed without comparison with alginate beads.

The evidence from this study suggests that probably the interactions between alginate and clay particles are responsible for the structural characterization of calcium alginate-clay beads. The mechanical resistance of these particles gives a considerable resistant to the structure to restrict the fluid absorption and the structure dissolution.

5.3.3 **Characterization of the beads**

The polar interaction between the hydroxyl groups of the alginate biopolymer and the uncharged siloxane moieties of the clay can lead to the formation of hybrid beads, as stated in literature (Cavallaro *et al.*, 2013). The calcium alginate-pyrophyllite beads were sphere-shaped with a 2-3 mm diameter. Some characteristics of alginate beads affects by introducing the pyrophyllite clay while most of the features still the same. As shown in Figure 5-2, a significant colour transformation from transparent to white can be easily noticed by the bare eye when clay minerals were added as confirmed by previous study (Barreca, Orecchio and Pace, 2014). Shape and size of alginate-clay beads are not affected by the incorporation of

clay. Dropping calcium alginate-clay suspension in the calcium chloride solution generates semi spherical beads, which is the same with only alginate suspension. Therefore, it seems that pyrophyllite clay is totally integrated into the beads' structure.

(a) Calcium alginate beads

(b) Calcium alginate-pyrophyllite beads

Figure 5-2(a) Calcium alginate beads, (b) calcium alginate-pyrophyllite beads

5.3.3.1 The Fourier transforms infrared spectroscopy analysis (FTIR)

The FTIR spectroscopy can be used to study the possibility of chemical interaction between the Pyrax clay and Sodium Alginate. The FTIR spectra of Sodium Alginate, Pyrax clay and Sodium Alginate- Pyrax clay beads are shown in the curves of Figure 5.3.

5.3.3.1.1 Sodium alginate spectrum

The spectrum in Figure 5-3 shows some characteristic peaks determined in sodium alginate. The main absorption featured bands displayed in the IR spectrum of sodium alginate are the hydroxyl (O-H), ether (C-O) and carboxylic (C=O) functional groups are (Daemi and Barikani, 2012). The broad peak observed at 3309 cm^{-1} was due to the stretching vibrations of O–H bonds. Carboxylate salt ion asymmetric and symmetric stretching vibrations are assigned to peaks at 1645 and 1416 cm^{-1}, respectively. The spectra of alginate samples present a band at 1034 cm^{-1} presumably due to the C–O stretching vibration of pyranosyl ring. These results match those observed in earlier studies (Daemi and Barikani, 2012; Leal *et al.*, 2008).

5.3.3.1.2 Spectrum of pyrophyllite

IR spectroscopy has a pivotal role in the investigation of the structure, bonding and chemical properties of clay minerals (Madejová, 2003). The infrared spectrum can provide a unique

fingerprint of each individual mineral but can also give information about mineral structure including the presence of both crystalline and non-crystalline impurities, and the nature of isomorphic substituents. The absorption bands corresponding to important stretching and bending vibrations of the mineral structure can be clearly-defined by the clay minerals IR spectra, such as OH and Si-O groups. The stretching vibration of OH group can absorb in the 3700-3500 cm^{-1} regions, while absorption in the 950-650 cm^{-1} regions can be assigned to be bending vibration of the same group. The most intense bending bands of the Si-O appear between 550–400 cm^{-1}, while the Si-O stretching modes arise in the 1050-1000 cm^{-1} (Greenwood, 2007).

In Pyrophyllite spectrum shown in Figure 5-3, an intense and sharp OH-stretching band was detected around 3673 cm^{-1} which is likely due to the stretching vibrations of the OH groups bonded to Al ions within the structure Al2OH and perpendicular to the planes of pyrophyllite layers (Kloprogge, Ruan and Frost, 2000; Kloprogge and Frost, 1999; Sánchez-Soto *et al.*, 1994; Farmer, 1974). The bending vibration of OH group appeared at 947-649 cm^{-1} and another characteristic beak at 1887 cm^{-1} indicated the hydroxyl bending of H2O. Si-O stretching vibration may contribute to the absorption bands centred at 1076 cm^{-1}, 1027 $cm^{-1}$and 1120 cm^{-1}. It is worth noting as shown in Figure 5-3 that for pyrophyllite sample, the weak band centered at 807 cm^{-1} and 853 cm^{-1} are assigned to out-plane OH libration and the band at 947 cm^{-1} relates to in-plane OH libration (Li *et al.*, 2014).

5.3.3.1.3 Spectrum of beads

The FTIR spectrum of pyrophyllite after interacting with sodium alginates and calcium chloride is shown in Figure 5-3. Based on the beads spectrum, there is no big difference in the chemical structure of alginate, which is the main constituent in the bead structure. The intensity of Carboxyl stretching vibration peaks of alginate decrease, which may attribute to the electrostatic interaction between the negative charges of the carboxyl groups and the positive charges sited at the edges of clay (Iliescu *et al.*, 2011).

The hydroxyl stretching peak of alginate at 3276 cm^{-1} is shifted into 3338 cm^{-1} when pyrophyllite clay was added. The peak assigned at 1016 cm^{-1} may be ascribed to the Si–O–Si stretching vibrational frequency of the clay on the alginate, whereas those at 1611 and 1421 cm^{-1} can be assigned to asymmetric and symmetric stretching vibrational modes of the COO^{-} groups. Almost the same wave number of the characteristics bands of the clay observes in the spectra obtained from the calcium alginate-pyrophyllite matrix. These observations indicate

the presence of the electrostatic forces and the intermolecular hydrogen bonding between alginate and pyrophyllite which confirm the chemical stability of this clay in calcium alginate beads.

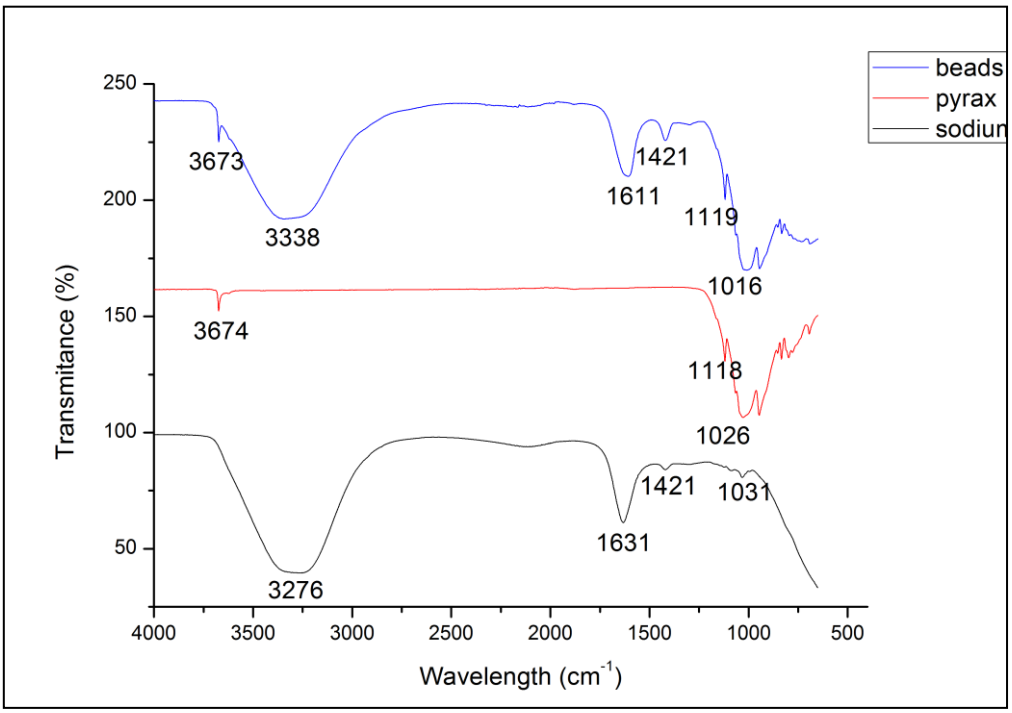

Figure 5-3 Fourier transforms infrared spectroscopy analysis of sodium alginate, pyrophyllite and calcium alginate-clay beads

5.3.3.2 Thermogravimetric analysis

Thermal analyses of dried samples with a mass of 16.8 mg were heated from 26.3 up to 792 ^{o}C with temperature programmed at certain heating rates in air.

5.3.3.2.1 Sodium alginate

It is apparent that generally, several consecutive steps of weight loss lead to the thermal decomposition of polysaccharides within sodium alginate (Figure 5-4), involving processes of the desorption of physically absorbed water molecules, the removal of structural water (dehydration reaction), depolymerisation (accompanied by the rupture of C–O and C–C bonds in the ring units resulting in the formation CO, CO_2 and H_2O), and, finally, the formation of poly nuclear aromatic and graphitic carbon structures (Parikh and Madamwar, 2006).

From Figure 5-4, two different regions can be observed. At the first region, a major weight loss was observed approximately 63% from 26.5-126^{o}C indicate the evaporation of free water. From the profile of this region, it can be noticed that sodium alginate sample contains more water than the other samples. This is expected since the alginates are largely used industrially for their water retention ability. The second thermal decomposition region showed weight loss of 5.63% from 126-793^{o}C indicating the occurrence of further thermal degradation of sodium alginate along with the rupture of alginate chains.

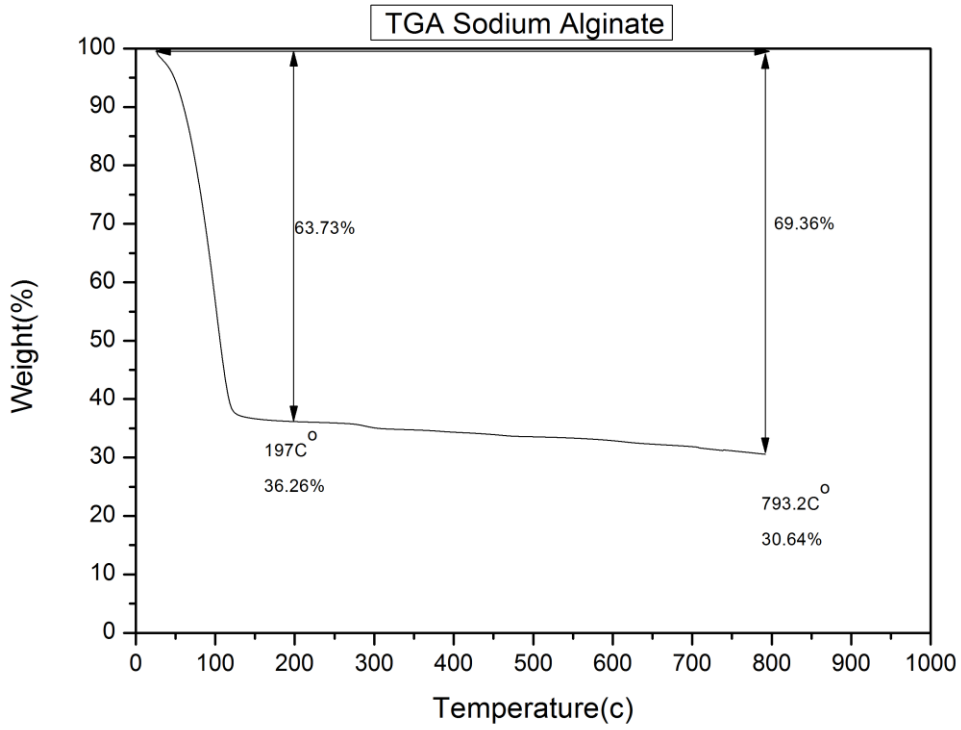

Figure 5-4 Thermogravimetric analysis of sodium alginate

5.3.3.2.2 Pyrophyllite

TGA curve Figure 5-5 showed that Pyrophyllite loses minute amounts of adsorbed water from 25^{o}C through 470^{o}C. This loss was about 1.18% and it may attribute to release of water molecules trapped at the clay surface. Hydroxyl water loss starts above 470^{o}C, and is nearly complete by 900^{o}C. A rapid weight loss was found between 840°C and 900°C. A possible explanation for this might be because the changing in crystalline structure and beginning of clay sintering.

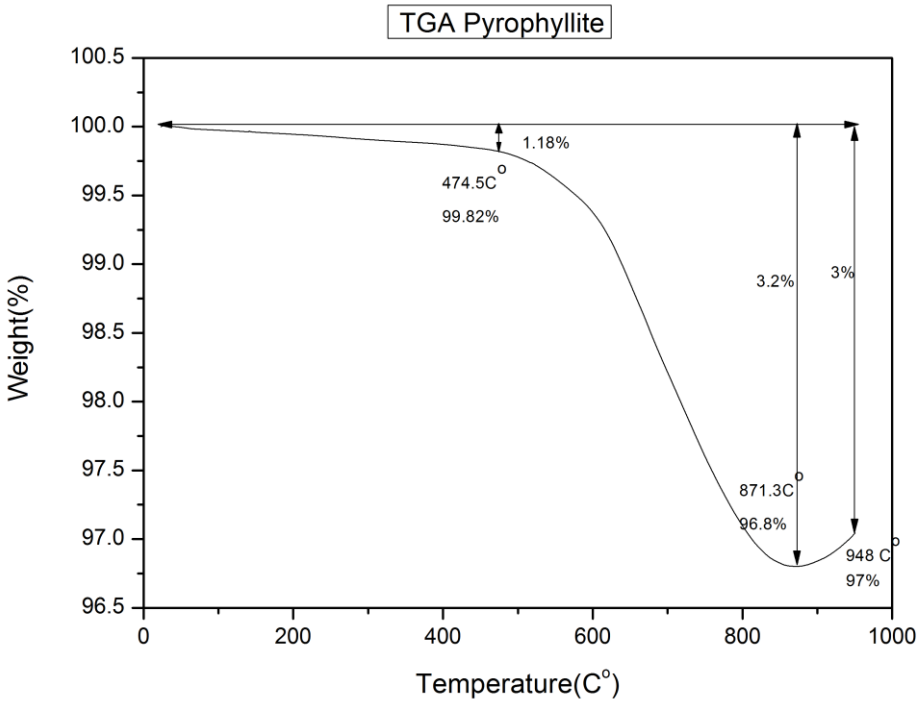

Figure 5-5 Thermogravimetric analysis of Pyrophyllite

5.3.3.2.3 Calcium alginate beads

As shown in Figure 5-6, the alginate beads start to lose their water molecules at temperature range between 26.5 and 177°C. These results were similar or comparable to previous study ((Laurienzo *et al.*, 2005). The initial temperature of polymeric decomposition started at 177.3°C for calcium-alginate beads, while the final decomposition temperature was observed at 837.1°C and residual left was 13.87%. At 200-800 °C, the weight loss rates of sodium alginate and calcium alginate beads remained basically the same. However, the major weight loss of calcium alginate beads occurred after 800 °C, which was 85.60%, whereas 69.36% of the weight of sodium alginate was lost before 800 °C (Figure 5-4). Between 100 °C and 200 °C, the weight loss of calcium alginate bead was higher than that of the sodium alginate, suggesting its moisture content was higher than that of the sodium alginate. Therefore, it can be inferred that the calcium alginate bead absorbed more water than the sodium alginate. This indicates the increment in the polarity and hygroscopicity of the calcium alginate bead that resulted from calcium intervention.

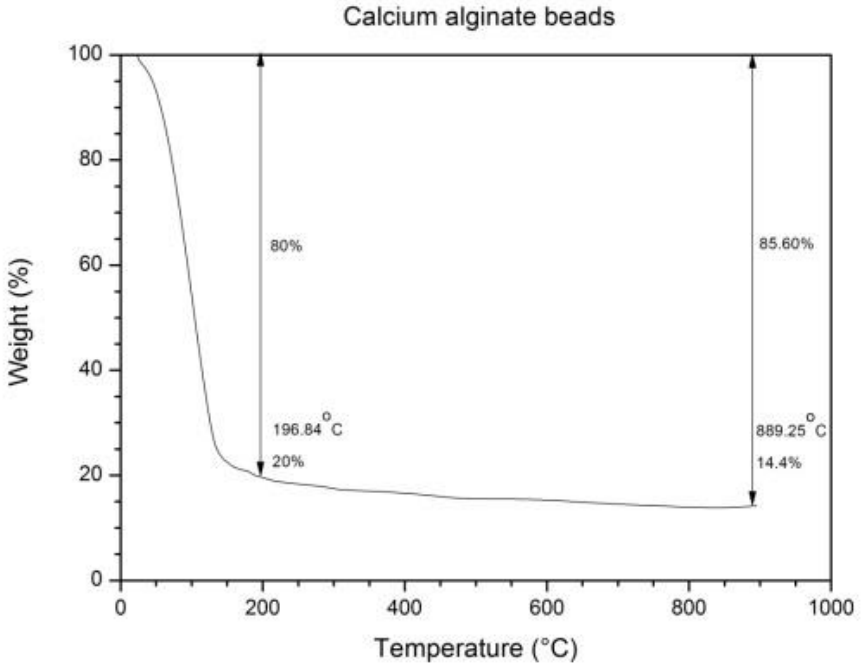

Figure 5-6 Thermogravimetric analysis of calcium alginate beads

5.3.3.2.4 Calcium-alginate –pyrax clay beads

The initial temperature of polymeric decomposition started at 173^{o}C for calcium alginate–pyrax clay beads, while the final decomposition temperature was observed at 774.7^{o}C and residual left was 42.8%. It is clear from Figure 5-7 that the calcium alginate–pyrax clay beads loss only 56.41% from their weight after 800 ^{o}C, which is apparently lower than that of the calcium alginate beads. Therefore, addition of pyrophyllite clay to the beads show an improvement of thermal stability compared with calcium alginate beads. This improvement was attributed to the high thermal stability of the Pyrophyllite (Pyrax clay) (Figure 5-7) and the strong interaction between the Pyrx particles in the alginate matrix. Pyrophyllite incorporation with the alginate matrix will restrict the alginate networks motions leading to a more stable matrix in the case of Ca-alginate- pyrophyllite beads. A more concentrated composition on the surface of the heat-exposed sample will develop to protect the majority of the sample from heat and reduces the mass loss rate during thermal decomposition (Leszczyńska *et al.*, 2007).

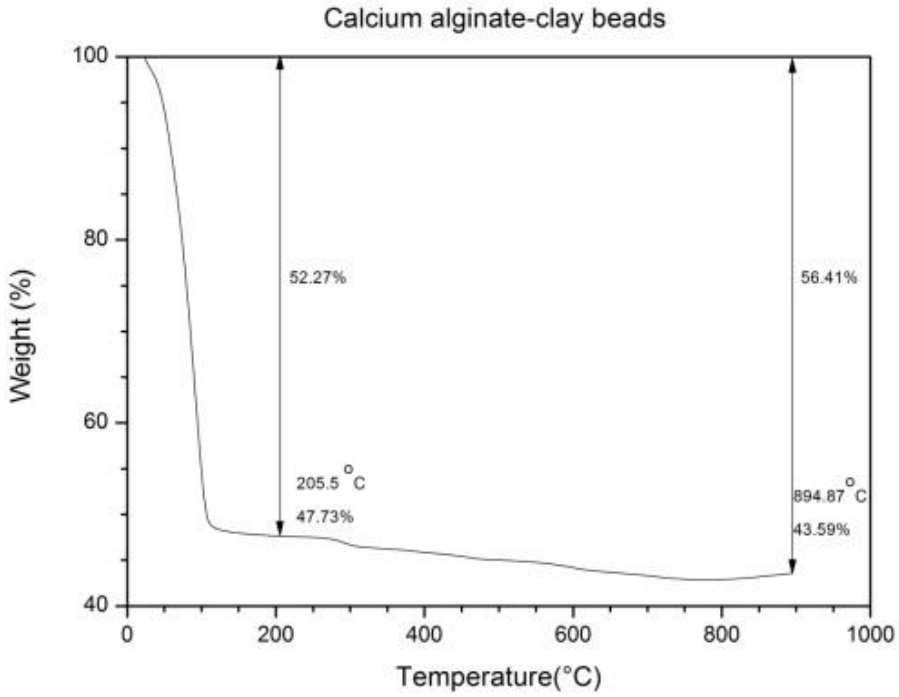

Figure 5-7 Thermogravimetric analysis of Calcium alginate-clay beads

5.3.3.3 Scanning electron microscopy analysis

The samples were dried at 50 °C for 24 h before coating with gold for scanning electron micrographs (SEM) analysis. SEM image of cross-section through Ca-alginate beads exhibited (Figure 5-8 A) a compatible homogeneous blends, whereas the Pyrophyllite particles were distributed homogeneously in the matrix.

The surface texture of Ca-alginate-clay beads (Figure 5-8 B) appears to be having caves surrounded by protruding barriers. However, the thickness and height of these barriers are small; this may be attributes to small particle sizes of pyrophyllite included as filler. The smaller the particle sizes of filler the smoother surface can be gained. Therefore the rougher surfaces can be achieved by using bigger particle size filler or no inclusion of filler can produce a rougher surface as well. However, such rough surfaces are believed to lead to predictable collapse (Zohar-Perez, Chet and Nussinovitch, 2004). It has been approved by Adzmi et.al. (2012,), that the addition of filler such as montmorillonite clay was found to improve the sphericity, flowability, density, visual quality and rigidity of the beads, which are desirable qualities for processing, handling and consumer usage. These characteristics stemmed from the filler's ability to fill-in the interstitial voids and strengthen the alginate hydrogel matrix (Adzmi *et al.*, 2012).

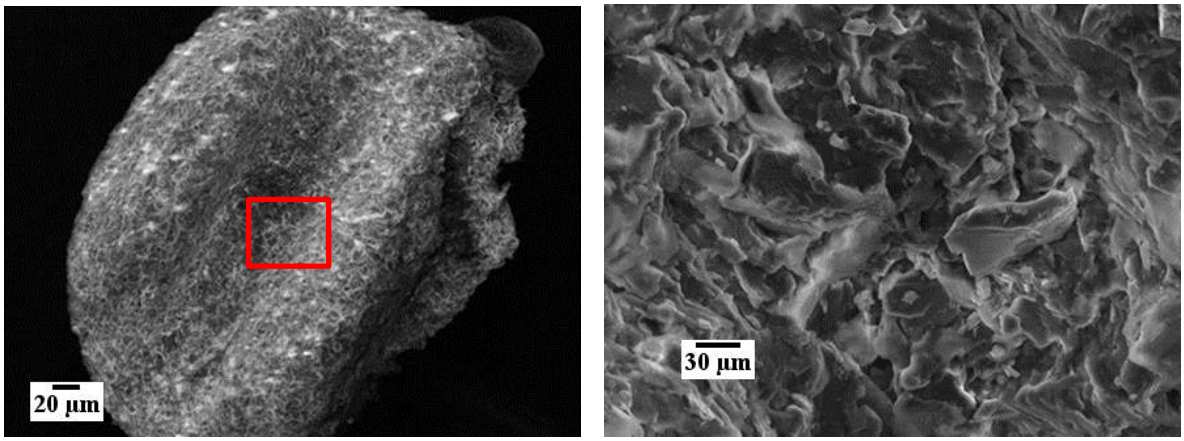

A) Surface texture of calcium alginate-clay beads B) Cross section of calcium alginate-clay beads

Figure 5-8 Scanning electron microscopy of calcium alginate-clay beads

5.3.3.4 EDAX analysis

EDAX analysis was used to study the elemental composition in the calcium alginate-clay beads. The area enclosed by a red square in Figure 5-8A has been examined and the elemental composition results as shown in Table 5-3 and Figure 5-9 indicate the presence of three main elements: Si, O and Al in high quantities. The beads composed mainly of 23.30 % Si, 53.02 % O and 9.40 % Al. These elements proved the presence of SiO_2 and Al_2O_3 that derived from clay material. As SiO_2 and Al_2O_3 are the major components of the pyrophyllite clay, it can be confirmed that the clay elements are existed in the beads.

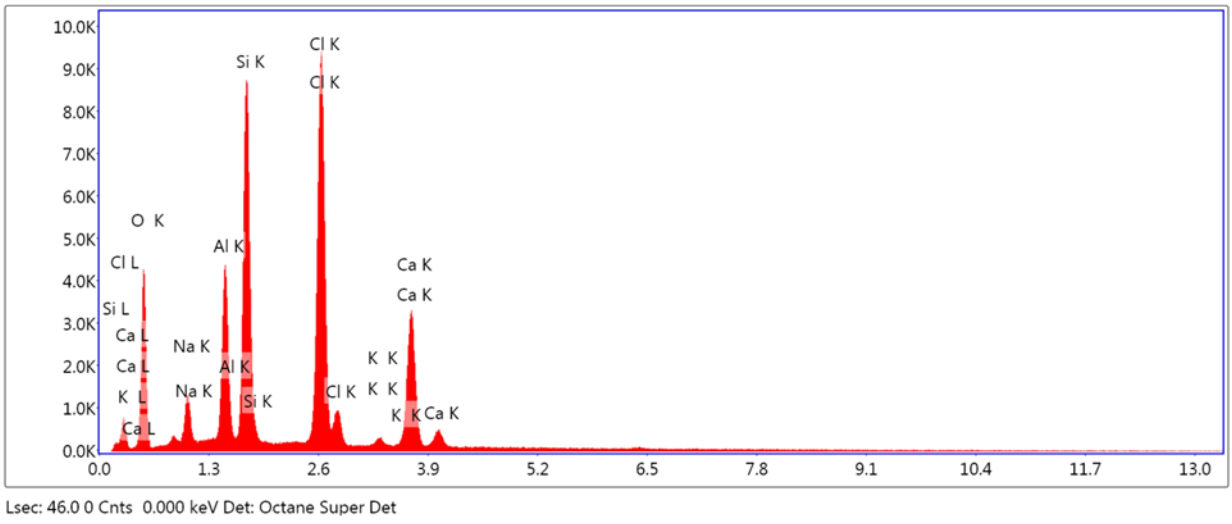

Figure 5-9 EDAX analysis of calcium alginate-clay bead

Table 5-3 Elemental of calcium alginate-clay bead analysis from EDAX

Element	Weight %	Atomic %	Net Int.	Error %
O K	36.17	53.21	592.80	9.80
NaK	3.21	3.28	151.73	9.04
AlK	7.44	6.49	742.36	4.80
SiK	15.70	13.15	1656.92	4.04
ClK	24.00	15.93	2067.58	2.79
K K	0.59	0.35	41.20	12.82
CaK	12.91	7.58	790.16	

5.4 Interim conclusions

The work in this chapter was undertaken to prepare a calcium alginate-clay beads to encapsulate B. sphaericus spores and evaluate beads ability to preserve Bacillus Sphaericus viability. The beads were prepared in this study by mixing sodium alginate and Pyrophyllite (Pyrax) clay solution and then cross-linking them with $CaCl_2$ solution. The characterization of calcium alginate-clay beads encapsulated with Bacillus Sphaericus was thoroughly examined. The followings conclusions are drawn from the experimental results presented in the chapter:

1) Microorganism's viability and survivability after long storage period requirements could be significantly more important than other basics one.
2) In beads formation, thus, incorporating an additional substance with the active ingredient seemed to be daunting task without affecting cells' viability.
3) Adding pyrophyllite clay provided a porous gel matrix with more spaces to occupy bacterial spores.
4) There established a strong interaction between the functional group of pyrophyllite and alginate.
5) Pyrophyllite was well dispersed in alginate matrix, therefore, the Calcium-alginate-pyrophyllite beads structure was stable and firm compared with alginate beads. The

surface and cross section characteristics of Ca-alginate-Pyrophyllite beads shown by the SEM micrographs and EDAX analysis have supported this conclusion.

6) Calcium-alginate- pyrophyllite beads had much improved thermal stability compared to calcium alginate beads, with the initial temperature of decomposition starting at 173^{o}C and final decomposition temperature at 774.7^{o}C and residual left 42.8%.
7) Furthermore, the matrix was suitable for Bacillus Sphaericus encapsulation and preservation of spore's viability over time.
8) The developed calcium-alginate-pyrophyllite was able to maintain the viability of the bacteria tested throughout capsulation preparation.
9) Calcium-alginate-pyrophyllite capsules/beads had excellent swelling capacity under alkaline condition with water absorption of 433%, while maintained their integrity.
10) For spore release, the swelling property of the matrix was crucial; however, excessive swelling could result in weak concrete. The swelling capacity of alginate-clay beads was still low (4.4 g/g of beads in cement filtrate) compared to the alginate beads without clay addition, the capsules showing 10% expansion only in the first hour. However this absorption capacity is pretty much enough for providing spores with essential water to germinate.

Chapter 6: Effect of bacterial spores encapsulated in calcium alginate-Pyrophyllite clay beads on mortar specimens

6.1 Introduction

Microbially induced calcium carbonate precipitation is an eco-friendly and cost effective repairing technique that offers huge potential in innovative engineering applications. Bacterial cells or spores incorporated in the concrete matrix may crash during mixing process or even during cement hydration. The reason is only limited space will be available during further hydration and formation of a dense cement matrix. As most of the bacterial size is bigger than the matrix pore diameters, which are smaller than the 0.5 ml, the probability of squeezing the bacteria squeezed inside the pores would be very high. Furthermore, the bacteria could be damage due to the mechanical stresses during mixing process. For these reasons, it is preferable to encapsulate the bacteria prior their addition to concrete matrix. The encapsulation material must possess a number of key features. It need to be semipermeable, have shell function to shield bacteria and should not affect the fresh and hardened concrete properties.

It is also important to investigate the effect of the amount of capsules added to the mixture on the mechanical properties of mortar specimens. The effect of bacteria on the compressive and flexural strength of concrete will also be investigated in this chapter. The calcite precipitates were visually examined by SEM and the characterised by EDAX. Even though many studies have been carried out to study the ability of applying microbial $CaCO^3$ as self-healing material in concrete, studies have not yet demonstrated the effect of different concentration of calcium source and nutrients altogether on the mechanical properties of cement mortar.

6.2 Materials

6.2.1 **Microorganisms**

Two species, Bacillus Sphaericus 57 and bacillus sphaericut 58 were taken from the microbiology bank at Brunel University London and used in this study. Nutrient agar medium was prepared to culture the two strains. This media consists of 2 g Yeast extract, 1g meat extract, 5g peptone, 5g sodium chloride and 15g agar per liter distilled water. To stimulate sporulation (spore formation), strains have to plate on a low nutrient medium to let them deplete the food source as starvation or nutritional depletion was found supporting sporulation (Su, Qi and Cai, 2012). Therefore, nutrient medium were modified by adding half

of the components with the same amount of agar (15g/L). Bacterial cultures were aerobically incubated at 30^{o}C for 4 days and vegetative growth and sporulation were observed periodically. To harvest the spores, cultures were collected by sterile disposable loops and washed by centrifuging and resuspending in 200ml ice-cold de-ionised water repeatedly. Spore concentrations in water suspensions were quantified by cell counting hemocytometer and the suspension were kept in a fridge at 4^{o}C and protected from light until use.

6.2.2 **Bio-reagents**

The bio-reagents used in this study included the nutrients for bacteria (yeast extract) and the deposition agents (urea and Calcium acetate). As B.sphaericus are ureolytic bacteria and proposed to heal cracks based on urea hydrolysis, urea and yeast extract are required as energy and carbon sources for grows. The bio-reagents added into the matrix of the specimens in a proportion of 1:2.25:3 yeast extract: urea: calcium acetate. The ingredients were used in proportions similar to those in research elsewhere. As the calcium acetate used in this study contains water, therefore, and in order to use the exact amount of the calcium salt, the final weigh of the mixing water added to mortar mixture was calculated by subtracting the amount of water in calcium acetate. Individual reagents were continuously dissolved in pure water before adding to mixing water.

6.2.3 **Immobilization of bacterial spores in calcium-alginate-clay beads**

Beads were fabricated using the sodium alginate (the most abundant polysaccharide distributed in the cell walls of brown alga) along with pyrophyllite (Pyrax clay) as a bulking agent. A droplet technique were used to obtain the alginate-clay beads, which involves preparing sodium alginate and clay solution in water and dropping this solution into the beaker containing 0.25 M calcium chloride solution through pasture pippette with a 1 mm diameter orifice to form alginate beads about 2 mm in diameter.

6.3 Methods

6.3.1 **The optimum ratio of calcium alginate-clay beads**

To investigate the optimum ratio of calcium alginate-clay beads, various mortar mixtures were designed. The addition of the beads was 0, 0.5, 1, 2, 3, 4, 5, 6, and 7% of the cement (by weight). For all mixtures, dry beads were wetted initially with a part of the mixing water before adding the remaining materials. Mixing was continued until a uniform and flowing mixture was obtained. After casting, the moulds were placed in an air-conditioned room

(20oC, >95% RH). In this study CEM I (CEMEX, Rugby, UK) complying with BS EN 197-1:2011 was used to make prismatic mortar specimens (40mm × 40mm × 160mm, n = 3). Water-to-cement ratio (w/c) of each mixture was 0.5 and cement-to-sand ratio was 1:3. Cement content is variable depending on the amount of beads added as presented in Table 6-1.

6.3.2 **The optimum ratio of precursors and nutrients**

A series of Portland cement mortar were made by replacing 0.5, 1, 3 and 5% of cement with bio-reagents, including the nutrients for bacteria (yeast extract and urea) and the precursor or deposition agent (calcium acetate). Mixing and curing procedures were followed similarly to the previous sub-section, 6.3.1. Cement content is variable depending on the amount of precursors and nutrients added as presented in Table 6-1.

6.3.3 **Bacterial spores incorporation method**

To study the effect of bacterial spores added directly or encapsulated in calcium alginate-clay matrix on the mechanical behaviour of cement mortar, six different series were used. Group R are the specimens without any additions. Group RP are the specimens with bio-reagents added, including the nutrients for bacteria (yeast extract and urea) and the precursor or deposition agent (calcium acetate). Group PPT58 is the specimens with bio-reagents and Bacillus Sphearicus spore 58 beads added. Group PPT 57 was the specimens added with bio-reagents, Bacillus Sphearicus spore 57 beads. Groups SP 57 and SP58 are the specimens with bio-reagents and Bacillus Sphearicus spore 57 and Bacillus Sphearicus spore 58 added, respectively. The bacterial spore's concentration used in SP 57 and SP58 series was 1×108 spores/cm3 of cement mortar. The amount of the bio-reagents was about 3% (by weight) of cement. Dry beads were wetted initially with a part of the mixing water before adding the remaining materials. The amount of beads added in PPT58 and PPT 57 series was 3% (by weight) of cement provided that the bacterial spore's concentration remains 1×108 spores/cm3 of cement mortar. Water-to-cement ratio (w/c), cement-to-sand ratio of each mixture, mixing and curing procedures was followed similarly to the previous sub-sections, 6.3.1 and 6.3.2. Cement content is variable depending on the amount of bio-reagents and beads added as presented in Table 6-1.

Table 6-1 Composition of the mortar (for three prismatic specimens (40mmx40mmx160mm))*

Series	Description of mixtures	Cement (g)	Sand (g)	Water (g)	Bead (g)	Calcium acetate (g)	Yeast extract (g)	Urea (g)
The optimum ratio of calcium alginate-clay beads								
PPT 0%	No calcium alginate-clay beads	450	1350	225	-----	------	------	-----
PPT 0.5%	Calcium alginate-clay beads (0.5%)	447.75	1350	225	2.25	------	------	-----
PPT 1%	Calcium alginate-clay beads (1%)	445.5	1350	225	4.5	------	------	-----
PPT 2%	Calcium alginate-clay beads (2%)	441	1350	225	9	------	------	-----
PPT 3%	Calcium alginate-clay beads (3%)	436.5	1350	225	13.5	------	------	-----
PPT 4%	Calcium alginate-clay beads (4%)	432	1350	225	18	-------	------	-----
PPT 5%	Calcium alginate-clay beads (5%)	427.5	1350	225	22.5	------	-----	----
PPT 6%	Calcium alginate-clay beads (6%)	423	1350	225	27	------	------	-----
PPT 7%	Calcium alginate-clay beads (7%)	418.5	1350	225	31.5	------	------	-----
The optimum ratio of precursors and nutrients**								
RP 0%	No Nutrients and precursors	450	1350	225	-----	-----	-----	-----
RP	Nutrients and precursors (1%)	445.5	1350	225	------	2.16	0.72	1.62

1%								
RP 3%	Nutrients and precursors (3%)	436.5	1350	225	------	6.48	2.16	4.86
RP 5%	Nutrients and precursors (5%)	427.5	1350	225	------	10.8	3.6	8.1
Bacterial spores incorporation method								
R	Nothing added	450	1350	225	-----	------	------	-----
RP	Nutrients and precursors (3%)	436.5	1350	225	-----	6.48	2.16	4.86
SP57	Bacillus Spearicus 57	436.5	1350	225	-----	6.48	2.16	4.86
SP58	Bacillus Spearicus 58	436.5	1350	225	-----	6.48	2.16	4.86
PPT57	Encapsulated Bacillus Spearicus 57(3%)	423	1350	225	13.5	6.48	2.16	4.86
PPT58	Encapsulated Bacillus Spearicus 58(3%)	423	1350	225	13.5	6.48	2.16	4.86

*Mortars were prepared in accordance with BS EN 196-1(BSI, 2005)

**The bio-reagents (Nutrients and precursors) added into the matrix of the specimens in a proportion of 1:2.25:3 yeast extract: urea: calcium acetate. (Wang *et al.*, 2014a).

6.3.4 **Analytical methods**

The Three-Point bending test is conducted on a loading frame to determine the flexural tensile strength on standard prism specimens of size 40mm x 40mm x 160mm. The specimens were cured in water for 28-days before testing. Compression test on the two cubic halves from the broken prismatic specimen of the flexural strength test was determined by using the Instron universal testing machine (UTM) in accordance with the British Standard BS EN 196-1:2016. All samples used for flexural, compression tests were water cured until reaching the testing age of 28 days. The Scanning Electron Microscope (SEM), an ultra-high performance field emission scanning electron microscope Zeiss Supra 35VP, was used to observe the microstructures, and the Energy Dispersive X-ray Analysis (EDXA) was used to

define the chemical composition of the resulting products. More details have been stated in Chapter 3.

6.4 Results and discussions

6.4.1 **Influence of calcium alginate-pyrophyllite beads on the mechanical properties of cement mortar**

6.4.1.1 Compressive strength

In this part of study, the effect of addition of calcium alginate beads without bacterial incorporation on compressive strength was investigated in order to find the optimum possible quantity of beads must be added without adversely affecting the strength properties of cement mortar. Figure 6-1 shows the variation in compressive strength of cement mortar with addition of 05%, 1%, 2%, 3%, 4%, 5%, 6% and 7% of beads.

As seen from the Figure 6-1and Table 6-2, there is a tendency for the calcium alginate-clay to induce a decrease of compressive strengths with high beads amount, when the amount of beads was 6% and 7%, the compressive strengths decreased by 18% and 25.7%, respectively. With a small amount of beads (0.5%), compressive strength increase up to 9.2% compressive strength. However, the highest value of compressive strength happened when the amount of beads added to the mortar mixture was 3%; the gain in strength as compared to control mix was 13.5%. It should be noted that in cement mortars small holes could be generated while making the specimens. The diameter of the beads is between 2 to 3 mm and it is supposed that the increase of strength for small amounts of calcium alginate-clay should come from the filler effect in the mortar specimens. These findings are consistent with another research showing that more defects may be formed and the strength decreases with further increases in the beads amount (Wang *et al.*, 2013). The reduction in compressive strength when larger amount of beads was used could be attributed to the negligible strength of the calcium alginate-pyrophyllite beads. Therefore, a higher concentration of beads yielded weaker compressive strength. This trend that has been observed in another study, since the beads added in cementitious materials are generally the weakest link within the matrix and do not contribute to strength (Hassan *et al.*, 2019).

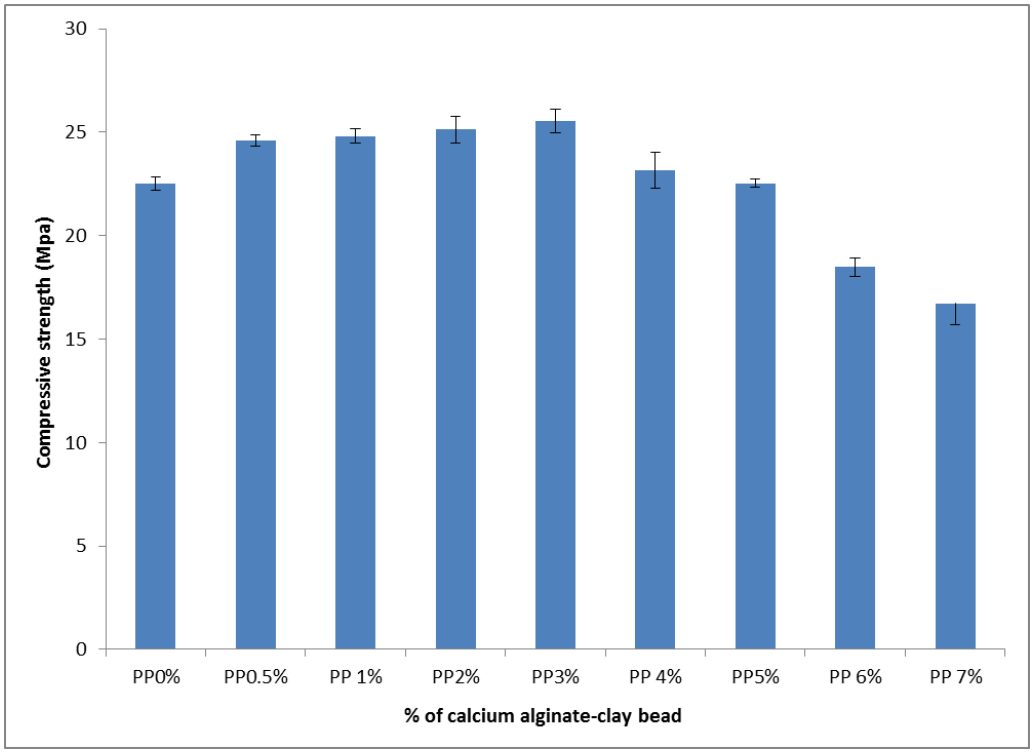

Figure 6-1 Compressive strength of the specimens (with different additions of beads, 0% (R), 0.5%, 1%, 2%, 3%, 4%, 5%, 6%, and 7% of cement by weight, respectively) at the age of 28 days

Table 6-2 Average of 28 days compressive strength of cement mortar with different additions of beads

Mix	% of beads	Compressive strength (Mpa)	SD	CoV%
R	0	22.51	0.34	1.51
PPT0.5%	0.5	24.59	0.28	1.14
PPT1%	1	24.82	0.35	1.42
PPT2%	2	25.13	0.65	2.60
PPT3%	3	25.54	0.56	2.20
PPT4%	4	23.16	0.86	3.71
PPT5%	5	22.54	0.22	0.96
PPT6%	6	18.48	0.44	2.40
PPT7%	7	16.72	1.00	6.00

6.4.1.2 Flexural strength

Figure 6-2 shows the variation of flexural strength versus the amount of calcium alginate-clay bead. The horizontal axis is the amount of bead in percent (%). The vertical axis is the flexural. Herein, for convenience of expression, sample with 0% beads was treated as a reference. Its flexural strength was 4.50 Mpa. The error bars in the figure indicated the standard deviation for each data, in which the maximum was 0.35.

For beads incorporating mixes, the flexural strength behaviour is slightly better comparing to control mixes; the flexural strength was slightly increased only for a dosage of capsules up to 3%. Then the flexural strength of the specimens starts to decrease gradually until the capsules addition of 7%. As can be seen in Figure 6-2 and Table 6-3, the flexural strength was increased from 2% to 17.8% with increasing addition of 0.5% to 3% capsules. While this increase in strength start to be less with addition of 4 and 5% of capsules. By increasing the addition to 6% and 7% capsules, the flexural strength start to decrease by 3.8% and 8.9% comparing to R specimen. The negative effect of adding larger amount of beads on flexural strength of mortar may be due to macro pore formation by the calcium alginate-pyrophyllite beads. A hollow macro pore remains as the beads absorb part of the mixing water and only release it during mortar setting. The flexural strength is reliant on the overall amount of macro pores and air voids in the cross sectional of the tested sample.

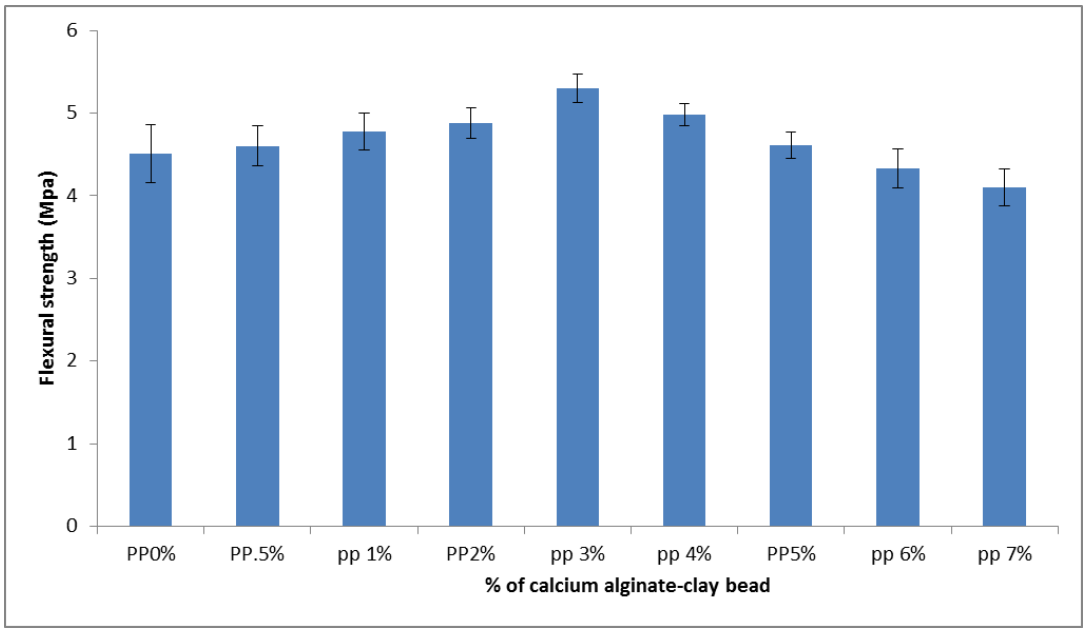

Figure 6-2 Flexural strength of the specimens (with different additions of Bacteria capsules, 0% (R), 0.5%, 1%, 2%, 3%, 4%, 5%, 6%, and 7% of cement by mass, respectively) at the age of 28 days.

Table 6-3 Average of 28 days flexural strength of cement mortar with different additions of beads

Mix	% of beads	Flexural strength (Mpa)	SD	CoV%
R	0	4.50	0.35	7.85
PPT0.5%	0.5	4.60	0.24	5.29
PPT1%	1	4.78	0.22	4.65
PPT2%	2	4.88	0.18	3.79
PPT3%	3	5.30	0.17	3.26
PPT4%	4	4.98	0.14	2.73
PPT5%	5	4.61	0.16	3.39
PPT6%	6	4.33	0.23	5.41
PPT7%	7	4.10	0.22	5.46

6.4.2 **Effect of nutrient on mortar strength properties**

The incorporation of the organic bio-mineral precursor compounds to the material matrix is essential to further improve the bacterial self-healing mechanism; however, they possibly have an unfavourable effect on strength characteristics. Therefore, current research focuses on the incorporation of the organic compounds with different dosages amounted to (0%, 1%, 3% and 5%) of cement weight and their potential influence on compressive and flexural strength (Figure 6-3).

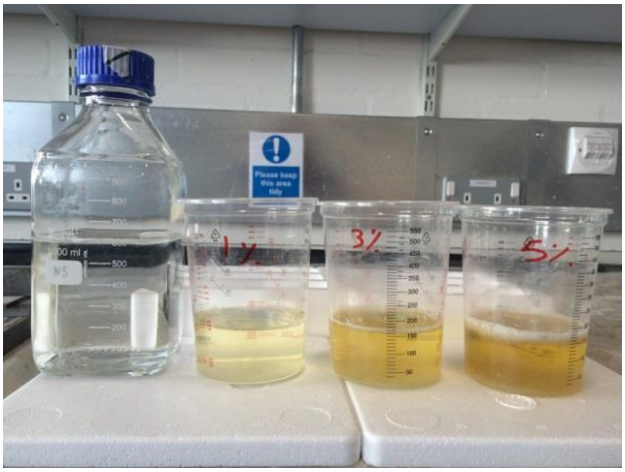

Figure 6-3 Different dosage of Organic Compound

Sets of 12 replicate test specimens with dimensions of 40×40×160 mm were prepared from Ordinary Portland cement and sand (1:3) and a water to cement weight ratio of 0.5 with and without (control) organic compounds additions and tested for compressive and flexural strength after 7 and 28 day curing.

In spite of its detrimental effect on the steel bar and durability of reinforced concrete, Calcium Chloride $CaCl_2$ is the most popular calcium source of microbially induced calcium carbonate precipitation MICP (Zhang, Guo and Cheng, 2014). For that reason, an alternative calcium source and its possibility to induce calcium carbonate precipitation without harming other mortar properties was used as deposition agents and investigated in this chapter.

As indicated by previous study, the microbial mortars treated with calcium acetate showed a higher compressive strength (about twice) than those of the mortars treated with the other calcium sources. Therefore, Calcium acetate Ca (CH3COO)2 is found to be the most suitable calcium source among other calcium compounds for the application of MICP. In addition to that, using calcium acetate shows significant benefit in inhibiting the chloride ion that causes steel bar corrosion (Zhang, Guo and Cheng, 2015). As B.sphaericus are ureolytic bacteria and proposed to heal cracks based on urea hydrolysis, urea and yeast extract are required as energy and carbon sources for grows. However, it has been stated that the compressive strength may decrease from 50% to 90% depending on the amount yeast extract added, while urea has no substantial effect on compressive strength of mortar specimens (de Rooij et al., 2013; Jonkers et al., 2010). In another study, it was observed that addition of urea and yeast extract to the mortar mixture reduces the compressive strength between 16% and 24% mostly because of the presence of 1% w/w cement of yeast extract (Erşan et al., 2015b) . It can thus be suggested that adding calcium acetate along with nutrients will possibly

overcome the negative effect of yeast on mortar compressive strength. Therefore, the combined effect of the calcium acetate, urea and yeast extract on the compressive strength has been studied in this part.

The results obtained from the test of cement mortar with 1, 3 and 5% w/w cement of nutrients are presented in Figure 6-4 and Table 6-4. In this figure; there is no significant increase in the 7 days compressive strength among all the mixtures. However, a clear trend of increasing in 28 days compressive strength can be noticed comparing to control specimen. The highest increment was 20.3% when 3% nutrient was added. Only 11.45% and 14.85% increase in compressive strength were detected in the mixture with 5% and 1%nutrient added. According to these data, it can be inferred that 3% is the optimum amount of reagent can be used not only to avoid the deterioration effect of nutrient, but to enhance the strength properties. As the bio-reagents added into the matrix of the specimens in proportion of 1:2.25:3 yeast extract: urea: calcium acetate, 3% of cement weight reagent means 1.44% of cement calcium acetate. In accordance with the present results, previous study has demonstrated that the compressive strength of cement mortar impaired by adding more than 2% calcium acetate. The reduction in strength has been caused by a decrease in both the pH of the cement paste and the acetic acid hydration (Kim et al., 2016). In another study which set out to determine the effect of using calcium acetate on the performance of silica fume blended cement, El-didamony et al. found that with addition of 2.0%wt of calcium acetate, the compressive strength will increase, whereas adding more calcium will negatively affect the compressive strength (El-Didamony et al., 1999).

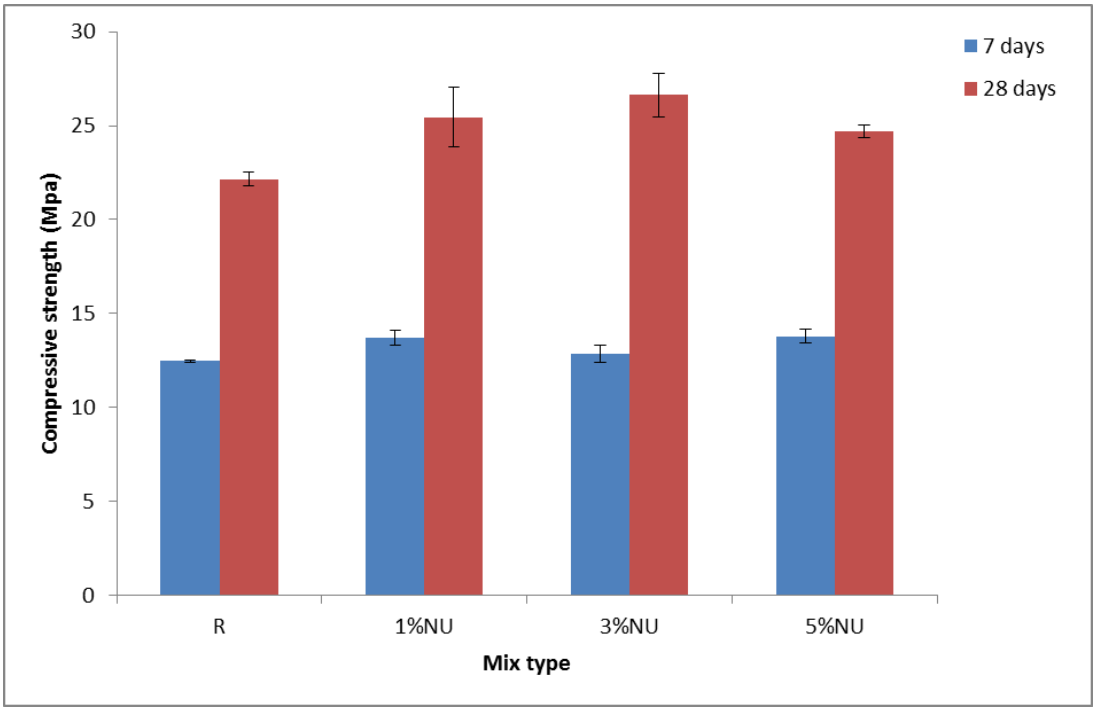

Figure 6-4 the effect of different amount of nutrients on compressive strength of cement mortar

Table 6-4 Average of 7 and 28 days compressive strength of cement mortar with different amount of nutrients

Mix	Compressive strength (Mpa)					
	7 days	SD	CoV%	28 days	SD	CoV%
R	12.47	0.04	0.34	22.15	0.39	1.74
1% Nu	13.71	0.39	2.87	25.44	1.59	6.24
3% Nu	12.86	0.44	3.42	26.65	1.16	4.34
5% Nu	13.79	0.39	2.79	24.69	0.35	1.42

6.4.3 **Influence of the directly added and encapsulated spores on the mechanical properties of mortar**

6.4.3.1 Compressive strength

Cement mortar specimens (40 mm×40 mm×160 mm) of similar ages with a water-to-cement weight ratio of 0.5 and with either incorporated encapsulated bacterial spores (1×10^8 B. Sphaericus 57 and 58 spores/cm^3) or direct addition of the same bacteria spores with same

concentration have been tested for compressive strength using a load-controlled universal testing machine and compared with control specimens. The compressive strength of the specimens with both bacterial strains (encapsulated and directly added spores) and the organic compounds (yeast extract, urea and calcium acetate) as a source of energy were examined to see what effect bio-healing agents would have when they were added together. The quantity of organic compounds used for each mixture was 3% of cement weight.

The compressive strength test in this study was performed for the samples with the same contents. Cement, sand, water, water-cement ratio and sand-cement ratio were the same for all mixtures, despite the addition of the calcium alginate beads and the organic compounds into some of the mixes.

The compressive strength of cubes at 28 days was tested in a load-controlled universal testing machine. Table 6-5 presented the compressive strength of all the specimens. It can be noticed from the table that the compressive strength of the mixture with PPT 57 is higher than those of controlled and PPT 58 specimens at 28 days. The maximum percentage increase in compressive strength of about 20.13% is found in the mortar sample of PPT 57 compared to controlled specimen. Figure 6-5 graphically presents the difference of the compressive strength of controlled, nutrients only, SP57 (directly added Bacillus Sphaericus 57), SP58 (directly added Bacillus Sphaericus 58), PPT57 (encapsulated Bacillus Sphaericus 57) and PPT58 (encapsulated Bacillus Sphaericus 57) at 28 day. The compressive strength of mortar sample for all types of healing agents (Nutrients, direct addition of spores and encapsulated spores) show an increase compared to controlled mix. However, the rate of compressive strength gain was dependent on the bacterial strains used and method of spore's incorporation. The highest compressive strength increase occurs when Bacillus Sphaericus 57 was added directly: this enhancement reaches to 25.5% at 28 days. However, the increase of the compressive strength was less with additions of Bacillus Sphaericus 58 to the mortar mixture (17%). Therefore, if it is essential to obtain cement mortar with improved compressive strength, the choice of strain for self-healing requirement is important (Ghosh *et al.*, 2005).

As discussed above, addition of nutrients had also improved the compressive strength of the cement mortar. The increase of the strength was therefore due to the combined effect of addition of bio-healing agents. Even though encapsulating nutrients with spores in one capsule could significantly help spores germination under appropriate conditions (availability

of water and oxygen), it was not practicable to encapsulate water soluble compounds into calcium alginate beads for the moment. Therefore, the organic compounds were added to the matrix by dissolving them with the mixing water. Although mixtures with encapsulated Sphaericus spores and nutrients have a lower amount of cement than the control mixture and the Ca-alginate-Pyrophyllite beads containing the spores are much vulnerable comparing to other filler constituents, the average compressive strength at 28 days of mixtures with a bio-based agent is higher than the average compressive strength of the control mixes. The reason for the difference in compressive strength between mixtures with encapsulated Sphaericus spores and directly added spores could be attributed to lack of the effective contact between the encapsulated spores and the essential nutrients (Nikolić *et al.*, 2010).

The increase in compressive strength after addition of these bio agents, hence, could be attributed to the modifications in the microstructure. Precipitation of new hydration products, or changing the density distribution of hydration products has led to this microstructural changes. Careful monitoring of hydration products of the samples containing bio reagents confirm the presence of individual crystals ($CaCO_3$) within the cement–sand matrix and plugging the pores within the mortar by calcite precipitation ((Achal *et al.*, 2009; Ghosh *et al.*, 2005; Ramachandran, Ramakrishnan and Bang, 2001; Ramakrishnan, Bang and Deo, 1998). Therefore, the compressive strength was increased as a result of the bio reagents incorporation. The composition and the microstructure significantly affected the strength of the specimen. The microstructure and the degree of hydration of the specimen can be influenced by different factors such as w/c ratio, age of the specimen, aggregates grading, different curing condition, and admixtures, which have direct impact on strength development (Wang *et al.*, 2014a).

High dense (less porous) microstructure can be achieved by continuing hydration as pore spaces become smaller when occupied with solid phase leading to improvements in strength properties. The strength of cement mortar, therefore, is closely related to its microstructure.

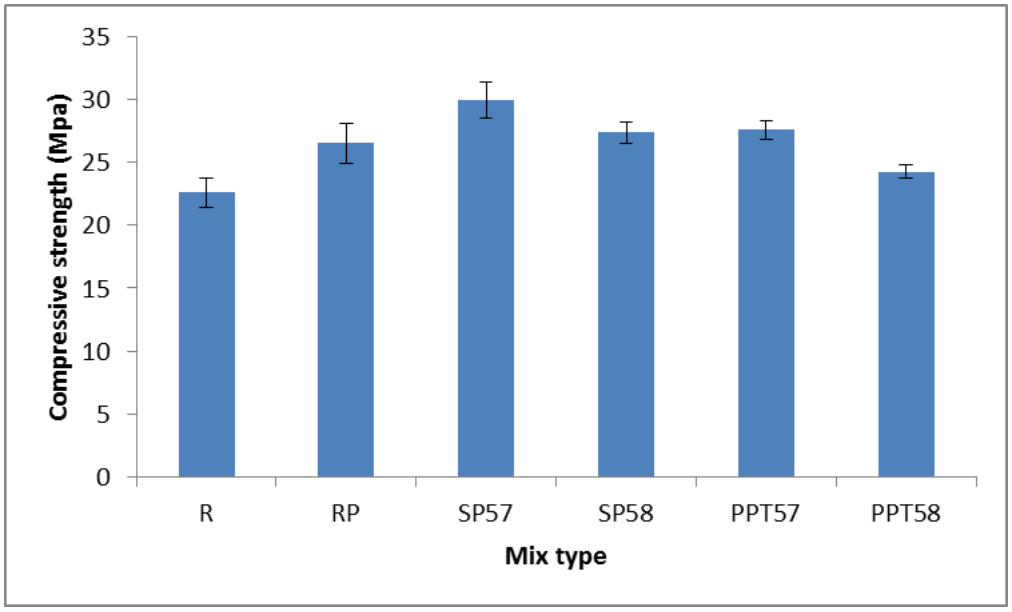

Figure 6-5 Compressive Strength of cement mortar with direct addition and encapsulated of bacterial spores

Table 6-5 Average compressive strength of cement mortar with directly added and encapsulated spores different bacteria strains

Mix	Average compressive strength(28 days) Mpa	Standard deviation SD	CoV%
R	22.38	1.15	5.15
RP	24.36	1.56	6.40
SP57	28.09	1.42	5.11
SP58	26.19	0.87	3.33
PPT57	26.89	0.74	2.74
PPT58	25.02	0.54	2.15

6.4.3.2 Flexural strength

Flexural strength of all cement mortar mixtures are found by testing mortar prisms of size (40mmx40mmx160mm) by three points loading. An average of three test samples of the same compositions was used. The average results are tabulated in Table 6-6 and Figure 6-6 the flexural strength of SP57 mortar is higher than the other mixes. This means that the precipitation of $CaCO_3$ with calcium acetate and the bio deposition agent (Urea and Yeast extract) by direct addition of bacterial spores (SP57) has increased the flexural strength of the mortar. The addition of 3% of calcium acetate and bio deposition agents in mortar containing SP57 has increased the flexural strength by 27.2% compared to control. However, to confirm that this improvement is caused by the self-healing process, the microstructural analysis is of

great importance to study the crack healing in order to understand the healing mechanisms with and without the bio-based agents.

In both types of addition, Bacillus Sphaericus 57 showed the highest improvement, which might attributed to the highly ureolytic activity of SP 57 in the presence of calcium acetate, urea and yeast extract comparing to SP58. Spores encapsulated in calcium alginate-Pyrophyllite beads have also improved the flexural strength of the mortar. Incorporation of PPT57 in mortar has increased the flexural strength by 25.6% compared to control. However, this increase is lower than that of the mortar with directly added spores. This behaviour correlates well with the results obtained from the compressive strength test.

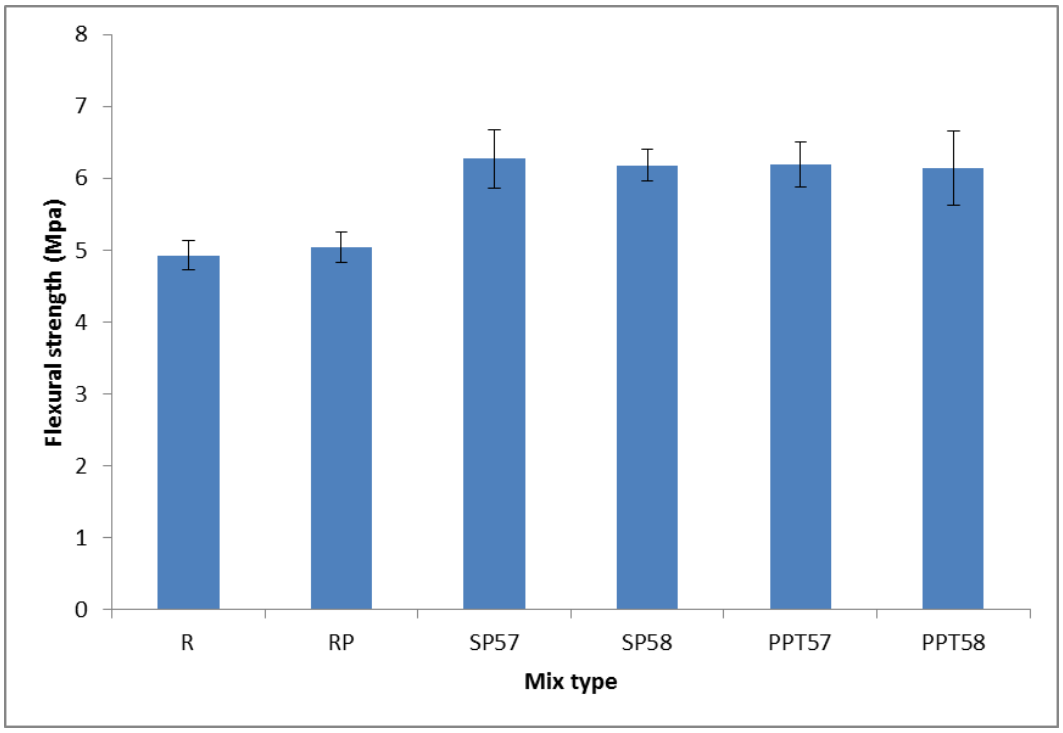

Figure 6-6 Flexural strength of mortar prisms with direct addition and encapsulated of bacterial spores

Table 6-6 Average flexural strength of cement mortar with directly added and encapsulated spores different bacteria strains

Mix	Average Flexural strength(28 days) Mpa	Standard deviation SD	CoV%
R	4.93	0.20	3.89
RP	5.04	0.21	4.08
SP57	6.27	0.41	6.51
SP58	6.18	0.22	3.56
PPT57	6.19	0.31	5.01
PPT58	6.14	0.52	8.40

6.4.4 **Influence of the encapsulated spores on the microstructure of mortar**

Specimens of all six mixes were subjected to scanning electron microscopy (SEM) analysis to examine the microstructural changes in concrete due to self-healing. Microstructural analysis was conducted on all specimens after 28 days of water curing to compare the self-healing process. In this study, attention is focused on production of calcium carbonate based crystals as it demonstrates the crack healing efficiency of individual mix. Three different polymorphs of calcium carbonate crystals; calcite, aragonite and vaterite are developed in the self-healing process (Rao *et al.*, 2013). Calcite is most abundant in nature, most thermodynamically stable structures and the least soluble mineral of the three forms. In Figure 6-7, all the calcium alginate-pyrophyllite beads are randomly distributed in the cross section of the prism sample of the cement mortar.

Figure 6-7 Mortar specimen contain 7% of cement weight calcium alginate-pyrophyllite beads

SEM images of all four mixes at 28 days specimens shown in Figures 6-10, 6-12 and 6-14 expressing the development of calcite crystals which are orthorhombic in nature (De Yoreo and Vekilov, 2003). The maximum calcium carbonate crystal precipitation is shown in the mixture of beads containing Bacillus Sphaericus 57 (Figure 6-12) comparing to nutrient only (Figure 6-10) and beads containing Bacillus Sphaericus 58 samples (Figure 6-14). The denser precipitation might indicate the highly ureolytic activity of bacillus 57 in the presence of calcium acetate, urea and yeast extract when they added directly. Figure 6-8 displays the SEM image of the fracture surface of control specimen (R). CH particle was clearly presented

with some unhydrated cement particles on the CH surface. The red arrow points to the area analyse by EDAX as shown in Figure 6-9.

Even though calcium carbonate can be created as a result of the catalysis action of both calcium acetate and bacteria, it can be produced in controlled samples as a by-product of CO_2 sequestration. In the presence of water, oxygen and adequate nutrients, bacteria play an important role in calcite formation by providing favourable environment for the bacteria to catalyse the conversion of calcium acetate (an organic calcium salt) into calcium carbonate. The calcite formation reaction by bacterial activity can be written as shown in equation 1.

$$CaC_4H_6O_4 + 4O_2 \longrightarrow CaCO_3 + 3CO_2 + 3H_2O \quad (1)$$

The concrete ability to precipitate calcium carbonate, is, as mentioned above, present in the controlled cement mortar samples. This deposition can occur due to penetration of moisture and gases such as carbon dioxide through pores in matrix and reaction with calcium hydroxide present in the hardened cement paste. This process is generally represented by the reaction shown in equation 2.

$$Ca(OH)^2 + CO_2 \longrightarrow CaCO_3 + H_2O \quad (2)$$

The mortar samples were further analysed by elemental distribution analysis (EDAX) spectra. It is a technique commonly used for qualitative analysis of materials, yet it is also able to provide a semi-quantitative results. The existences of calcium carbonate crystals are obvious but in small amounts in the nutrient only cement mortar through scanning electron microscopy and EDAX (Figure 6-11). This suggests that there is potential for calcium carbonate production through the carbonation process, albeit at a rate slower than that produced by bacterial metabolic activity.

Moreover, as calcium carbonate formed through carbonation process is directly related to the availability of dissolved carbon dioxide, thus, CO_2 in permeated water is generally not enough to convert calcium hydroxide to calcium carbonate. Additionally, upon contact with water, portlandite ($Ca(OH)_2$) dissolves because of its solubility reducing the amount of calcium hydroxide necessary to calcium carbonate formation.

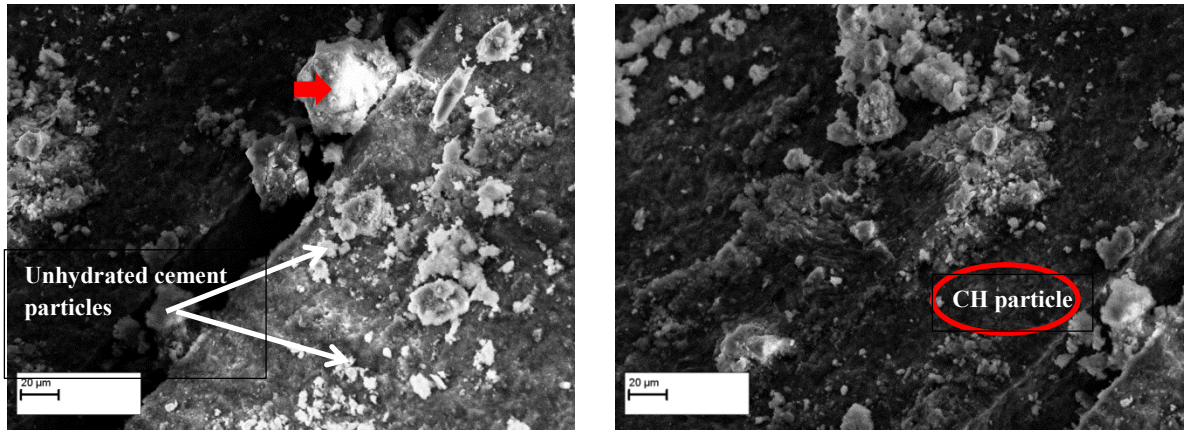

(a) (b)

Figure 6-8 SEM image of a fracture surface of control specimen (R) at 1000 x magnification,(a) showing unhydrated cement particles on the CH surface, the red arrow points to the area analyse by EDAX, (b) showing CH particle

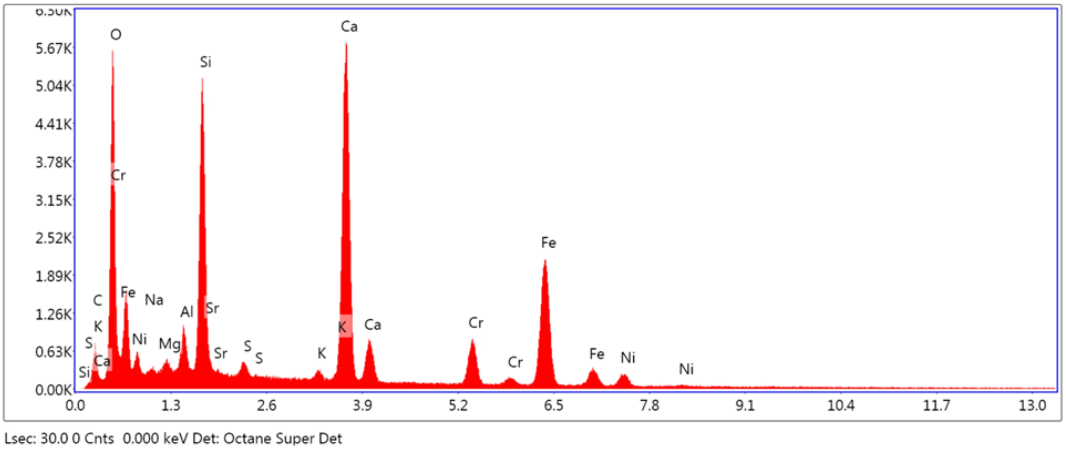

Figure 6-9 EDAX analysis of control mortar sample (R)

Table 6-7 Elemental composition of control mortar sample (R)

Element	Weight %	Element	Weight%
C K	6.2	O K	36.7
NaK	0.5	MgK	0.6
AlK	1.6	SiK	8.9
SrL	0.5	S K	0.6
K K	0.4	CaK	19.0
CrK	4.1	FeK	18.6
NiK	2.2		

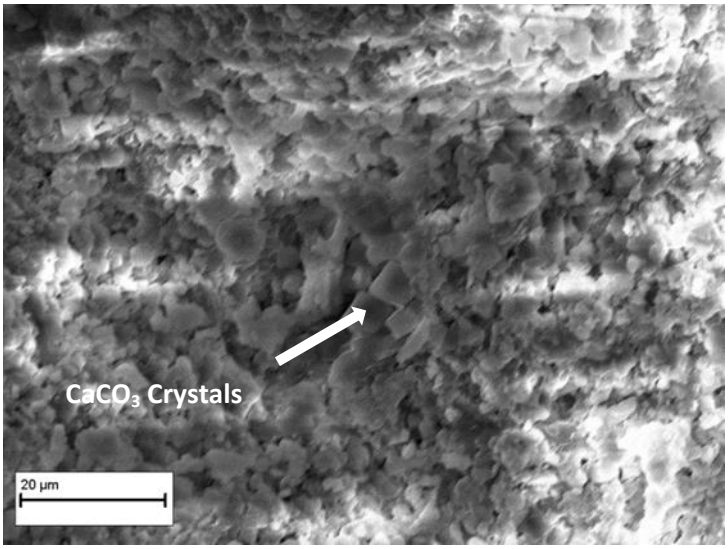

Figure 6-10 SEM image of Nutrients only specimen (RP) under 300 x magnification

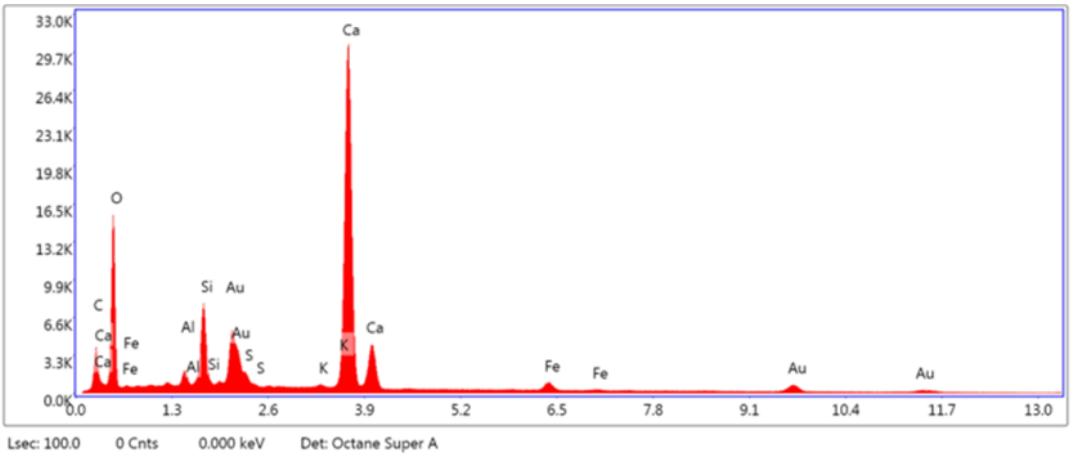

Figure 6-11 EDAX analysis of Nutrients only specimen (RP)

Table 6-8 Elemental composition of Nutrients only specimen (RP)

Element	Weight %	Element	Weight %	Element	Weight %
C	2.04	Si	4.16	Ca	53.20
O	19.16	S	0.89	Fe	2.64
Al	0.43	K	0.22	Au	17.27

In bacterial mortar, on the other hand, calcium carbonate precipitates in a different method with the existence of calcium acetate and bacteria. Bacterial metabolic conversion of calcium acetate into calcium carbonate leads directly to the formation of excess carbon dioxide which in turn used in the carbonation of calcium hydroxide. More calcium carbonate therefore can

be produced (Schlangen *et al.*, 2010). Here, the two Bacillus Sphaericus strains demonstrated urease activity that drove the biologically induced calcite precipitation confirming that these species are able to form calcium carbonate when grown under alkaline environmental conditions.

The area in fractured surface of sample PPT 57 with the most intense precipitate formation compared to sample PPT 58, produced an amorphous phases of calcium carbonate. These observations confirmed that the bacterial spores was successfully released, germinated and activated by the precursor (calcium acetate) and nutrients leading to produce a surplus of hydration products. SEM image of the reference sample (0% beads) is shown in Figure 6-8.

Apart from the network of hydration product created in the reference sample, an amorphous phases and crystalline have been autogenously deposited at the surface fracture, yet these crystals appear not be able to pack densely as the formed products in the bacterial capsules embedded samples. Figure 6-12 of PPT 57 display calcium carbonate crystals in a numerous, more densely packed than in the PPT 58 (Figure 6-14).

The EDAX- inspected areas of the surface fracture of PPT57 and PPT58 samples are marked as red box in Figures 6-12 and 6-14. It has been demonstrated by EDAX analysis of PPT 57 that the composition of precipitates was Ca, C, and O. According to theoretical calculations on the percentage of weight of $CaCO_3$, carbone, calcium and oxygen contents should be 12%, 40% and 48%, respectively. The weight percent (wt. %) of chemical elements has been found as follows: Ca = 25.53%, C = 11.54%, O = 62.12%. Typical differences in weight percent between theoretical and actual values are shown as 0.46%, 14.12 % and 14.47% for C, O and Ca, respectively (Table 6-9). The EDAX analysis of PPT58 sample showed the presence of the Ca, C and O elements in the precipitates with weight percent as follows: Ca = 36%, C = 10.7 %, O = 49.8%. Differences in actual and theoretical values are mainly caused by the other hydration products. The samples also contained traces of silica, which can be attributed to the production of other hydration product. Presence of Si, Al and Fe in the EDAX elemental analysis of reference sample proved the development of hydration products such as portlandite, calcium silicate hydrate and ettringite as well as calcium carbonate crystals (Figure 6-9). Due to the formation of these products, most cracks will be sealed quickly by a network of crystal filling and finally heals the materials. The dense network formed in the cracking area can support good healing. Since compositional data of the EDAX examination provide information only about the topmost part of the assessed area, there could be extra

precipitates that may form inside the matrix where the microscopic or EDAX analysis cannot be obtained. It is concluded that existence of crystalline calcium carbonate associated with bacteria suggested that bacteria provide nucleation sites for calcite formation during the mineralization process.

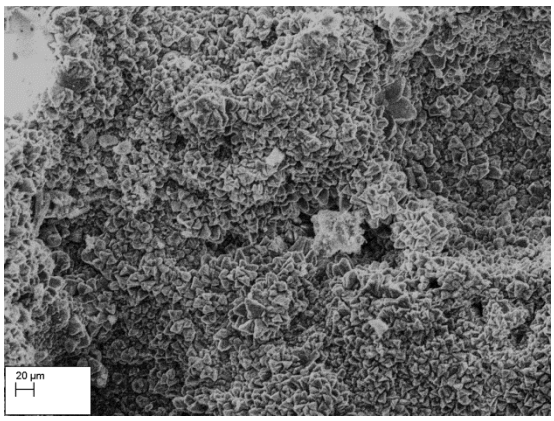

(a)

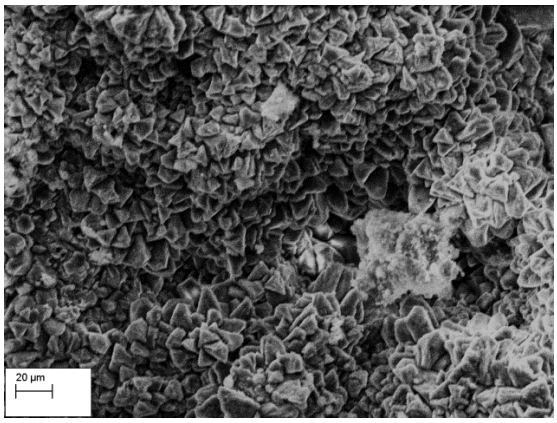

(b)

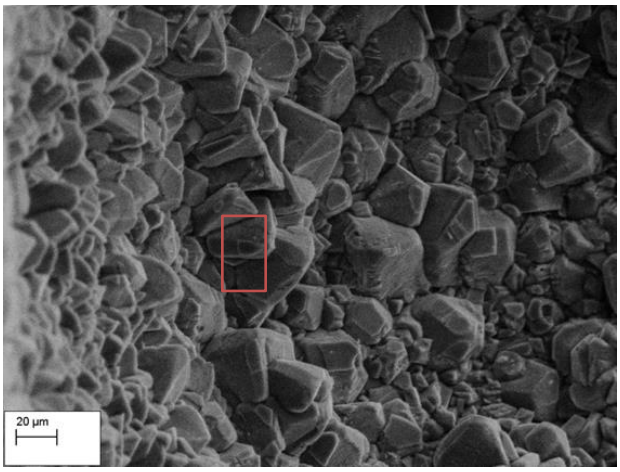

(c)

Figure 6-12 SEM image of PPT 57 showing calcium carbonate crystals under different magnifications (a) 500x, (b), 1000x, (c) showing a selected area for EDAX analysis, 1000x

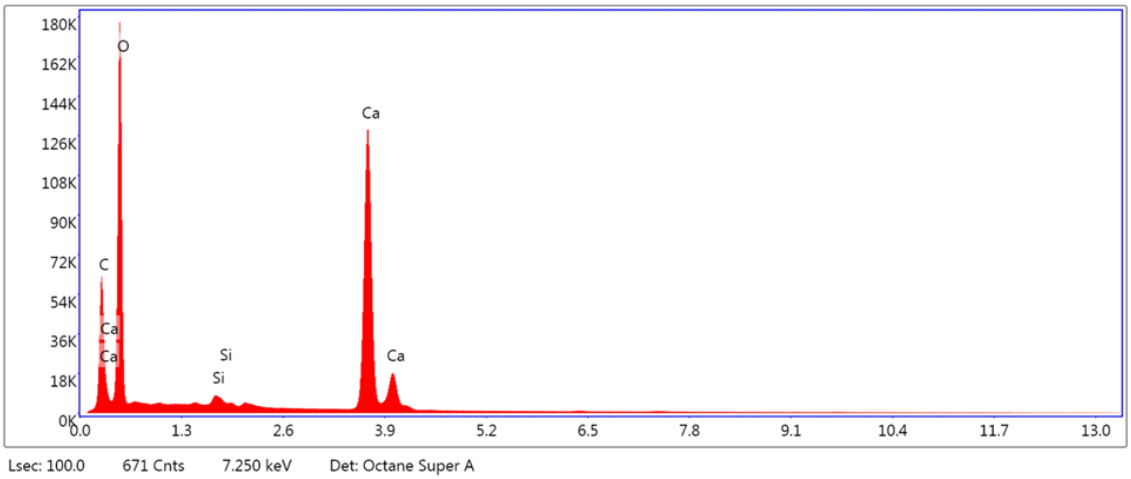

Figure 6-13 EDAX analysis of PPT 57 mortar sample

Table 6-9 Elemental composition of PPT 57 mortar sample

Element	Weight %		Difference between actual and theoretical
	Actual value	Theoretical value	
C K	11.54	12	0.46
O K	62.12	48	14.12
SiK	0.81	----	----
CaK	25.53	40	14.47

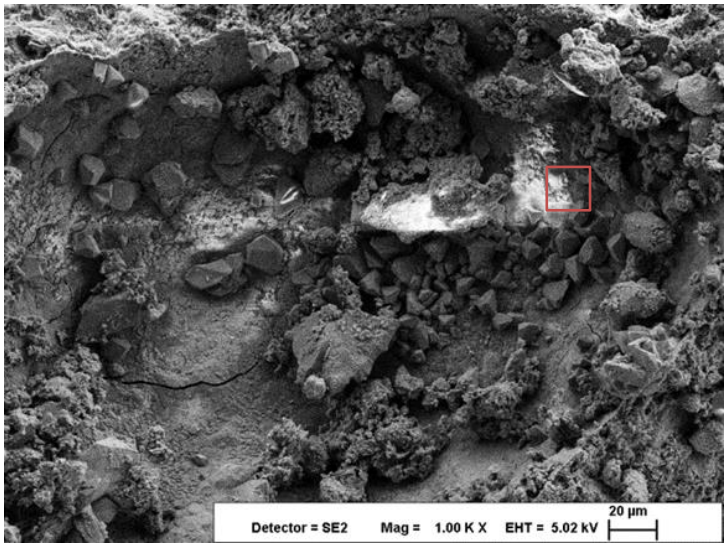

Figure 6-14 SEM image of PPT 58 under 1000x magnification

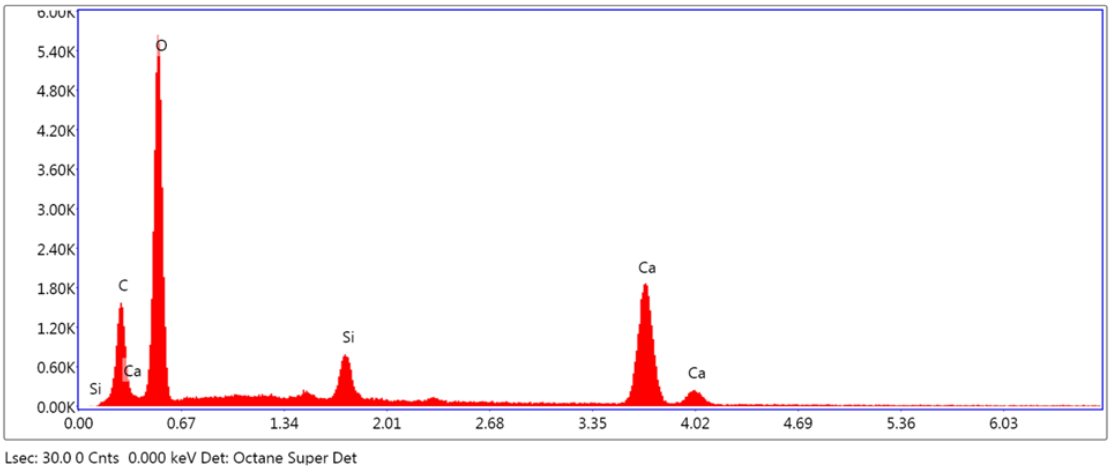

Figure 6-15 EDAX analysis of PPT 58 mortar sample

Table 6-10 Elemental composition of PPT 58 mortar sample

Element	Weight %		Difference between actual and theoretical
	Actual value	Theoretical value	
C K	10.7	12	1.3
O K	49.8	48	1.8
SiK	3.5	----	----
CaK	36.0	40	4

Figures 6-16, 6-17 and 6-18 show the SEM micrographs of the embedded capsule, the surrounding mortar matrix and the healing product at the fractured surface of each mix. Scanning electron microscopic images is able to display fine morphological features and distribution of the healing agent. In the first seven days of water curing, SEM micrograph in Figure 16 shows obvious gaps between the mortar matrix and the capsules. This indicates the weak bonding between the capsules and the bulk cementitious matrix and the main reasons behind this separation may include:

1. Early-age autogenous shrinkage deformations accompanying the hydration of cement.
2. The high formation of cement hydration products in the region around the beads interfaces (De Yoreo and Vekilov, 2003).

However, by carefully examining the images of near the gab, there is no visible micro-cracking in the mortar matrix near the beads (Figure 6-16) because the hydration products that connected the capsule to the matrix did not undergo fracture. Scanning electron microscopy images presents the intercorrelations between the capsules and the matrix's hydration products (Figure 6-17).

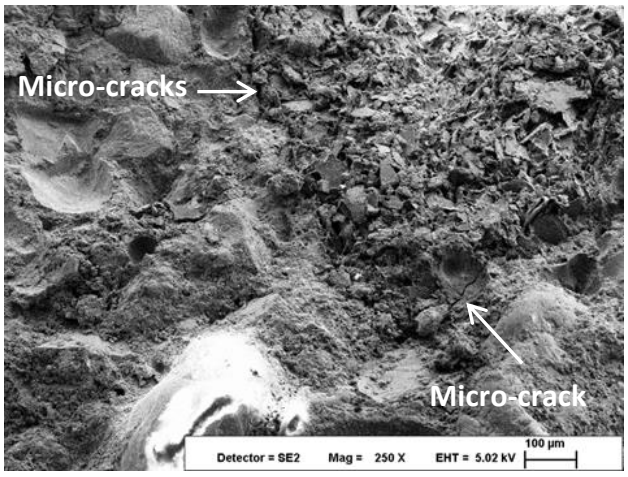

Figure 6-16 SEM image of PPT 57 showing the interface between the embedded beads and the surrounding mortar matrix under 250 x magnification

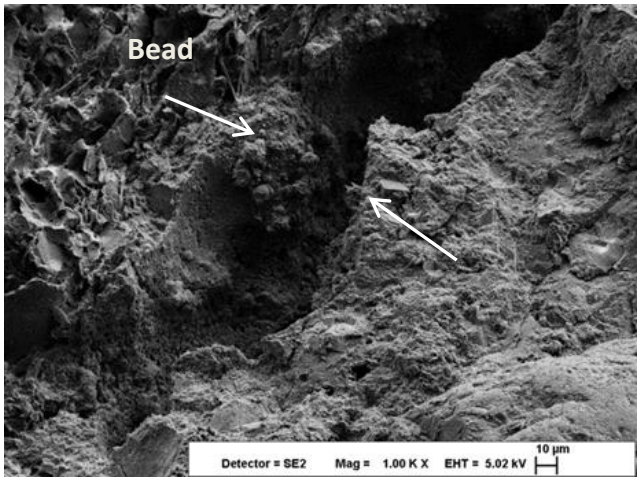

Figure 6-17 SEM image of PPT 57 showing the interface between the embedded bead and the surrounding mortar under 1000x magnification

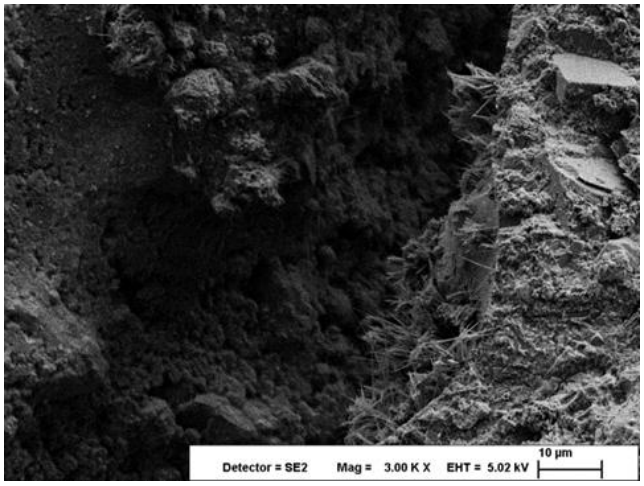

Figure 6-18 SEM image of PPT 57 showing the interface between the embedded bead and the surrounding mortar under 3000x magnification

The capsules were locked into position with mortar matrix by connecting rods that have been developed between the embedded capsule and the surrounding mortar matrix as hydration products (Rao *et al.*, 2013). Ettringite and calcium silicate hydrates (C-S-H) were the main hydration products bonding the beads and the matrix as shown in Figure 6-18. This indicates that there is no adverse interactions occurred via inclusion of calcium alginate capsules thus the hydration gradients close to the capsules were not affected.

6.5 Interim conclusions

The aim of this chapter was to study the effect of bacterial spores encapsulated in calcium alginate-Pyrophyllite clay beads on mortar specimens. Microstructural and mechanical properties were intensively investigated to examine the suitability of such bacterial spores' beads as a self-healing material.

The overall conclusions and major outcomes can be drawn as follows:

1) The optimum quantity of beads must be added to cement mortar mixture was found to be 3% without adversely affecting the strength properties of cement mortar.
2) The compressive strength was increased by 9.22% to 14.77% with increasing addition of 0.5% to 3% beads and the flexural strength was slightly increased only for a dosage of beads up to 3% and then starts to decrease gradually until the beads addition of 7%.
3) It has been found that 3% is the optimum amount of reagent can be used not only to avoid the deterioration effect of nutrient, but to enhance the strength properties. The highest increment of compressive strength was 20.28% when 3% nutrient was added.

4) The calcium alginate-pyrophyllite beads are randomly distributed in the cross section of the prism sample of the cement mortar.
5) For bacterial mortar, the rate of compressive strength gain was dependent on the bacterial strains used and method of spore's incorporation. The highest compressive strength increase occurs when Bacillus Sphaericus 57 was added directly: this enhancement reaches to 25.5% at 28 days.
6) The flexural strength of mortar specimen with direct addition of Bacillus Sphaericus 57 has increased by 27.2% compared to control.
7) In both types of addition, Bacillus Sphaericus 57 showed the highest improvement, which might attributed to the highly ureolytic activity of SP 57 in the presence of calcium acetate, urea and yeast extract comparing to SP58.
8) Mechanical properties of self-healing mortar with directly added spores were higher than that with encapsulated spores. In addition to that, 3% calcium alginate-clay bead concentration has a low density, and positioned on the surface of the specimens. Non uniform distribution of beads in mortar matrix could result in difficulty in delivering bacterial spores into matrix. Therefore, the spores have been added directly in the preparation of mortar in the subsequent chapters (Chapter 7, 8 and 9).
9) The maximum calcium carbonate crystal precipitation is shown in the mortar mixture containing encapsulated Bacillus Sphaericus 57 (PPT57) based on SEM images.
10) On the bases of EDAX analysis of the precipitates from the bacterial samples, it has been found that the precipitates are composed of calcium carbonate crystals.
11) There is no adverse interactions occurred via inclusion of calcium alginate capsules thus the hydration gradients close to the capsules were not affected.

Chapter 7: Effect of Freeze-Thaw action on the Microstructural and Mechanical properties of bacterial Mortar

7.1 Introduction

Cement-based material is one of the important structural materials and is extensively used in civil engineering. In recent years, there are more and more of constructions built in cold regions. The abrupt temperature change in the environment is one of the most destructive actions affecting cementitious materials. Repetitive freeze-thaw cycles in cold environments, can be detrimental to a porous and brittle material such as cementitious materials, when it is exposed to lower temperatures, it may deteriorate rapidly by losing strength and/or crumbling. When water begins to freeze in a capillary pores, the increase in volume accompanying the freezing of the water requires an expansion of the pores equal to 9% of the volume of frozen water, or forcing of the amount of excess water out through the boundaries of the specimen, or combination of both effects (Mehta and Monteiro, 2017). Different parameters control the amount of this hydraulic pressure, such as the permeability of the material, the degree of saturation, the distance to the nearest unfilled void and the rate of freezing. Local cracking will occur if the pressure exceeds the tensile strength of the material at any point. Cementitious materials will suffer a progressive damage when exposed to frequent cycles of freezing and thawing in a wet environment, because water will enter the cracks during the thawing period of the cycle to freeze again later. Therefore, the strength of the sample decreases with the freeze-thaw cycle. Freeze-thaw cycling is one of the main causes of degradation of cementitious in cold regions and can result in engineering failure; its frost resistance has been an issue of major concern for cement mortar engineering designers and constructers.

There is little work on the effect of FT cycle on the self-healing concrete, especially the effect of FT cycle and effect of self-healing agent and processes or their combined effect on the performance of self-healing concrete. Therefore, the present work focused on the effect of freeze-thaw action on the mechanical properties and microstructural behaviour of bacterial cement mortar. The evaluation of self-healing capability against freeze-thaw cycles is of utmost importance for durability assessment of bacterial concrete.

7.2 Materials and methods

7.2.1 **Bacterial Selection**

To study the durability of bacterial mortar subjected to freeze-thaw cycles, Bacillus Sphaericus 57 and 58 (taken from Brunel University microbiological bank) and Bcillus Megaterium 33 (isolated from soil) were used in this study. The properties and specification of these strains were described in details in Chapter 4. The three strains of Bacillus have been selected and used for this study based on their ability to survive in concrete environment, inducing calcium carbonate precipitation and spore formation. A modified nutrient agar plates with bacterial cultures were incubated upside down (agar up) for 3–7 days under 30^{o}C before harvesting spores. Bacterial cells were collected and suspended in a saline solution after approving the spore formation by spore staining method. The spores were harvested by subsequent centrifugation at 10,000 rpm for 15 minutes and washing with chilled deionized sterile water. After that, counting slide was used to determine the spore's concentration. Spores concentration was 10^{8} cell/cm^{3} of mortar as an optimum concentration based on previous studies. The spores were stored at 4^{o}C until the start of cement mortar casting.

7.2.2 **Cementitious materials**

General purposes Ordinary Portland Cement (OPC) CEM I (CEMEX, Rugby, UK) complying with BS EN 197-1:2011 and locally available sand were used in preparation of test specimens. The maximum size of sand was 1 mm. Nutrients were added to the mixture as an energy source to convert a spore into a vegetative cell. In this study, urea and yeast extract were added as nutrients for bacteria. Additionally, calcium acetate hydrate was included in the mixture as a precursor or deposition agent, which is essential to produce calcium carbonate. The addition ratio nutrients and precursors were 3% of cement weight.

7.2.3 **Mix design**

The mortar mix was designed accordance with BS EN 196-1(BSI, 2005) with a constant water cement ratio of 0·5 and cement to sand ratio 1:3. The bio-reagents were added into the matrix of the specimens in a proportion of 1:2.25:3 yeast extract: urea: calcium acetate hydrates. The final percentage of bio-reagents added to the mixture was 3% of cement weight as an optimum amount based on earlier investigations (Table 7-1).

Table 7-1 Mix Proportion*

Mix	Mortar contents (for three prismatic specimens (40mmx40mmx160mm))							
	W/C	S/C	Cement	Sand	Water	Calcium acetate	Yeast extract	Urea
R	0.5	3.0	450g	1350g	225g	------	------	------
RP	0.5	3.0	436.5g	1350g	225g	6.48g	2.16g	4.86g
SP57	0.5	3.0	436.5g	1350g	225g	6.48g	2.16g	4.86g
SP58	0.5	3.0	436.5g	1350g	225g	6.48g	2.16g	4.86g
SP33	0.5	3.0	436.5g	1350g	225g	6.48g	2.16g	4.86g

*Mortars were prepared in accordance with BS EN 196-1(BSI, 2005)

7.2.4 **Specimen preparation and freeze–thaw process**

Prisms of size, 40mm×40mm×160mm were cast to study the mechanical and microstructural properties of the mortar. Table 7-1 shows the composition of the specimens in each series. Five groups of specimens were casted. Group R are the control specimens without any additions. Group RP are the specimens with bio-reagents added, including the nutrients for bacteria (yeast extract) and the deposition agents (urea and Calcium acetate). Group SP58 is the specimens with bio-reagents and Bacillus Sphearicus spore 58 added. Group SP57 was the specimens added with bio-reagents, Bacillus Sphearicus spore 57. The last group was SP33 which is the specimens with bio-reagents and Bacillus Megaterium spore 33 added. The mixture was mixed for three minutes and compacted using a table vibrator. After 24 hrs, Group R specimens were demoulded, whereas the other group's specimens were demoulded after 48 hrs because of the delaying action of the bio-reagents added. All specimens were cured in water for 28 days before starting freeze-thaw cycles. The mortar specimens were left to dry overnight and weighed before subjecting to freezing and thawing. Each cycle lasted for 24 hrs (7 h freezing at -15^{o}C, after that the sample will allow equilibrating for 1 h at 24^{o}C, then 16 h thawing periods at water at 20 °C). After 1, 3, 10 and 30 cycles, the flexural and tensile strength of the specimens were measured.

7.2.5 **Analytical method**

An average of three test samples of the same compositions was used for flexural strength. The test was conducted as described in Chapter 3, section 3.4.6.1, after subjecting to 1, 3, 10 and 30 Freeze-Thaw cycles. Before applying the freezing and thawing actions, the samples were cured for 28 days. The compressive strength test was conducted on the two cubic halves from the broken prismatic specimen of the flexural strength test as described in Chapter 3, section 3.4.6.2. The test was performed after exposing to 1, 3, 10, and 30 freeze-thaw cycles.

The broken pieces of the specimens obtained from compressive strength were collected and subjected to Scanning electron microscopy (SEM) to examine the microstructural changes due to freezing and thawing action. An Energy Dispersive X-ray (EDAX) analyses connected with SEM was used to detect the elemental compositions in different spots on the same surface specimens. All the selected samples were gold coated prior to examination. These analyses have been outlined with more details earlier in the thesis (Chapter 3, section 3.4.7).

7.3 Results and discussions

7.3.1 **Effect of freeze-thaw cycles on mechanical properties**

7.3.1.1 Compressive strength

The effect of freeze–thaw action on the compressive strength of bio-cement mortar specimens was determined as a function of bacterial type and the number of freeze–thaw cycles (F–T cycle). The test was first done on the same mortar mixture without subjecting to freeze-thaw cycles. This can be the basis for determining the relative change in compressive strength due to freeze-thaw action. The results are based on the average of three specimens.

The results of compressive strength test for control specimen, the specimens contain only nutrients, sp33, sp57 and sp58 mortar mixtures after different cycles of freeze-thaw are given in Table 7-2. As presented in Figure 7-1, the compressive strength of controlled specimen, shows a sharp decrease due to the action of freeze-thaw cycles; after the first 1 cycles, it have fallen by 1.4% from the initial compressive strength, while it decreased by 21% of its initial compressive strength after 10 cycles. As the freeze-thaw cycles were repeated 30 times, the decrease in compressive strength was 36.4% percent of the initial value.

Table 7-2 Effect of F-T cycles on compressive strength of control and cement mortar

Mix	Compressive Strength (MPa) per number of F-T cycles (CoV%)				
	Before FT	1st	3rd	10th	30th
R	38.45(6.1)	37.90(0.94)	36.95(2.0)	28.04(5.1)	24.45(1.0)
RP	35.75(2.5)	34.53(7.5)	32.94(3.1)	24.88(6.4)	23.02(6.1)
SP57	42.95(5.4)	42.73(3.7)	38.53(2.2)	35.25(4.3)	33.87(2.9)
SP58	41.97(3.8)	41.54(1.5)	37.50(3.9)	35.04(4.9)	34.26(4.4)
SP33	43.77(3.7)	43.40(0.4)	40.78(5.1)	36.82(1.6)	35.30(2.0)

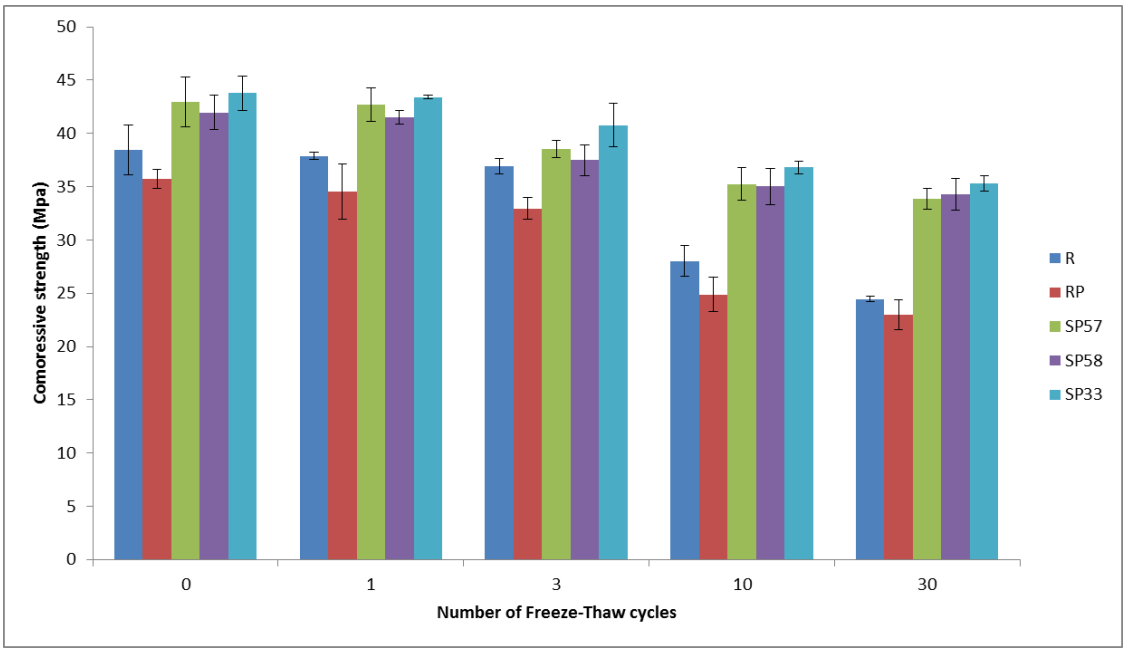

Figure 7-1 Effect of F-T cycles on compressive strength of control and bacterial mortar

The specimens contain only nutrients underwent drastic reduction in their compressive strength after exposure to 3 cycles of freezing and thawing. However, no significant differences in compressive strength were noticed after exposing to 10 and 30 cycles, indicating that the strength reduction took place mainly after the first few cycles. In more general terms, for specimens contain only nutrients, it can be detected that a decrease in the compressive strength is associated with an increase in the number of FT cycles. The primary reason for this reduction during freeze-thaw cycles is due to the propagation and growth of micro-cracks in the matrix after formation of ice within the pore throughout the freezing action.

In the SP33 bacterial mortar, the efficiency of microbialy induced calcium carbonate precipitation MICP in terms of strength development was greater than that of the SP57 and SP58. There is only small reduction observed in compressive strength of all bacterial mortar specimens subjected to one freeze-thaw cycles. After one freezing and thawing cycles, the compressive strength of SP 33, SP57 and SP 58 only change slightly. While the compressive strength reduction in all of bacterial mortar samples was low even after exposing to 30 F-T cycles (19.4% in SP33, 18.37% in SP58 and 21% in SP57) this could be attributed to the

dense microstructure of the bacterial specimens. It also evident that the bacterial mortar had higher strengths compared to control mortar even though it has lost some of its strength after exposed to a given number of freeze-thaw cycles. Additionally, all bacterial mortar samples after freezing and thawing, exhibited more strength than control not subjected to freezing and thawing.

Moreover, exposing the control specimens to 30 freeze-thaw cycles results in a significant distortion. In the meantime, bacterial specimens endure 30 cycles of freezing and thawing without noticeable distortion. With regard to above mentioned, a bacterial cement mortar withstands freeze– thaw cycles better than control cement mortar.

It is indicated that the mortar contained biological agents (bacterial spores, nutrients and biodeposition agent) has excellent freeze-thaw durability. This is so because cracks initiated by freeze thaw cycles were sealed by generating calcium carbonate crystal through MICP. Therefore, the resistance to the freeze-thaw cycles increased.

7.3.1.2 Flexural strength

Table 7-3 shows the flexural strength of control specimen(R), the specimen contain only nutrients (RP), sp33, sp57 and sp58 after 1, 3, 10 and 30 cycles of freeze-thaw. It can be seen that the average flexural strengths were 6.28 and 6.89 MPa for R and RP specimens, and 7.25, 8.48 and 7.24 MPa for SP57, SP58 and SP33 specimens, respectively, just prior to freezing and thawing cycles. It can be realized that the drop rate in flexural strength of control and bacterial specimens is evident and increases gradually after the simultaneous actions of freeze-thaw cycles. It is also observed that the rate of this decrease in control cement mortar after the 30th repetition cycle reaches 38.2% of the initial strength. This may be attributed to the increase in micro-cracks caused by tensions initiated as a result of these cycles. For the specimens with the three different types of bacterial spores, the flexural strength is higher compared to control mortar. The influence of freeze-thaw action on flexural strength is very modest after the 1st cycle. This may be due to the increase in frost resistance of bacterial mortar as a result of the dense internal structure and the filling effect of the calcium carbonate. Flexural strength test results after one cycle were 5.63, 5.38, 5.49 and 5.12 MPa for sp33, sp58, sp57 and nutrient only compared to control of 3.88MPa. This reduction in strength can be attributed to the gradual decomposing of calcium carbonate crystal caused by the osmotic and swelling pressures cause by water movement. Flexural strength variations of all specimens versus the number of freeze-thaw cycles are presented in

Figure 7-2. Flexural strength was higher after 30 cycles of freezing and thawing for all bacterial mortar.

Table 7-3 Effect of F-T cycles on the flexural strength of control and bacterial mortar

Mix	Flexural Strength (MPa) per number of F-T cycles (CoV%)				
	Before FT	1st	3rd	10th	30th
R	6.28(7.0)	3.88(4.0)	3.87(4.0)	3.72(3.1)	3.06(8.0)
RP	6.89(15.0)	5.12(3.6)	5(4.5)	4.64(8.8)	4.2(3.9)
SP57	7.25(4.2)	5.49(2.5)	6.48(7.5)	5(13.2)	4.7(2.4)
SP58	8.48(7.0)	5.38(4.8)	8.48(6.0)	5.58(5.8)	4.83(2.0)
SP33	7.24(10.0)	5.63(1.3)	7.04(1.4)	5.5(9.1)	4.61(3.7)

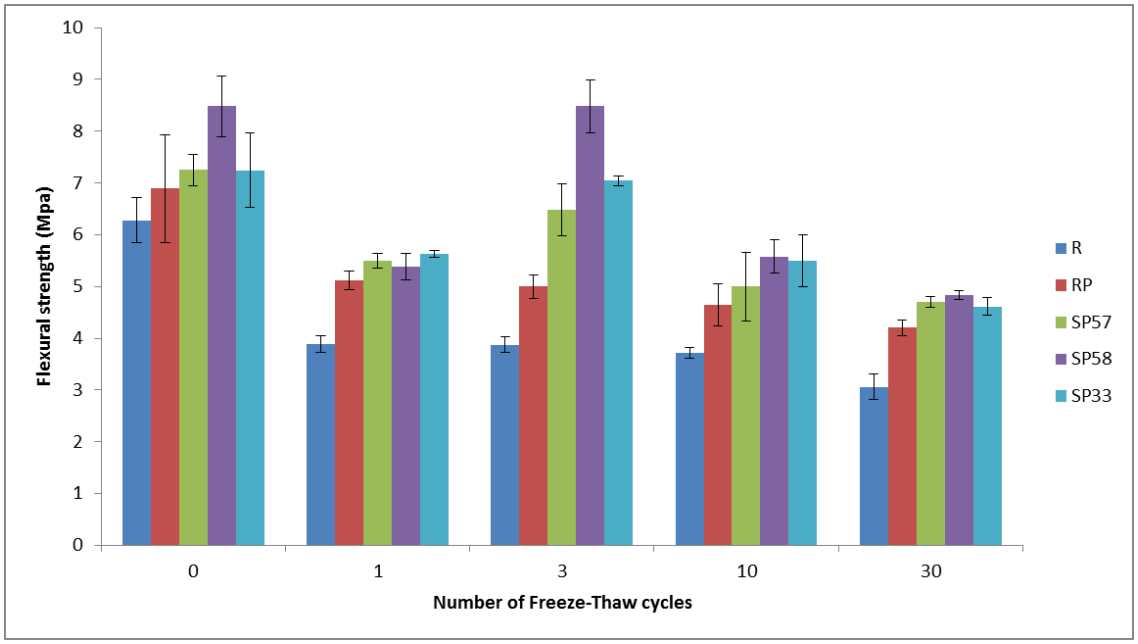

Figure 7-2 Effect of F-T cycles on flexural strength of control and bacterial mortar

7.3.2 **Effect of freeze-thaw on the microstructure**

7.3.2.1 Non-bacterial samples

SEM micrographs were used to monitor the changes in the microstructure of mortar during freeze-thaw exposure. The sound cement mortar (before FT cycle) were characterised by a relatively dense microstructure. Few cracks were detected under scanning electron microscopy and no significant alteration in microstructure or recrystallization was generated

(Figures 7-3 and 7-4). The principle hydration products of controlled and nutrients only cement mortar are ettringite needle-like crystals, calcium silicate hydrate (CSH) gel and calcium hydroxide (CH) plates.

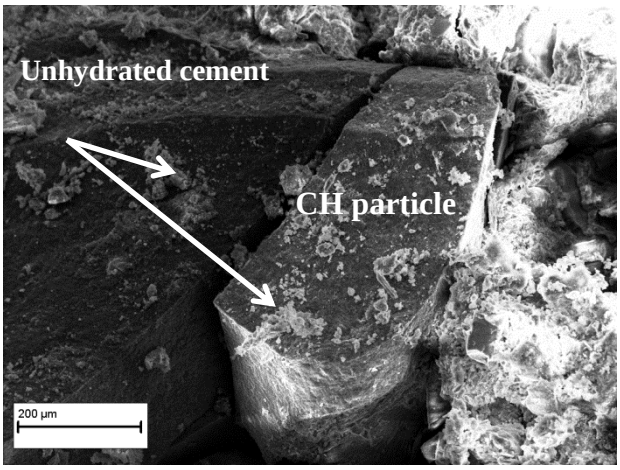

(a)

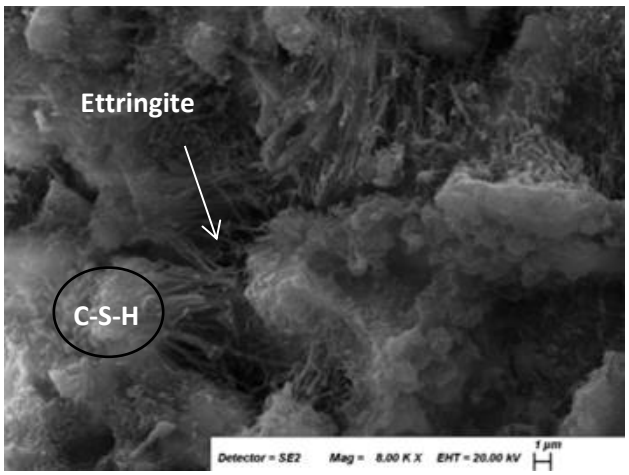

(b)

Figure 7-3 SEM images of control mortar before Freeze-Thaw cycles showing cement hydration product, (a) CH and unhydrated particles,400x (b) C-S-H and ettringite,8000x

RP sample also contains voids; however, additional confirmation is required to identify the remnant hydrates as they are not clearly recognisable using SEM image. The structure of RP was also characterised by the presence of the perfect cleavage of blocky Ca $(OH)^2$ crystals. Therefore, the accumulated cleaved Ca $(OH)^2$ crystals are maybe the most noticeable feature.

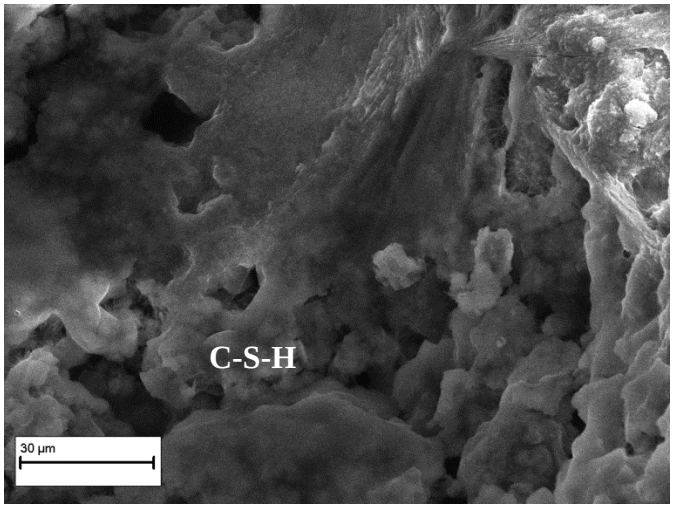

(a)

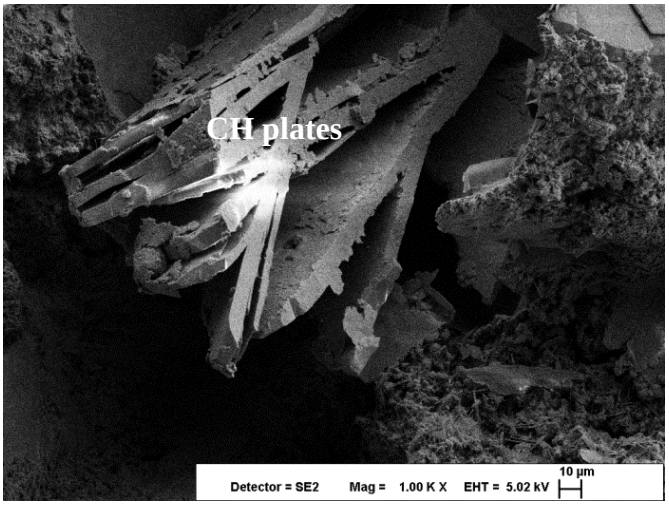

(b)

Figure 7-4 SEM images of RP mortar before Freeze-Thaw cycles showing cement hydration product, (a) C-S-H gel, 2000x, (b) CH plates,1000x

Based on SEM analysis, it has been found that subjecting the control sample to one freeze-thaw cycle led to formation microcracks and such as needle-like ettringite crystals and other hydration products (Figure 7-5a). EDAX analysis results of the marked area in Figure 7-5 (a) showed that the chemical composition of these crystals had three dominating ingredients (Figure 7-5(b)): carbon, oxygen, and calcium, suggesting that calcium hydroxide ($Ca(OH)_2$) together with calcium carbonate ($CaCO_3$) were possibly formed.

After enduring three freezing-thawing cycles, it appears that most of the clinker particles of the samples without any addition (R) may be nearly fully hydrated and the surface of the

samples were covered with hydration products in small sizes, including the crystals that is visible in a cavity as shown in Figures (7-5 (d)). The EDAX analysis conducted on the crystals in the cavity showed that silicon element was present (16.7%), suggesting the significant presence of calcium silicate hydrate (Figure 7-5 (c)).

It was also noticed that the crack amount in the cement mortar deteriorated by freeze thaw actions (F/T) were considerably higher than those of sound mortar (Figure 7-5 (c)), and basically, there appears to be nothing detected in the cracks, hence no new hydration products other than those part of the original cement mortar are produced. Apparently, because of curing for a short period prior to freeze thaw action, there was an inadequate amount of moisture for continued hydration (Figure 7-5).

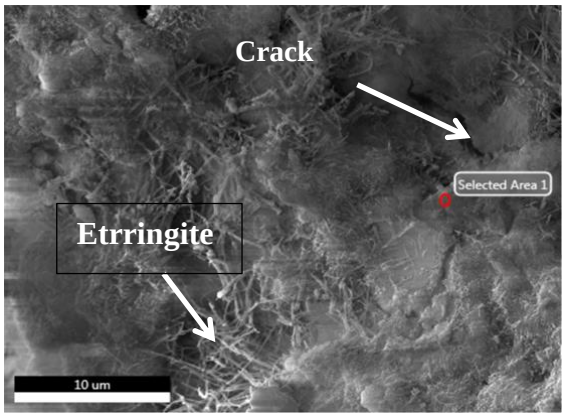

(a)

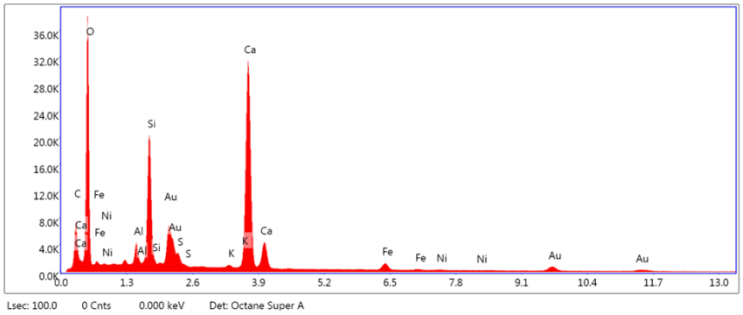

(b)

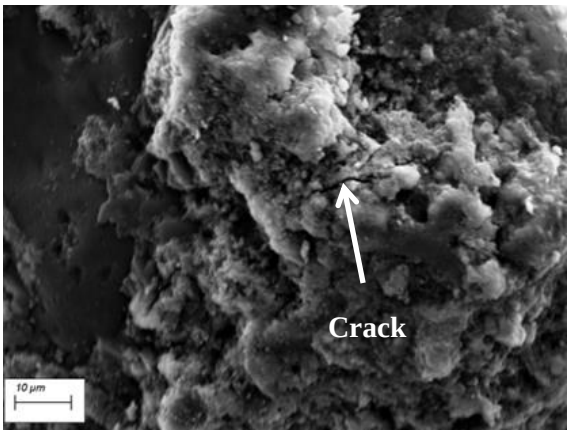

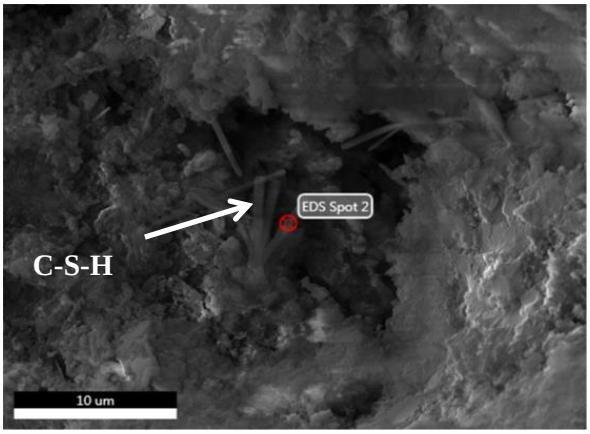

(c) (d)

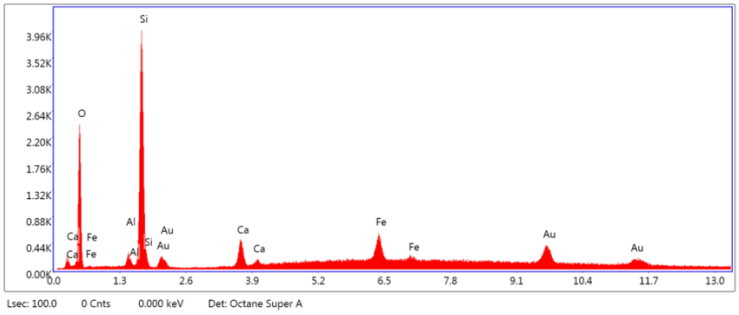

(e)

Figure 7-5 Control sample (R) under F-T cycles, (a) SEM image of the sample after enduring one F-T cycles showing ettringite formation (b) EDAX analysis of the marked area in (a), (c)SEM image of the sample after subjecting to three F-T cycles, showing crack formation, (d) SEM of the surface of the samples after 3 F-T showing a cavity filled with hydration products and (e) EDAX analysis of the marked area in (d) suggesting the presence of C-S-H

A closer examination on the RP sample subjecting to three freeze-thaw cycles (Figure 7-6 (a) and (b)) shows a pocket filled with hydration products mainly inner C-S-H. This pocket was surrounded by voids showing eroded hydrates and outer product C-S-H.

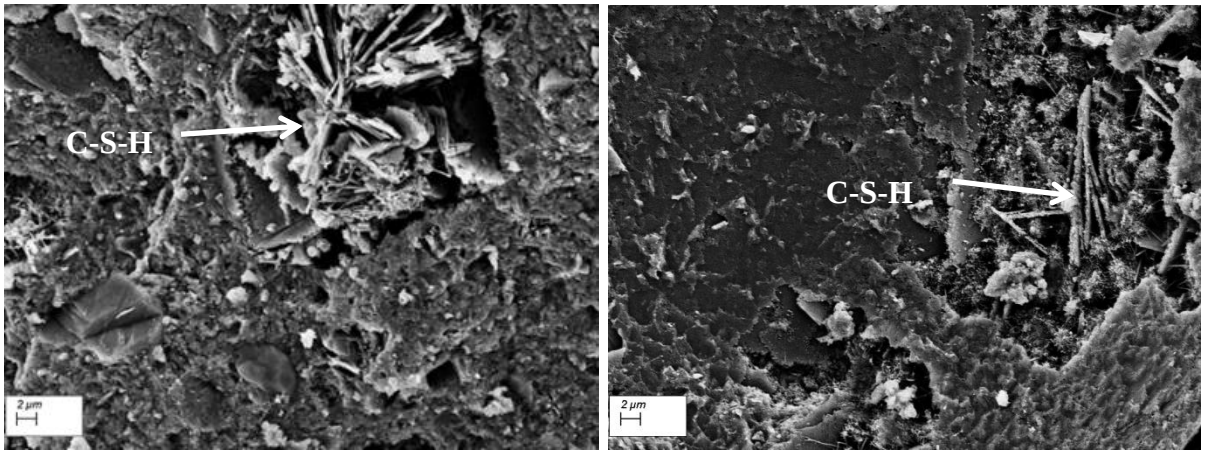

(a) (b)

Figure 7-6 SEM images of RP samples subjecting to three Freeze-Thaw cycles at 5000x magnification, (a) pocket filled with hydration products mainly inner C-S-H, (b) C-S-H on the surface of the sample

However, observing the controlled (R) sample after 3 cycles, by the SEM image, reveals that pores and micro-cracks are also present on the surface fracture (Figures 7-7 and 7-8). The shapes of the pores are circular or oval and in a different sizes. The location of the micro-crack initiation was around the sand particle and through the air void. The primary cause of the cracks was difficult to determine because the sample preparation process for SEM includes crashing the mortar specimen. The outcomes above demonstrate that the reference cement mortar may be internally damaged. Such outcomes can reasonably be expected to be achieved.

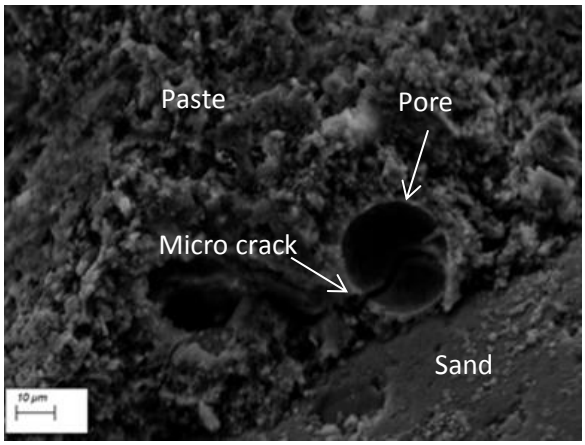

Figure 7-7 R subjecting to three Freeze-Thaw cycles under 2000x magnification (circular pores)

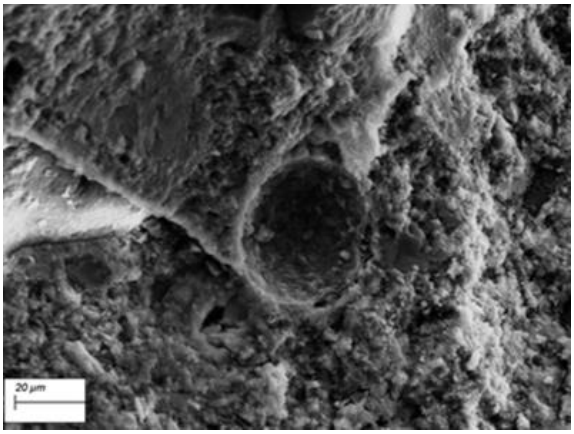

Figure 7-8 R subjecting to three Freeze-Thaw cycles under 2000x magnification (oval pores)

The cross section of the RP specimen after 3 FT cycles reveals the distribution of pores of various diameters (Figure 7-9). The internal damage of RP cement mortar after a number of freeze-thaw cycles are expected to form, resulting in the formation of cracks throughout the cross section.

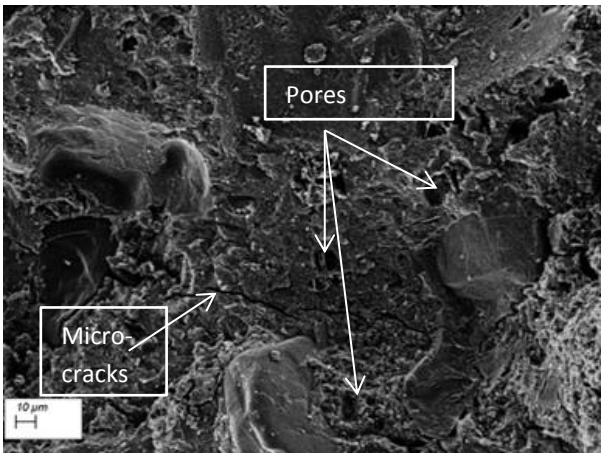

Figure 7-9 RP subjecting to three Freeze-Thaw cycles under 1000x magnification

After exposing to 10 F-T cycles, the typical hydration products of R and RP specimens were the formation of ettrimgite agglomerates and C-S-H particles mixed with portlandite as shown in Figures 7-10 and Figure 7-11 (a) and (b). Few pores and fissures can be detected in the microstructure of these specimens.

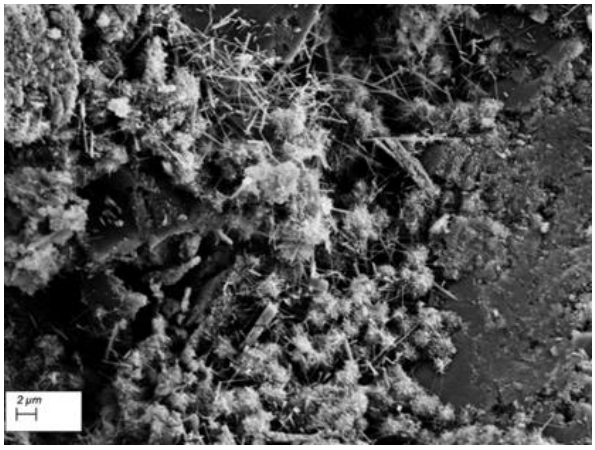

Figure 7-10 R subjecting to ten Freeze-Thaw cycles under 5000x magnification

The presence of ettringite needle-like crystals was the predominant feature of the RP samples. Ettrigite crystals development in the presence of water may promote volume expansion of the matrix leading to construction failure. Ettringite crystals could be formed by the recrystallization of the primary components (SO_4^{-2}, Al^{+3}, and Ca^{+2}) that were present in the mortar pore fluid.

The environment surrounding the specimens mainly controls the amount of ettringite crystals developing in cement mortar. A small amount of ettringite was found under normal curing conditions and before exposing to freeze-thaw actions, while greater quantity of ettringite can be seen in mortars after exposing to F-T cycles. These findings were comparable to those reported by Batic et al (Batic *et al.*, 2000).

The morphology of ettringite crystals formed in cement mortar was also changed depending on the available space. If the space available for the ettringite to grow was small, it will develop as short and thin crystals. However, ettringita crystals have better development when they grow inside pores or cracks. Crystalline ettringite formation, thus, does not necessary exerts any expansive action in the case of forming dense clusters to fill the available spaces.

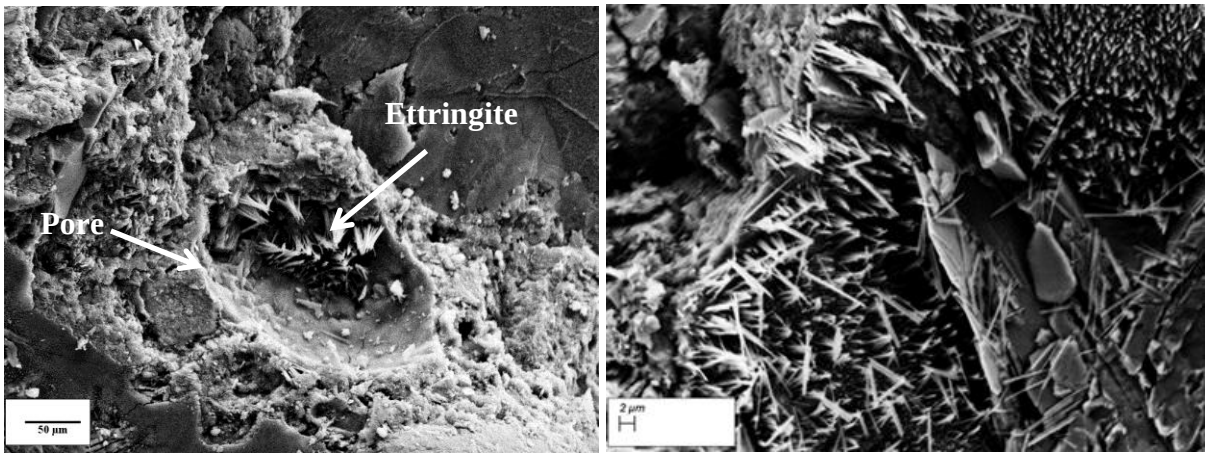

(a) (b)

Figure 7-11 SEM images of RP subjecting to ten Freeze-Thaw cycles; (a) image of RP sample showing etrringite formation inside the pore at1000x, (b) image of RP samples showing formation of ettringite agglomerates at 5000x

After subjecting to 30 FT cycles, R and RP mortar gave rise to micro-cracks. Surface and internal cracks can be observed by SEM images (Figures 7-12 and 7-13). Therefore, the non-bacterial mortar could develop internal deterioration and fasten damage accumulation at this stage. Abundant portlandite developed in the control sample, but no ettringite was detected as shown in Figure 7-12. The hydration products in the surface fracture of control sample (R) may be eroded and provided channels for more crack propagation and probably water and ion movement.

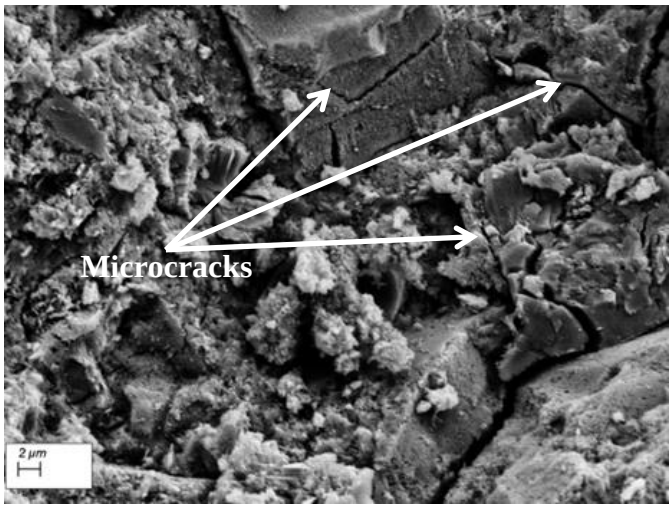

Figure 7-12 SEM image of control (R) subjecting to 30 Freeze-Thaw cycles at 5000x magnification

Unlike the control, ettringite crystals were observed in RP specimen exposing to 30 freezing and thawing cycles. However, the amount of ettringite found in the surface fracture of this specimen was limited compared to that exposed to ten cycles (Figures 7-11 and 7-13). There is also a massive deposition in fracture areas.

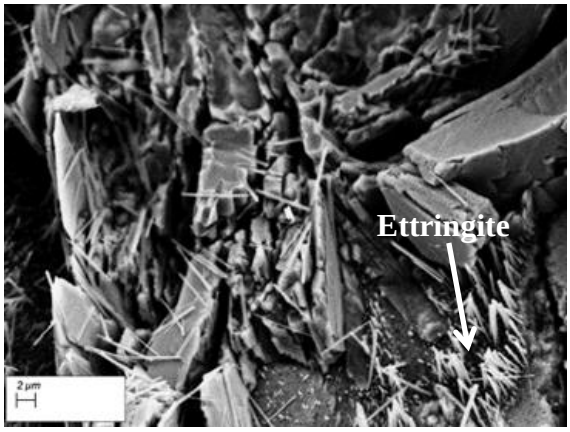

Figure 7-13 SEM image of RP sample subjecting to 30 Freeze-Thaw cycles at 5000x magnification

Any deterioration of concrete by freeze-thaw action accelerates the rate at which ettringite leaves its original location in the paste to go into solution and recrystallize in larger spaces such as voids or cracks. This is because both water and space must be present for the crystals to form. The space can be provided by cracks that form due to damage caused by frost action. In addition, deterioration caused by such mechanisms provides greater surface area of exposure and easier paths for ingress and egress of water (Thomas and Ramlochan, 2004; Portland Cement Association, 2001). Ettringite did not cause the cracking, nor did it contribute to the propagation of existing cracks. Cracks due to frost damage created space for ettringite crystals to grow.

7.3.2.2 Bacterial samples

The microstructure of bacterial cement mortar examined by SEM shows that all mortar samples contain calcium hydroxide crystals (CH), calcium silicate hydrate (CSH) and pores. However, the presence of calcium carbonate crystals (C) in the SEM images of mortar samples incorporated bacteria is also obvious. The calcite deposits formed predominantly as separated crystals in the pores, which is one of the prominent reasons of strength and permeation properties enhancement. Calcite precipitation in the pore spaces of a microbial mortar has also been confirmed (Zhang, Guo and Cheng, 2015). SEM images of all the

bacterial mortar exhibited more compacted and denser microstructure compared to controlled specimens (without bacteria).

The Figures 7-14((a) and (b)), 7-15 ((a) and (b)) and 7-16 ((a) and (b)) display the microstructures of samples SP33, SP57 and SP58 before subjecting to freeze-thaw action. Their microstructure was shown to have more compact morphologies and less porous and denser than those of the R and RP samples. The big crystalline calcium hydroxide [Ca $(OH)_2$] were not present in the samples. A layer of crystals was observed to cover the majority of the surface of the bacterial samples. However, major differences have been revealed in the thickness of the carbonate layer among the bacterial treated mortar specimens through SEM examination. Compared to the samples SP33 and SP57, the microstructure of the sample SP58 was different, showing some of the area across the surface without carbonate crystals. The precipitation of these crystals is an indication of bacterial mediation of mineralisation process. The internal structure of the bacterial specimens is denser than the controlled and nutrients only due to the filling effect of the calcium carbonate.

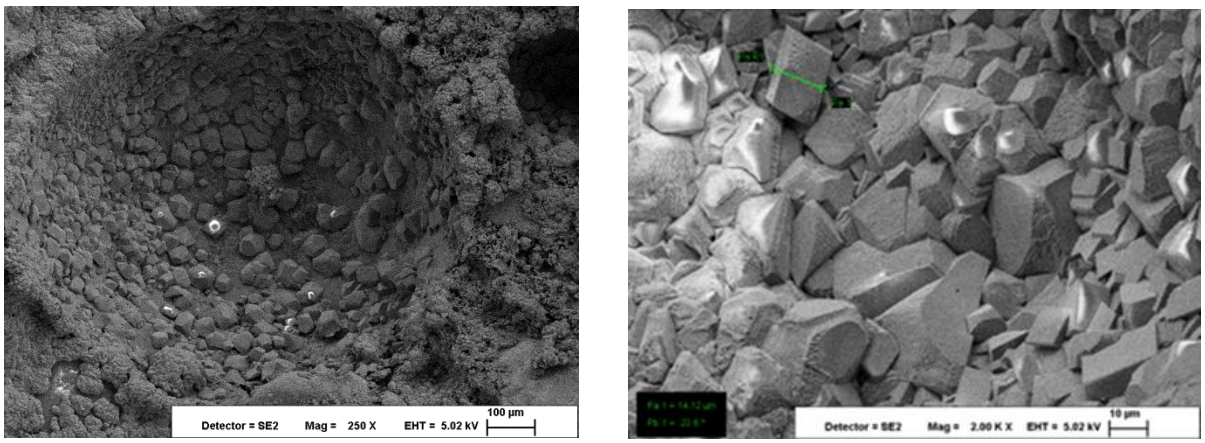

(a) (b)

Figure 7-14 SEM images of SP33samples before exposing to Freeze-Thaw Cycles at (a) 250x magnification and (b) 2000x magnification

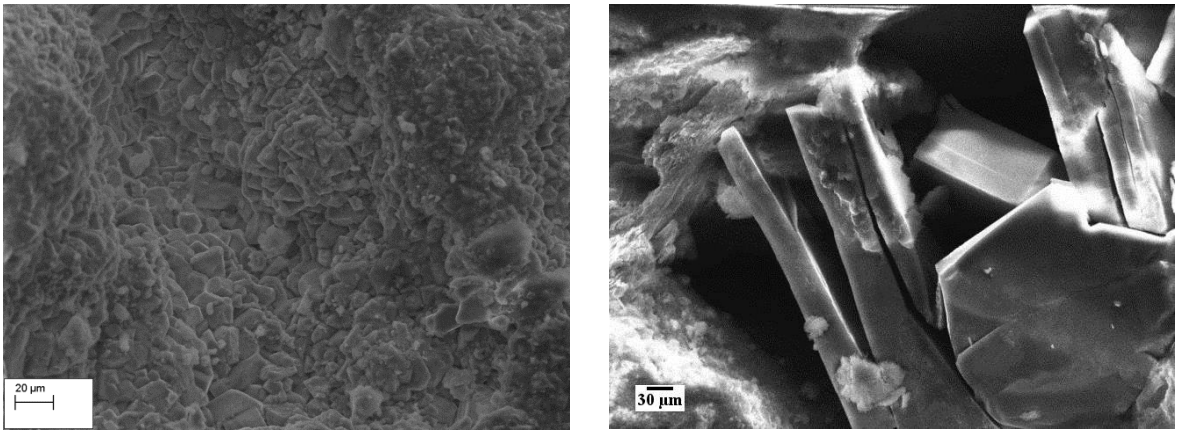

(a) (b)

Figure 7-15 SEM images of SP57samples before exposing to Freeze-Thaw Cycles at (a)1000x magnification and (b) 2000x magnification

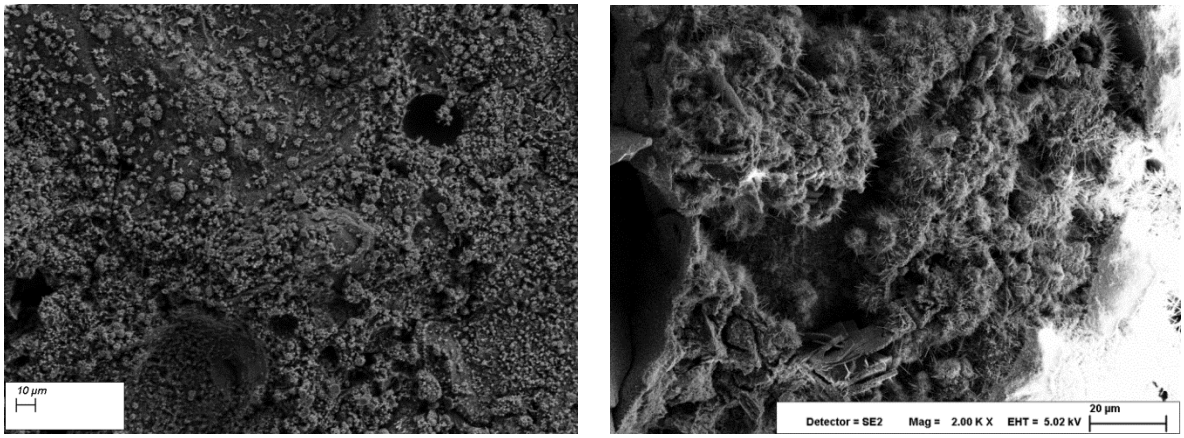

(a) (b)

Figure 7-16 SEM images of SP58samples before exposing to Freeze-Thaw Cycles at (a)1000x magnification and (b) 2000x magnification

After 10 freeze-thaw cycles, the whole structures of SP33 mortar samples remain very dense as shown in Figure 7-17 and sufficient hydration products (CH plates) were observed. It is noted that the micro pores are filled with large amount of calcite deposition as confirmed by EDAX analysis of the deposited layer (Figure 7-18). The EDAX analysis shows that this structure contains a large amount of calcium.

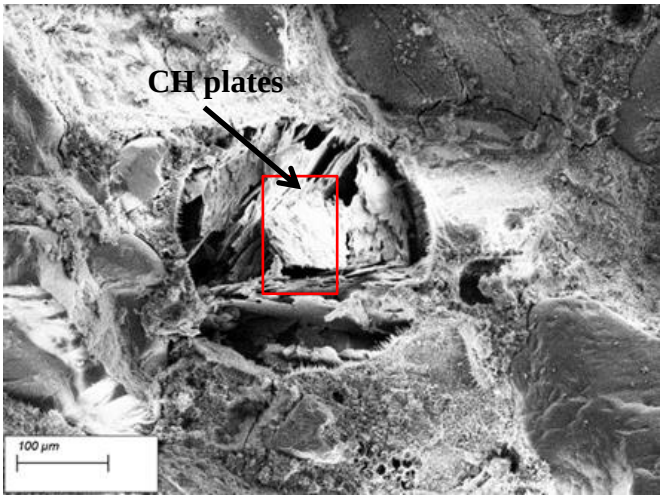

Figure 7-17 SP33 exposing to 10 F-T cycles

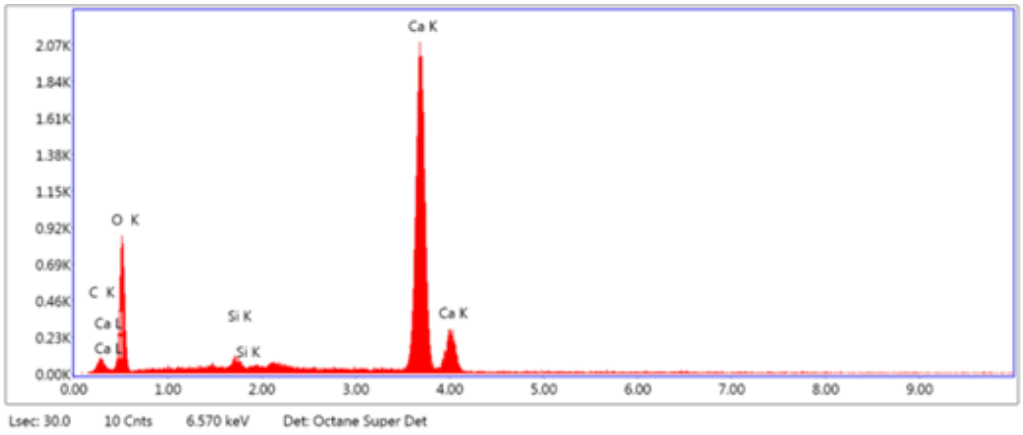

Figure 7-18 EDAX analysis of SP33 exposing to 10 F-T cycles

The SP33 specimen exhibited abundant ettringite after exposing to 30 F-T cycles, which developed both in voids and on the interface fractures as shown in Figure 7-19. Ettringite can be formed during freeze-thaw actions by transforming part of monosulfate (one of the cement hydration products). As freezing and thawing actions causes osmotic and swelling pressures of water, the calcium carbonate precipitated in the pores is gradually decomposed with increasing the cycle's number. Therefore, moisture and phase component transformation will take place through the micro pores leading to the late ettringite formation (Stark and Bollmann, 2000). S, Al, O, and Ca were detected in the EDAX spectrum (Figure 7-20). The high increase in calcium could be attributed to the presence of Ca $(OH)^2$.

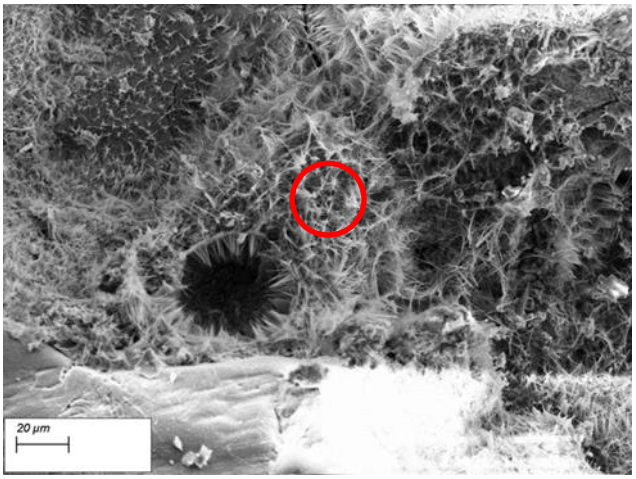

Figure 7-19 SP33 exposing to 30 F-T cycles

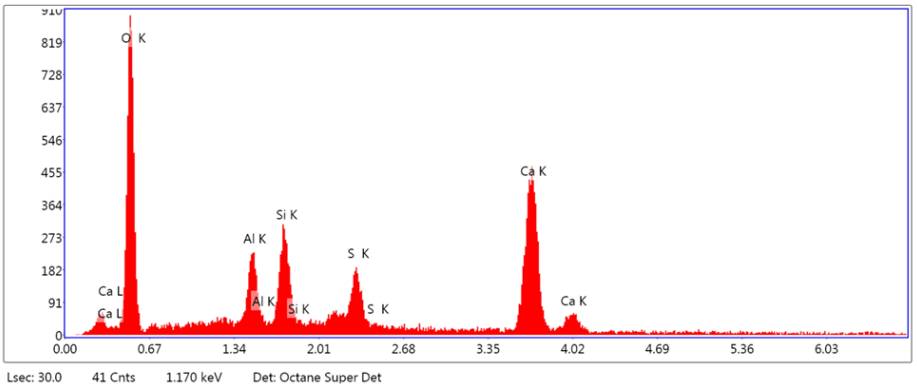

Figure 7-20 EDAX spectrum of the selected area of the SP33 exposing to 30 F-T cycles

Exposing the SP57 and SP58 samples to 10 freeze-thaw actions resulted in the pores filled with hydration products (Figures 7-21((a) and (b)) and 7-23) and the microcracks are almost occupied with calcite precipitations and hydration products. However, SEM image of SP 57 and SP58 after 30 F-T cycles shows conspicuous formation of ettringite in voids and microcracks (Figures 7-22((a) and (b)) and 7-24((a) and (b))). It was proved that ettringite formation in hardened concrete can form as a consequence of the influence of freezing and thawing (ibid). An ettringite formation in hardened concrete does not in every case lead to a direct damage of the concrete structure. At present, there is still controversy whether different types of ettringite exist; whether the damage mechanism can be initiated by coarse or fine crystalline ettringite; whether the formation of large ettringite crystals in hardened concrete, which also occur without heat treatment, is the primary cause of damages in the micro structure or if it only causes damage-promoting changes in the micro structure; and which practical consequences the ettringite filling of artificial air voids may have.

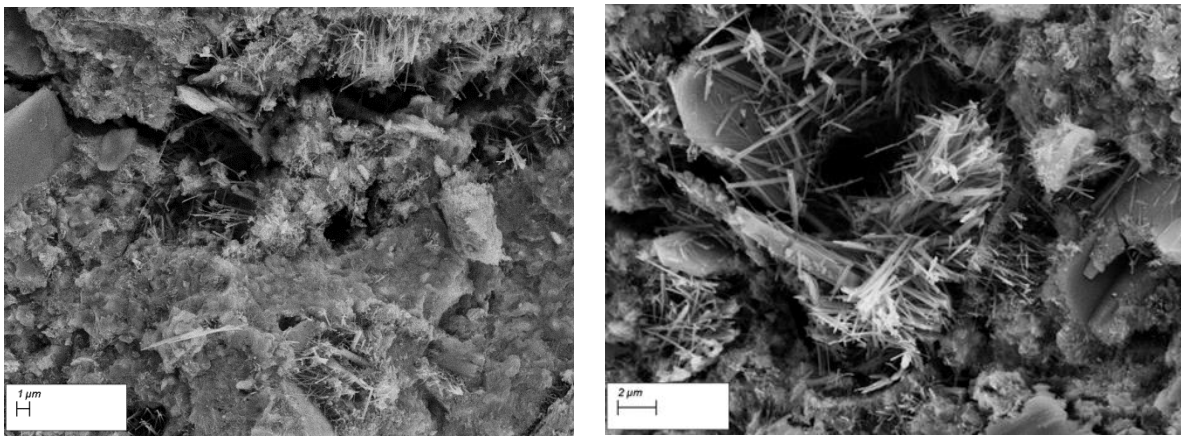

(a) (b)

Figure 7-21 SEM image of SP57samples subjected to 10 F-T cycles at (a) 6840x magnification and (b)10000x magnification

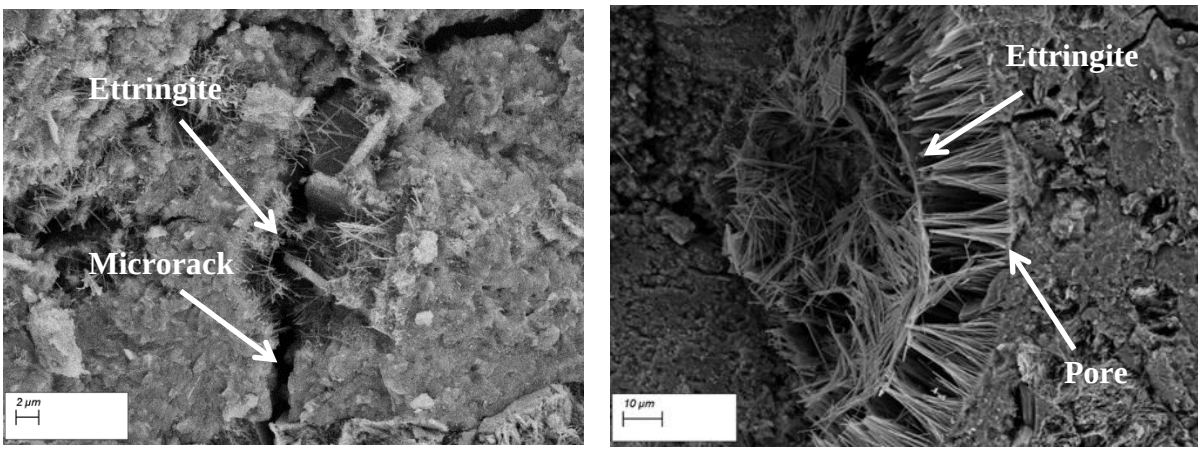

(a) (b)

Figure 7-22 SEM image of SP57samples subjected to 30 F-T cycles at (a) 5790x magnification and (b)2000x magnification SP57 subjected to 30 F-T cycles

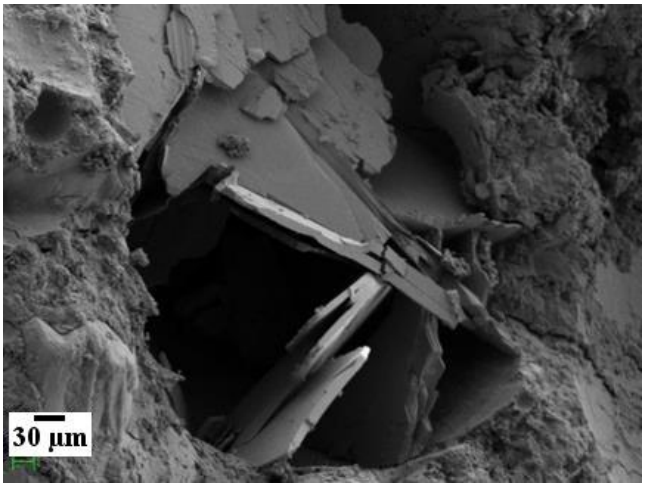

Figure 7-23 SP58 subjected to 10 F-T cycles

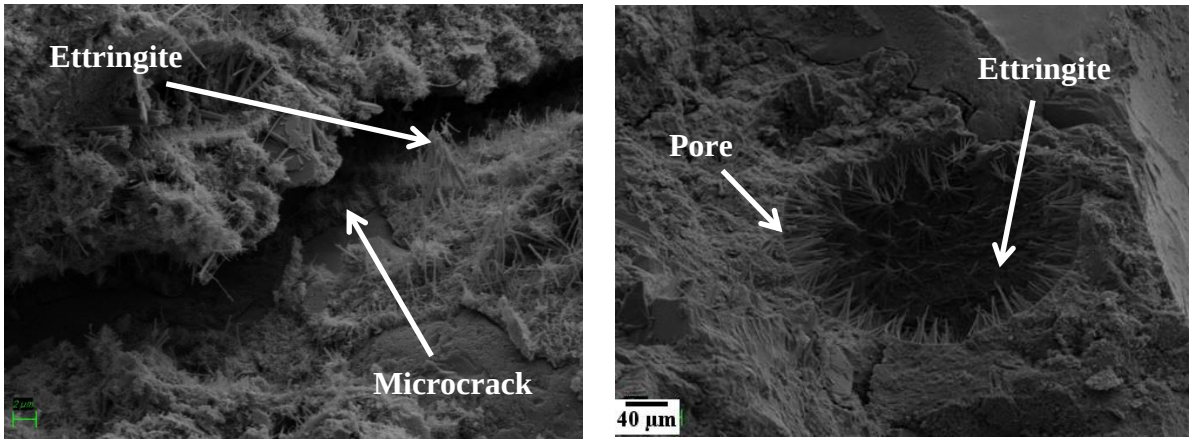

(a) (b)

Figure 7-24SEM image of SP58 samples subjected to 30 F-T cycles at (a) 6000x magnification and (b)3000x magnification

SEM images of surfaces of cement mortar containing SP 57, SP58 and SP33 exposed to the frequent freeze–thaw cycles showed a presence of dense deposit of calcium-carbonate crystals. This deposit creates a cover (surface II) on top of the original surface of the cement mortar specimen (surface I). The elemental composition of the surface I of the three mixtures (Figures 7-27, 7-30 and 7-33) as performed by EDAX, have confirmed the similarity with control cement hydration products, while the existence of Ca, C and O in the elemental composition of surface II can be assigned to calcium carbonate (Figures 7-26 and 7-32). The elemental composition shown in Tables 7.4 and 7.8 are close to each other's, while the compositions shown in Tables 7.6 seem to be affected by the gold coating during preparation for SEM investigation. Based on the theoretical calculations on the percentage of weight of $CaCO_3$, Carbone, calcium and oxygen contents should be 12%, 40% and 48%, respectively. The weight percent (wt. %) of chemical elements of surface II of SP33 (Table 7-4) has been

found as follows: Ca = 33.9%, C = 12.5%, O = 53.5%, which are relatively close to the theoretical percentage of weight of calcium carbonate. The analysis of surface II of SP58 (Table 7-8) shows that the weight percentages of Ca, C and O are 35.5%, 10.1 and 53.6, respectively, with little traces of Si. The variances in the actual and theoretical values are probably caused by the other hydration products. The differences between the actual and theoretical values of Ca, O and C in Tables 7.6(surface II of SP57) are relatively high. This means that surface II could be a result of the precipitation of hydration products.

The samples with precipitated calcite layer over the surface were found to have a very low permeability (Verma *et al.*, 2015b).

Therefore, the durability of cement structure could be improved by enhancing its resistance to adverse environmental factors such as prolonged exposure to freeze-thaw actions.

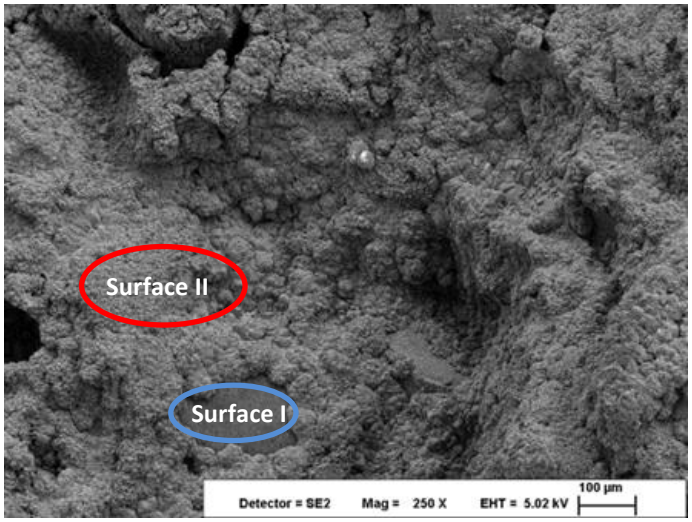

Figure 7-25 SEM images of a layer (surface II) newly formed over the cement mortar specimen (surface I) cast with SP33

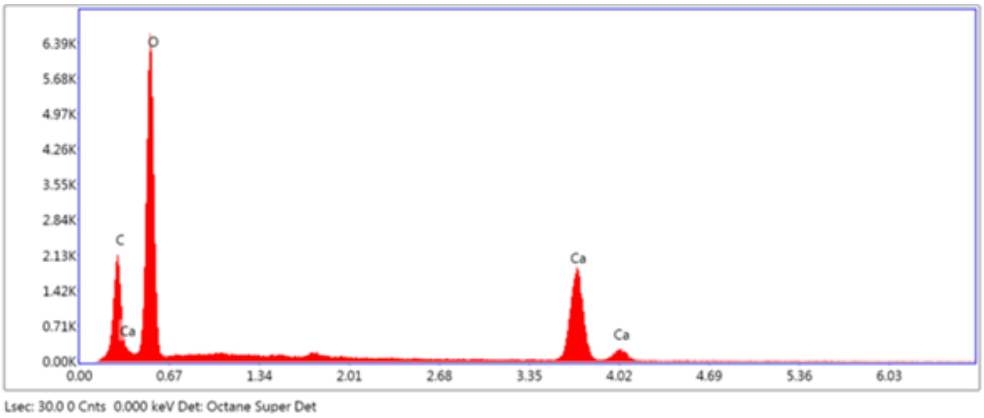

Figure 7-26 EDAX analysis of surface II of SP33 (the red marked area in Figure 7-25))

Table 7-4 Elemental analysis of surface II of SP33

Element	Weight %		Difference between actual and theoretical
	Actual value	Theoretical value	
C K	12.5	12	0.5
O K	53.5	48	5.8
CaK	33.9	40	6.1

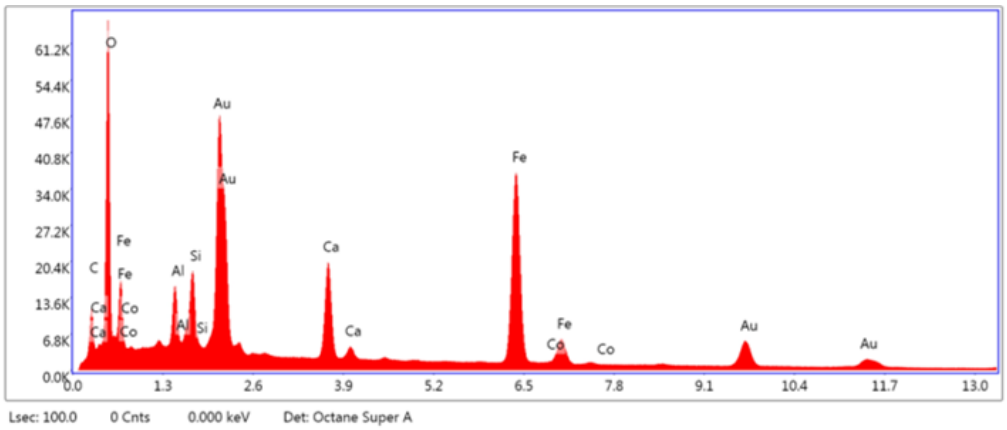

Figure 7-27 EDAX analysis of surface I of SP33 (the blue marked area in Figure 7-25))

Table 7-5 Elemental analysis of surface I of SP33

Element	Weight %
C	2.37
O	12.89
Al	2.33
Si	2.70
Ca	8.70
Fe	35.98
Co	0.20
Au	34.84

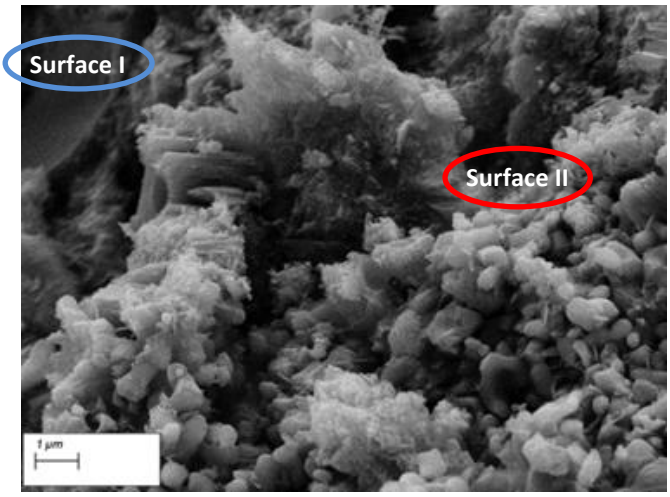

Figure 7-28 SEM images of a layer (surface II) newly formed over the cement mortar specimen (surface I) cast with SP57

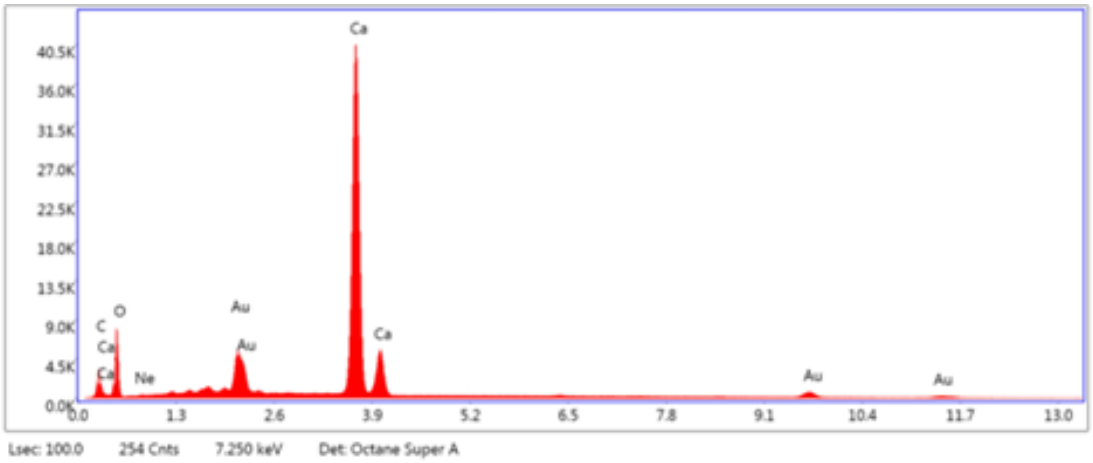

Figure 7-29 EDAX analysis of surface II of SP57 (the red marked area in Figure 7-28))

Table 7-6 Elemental analysis of surface II of SP57

Element	Weight %		Difference between actual and theoretical
	Actual value	Theoretical value	
C	4.13	12	7.87
O	27.68	48	20.32
Ne	0.00	----	-----
Ca	52.54	40	12.54
Au	15.64	-----	------

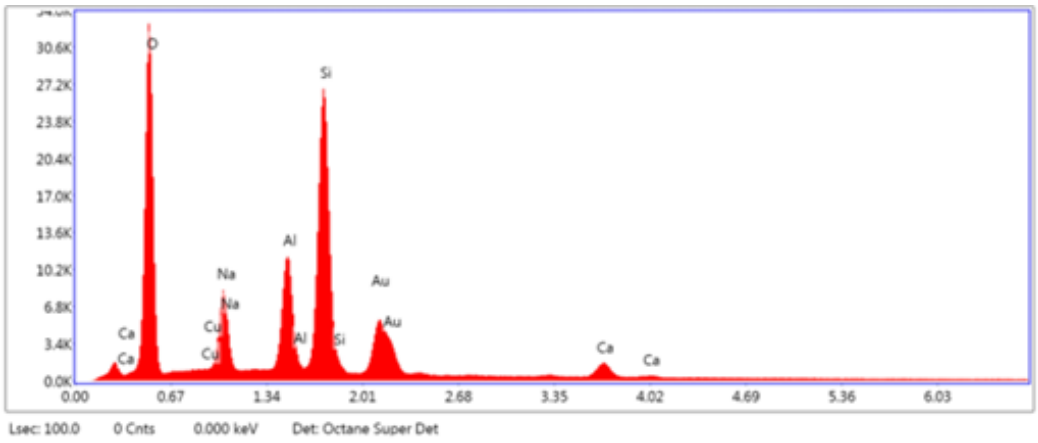

Figure 7-30 EDAX analysis of surface I of SP57 (the blue marked area in Figure 7-28))

Table 7-7 Elemental analysis of surface I of SP57

Element	Weight %
O	35.93
Cu	0.00
Na	7.22
Al	9.69
Si	26.42
Au	15.42
Ca	5.32

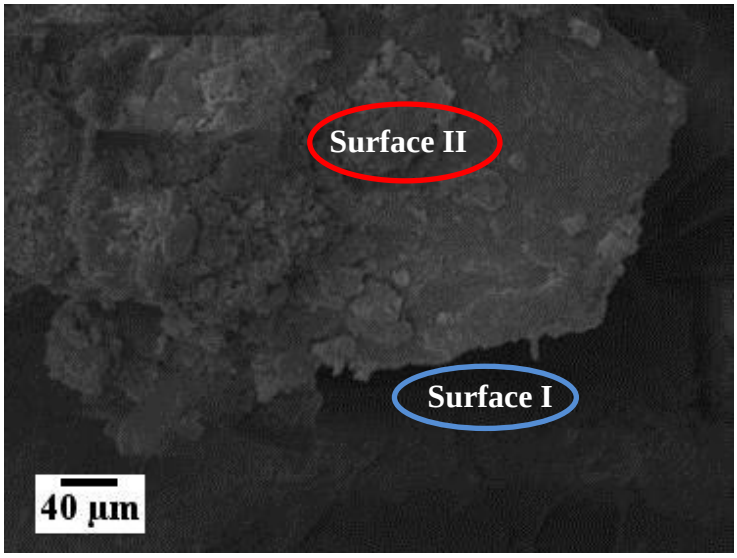

Figure 7-31 SEM images of a layer (surface II) newly formed over the cement mortar specimen (surface I) cast with SP58

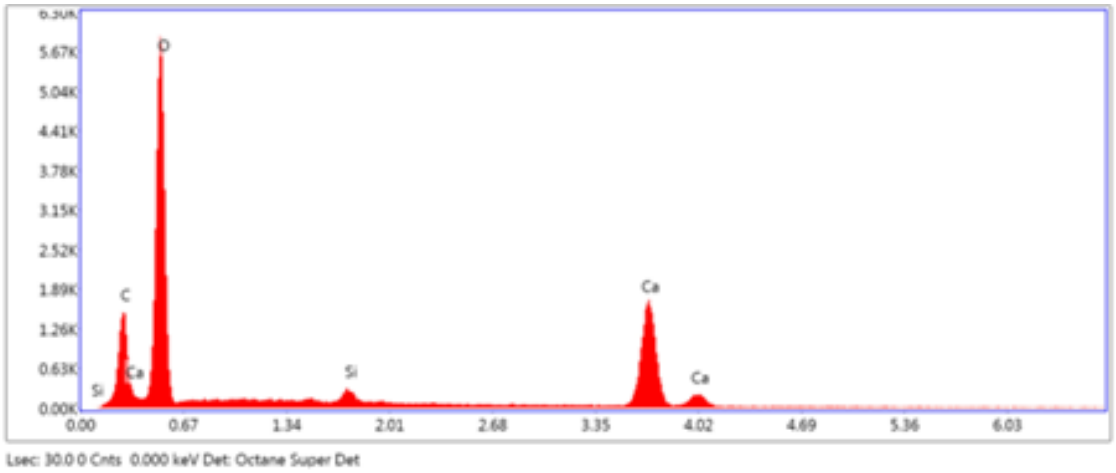

Figure 7-32 EDAX analysis of surface II of SP58 (the red marked area in Figure 7-31))

Table 7-8 Elemental analysis of surface II of SP58

Element	Weight %		Difference between actual and theoretical
	Actual value	Theoretical value	
C	10.1	12	1.9
O	53.6	48	6.5
Si	1.1	-----	-------
Ca	35.2	40	4.8

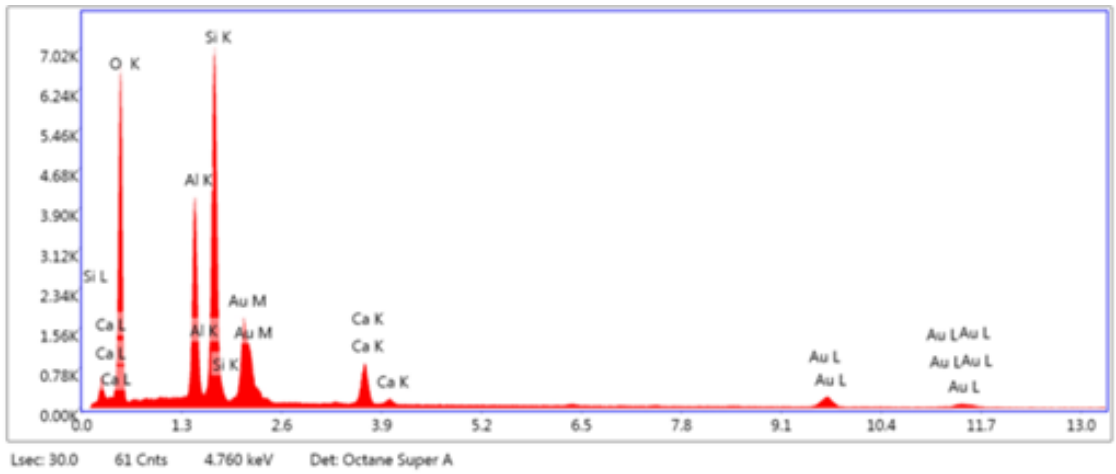

Figure 7-33 EDAX analysis of surface I of SP58 (the blue marked area in Figure 7-31))

Table 7-9 Elemental analysis of surface I of SP57

Element	Weight %
O	41.28
Al	11.30
Si	19.30
Ca	5.07
Au	23.05

The bacterial mortar is characterized by dense structure through which moisture migration is relatively difficult. Therefore, bacterial incorporation enhanced the mortar freezing resistance to a certain degree.

The mechanisms of dilation deformation of concrete affected by repeated cycles of freezing and thawing have long been a topic of intense debate with various plausible theories (Powers, 1955; Powers and Helmuth, 1953). Ice accretion, hydraulic pressure and osmotic pressure are the three basic internal mechanisms of freeze-thaw deterioration that have been proposed. Damage is assumed to occur within the microstructure, in all of three cases, if the pressure exerted within the microstructure exceeds the tensile strain capacity of the cement paste. The hydraulic pressure theory is the most common accepted mechanism for freeze-thaw damage in concrete. The principle behind this theory is that, the water present in gel and capillary pores of the cement paste microstructure expands 9% in volume after freezes into ice. Theoretically, the critical saturation level of the cement paste is 91.7% (Powers, 1955), meanwhile the unfilled pore spaces can accommodate the volume increase. However, in reality, the overall critical saturation level may decrease, because the critical saturation occurs locally as a result of the uneven distribution of pore water within the concrete. During freezing, formation of ice must accommodate within capillary pores, while any melted water must reallocate itself to nearby pores or air voids to accommodate the volume expansion. Otherwise, cracks can initiate as the pressure within the pore void exceeds the tensile strength of the cement paste (Powers and Helmuth, 1953).

Internal pressure can also be generated by the osmotic pressure theory (Powers, 1955). The principle of the osmotic pressure theory depends on the concentration of metal hydroxides in

the ice-liquid interface between the frozen and unfrozen water. Because only nearly pure water can form ice during freezing of pore water, metal hydroxides will accumulate in the surrounding melted water and its concentration will increase. The resulting concentration gradient in the ice-liquid interface will restore the equilibrium by drawing in more water into the pore allowing further water to enter and freeze; then the cycle is repeated (ibid).

Ice accretion is another theory to explain the ice formation within the cement paste structure, and it is also known as capillary ice growth. This theory depends on the energy equilibrium between the ice inside the pore and the liquid in the neighbouring paste. The filling capacity of capillaries is much higher than that of air voids, therefore, the pressure exerted from capillary ice during expansion of freezing ice is greater. Thus, air void ice has less free energy than that of capillary ice (Powers and Helmuth, 1953). As the gel pore water hag greater free energy than that in the capillary ice, it must be redistributed to air void or capillary pore in order to be able to freeze. To decrease its energy potential, gel pore water tend to move into the pores leading to more ice crystal formation (ibid). As no single theory can alone account for the performance of concrete subjected to freezing conditions, the frost damage of concrete is more likely to develop under a combined effect of different freeze-thaw mechanisms (Pigeon, 1994).

The frost resistance of the bacterial mortar samples enhanced as the calcium carbonate crystals generated from microbialy induced calcium carbonate precipitation blocked the capillary pores.

7.4 Interim conclusions

The main aim of this chapter was to study the effect of freeze-thaw cycles on the microstructural and mechanical properties of bacteria based self-healing mortar. Three Bacillus species were used in this study, namely; Bacillus Sphaericus 57, Bacillus Sphaericus 58 and Bacillus Megaterium 33.

The major outcomes of the test can be drawn as follows:

1) Bacterial based self-healing mortar endures freezing and thawing action better than control cement mortar. After exposing to 30 F-T cycles, the compressive strengths of SP33, SP58 and SP57 have been reduced by 19.4%, 18.37% and 21%, respectively, while the reduction in compressive strength of control mortar was 36.4% percent of

the initial strength. This could be attributed to the dense microstructure of the bacterial specimens.

2) In the SP33 bacterial mortar, the efficiency of microbialy induced calcium carbonate precipitation MICP in terms of strength development was greater than that of the SP57 and SP58.
3) The effect of F-T cycles on flexural strength was very modest after the 1st cycle. This behaviour could be attributed to the increase in frost resistance of bacterial mortar as a result of the dense internal structure and the filling effect of the calcium carbonate.
4) Although the flexural strength of the specimens with the three different types of bacterial spores was higher compared to control mortar, a decrease in strength with increase the number of the cycles has been notices. This reduction in strength can be explained by the gradual decomposing of calcium carbonate crystal caused by the osmotic and swelling pressures cause by water movement.
5) After subjecting to 30 FT cycles, non-bacterial mortar samples have more internal deterioration than bacterial mortar. The amount and intensity of internal cracks of R and RP samples comparing to bacterial samples indicated more damage accumulating after subjecting to 30 FT cycles. This outcome was further supported by the compressive and flexural strength for bacterial cement mortar through a number of FT cycles.
6) The substantial decrease in strength with FT cycles was only seen after 30 FT cycles and this was believed to be a consequence of the abundant ettringite formation after exposing the bacterial mortar samples to 30 F-T cycles, which developed both in voids and on the interface fractures.
7) Deterioration processes operating in cement mortars exposed to FT cycles were attributed to the involvement of two factors: the hydraulic pressure from osmotic phenomena and water crystallisation. However, there are some suspicions regarding the effect of the massive ettringite formation in the matrix-aggregate interface, on the deterioration mechanism of the material.

Chapter 8: Effect of Wet-Dry cycles on the Microstructural and Mechanical properties of bacterial Mortar

8.1 Introduction

In the last twenty years, there are number of studies specifically addressing the durability issues relating to the formation of cracks in concrete developing bio-based repair system a new generation of self-healing concretes. The physical and mechanical properties of concrete are substantial influenced by the environmental conditions. The strength and integrity of the structure does not necessarily affected by the early age crack formation. Nevertheless, under a moist or environment, these cracks cause permeation and durability problems.

Wet-dry cycling is one of the most crucial factors causing the degradation and failure of cement-based materials. It is well known that the microscopic properties of cement-based materials could be determined by its microstructures characteristics (Korb, 2007). However, earlier studies have been concentrated on the deterioration of macroscopic properties, such as the reduction in the flexural strength and the compressive strength, the dynamic elastic modulus loss and the weight loss. Therefore, the main objective of this research is to study the effects of exposure to wetting and drying cycles, on the microstructure, durability and mechanical properties of concretes prepared with biological agents.

The present study was carried out to evaluate the changes occurring in the mechanical properties and the microstructure of bacteria based self-healing concrete when exposed to 30 wetting and drying cycles. For comparison, a set of mortar prisms were made and water cured during the same period prior to testing.

8.2 Materials and methods

8.2.1 **Materials**

Ordinary Portland Cement (OPC) was general purpose cement CEM I (CEMEX, Rugby, UK) complying with BS EN 197-1:2011 and sand was locally available with a maximum particle size of 1 mm. Three types of bacterial strains were selected for this research (Bacillus Megaterium 33 isolated from soil and Bacillus Sphaericus 57 and 58 from Brunel University Biological bank), their properties and specification were explained in Chapter 4. Bacterial strains were grown by the same method as described in “Cultivation media and bacteria culturing” section. The spores were prepared from an overgrown cell cultures. The cultures were streaked on a modified nutrient broth media and were incubated at 30^{o}C for at least

three days. Once spore formation was approved by spore staining method, the cultures were collected and suspended in a saline solution. Then the suspensions were centrifuged at 10,000 rpm for 15 minutes. The spore pellet was washed with chilled deionised water and centrifuged again. This process was repeated three times. The spores were stored at $4^{o}C$ until the start of cement mortar casting. To obtain the total number of spores in each bacterial spore suspension, counting slide was used with chamber depths of 0.02mm. Bacterial spores' concentration used in this study was 10^{8}spores/cm^{3} of mortar. Calcium carbonate precursor used was calcium acetate ($Ca(C_2H_3O_2)_2$). In addition, urea and yeast extract were added as nitrogen source and nutritional carbon for bacteria. The final concentration of bio-reagents (nutrients and precursor) added into the matrix was 3% of cement weight in a proportion of 1:2.25:3 yeast extract: urea: calcium acetate. Bio-reagents were dissolved in water before adding to mortar mixture. The bacterial spores' along with the nutrient solution constitutes the healing agent.

8.2.2 **Methods**

8.2.2.1 Mix and specimens casting

Ordinary Portland cement with water to cement ratio of 0.5 and cement to sand ratio 1:3 were used to prepare the cement mortar prisms with dimensions of 40 mm x 40 mm x 160 mm. There were 5 different mixes with 12 specimens for each mix was prepared. The mix design used in the chapter is the same as that used in Chapter 7 (Table 7.1). Bacterial mixes were prepared by adding 3 different bacterial spores (Bacillus Sphearicus spore 5, Bacillus Sphearicus spore 58 and Bacillus Megaterium spore 33), nutrients for bacteria (yeast extract and urea) and the deposition agents or the precursor (Calcium acetate). Control specimens were prepared in a similar way without adding bacterial cells. The last mix was prepared with the addition of nutrients and precursor. The spores' suspension was diluted to the required concentrations and the bio-reagents were added to the water used for making cement mortar. The mortar mixture was allowed to mix for 3 min. All the specimens were well compacted using table vibrator. All specimens were demoulded after 24 h, apart from the last mix and then cured in an air-conditioned room ($20^{o}C$, >95% RH) until testing. After 28 days of curing, the specimens were allowed to air dry in the laboratory for 12 hrs prior to the start of wet-dry cycling and testing.

8.2.2.2 Wetting and drying cycling

Concrete infrastructure commonly exposes to a wide range of environmental exposure conditions. To examine the durability of self-healing of bacterial concrete, different exposure regimes have been adopted to simulate these conditions. One of these procedures is subjecting concrete to the repeated action of the wetting and drying cycles. After 28 days curing, the specimens were taken out of the water and the alternate cycles of wetting and drying was started. At this time, the specimens were submitted to 30 wet/dry cycles. The exposure procedure was used to mimic real-life outdoor weathering changing from days with sunshine to the elevated temperatures and rainy days. Therefore, each cycle consisted of 24hrs periods of immersion in water at 20°C followed by 22hrs of oven drying at 55°C and then cooling the specimens in laboratory air at 21±1°C for 2hrs (Yang, Yang and Li, 2011; Yang *et al.*, 2009).

A total of 60 specimens distributed in five series were subjected to wet-dry cycles, each series containing three specimens. All specimens belonging to one series had the same characteristics. Specimens without bacterial strain and bio-reagents material were referred as reference R with number from 1-12, while specimens with no bacteria yet have bio-reagents were called RP with number from 1-12. For bacterial samples, the name given to each series follows the format "SP x" with x the name of Bacillus strain and WD, which means if the specimens were or not subjected to wet-dry cycles with number from 1-12. After the 1^{st}, 3^{rd}, 10^{th} and 30^{th} cycles, the specimens were tested for their respective compressive, flexural strengths and microstructural systems.

8.2.2.3 Analytical methods

For each mixture, three specimens were prepared for the flexural strength. The test was determined by using Instron universal testing machine (UTM) in accordance with BS EN 196-1:2016 after subjecting to 1, 3, 10 and 30 wet-dry cycles. The samples were cured for 28 days before applying the wetting and drying actions. The samples were placed centrally between the two steel supporting rollers of the flexure device and the third steel loading roller with a constant rate of (50 ± 10) kN/minute. More details have been stated in Chapter 3. Compressive strength test was carried out by using the Instron universal testing machine (UTM) in accordance with BS EN 196-1:2016. The test was conducted on the two cubic halves from the broken prismatic specimen of the flexural strength test. The broken pieces of the specimens obtained from compressive strength were collected and subjected to Scanning electron microscopy (SEM), an ultra-high performance field emission scanning electron microscope Zeiss Supra 35VP to examine the microstructural changes due

to wetting and drying cycles. An Energy Dispersive X-ray (EDAX) analyses connected with SEM was used to detect the elemental compositions in different spots on the same surface specimens. All the selected samples were gold coated prior to examination. Two SEM images per samples have been captured. More details have been stated in Chapter 3.

8.3 Results and discussions

8.3.1 **Effect of wet-dry cycles on Mechanical properties**

8.3.1.1 Compressive strength

The compressive strengths development of the samples under wet/dry cycles is shown in Table 8-1. The variation of compressive strength of controlled (R), the specimen contain only nutrients (RP), SP57, SP58 and SP33 bacterial mortar samples against number of wetting and drying cycles are presented in Figure 8-1. The results show that after one cycle of wet-dry, the incorporation of strains SP57, SP58 and SP33 in mortar mixture resulted in significant increase in the strength compared to nonbacterial mortar specimens (R and RP). Apart from SP58 bacterial mortar mixture, the compressive strength of all mixture groups increased when subjected to three wet-dry cycles. SP57 bacterial mortars possess the highest compressive strength (40.88Mpa) after exposing to this number of cycles, while, RP and SP 33 mortar specimens show their compressive strength as 33.7 and 31.8Mpa, respectively. The controlled mortar specimen shows a compressive strength of 29.9Mpa after the same number of cycles. This reduction in compressive strength in SP58 bacterial mortar could be attributed to the micro-cracks propagated due to dissimilarities in the thermal expansion coefficient and dry shrinkage of ordinary Portland cement mortar. On the other hand, both groups (SP57 and SP58) had similar results when subjected to ten wetting and drying cycles. The SP33 showed slightly higher strength compared to other bacterial groups, but the results are still lower than the nonbacterial groups.

After 30 cycles of wetting and drying, the controlled specimen shows 41.5% and 15.6% increase in its value over 3 and 10 cycles, respectively. RP, SP58 and SP33 mortar samples exhibit their strength increment after 30 cycles as 36.2%, 41% and 20.4% over 3 cycles strength and 31%, 19.3% and 37.7% over10 cycles strength (Figure 8-1). It can also be seen that there is very little difference in compressive strength values of all bacterial mixes at the end of the test and the rate of increase in strength is almost nil in bacterial specimens whereas controlled mortar specimen showed significant improvement. The reason for this significant increase in strength of control specimens is the longer curing time provided by the wet and

dry exposure. It is evident that the repeated wet exposure and the high drying temperature promoted the development of strength of these specimens. With the frequent cycles, the hydration products will gradually crystallise in the pores and the pore structure becomes denser. The considerable increase in compressive strength of control mortar specimens could also attributed to an increased rate of carbonation and hydration.

It is clear that bacterial mortar samples exhibited lower compressive strength than the control after 30 cycles of wetting and drying while this trend was inversed in the first wet-dry cycle. A 21% decline was observed in compressive strength for SP57, whereas for SP58 and SP33 strength dropped by 18.3% and 9.4%, respectively, relative to the control at that same wet-dry cycle. The lower strength performance of mortars containing bacterial spores could be attributed primarily to the reduction in the bacterial metabolic activities which responsible for precipitation of calcium carbonate as the temperature increased to 55 ^{o}C during the drying time of the cycle. However, most Bacillus spores will survive and withstand comparatively higher temperatures. The maximum growth temperature (the highest temperature at which growth can occur) has been found to be 45 ^{o}C for Bacillus Sphaericua and 48 ^{o}C for Bacillus Megaterium. The temperature at which the spores will die (formerly known as spore death temperature) has also been reported to be 88 ^{o}C for Bacillus Sphaericus and 89 ^{o}C for Bacillus Megaterium (Warth, 1978). In a study to investigate the role of urease in calcium carbonate precipitation, it has been found that the enzymatic activity of Bacillus megaterium reduced by nearly 47% as the temperature increased to 55 °C (Dhami, Reddy and Mukherjee, 2014).

It can also be indicated that the majority of strength increment occurs within the first three cycles, even though the improvement in compressive strength under wet/dry cycles is dependent on the age of the specimen. This improvement under wet-dry cycles could be attributed to the availability of sufficient additional water for further hydration of unhydrated cement (the mechanisms of autogenous healing) and the formation of calcium carbonate crystals (Snoeck and De Belie, 2016). As observed in the literature, additional hydration together with calcium-carbonate precipitation happens at early age, but later, the $CaCO_3$ crystallization will dominate the entire healing (Van Tittelboom *et al.*, 2012). It was suggested that the formation of calcium carbonate during exposing to wetting and drying cycles was attributed to the reaction of unhydrated cement and carbon dioxide (CO_2) dissolved in the cement pore solution (Van Balen, 2005). The older the specimen, the lower is the increment in compressive strength. This is due to the further hydration and hardening of

the cementitious matrix in time. This leads to a lower amount of calcium carbonate precipitating for the self-healing mechanisms in case of bacterial specimens.

Table 8-1 Effect of W-D cycles on the compressive strength of control and bacterial mortar

Mix	Compressive Strength (MPa) per months of W-D cycles (CoV%)			
	1st	3rd	10th	30th
R	26.12(4.4)	29.9(1.0)	36.61(6.6)	42.31(3.2)
RP	26.74(7.0)	33.68(2.9)	35.03(3.3)	45.9(2.5)
SP57	31.6(5.2)	40.89(3.3)	33.59(1.9)	33.45(4.0)
SP58	30.66(1.8)	24.56(4.5)	29.04(3.0)	34.56(2.6)
SP33	29.5(1.5)	31.8(3.1)	27.84(4.8)	38.34(3.6)

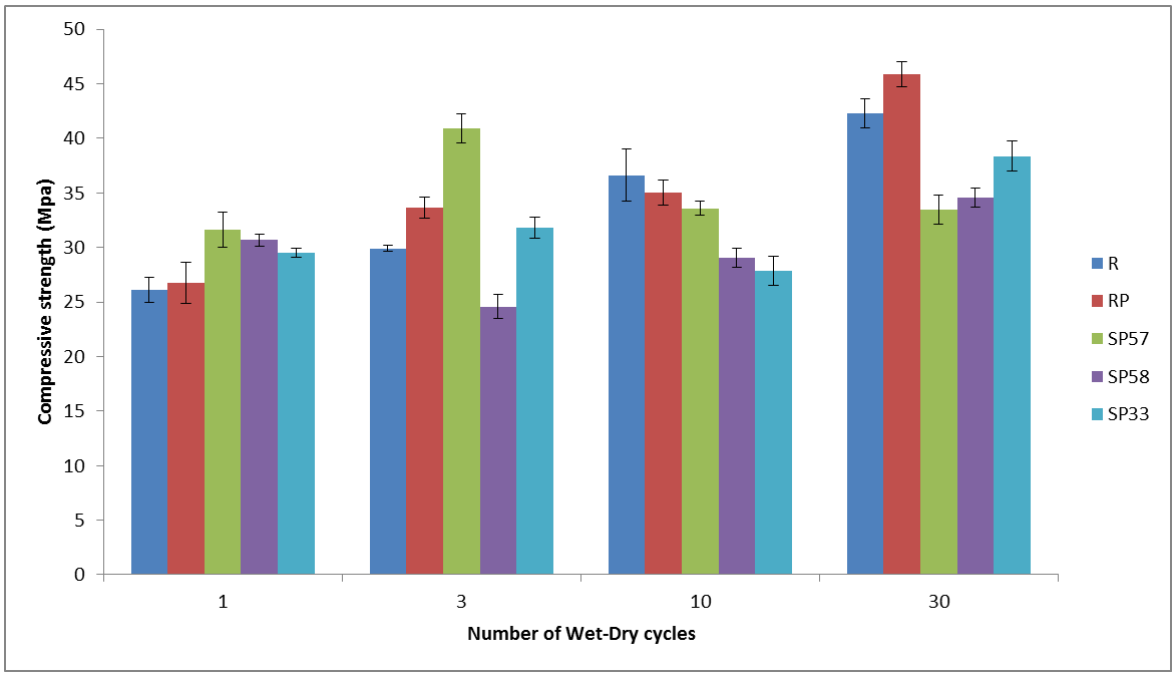

Figure 8-1 Effect of W-D cycles on the Compressive Strength of control and bacterial mortar

8.3.1.2 Flexural strength

The results obtained from flexural strength test of control specimen (R), the specimen contain only nutrients (RP), SP57, SP58 and SP33 cement mortar prisms under the effect of 1, 3, 10 and 30 wet/dry cycles are shown in Table 8-2. Flexural strength test results after one cycle were 5.54, 5.35, 5.51 and 5.18Mpa for SP33, SP58, SP57 and RP compared to control of

3.975MPa. In this study, there is a slight increase in the flexural strength of the bacterial mortar specimens exposed to wet-dry cycles compared to the controls. This is may be because of the potential ability of the self-healing process of bacteria self-healing system to promote flexural strength of the cement mortar. It was assumed that the C-S-H from the cement hydration is usually stronger than the main constituents of healing products. On the other hand, the tensile strength of the matrix is still stronger than the bond strength between the newly formed C-S-H and crack surface, even if C-S-H is formed inside the crack as a result of rehydration of unhydrated cement (Yang *et al.*, 2009).

Variations in flexural strength of specimens with number of wet-dry cycles are presented in Figure 8-2. According to this figure, flexural strength of all specimens except RP present increase-reduce-increase phenomenon along with wet-dry cycles. For Bacillus Spaericus 57 and 58 specimens, flexural strength gradually increases to 6.09 Mpa and 6.50 Mpa, respectively from 1 to 3 cycles, then gradually decreases to 4.72 Mpa and 4.42 Mpa, respectively from 3 to 10 cycles and slightly increased to 4.89 Mpa and 5.23 Mpa, respectively from 10 to 30 cycles. The flexural strength of Bacillus Megaterium 33 specimen from 5.54 Mpa at 1 cycle increases to 9.25 Mpa at 3 cycles then decreases suddenly from 3 to 10 cycles, 10 cycles becomes 4.91Mpa, 10 to 30 cycles increases to 5.41Mpa. But flexural strength of RP specimens presents reduce-increase-reduce phenomenon in the process of wet-dry cycles. 5.18 Mpa at 1 cycle reduces to 3.39 Mpa at 3 cycles, increases to 6.37 Mpa from 3 to 10 cycles and then reduces to 5.36 Mpa at 30 cycles. For bacterial mortar samples, the flexural strength change rule has a clear difference with RP. This finding can be explained by that in the early stage of wet-dry exposure, there was crystal (hydration products) accumulate in the pores inside the mortar, while the crystallisation pressure is not enough to make the mortar cracked, so the flexural strength increased. However, as the dry–wet cycles increased, excessive crystal products cause cracks in the specimen, and the crack further expands and connects, which leads to decrease the flexural strength. With the accumulation of crystal, crystal filled the pore and the crack, the flexural strength increased. For RP sample, the majority of flexural strength loss occurs within the first three cycles. However, after 10 cycles, values for flexural strength increased relative to these minimum values by 88 %. In these samples, the flexural strength measured after 30 cycles of wet-dry reduced by 15.86% relative to that after 10 cycles. The initial damage of RP sample after subjecting to 3 wet-dry cycles can be attributed to the retarding effect of yeast extract and urea used in this mixture. It has been found that yeast extract acts as retarder, decreasing the degree of hydration in

cement paste samples(Wang *et al.*, 2014b) and this reduction is caused by the presence of carbohydrates in yeast extract that are known to cause retarding effect (Bolobova and Kondrashchenko, 2000). Urea can also influence the hydration behaviour of the cementitious material by depressing the heat of hydration and retarded the initial setting (Mwaluwinga, Ayano and Sakata, 1997). The presence of the retarder delayed the ettringite and the C–S–H gel formation which are the main strength-contributing compounds.

It can be observed that with bacterial spores' incorporation, the flexural strength of SP33 mortar after 3 W-D cycles was further enhanced (i.e., from 5.54 MPa to 9.25 MPa) with an additional increase of 53% compared to control specimens. In addition, SP33 samples show the highest increase during the 1st, 3rd, 10th and 30th W-D cycle. The flexural strength of specimens containing SP58, SP57 and RP subjected to three wet-dry cycles was increased by 7.3, 0.5 and 5.4%, respectively compared to control specimen. However, there is a little increase in flexural strength of bacterial mortar after subjecting to 10 wet/dry cycles comparing to their values after 3 cycles.

Table 8-2 Effect of W-D cycles on the flexural strength of control and bacterial mortar

Mix	Flexural Strength (MPa) per months of W-D cycles (CoV%)			
	1st	3rd	10th	30th
R	3.98(9.4)	6.06(2.3)	2.61(15.8)	5.65(7.5)
RP	5.18(2.6)	3.39(9.4)	6.37(6.6)	5.36(5.2)
SP57	5.51(7.3)	6.09(1.6)	4.72(9)	4.89(13.6)
SP58	5.35(4.4)	6.50(5.5)	4.42(19.9)	5.23(3.7)
SP33	5.54(10.1)	9.25(4.8)	4.91(10.6)	5.14(3.0)

Generally, the wet-dry action exhibited the optimum mechanical recovery among different accelerated exposure conditions. It can be assumed that, the additional water has been evaporated during the drying period leading to increase the ions concentrations in the water remaining in the cracks. Significant amounts of reactant were concentrated; in this case, for further reactions and the through-solution reactions were also available in the presence of adequate amount of water. Furthermore, the additional precipitation of $CaCO_3$ due to carbon dioxide penetration into the crack during the drying time would be beneficial for crack

closing (Sisomphon, Copuroglu and Koenders, 2013). It has also been stated that the interaction of unhydrated cementitious materials, H_2O and carbon dioxide can be stimulated by subjecting to this type of exposure condition (Qian, Zhou and Schlangen, 2010). It can be indicated, from another opinion, that wet-dry action exhibited more regaining in the mechanical properties compared to water-cured regimes due to the high internal moisture content and the action of unnecessary water inside the specimen (Yang *et al.*, 2011).

In this work, the biological agents (bacterial spores, deposition agents and nutrients) served as self-healing agents to trigger the mineralization of calcium carbonate in cement mortar. The significant enhancement in flexural strength for bacterial mortar specimens is mostly qualified to their microstructural change. This enhancement clearly indicates the efficiency of biological agents in precipitating calcium carbonates and filling the micro-pores and thereby strengthening the matrix. Therefore, the higher flexural strength, particularly in the case of using SP33 bacterial spores, indicates the formation of dense microstructure comparing to controlled matrix.

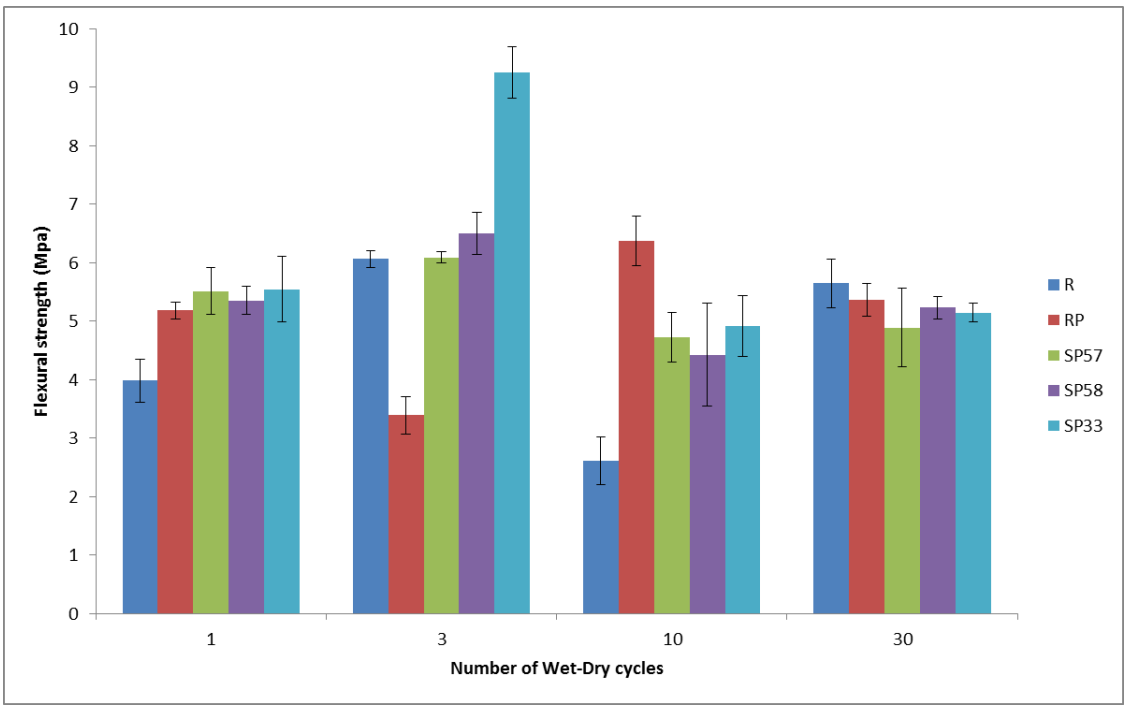

Figure 8-2 Effect of W-D cycles on the Flexural Strength of control and bacterial mortar

8.3.2 **Effect of wet-dry on the microstructure**

8.3.2.1 Microstructure prior to wet/dry cycling

Figures 8-3 and 8-4 display the microstructure of control mortar and that containing nutrients only (3% of cement weight) before exposing to wet-dry cycles. The similar micro topographies from the SEM micrographs of control mortar and mortar containing nutrients were used as confirmation of the comparable values of the compressive strength of these samples. However, unidentified crystals can be found disconnected to the C-S-H structure in the RP sample.

The dominant phase present in the matrix of controlled specimen, as seen in Figure 8-3, is an entangled mass of calcium silicate hydrates (C-S-H) and voids. C-S-H is a rigid gel produced from cement hydration as a major hydration product contributes to compressive strength enhancement of concrete.

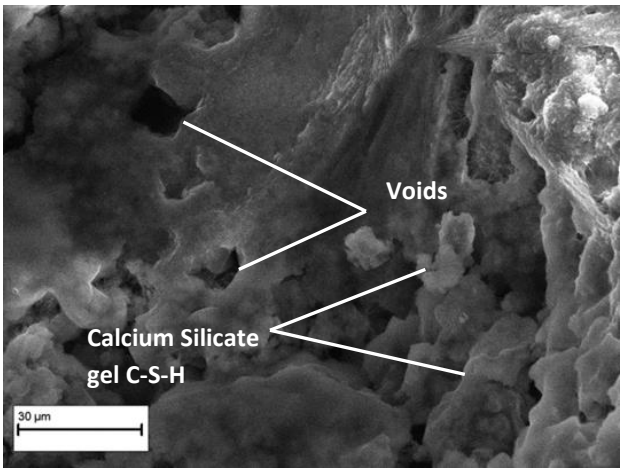

Figure 8-3 Control specimen R before subjecting to WT cycles

The microstructure observed in Figure 8-4 for RP sample after 28 days of water curing was similar to the controlled mortar, yet, less voids and more Calcium Silicate Hydrate (C-S-H) were detected. This is attributed to the ability of the calcium acetate to reduce the pH value of the mortar mixture, enhancing the C-S-H and ettringite formation (Kim *et al.*, 2016).

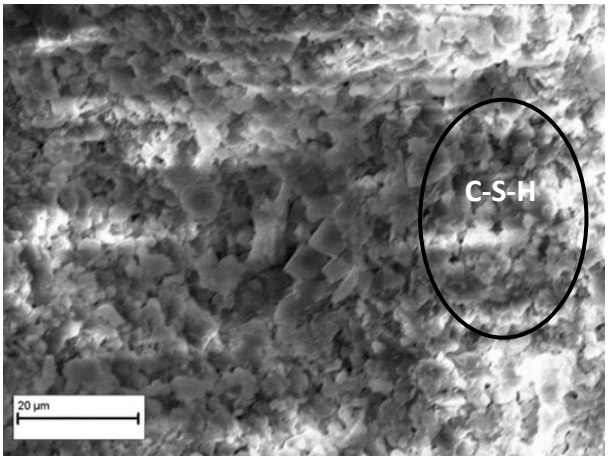

Figure 8-4 Specimen with only nutrient added RP before subjecting to WT cycles

Figures 8-5, 8-7 and 8-9 exhibit the structural analysis of bacterial (SP33, SP57 and SP58) blended cement mortars, which were not exposed to wet/dry cycling. In general, the structure of the three types bacteria cement mortar was denser and less porous comparing to control mortar at 28 days of curing due to the compact formation of calcium carbonate, which is probably the reason for the high compressive strength compared to control mortar. SEM image illustrated the presence of calcium carbonate crystals formed by Bacillus Megaterium 33, Bacillus Sphaericus 57 and Bacillus Sphaericus 58, in different shape and amount. As bacteria provided nucleation sites for the mineralisation process, the surfaces of bacteria were found to be enclosed by calcite crystals. The calcium carbonate crystals in the SP33 bacterial mortars were observed in a flower-shaped clusters made with many well-arranged thin (or rod-like) crystals of $CaCO_3$ (Figure 8-5(a) and (b)). The chemical composition of a selected area in the surface fracture was analysed using EDAX, which revealed the presence of only three elements in the samples.

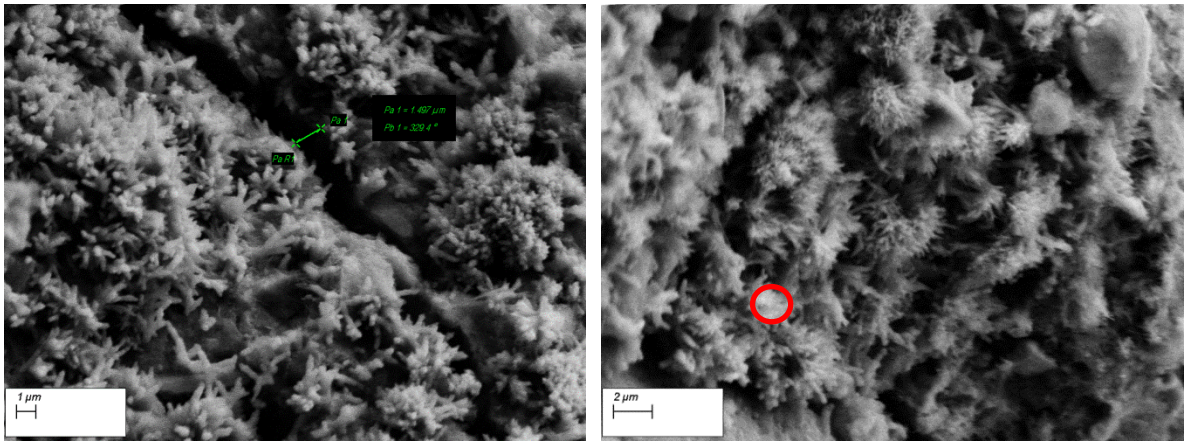

(a) (b)

Figure 8-5 SEM images of SP33 specimen before subjecting to WT cycles at 1000x magnification; showing precipitation of (a) rod-like crystals of $CaCO_3$ (b) flower-shaped clusters of $CaCO_3$

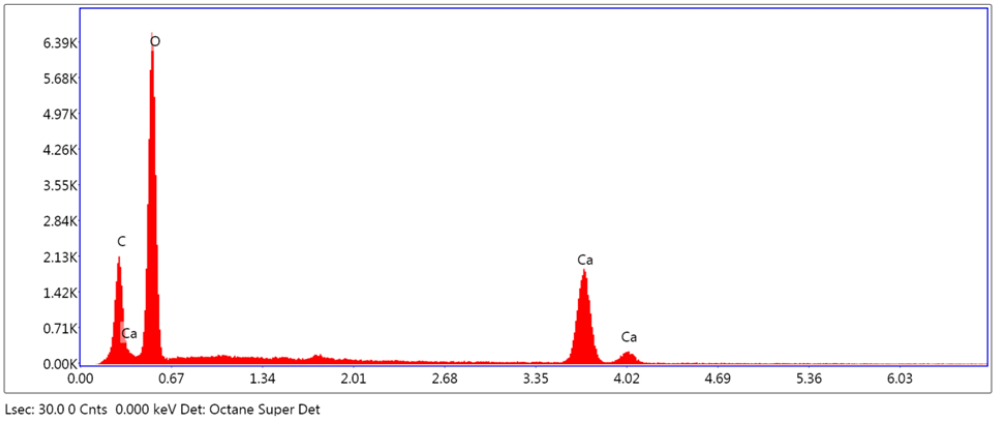

Figure 8-6 EDAX analysis of SP33 specimen before subjecting to WT cycles (the area enclosed by the red circle in Figure 8-5)

As indicated in Tables 8-3, the samples contained calcium, oxygen and carbon with different weight percentages. The weight percentages of these elements were nearly identical to the theoretical values of elemental compositions of $CaCO_3$ (Meiron *et al.*, 2011).

This analysis proves that the composition of the calcium carbonate produced by SP33 is 100% pure due to the absence of any other elements.

Table 8-3 Elemental analysis of SP33 specimen before subjecting to WT cycles

Element	Weight %
C K	12.5
O K	53.5
CaK	33.9

The microstructure of the SP57 samples before subjecting to wet-dry cycles was characterised by an arrangement of planar arrays of coarse hexagon-shaped of either $CaCO_3$ crystal or plates of calcium hydroxide (Figure 8-7(a) and (b)). Figure 8-7(a) show a great number of merged plates crystals. These crystals are more compact and regular distributed.

This calcium carbonate crystal morphology is consistent with other studies of a microbial induced calcium carbonate precipitation (MICP) process (Choi, Wang and Chu, 2016; Abo-El-Enein *et al.*, 2012). Under normal conditions, this form of calcium carbonate is considered thermodynamically stable.

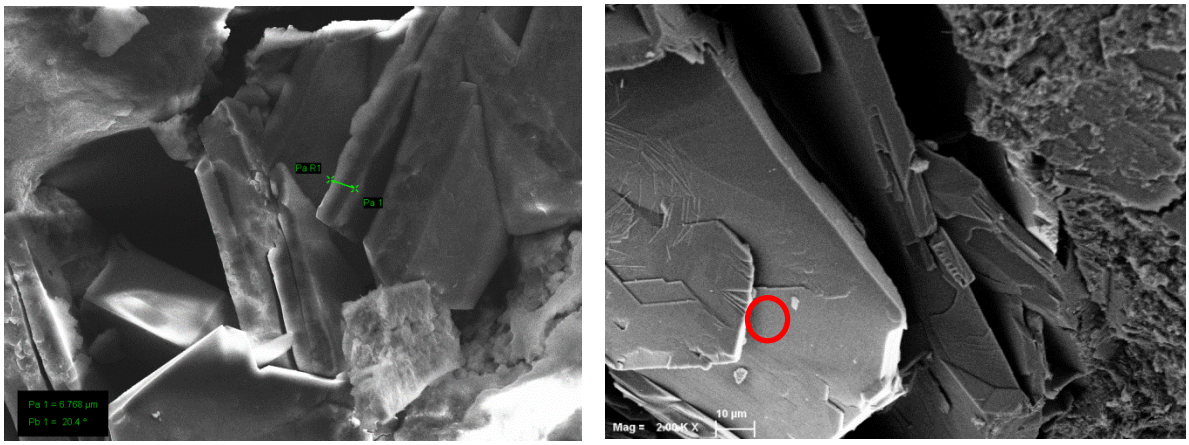

(a) (b)

Figure 8-7 SEM images of SP57 specimen before subjecting to WT cycles at 2000x magnification, (a) compact and regular distributed plates, (b) planar arrays of coarse hexagon-shaped plates

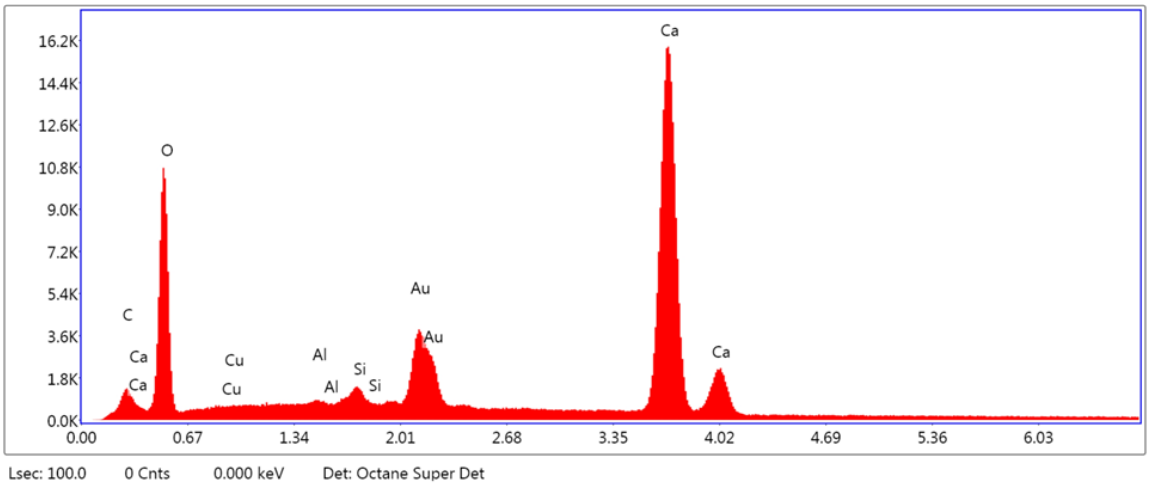

Figure 8-8 EDAX analysis of SP57 specimen before subjecting to WT cycles

Elemental analysis of SP57 specimen as indicated in Table 8-4 and Figure 8-8 shows that the sample contained negligible traces of elemental silicon and a minute percentage of Au. The peak of Au element was present in the EDAX analysis because of gold sputter coating. Due to the big differences between the actual and theoretical values of the composition of calcium carbonate, the hexagonal plates could be either a not 100% pure calcium carbonate as a result of the presence of other elements such as silicon, or other hydration products like CH.

Table 8-4 Elemental analysis of SP57 specimen before subjecting to WT cycles

Element	Weight %		Difference between actual and theoretical
	Actual value	Theoretical value	
C K	1.55	12	10.45
O K	26.14	48	21.86
CuL	0.00	----	----
AlK	0.00	----	----
SiK	0.57	----	----
AuM	8.07	----	----
CaK	63.68	40	23.68

It is clear that the amount of calcite precipitation in SP58 specimen (Figure 8-7) is less comparing to other bacterial mortar samples. This could explain the low compressive strength results with SP58 added. The crystal morphology observed in Figure 8-9 was close to that in SP33 bacterial sample. The calcium carbonate can be identified as a cluster of small rod crystals. The chemical composition of this cluster found in the surface fracture was analysed using EDAX, which revealed the presence of the main elements of calcium carbonate ($CaCO_3$) as presented in Figure 8-9.

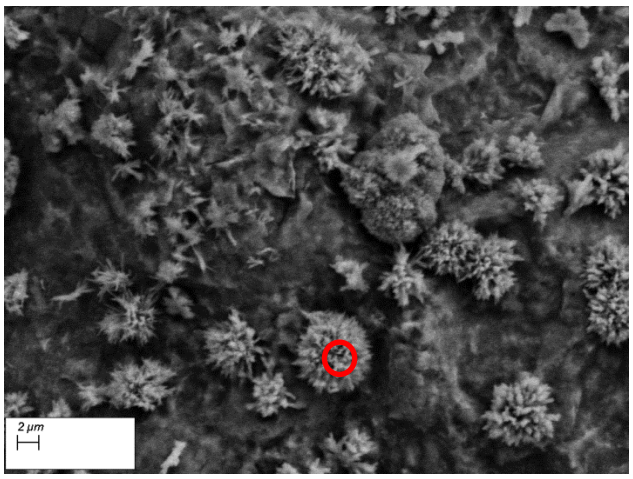

Figure 8-9 SP58 specimen before subjecting to WT cycles (Mag=5000X)

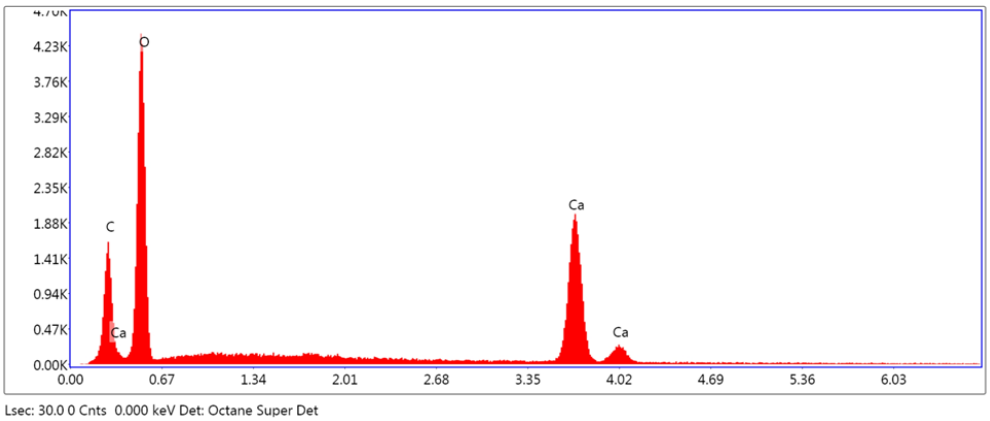

Figure 8-9 EDAX analysis of SP58 specimen before subjecting to WT cycles

Elemental analysis of SP58 specimen as indicated in Table 8-5 revealed that the sample contained the same elements as SP33 specimen, with no significant variances noticed between the elements found in the two samples analysed.

Table 8-5 Elemental analysis of SP58 specimen before subjecting to WT cycles

Element	Weight %
C K	11.1
O K	46.2
CaK	42.6

Despite the similarities in the test conditions (bacterial concentration, mix design, calcium source and the nutrients added), differences in crystal morphologies and amount of crystals precipitated can be detected among all the bacterial samples in this study. It has been proved that, in the presence of calcium acetate, calcium carbonate crystals can be precipitated by most of the soil bacteria and that calcite precipitation is just a function of the medium composition (Boquet, Boronat and Ramos-Cormenzana, 1973). It was also found that, calcium carbonate crystals exhibit a wide range of morphologies and crystal sizes when precipitated in the media containing Ca (such as calcium acetate) (Urzi et al., 1999).

8.3.2.2 Microstructure after wet-dry cycling

8.3.2.2.1 Non-bacterial mortar

In order to better understand the effect of wet-dry cycles on the microstructural properties of plain mortar, micrographs were captured from fracture surface of specimens subjected to 1, 3, 10 and 30 wet-dry cycles and compared to that for specimens without wet/dry cycling . The SEM image of the control specimen subjected to three wet-dry cycles action is shown in Figure 8-10. Different scales pores are major defects in control specimen, and micro-cracks are also observed in this micrograph.

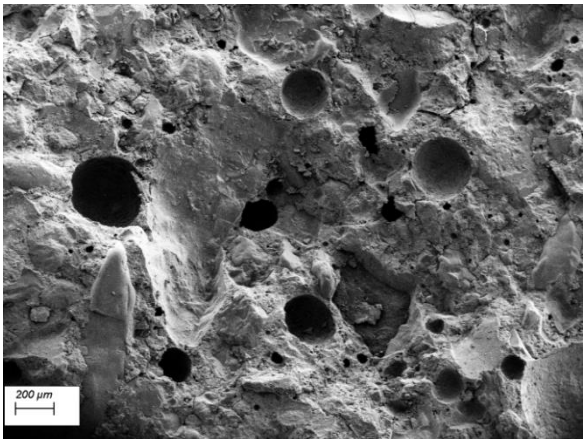

Figure 8-10 Control (R) specimen subjected to Three WT cycles

Both small plate crystal of tobemorite and big hexagonal plate of portlandite are visible on the surface fracture in Figure 8-11 for the mortar specimen containing nutrient only under three wet and dry cycling conditions.

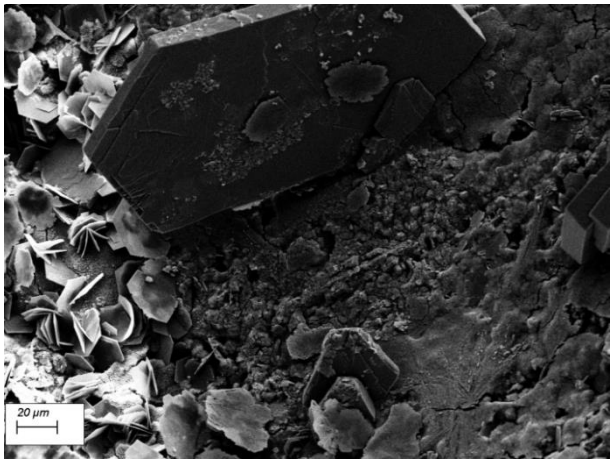

Figure 8-11 RP specimen subjected to three WT cycles (Mag=1000X)

After 30 wet-dry cycles, the microstructure of control mortar (R) exhibits a distribution of C-S-H gel in a form of tiny fibres which gathers to make a mesh, known as “honeycomb” (Figure 8-12(a)). A large amount of ettringite formed at the interfaces of cement paste or in the pores can also be seen in the microstructure of control sample (Figure 8-12(b)). These features can be seen as a result of carbonation reaction. It has been approved that the wet-dry cycle could result in quicker carbonation reaction by affecting the chemical part of this process (Neves, Branco and De Brito, 2013). Diffusion of carbon dioxide through cement matrix leads to concrete carbonation (Pade and Guimaraes, 2007). If the cement mortar was entirely dry or in a water-saturated state, carbonation cannot occur. Upon drying, no dissolution and transport can take place; in contrast, no carbonation will happen if the cement

mortar is continuously immersed in water. Instead of carbonate formation, precipitation inhibition and binder leaching will be preferred.

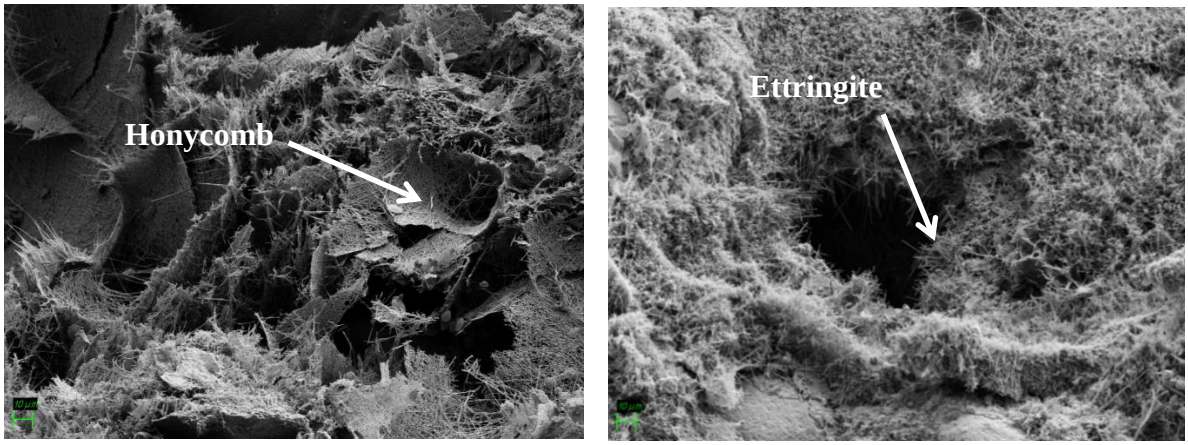

(a) (b)

Figure 8-12 SEM images of control (R) specimen subjected to 30 WT cycles at 1000x magnification (a) formation of C-S-H gel in a form of honycomb, (b) ettringite formation

The existence of ettringite crystals was more noticeable and the development of the needle-like crystals was clearly enhanced after subjecting to 30 wetting and drying cycles.

Specimens made with nutrients only (RP) contained very little or no visible amounts of these features (Figure 8-13(a) and (b)). The formation of ettringite in the control test specimens implies that the expansion and cracking phenomena could be described as internal sulphate attack, where sulphates are supplied by the cement paste itself. Therefore, the wet-dry cycles has some influence on the microstructures of the control specimen.

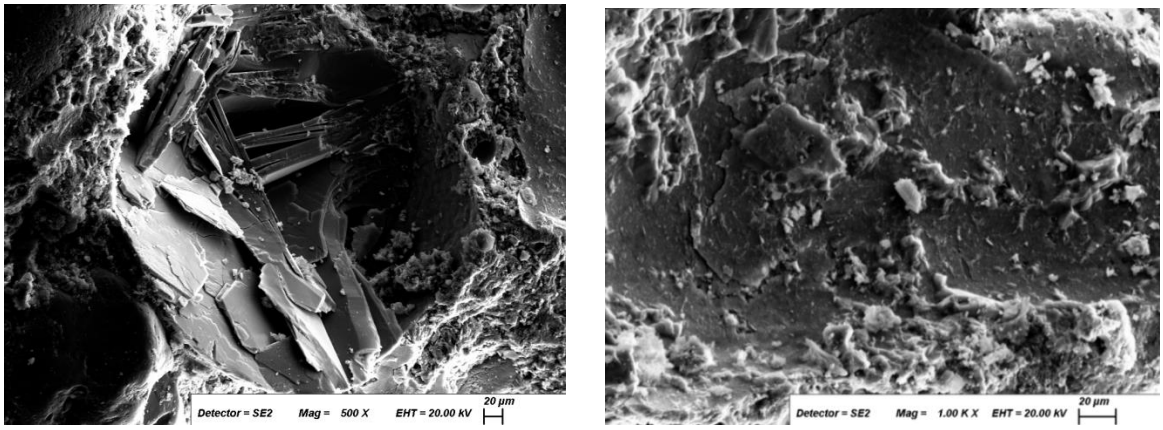

(a) (b)

Figure 8-13 SEM images of RP specimen subjected to 30 WT cycles at (a) 500x magnification and (b)1000x magnification

8.3.2.2.2 Bacterial mortars

The SEM observation of bacterial samples taken after each cycle allowed the spread of the first cracks caused by W-D cycles to be located and tracked. After 10 and 30 wet-dry cycles, the microstructure of all bacterial test specimens showed features in the paste matrix on crack surfaces and in voids. These features contain large platelet crystal phases and column aggregates interspersed between finer phases and accumulated in voids as presented in the micrographs of SP33, SP57 and SP58 samples after exposing to 10 wet-dry cycles action (Figures 8-14, 8-17 and 8-20(a) and (b) respectively). In the literature, calcite formation can be proved by the aggregation of several small hexagonal platy crystals in the form of column (Cultrone, Sebastian and Huertas, 2005). Commonly, calcite occurs in a variety of crystal shapes (rhombohedra, prisms, tabular and scalenohedra forms), and the difference in the crystal habit and size depends on the thickness of the sample (Cizer *et al.*, 2012).

However, based on the EDAX analysis of the selected area of all bacterial mortar samples subjected to 30 W-D cycles presented in Figures 8-15, 8-18 and 8-21, it has been found that the weight percent of the element compositions shows big differences between the actual and theoretical values of Ca, O and C. This means that the features showed in the microstructure of the bacterial mortar could be either a result of the precipitation of hydration products like CH or a not 100% pure calcium carbonate.

It can also be needle like features (needle aragonite) within the paste matrix and inside the pore as shown in Figures 8-16(a) and (b), 8-19 and 8-22 of SP33, SP57 and SP58 samples

subjected to 30 wet-dry cycles action, respectively. It is seen from the bacterial cement mortar of SP 33, SP57 and SP58 that the cracks and the micropores were fully occupied with abundant residue after wet–dry conditioning cycles. The amount of cracks in this bacterial mortar greatly reduced compared to non-bacterial mortar. Therefore, the microstructure of bacterial mortar with calcite crystals and rehydration products possesses different characteristics from non-bacterial cement mortar. This observation suggested that bacterial mortar with very low amount of micro cracks will most likely have lower permeability and better durability than non-bacterial mortar.

While precipitation of considerable quantities of these obvious calcium carbonate polymorphs was only detected on the surface fracture of bacteria-based samples, it suggests that its formation was associated to bacterial activity. Formation of such a structure determines the increase in the strength of bacterial cement mortar.

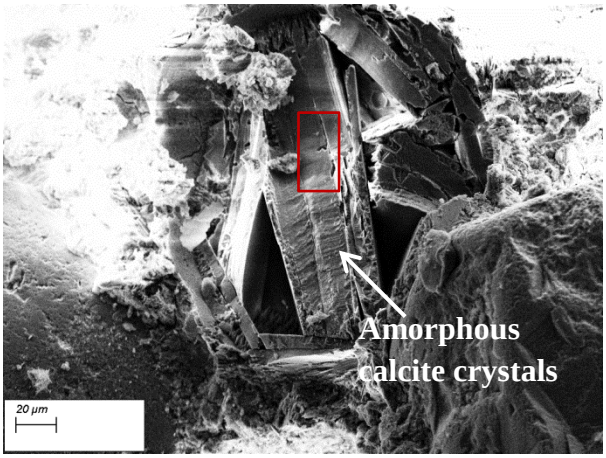

Figure 8-14 SP33 specimen subjected to TEN WT cycles (Mag=10000X)

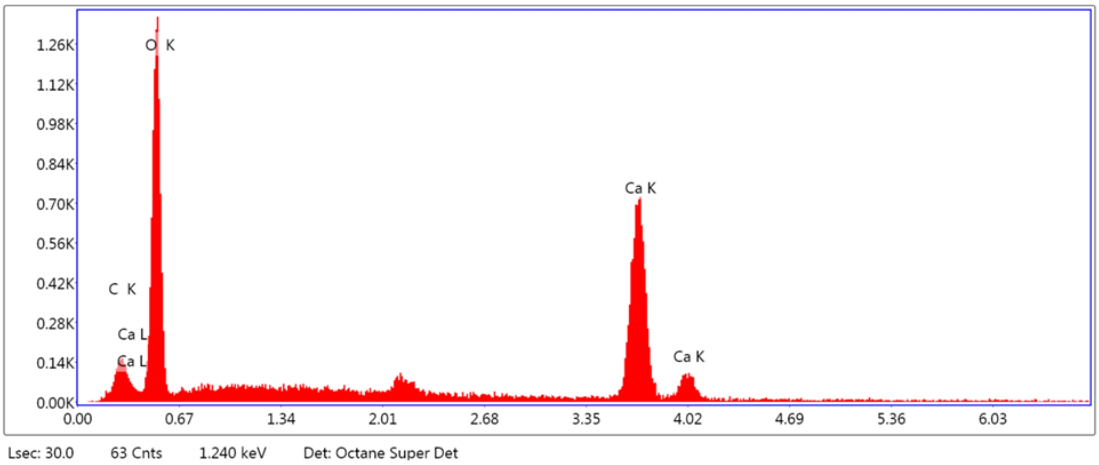

Figure 8-15 EDAX analysis of SP33 specimen subjected to TEN WT cycles

Table 8-6 Elemental analysis of SP33 specimen subjected to TEN WT cycles

Element	Weight %
C K	2.80
O K	33.31
CaK	63.89

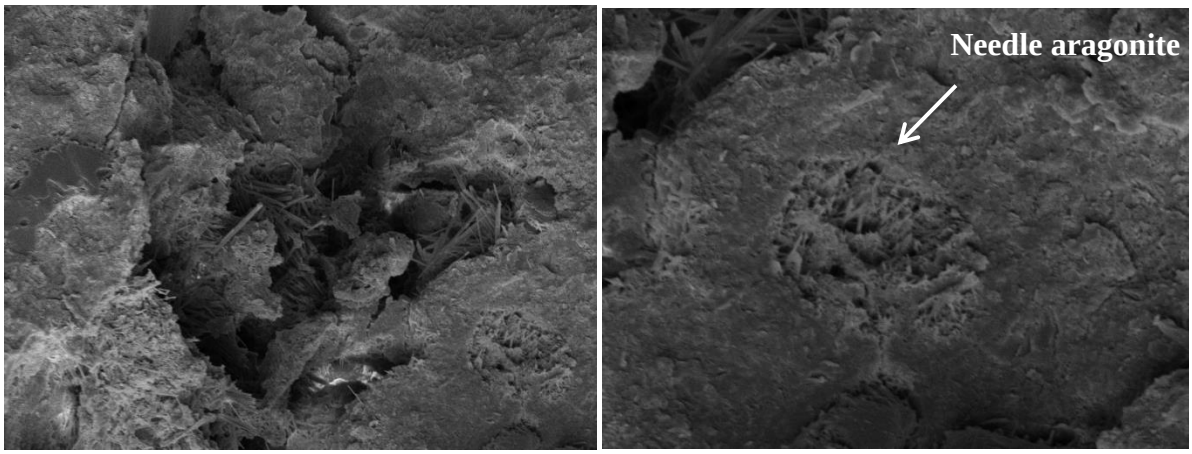

(a) (b)

Figure 8-16 SEM images of SP33 specimen subjected to 30 WT cycles at 5000x magnification showing formation of aragonite (a) within the paste matrix and (b) inside the pore

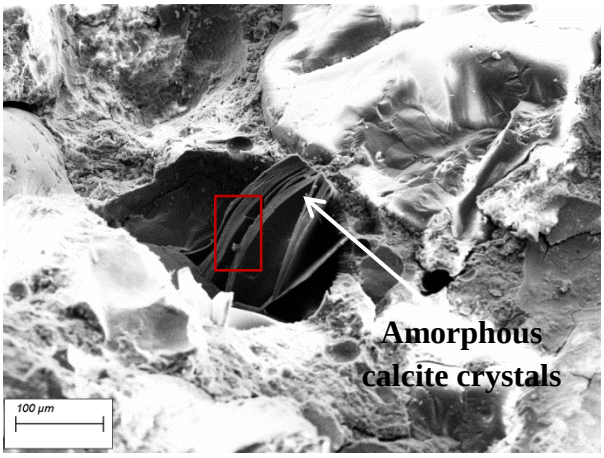

Figure 8-17 SP57 specimen subjected to TEN WT cycles

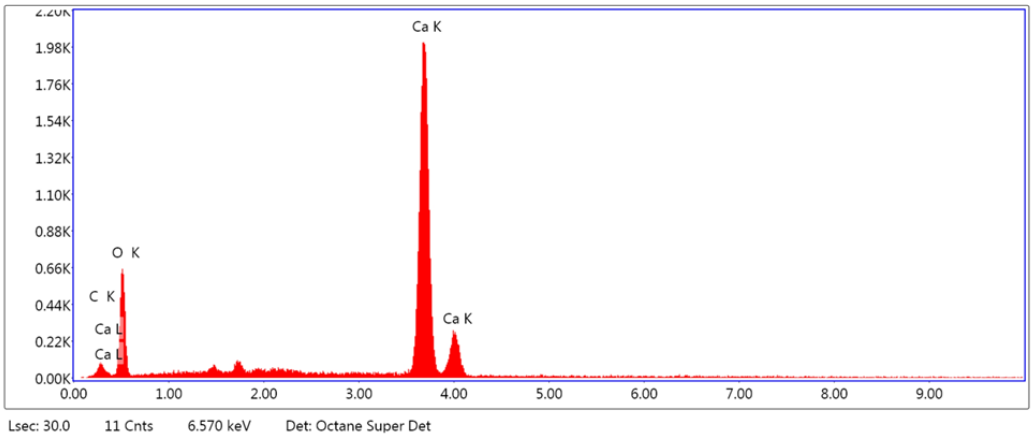

Figure 8-18 EDAX analysis of SP57 specimen subjected to ten WT cycles

Table 8-7 Elemental analysis of SP57 specimen subjected to TEN WT cycles

Element	Weight %
C K	1.30
O K	19.29
CaK	79.41

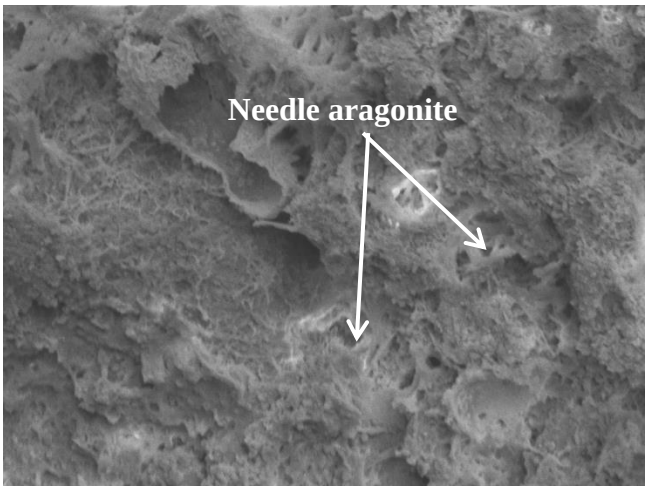

Figure 8-19 SEM image of SP57 specimen subjected to 30 WT cycles at 10000x magnification

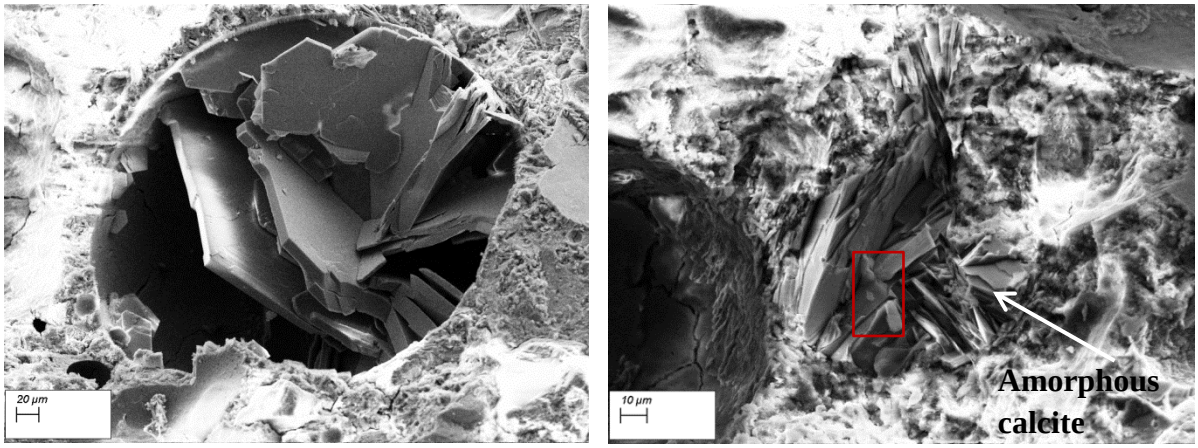

(a) (b)

Figure 8-20 SEM images of SP58 specimen subjected to ten WT cycles at 10000x magnification showing formation of large platelet crystal phases and column aggregates (a) accumulated in voids and (b) interspersed between finer phases

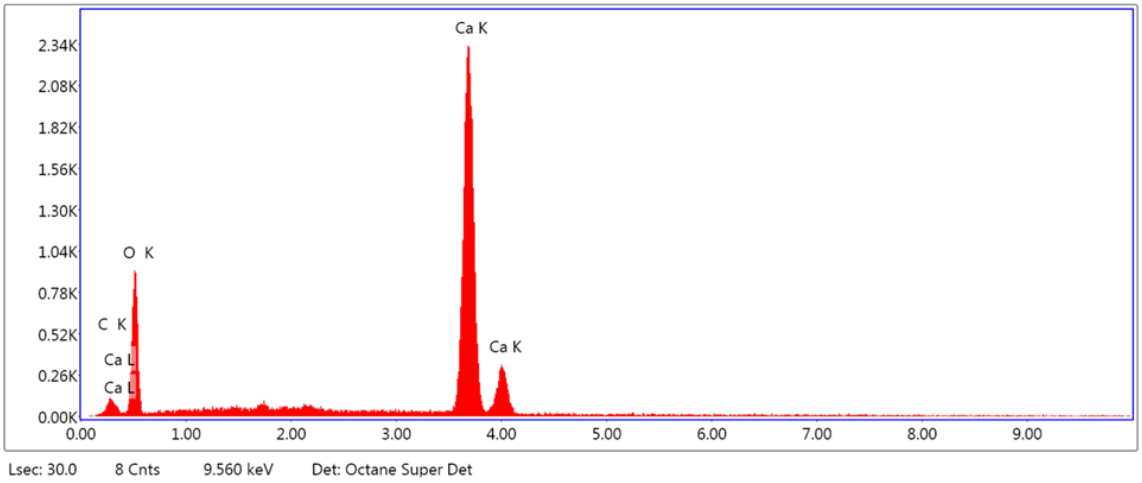

Figure 8-21 EDAX analysis of SP58 specimen subjected to ten WT cycles

Table 8-8 Elemental analysis of SP58 specimen subjected to ten WT cycles

Element	Weight %
C K	1.36
O K	22.57
CaK	76.07

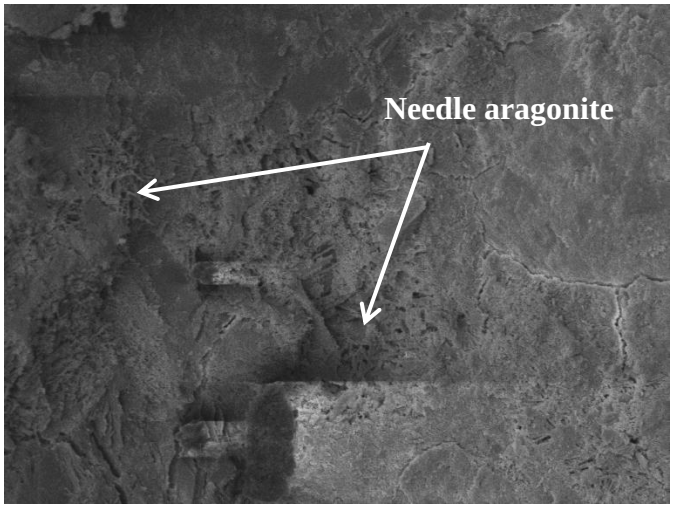

Figure 8-22 SEM image of SP58 specimen subjected to 30 WT cycles at 5000x magnification

The microstructural features shown were found primarily in bacterial specimens that exhibited higher compressive strength after three wet-dry condition cycles, specifically made of SP33 and SP57. Non-bacterial specimens contained very little or no visible amounts of these features. Thus, the extent to which the features formed within the microstructure of the test specimens correlates very well with the bacterial activity. One more important observation from EDX analysis results (Tables 8-7, 8-8 and 8-9) is that the amount of calcite crystal precipitation of the bacterial cement mortar is higher with SP57 after ten wetting-drying compared to SP58 and SP33 specimens.

As the Bacillus Sphaericus used in the SP57 mortar sample is capable to generate more urease enzyme through its microbial activity under wet-dry action compared with the Bacillus Megaterium (33) and the other Bacillus Sphaericus (58) used in this research, hence more calcium carbonate was precipitated. Therefore, SP57 mortar sample performed better during wetting-drying cycles.

8.4 Interim conclusions

This chapter presents the findings of an investigation into the bacteria based self-healing cement mortar subjected to 30 wetting and drying condition cycles. Some major conclusions could be drawn as follows:

1) After 30 cycles of wetting and drying, bacterial self-healing mortar samples exhibited lower compressive strength than the control. A 21% decline was observed in compressive strength for SP57, whereas for SP58 and SP33 strength dropped by 18.3% and 9.4%, respectively. This trend could be attributed primarily to the

reduction in the bacterial metabolic activities which responsible for precipitation of calcium carbonate as the temperature increased to 55 ^{o}C during the drying time of the cycle.

2) According to the flexural strength of all specimens except RP, the results show increase-reduce-increase phenomenon along with wet-dry cycles.
3) SP33 samples show the highest increase during the 1st, 3rd, 10th and 30th W-D cycle. The flexural strength of specimens containing SP58, SP57 and RP subjected to three wet-dry cycles was increased by 7.3, 0.5 and 5.4%, respectively compared to control specimen.
4) This study revealed that mechanical property enhancement due to bacterial calcite precipitation was achievable in cementitious materials in commonly encountered exposure environments, especially, the continuous or occasional contact with external water.
5) The strength data suggested a rapid rate of self-healing for the first few cycles of water exposure and drying, but a substantially lower rate after 10 cycles and reaching a plateau beyond 30 cycles.
6) It has been found by surface chemical analysis (EDAX) that the crystals formed within and on the surface of the bacterial samples were either a precipitation of hydration products like CH or a not 100% pure calcium carbonate.
7) Bacterial cement mortars exhibited significant differences in the calcite polymorph when subjected them to wet-dry cycles. Amorphous calcite crystals accumulated in voids, whereas the paste matrix covered with needle like features (needle aragonite).
8) The self-healing of micro-cracks in bacterial mortar was expected to overcome the problem of cracking in cementitious materials for structures exposed to wetting and drying environmental conditions. Thus self-healing should maintain strength and durability even when subjected to these conditions. Outdoor exposure studies should be conducted to confirm this expectation in bacterial mortars exposed to natural environments.
9) The test results achieved in this study showed that the test procedure adopted could be useful in assessing the durability of bacteria based self-healing materials.

Chapter 9: Effect of outdoor exposure on the Microstructural and Mechanical properties of bacterial Mortar

9.1 Introduction

The service life of structures is significantly influenced by the environmental or exposure conditions. One of the main deterioration factors affecting cementitious conditions is carbonation. Therefore, substantial efforts have been made to determine the influence of carbonation on concrete material in the lab and field throughout the world (Verma, Bhadauria and Akhtar, 2015). Under the influence of long exposure to carbone dioxide, carbonation reaction takes place as a combination of physical and chemical concrete transformation. Carbonation leads to break down the passive layer covering the steel in reinforcement concrete. Despite the positive effect of the steel bar on minimising the crack width, the original crack formation cannot be prohibited. Many cracks repair techniques have been used when cracks become visible. One of these techniques is incorporating bacterial agents into the concrete matrix to induce its self-healing ability.

Bacteria-based self-healing concrete has been developed with the availability of new generations of self-healing in recent years. The structural performance and durability of concrete structures is expected to be enhanced by using bacterial concrete. This is because the dense microstructure that decreases water permeability and restricts ingress of harmful substances to concrete matrix. Although the process of self-healing in concrete is well understood, the details concerning self-healing in bacterial concrete are insufficient, particularly in regard to exposing to different environmental conditions. These conditions can vary greatly and include the concrete exposing to the outdoor environment such as the action of wind, sun and rain-water.

The present investigation focuses on the self-healing of bacterial mortars after 18 months of outdoor exposure. Visual control assessment and measurement of the physical properties such as compressive strength and flexural strength were used to evaluate changes in mortar samples subjected to outdoor exposure. To study the microstructure, the crashed specimens after the compressive strength test were used for microstructural investigation for each specific age using scanning electron microscopy (SEM) and energy dispersive X-ray analysis (EDAX).

9.2 Materials and methods

9.2.1 **Materials**

Ordinary Portland Cement (OPC) was general purpose cement CEM I (CEMEX, Rugby, UK) complying with BS EN 197-1:2011 and sand was locally available with a maximum particle size of 1 mm. Three types of bacterial strains were selected for this research (Bacillus Megaterium 33 isolated from soil and Bacillus Sphaericus 57 and 58 from Brunel University Biological bank), their properties and specification were explained in Chapter 4. Bacterial strains were grown by the same method as described in "Cultivation media and bacteria culturing" section. The spores were prepared from an overgrown cell cultures. The cultures were streaked on a modified nutrient broth media and were incubated at 30^{o}C for at least three days. Once spore formation was approved by spore staining method, the cultures were collected and suspended in a saline solution. Then the suspensions were centrifuged at 10,000 rpm for 15 minutes. The spore pellet was washed with chilled deionised water and centrifuged again. This process was repeated three times. The spores were stored at 4^{o}C until the start of cement mortar casting. To obtain the total number of spores in each bacterial spore suspension, counting slide was used with chamber depths of 0.02mm. Bacterial spores' concentration used in this study was 10^{8}spores/cm^{3} of mortar. Calcium carbonate precursor used was calcium acetate (Ca $(C_2H_3O_2)_2$). In addition, urea and yeast extract were added as nitrogen source and nutritional carbon for bacteria. The final concentration of bio-reagents (nutrients and precursor) added into the matrix was 3% of cement weight in a proportion of 1:2.25:3 yeast extract: urea: calcium acetate. Bio-reagents were dissolved in water before adding to mortar mixture. The bacterial spores' along with the nutrient solution constitutes the healing agent.

9.2.2 **Methods**

9.2.2.1 Mix and specimens casting

Mortar specimens were prepared using general purpose Ordinary Portland Cement CEM I (CEMEX, Rugby, UK) complying with BS EN 197-1:2011 and locally available sand with maximum size of 1 mm. The mortar mix was designed with a constant water cement ratio of 0·5 and cement to sand ratio 1:3. Samples were cast in prismatic moulds 40mm×40mm×160mm in size. The mix design and sample naming used in the chapter are the same as that used in Chapter 7 (Table 7.1). Bacterial mortars specimens were prepared with three different types of bacterial spores (Bacillus Sphaericus 57, Bacillus Sphaericus 58 and

Bacillus Megaterium). To prepare bacterial spores, mature cultures (3–7 days) were collected and the spores were harvested by centrifugation and washing with deionized sterile water three times. Bacterial spore concentration used in this study was 10^8 cell/cm^3 of mortar. A counting chamber slide was used to determine the spore's concentration. Yeast extract, urea and calcium acetate (Ca $(C_2H_3O_2)_2$) were added to the mortars specimens as a nutrient for bacteria with a total additional ratio of 3% by weight of cement. The addition of the nutrients in cement mortars was in a proportion of 1:2.25:3 yeast extract: urea: calcium acetate. Table 9-1 shows the composition of the specimens in each series. Group R are the specimens without any additions. Group RP are the specimens with bio-reagents added, including the nutrients for bacteria (yeast extract and urea) and the deposition agent (calcium acetate). Group SP58 is the specimens with bio-reagents and Bacillus Sphearicus spore 58 added. Group SP57 was the specimens containing bio-reagents and Bacillus Sphearicus spore 57. The last group was SP33 which is the specimens with bio-reagents and Bacillus Sphearicus spore 33 added. Now mortar was allowed to mix for 3 min. All the specimens were well compacted using table vibrator. After casting, the moulds were placed in an air-conditioned room (20^{o}C, >95% RH). The specimens in Group R were demoulded after 24hrs, while the other specimens were demoulded after 48hrs because of the delaying action of the bio-reagents added. After demoulding, all specimens were cured in water.

9.2.2.2 Outdoor Exposure process

After 28 days curing, the specimens were taken out of the water and kept outside the lab in a wire shelving unit in order to provide full exposure. The specimens were positioned in a 45^o toward the south direction and left 18 months under exposure to different environmental conditions during this period of time as shown in Figures 9-1 and 9-2. A total of 105 specimens distributed in five series were subjected to weathering. All specimens belonging to one series had the same characteristics. Specimens without bacterial strain and nutrient material were referred as reference R with number from 1-21, while specimens with no bacteria yet have nutrient were called RP with number from 1-21. For bacterial samples, the name given to each series follows the format "SP x" with x the name of Bacillus strain with number from 1-21. After 1, 3, 6, 9, 12, 16 and 18 months, the specimens were tested for their respective compressive, flexural strengths and microstructural analysis. Samples were then moved to the next conditioning stage and the process repeated.

Figure 9-1 Outdoor Exposure (wire shelving unit) Figure 9-2 Samples were positioned 45^{o}

9.2.2.3 Analytical methods

After the end of the respective exposure time (i.e. after 1, 3, 6, 9, 12, 16 and 18 months), all of the series were submitted to mechanical testing. Firstly, flexural strength test according to BS EN 196-1:2016 (BS EN 196-1: 2016, 2016) was performed on 40mmx40mmx160mm mortar specimens. The samples were tested by placing them centrally between the two steel supporting rollers of the flexure device and the third steel loading roller with a constant rate of (50 ± 10) KN/minute. More details have been stated in Chapter 3. The compressive test was performed on the specimen halves that were created after the flexural test according to BS EN 196-1:2016 (ibid). The specimens were evenly loaded with force at the rate of 144 KN/minute. The maximum applied load was recorded and analysed using Instron software. For the purpose of comparing the impact of outdoor exposure, the obtained values were averaged by the mean and their standard deviation (SD) was determined. SEM imaging was performed on an ultra-high performance field emission scanning electron microscope Zeiss Supra 35VP. SEM was used to study the characterization of the microstructure of mortars under different magnifications. For SEM examination, small fractured specimens from compressive test were prepared. The specimen was mounted on an aluminium stud. The top surfaces of the SEM specimens were coated with a thin layer of gold to obtain clear photomicrographs. The chemical composition in different spots at crack surfaces was determined by Energy Dispersive X-ray (EDAX) analyses. Two SEM images per samples have been captured. More details have been stated in Chapter 3.

9.3 Results and discussions

9.3.1 **Effect of outside exposure on strength properties**

9.3.1.1 Compressive strength

In this chapter, the influence of environmental exposure on bacterial self-healing behaviour was analysed by the changes in the compressive strength of cement mortar, which had been exposed to outdoor environment for 18 months. The compressive strength test results are presented in Table 9-1.

Table 9-1 Effect of weathering exposure on Compressive Strength of control and bacterial Mortar

Mix	Compressive Strength (MPa) per months of outdoor exposure (CoV%)						
	1st month	3rd month	6th month	9th month	12 months	16 months	18months
R	33.16(4)	34.35(0.6)	35.45(3.9)	33.08(2.8)	31.82(3.6)	30.04(3.3)	28.88(2.6)
RP	35.43(5.4)	37.1(1.7)	39.15(2.9)	37.05(2.7)	35.53(3.3)	33.87(0.9)	31.12(3.8)
SP57	38.48(3.9)	41.5(2)	44.95(3.6)	43.21(2.1)	47.89(1.6)	50.73(1.8)	52(0.7)
SP58	37.79(3.5)	38.88(1.8)	40.2(4.2)	41.87(3.9)	42.17(2.3)	43(2.7)	45.76(1.6)
SP33	40.63(4.4)	41.48(1.6)	43.21(2.8)	45.46(1.6)	46.61(1.4)	48.87(4.7)	53.45(3.8)

The variation curves of compressive strength of bacterial and non-bacterial cement mortars with age of exposure are shown in Figure 9-3. It can be seen that there is relationship between the compressive strength and the age of exposure. The compressive strength of all bacterial mortar samples increased with the increase of exposure time, under the same environmental conditions. However, this increment is not the same among the different mortar samples.

Generally, bacterial mortars exhibit more compressive strength change compared to non-bacterial mortars. For R and RP samples, the compressive strength increased constantly from 1 to 6 months, and decreased since then until 18 months, whereas, for bacterial samples, this parameter rose from 1 to 18 months. The increase in compressive strength could be explained as follows. During long time weathering exposure, the carbon dioxide (CO_2) from the atmosphere may diffuse through tiny pores into the mortar and react with the cement hydration products such as ettringite, calcium silicate hydrate, calcium hydroxide and

calcium aluminate hydrate. These hydration products may decompose to new product like calcium silicate and carbonate leading to increase the mortar mass and improving the mechanical properties.

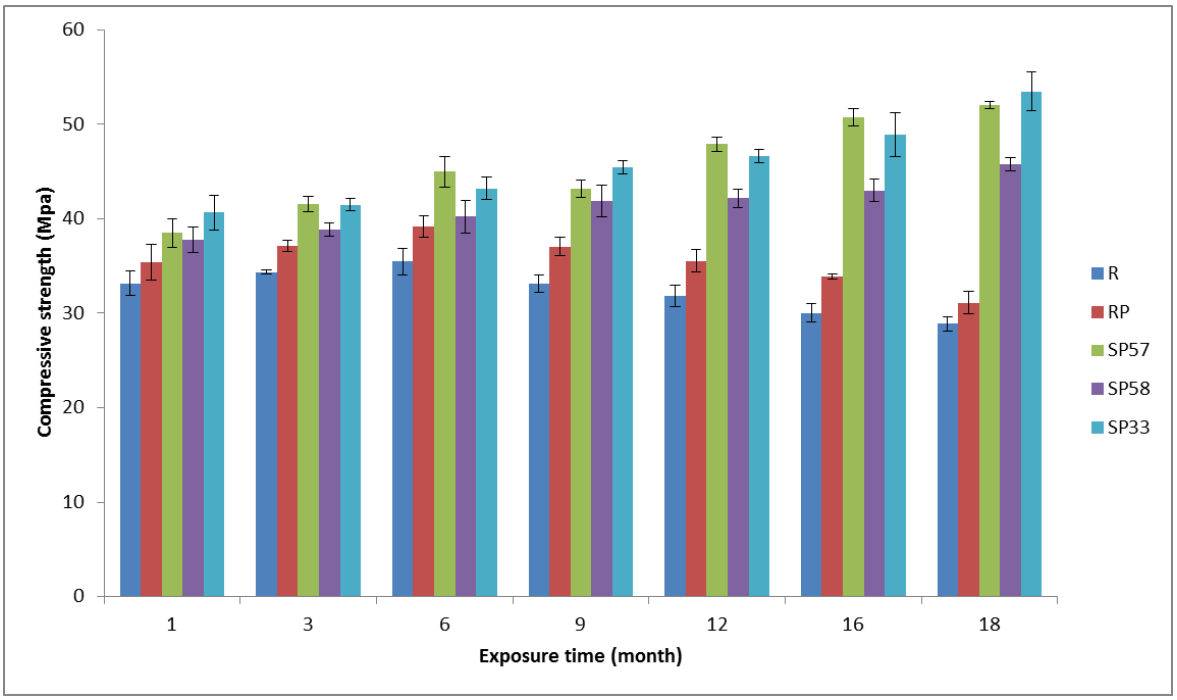

Figure 9-3 Effect of Weathering Exposure on the Compressive Strength of control and bacterial mortar

The decrease in the compressive strength of control specimens (R) was 13% percent, while it was 12% percent in the case of the specimens contains nutrients only (RP), when exposed to 18 months outdoor weathering effect compared to the first month exposure. This reduction in compressive strength could be explained to be a result of an increase of the micro-cracks in the mortar structure which leads to damage the mortar microstructure, thus changing the hydration products and destroying the chemical equilibrium of the system. The reduction in strength also probably relates to the fact that no additional water was added to the samples and due to the small sample size the test specimens gradually became drier. The compressive strength of the mortar specimens containing different bacterial strains increased at all of environmental exposure. The highest compressive strength was achieved by mortar incorporated Bacillus Megaterium SP33: the compressive strength value reached 53.453 MPa after 18 months of exposure with improvement of 85% comparing to control. This increase in compressive strength is possibly attributed to precipitation of calcium carbonate within the cracks and pores of mortar matrix (Ramachandran, Ramakrishnan and Bang, 2001; Santhosh *et al.*, 2000; Ramakrishnan, Bang and Deo, 1998).

By incorporating two Bacillus Sphaericus strains (SP57 and SP58) with same concentrations (10^8 spore/cm^3), the compressive strength values after 18 months of exposing were also improved comparing to control. However, the observed improvements were less than that for Bacillus Megaterium SP33. This gives a recommendation that the bacterial strain choice is essential in improving the compressive strength of mortar (Ghosh *et al.*, 2005).

Experimental results positively indicate that all bacterial mortars specimens are more resistant to weathering effect than non-bacterial concrete. The phenomenon may be explained by the fact that bacterial mortar microstructure are more compact and dense and thus are able to withstand weathering effects. According to the mechanism of microbially induced calcium carbonate precipitation MICP, the calcite crystals generated; this, along with other hydration products clogged mortar pores, resulting in decreased porosity, hence the compressive strength improved. The highest compressive strengths corresponded to all bacterial mortars at the majority of testing ages could be attributed to the good mechanical behaviour in the long term when they are exposed to outdoor conditions (Figure 9-3).

9.3.1.2 Flexural strength

The test results, in terms of flexural strength of control specimens (R), specimens contained nutrients only (RP), SP33, SP 57 and SP58 bacterial mortar specimens exposed to the outdoor environment up to 18 months are presented in Table 9-2. The control specimens and the specimens contained nutrients only, suffered some kind of degradation due to weathering and/or aging. Not counting a slight change in colour, no visible cracks or other exterior signals of deterioration were found on the test specimens.

In general, the bacterial cement mortars showed a better weathering performance than the non-bacterial ones, with a higher retained flexural strength. After a one-year exposure to the outdoor environment, an average loss of 32% in the flexural strength occurred for the RP specimens, against an average decrease by 8.6% for the R mortars.

With time, the bacterial mortar placed outdoor underwent some kind of post cure process, which led to an increased flexural strength after six and twelve months of weathering. Conversely, the non-bacterial mortar showed the evidence of some degradation processes due to weathering: after six and twelve months of outdoor exposing, the flexural strength slightly decreased. Nevertheless, no unequivocal conclusions can be drawn regarding the presence of clear trends about the performance of the bacterial mortar under weathering exposure,

because of the relative short time frame of weathering exposure as well as the small number of test samples (bacterial mortar).

Table 9-2 Effect of Weathering Exposure on the Flexural Strength of control and bacterial mortar

Mix	Flexural Strength (Mpa) per months of outdoor exposure (CoV%)						
	1st month	3rd month	6th month	9t month	12month	16month	18month
R	7.12(3.5)	7.27(5)	7.04(3.2)	6.82(3.2)	6.51(4)	6.38(4.9)	6.08(5.2)
RP	8.11(2.4)	6.95(3)	6.36(6.6)	5.98(4.4)	5.44(5.7)	5.01(3.7)	7.25(7.6)
SP57	6.75(5.7)	6.56(2)	4.88(6.8)	5.55(1.5)	6.49(6.8)	7.34(6.6)	7.83(6.9)
SP58	8.96(4.8)	6.40(7)	4.78(7.2)	4.63(6.2)	5.82(5.6)	6.84(7.8)	7.26(6.8)
SP33	9.44(5.2)	6.34(3.2)	5.32(6.4)	4.96(3.4)	4.38(8.3)	4.71(6.3)	7.11(1.8)

The flexural strength behaviour of all specimens is also highlighted in Figure 9-4. There were considerable differences between the spring/summer and fall/winter periods that could ex plain the fluctuation in flexural strength. This fluctuation can be explained by that in the first few months of exposure, the crystallisation pressure of the hydration products present in the pores is not sufficient to make the mortar cracked, so the flexural strength increased. More crystal products accumulate with time and the presence of water, thus increasing the pressure leading to crack. The crack further expands and connects with time, which results in decrease the flexural strength. The flexural strength increased again with the growth of crystal formation, filling the pore and the crack.

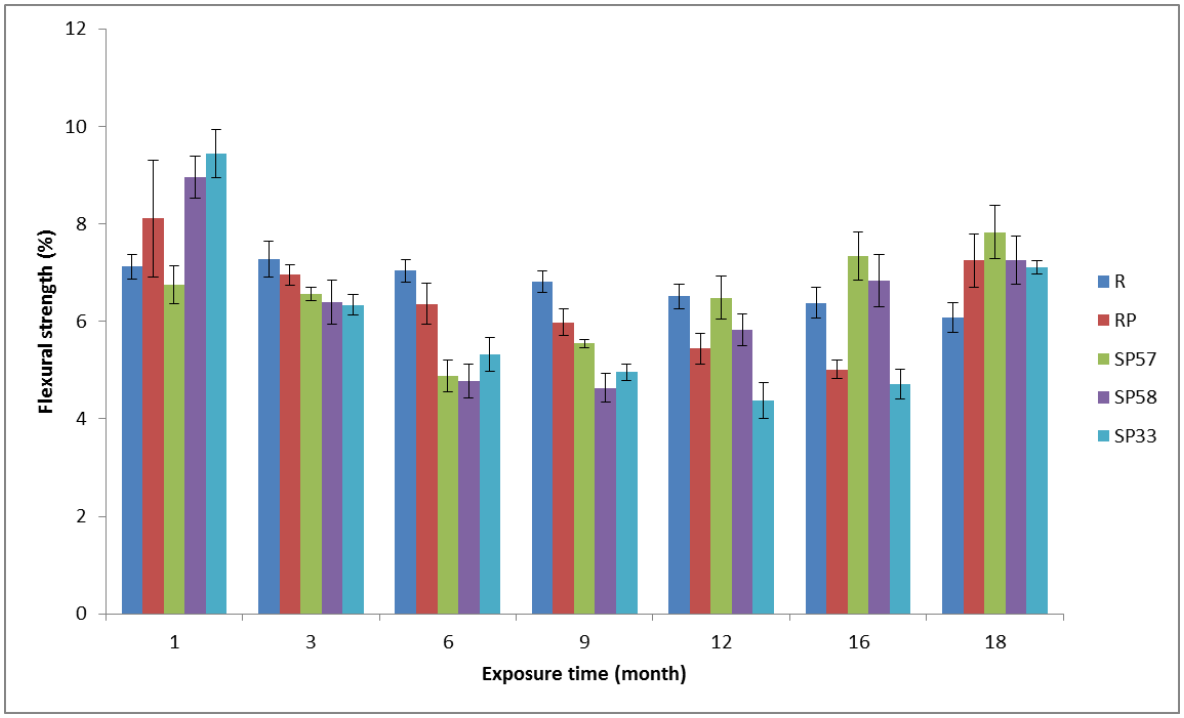

Figure 9-4 Effect of Weathering Exposure on Flexural Strength of control and bacterial mortar

9.3.2 **Prediction of long term performance of self-healing cementitious composites subjected to outdoor exposure based on mechanical properties**

9.3.2.1 Prediction of compressive strength under outdoor exposure

Based on the results presented in section 9.3.1.1, a polynomial function was proposed to describe the relationships between compressive strength and outdoor exposure time for 5 different mixtures, as Eq. (1)

$$Fc=at^2+bt+c \quad (1)$$

Where Fc is the compressive strength of mortar subjected to outdoor exposure at t days. And the fitting parameters corresponding to the type of mixtures were listed in Table 9-3. Fig. 9-5 (d) - (b) show that these propose formulas had good fitting performance.

It is also very important to know the relationship between compressive strength of mortar and exposure time because usually, quality of mortar and its fitness for construction is judged based on the compressive strength. So, it is important to have a relationship between compressive strength and exposure time. Figure 9-5 shows relationships between compressive strength and exposure time of nonbacterial and bacterial cement mortar.

The data points in Figure 9-5 (c, d and e)) distribute to the right oblique upward, forming a zonal shape. Although data points present discreteness for each bacterial mortar mixture, it is clear that as the increasing of exposure time, the compressive strength of the same mortar tends to increase as well. The correlation coefficient between compressive strength and exposure time of SP57, SP58 and SP33 are 0.968, 0.971and0.983, respectively, demonstrating that the compressive strength and exposure time are still well positively correlated under environmental effects for long period of time. This could be due to the continuing calcite precipitation due to microbial activity, which gives rise to strength growth.

However, the compressive strength of the non-bacterial mortar tends to decrease as the increasing of exposure time. Under long-term environmental effects, the expansions or shrinkages caused by environments would induce cracks within cement mortar. Once the cracks are initiated, it allows the further penetration of more harmful and corrosive substances, which ultimately reduces the durability and strength of mortar in a substantial manner.

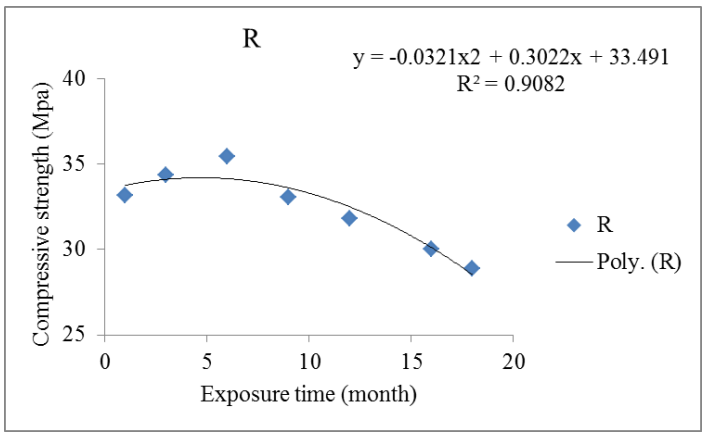

(a)

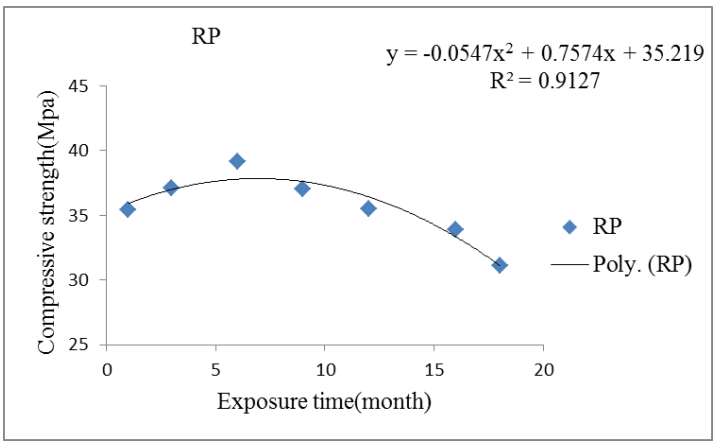

(b)

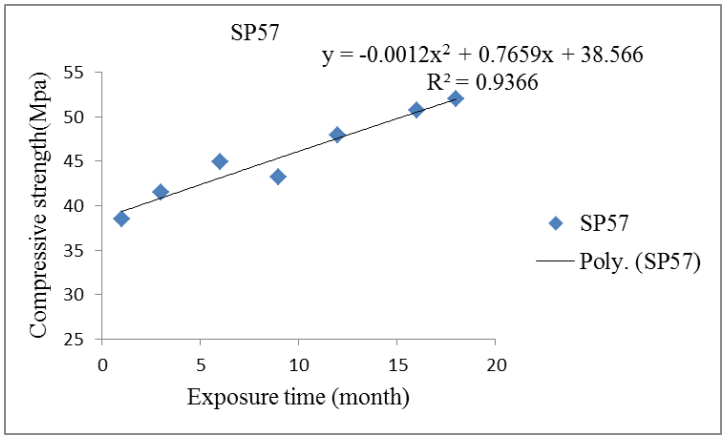

(c)

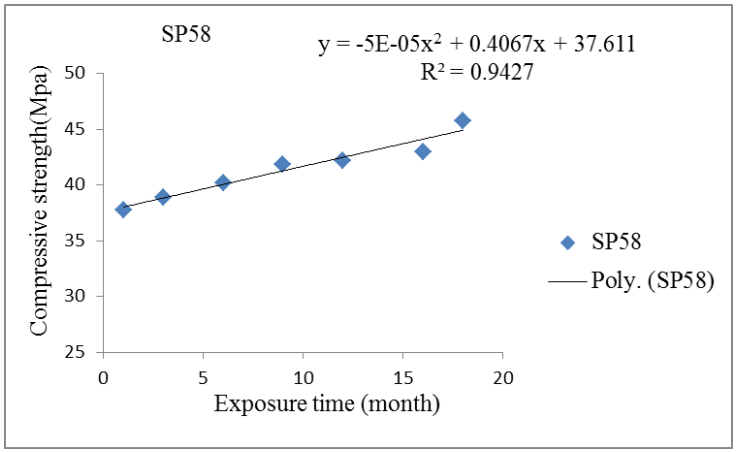

(d)

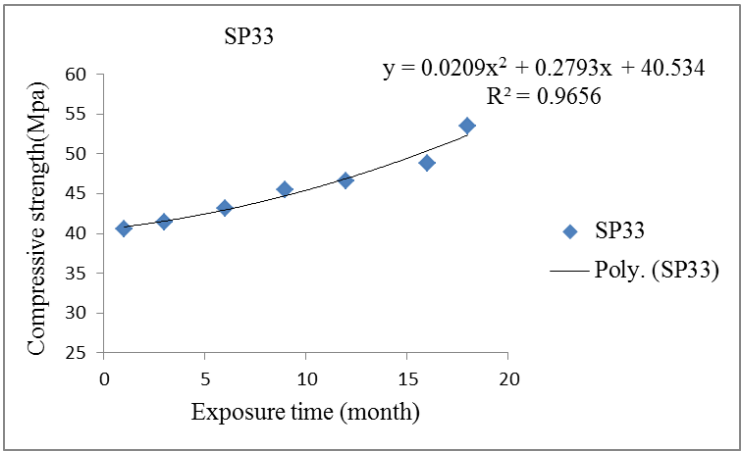

(e)

Figure 9-5 Fitting curves of compressive strength versus outdoor exposure time of control (a), nutrients only(b), SP57self-healing mortar(c), SP58self-healing mortar(d) and SP33self-healing mortar(e)

As can be seen from Table 9-4, the average correlation coefficient of the compressive strength curve under different exposure time was relatively high, which confirmed the good quality and repeatability of the results.

Table 9-3 Fitting parameter, R, R-square and SEE of the formulas for compressive strength of self-healing mortar subjected to outdoor exposure

Mix	a	b	c	Proposed functions	R^2	R	SSE
R	-0.0321	0.3022	33.491	$Fc = -0.0321t^2 + 0.3022t + 33.491$	0.9082	0.953	2.98
RP	-0.0547	0.7574	35.219	$Fc = -0.0547t^2 + 0.7574t + 35.219$	0.9127	0.9554	3.50
SP57	-0.0012	0.7659	38.566	$Fc = -0.0012t^2 + 0.7659t + 38.566$	0.9366	0.968	9.35
SP58	-5×10^{-5}	0.4067	37.611	$Fc = -5E\text{-}05t^2 + 0.4067t + 37.611$	0.9427	0.971	2.47
SP33	0.0209	0.2793	40.534	$Fc = 0.0209t^2 + 0.2793t + 40.534$	0.9656	0.983	4.16

The fitting formulations have different values of compressive strength with different mortar mixture with R^2 ranging from 0.9082 to 0.9656. R^2 represents the determination coefficient and R represents the correlation coefficient. R^2 is a measure of how well the independent variables approximate the measured dependent variable, high values of R^2 are generally indicative of a good performance. The SSE (sum of squares due to error, calculated as (2)), which is one of important indexes presenting goodness of curve fitting, is shown in Table 9-3.

$$SSE=\sum_{i=1}^{n}(yi-\hat{y}i)\text{^}2$$

where yi and $\hat{y}i$ represent the experimental and predicted (through the proposed functions) compressive strength of mortar and n is the number of data analysed. The SSE statistic is the least-squares error of the fit, with a value closer to zero indicating a better fit. The SSE of all proposed functions listed in this study is small, together with big R-square statistics, indicating good fitting effects to the experimental results. In addition, the index as (predicted value−experimental value)/experimental value are used to reflect the errors between experimental values and predicted values. The figures for these errors of five different mortar samples are presented in Appendices (A, Figures A-1 (a-e)).

It is shown that all the compressive strength-exposure time relationships for all mortar mixtures listed in this study are applicable to the bacterial-based self-healing mortar with satisfactory accuracy.

9.3.2.2 Prediction of flexural strength under outdoor exposure

A polynomial function, based on the results obtained from section 9.3.1.2 was proposed to describe the relationships between flexural strength and time of outdoor exposure for bacterial and non-bacterial mortar mixtures, as Eq. (1)

$$F_f = dt^2 + et + f \quad (1)$$

Where F_f is the flexural strength of mortar subjected to outdoor exposure at t days. And the fitting parameters corresponding to the type of mixtures were listed in Table 9-4. Figure 9-6 (a) shows the measured flexural strength values for control mortar (R). It shows the regression curve represented by the second-degree polynomial function. The regression curve describes the measured points with an accuracy of 95.8%. Based on the shape of the regression curve, it could be stated that increasing the outdoor exposure time reduced the flexural strength of the test samples. Figure 9-6 (b, c, d and e) also shows the regression curve represented by the second-degree polynomial function of RP, SP57, SP58 and SP33, respectively. The regression curve describes the measured points with an accuracy of 75.74%, 81.69%, 83.46% and 88.68%. Based on the shape of the regression curves of the three bacterial mortar, it could be stated that the flexural strength continue to increase and reach a point of highest development after subjecting to 18 months of outdoor exposure. The reason behind the flexural strength increase in the bacteria mortar specimens is that the presence of calcium carbonate crystals generated during MICP process and carbonation process.

Table 9-4 Fitting parameter, R, R-square and SEE of the formulas for flexural strength of self-healing mortar subjected to outdoor exposure

Mix	d	e	f	Proposed functions	R^2	R
R	-0.0019	-0.0288	33.491	$F_f = -0.0019t^2 - 0.0288t + 7.2486$	0.958	0.979
RP	0.0248	- 0.5625	8.6493	$F_f = 0.0248t^2 - 0.5625t + 8.6493$	0.7574	0.8703
SP57	0.0246	- 0.388	7.0921	$F_f = 0.0246t^2 - 0.388t + 7.0921$	0.8169	0.904
SP58	0.0453	- 0.8912	9.1528	$F_f = 0.0453t^2 - 0.8912t + 9.1528$	0.8346	0.914
SP33	0.048	- 1.0573	9.9357	$F_f = 0.0487t^2 - 1.0573t + 9.9357$	0.8868	0.942

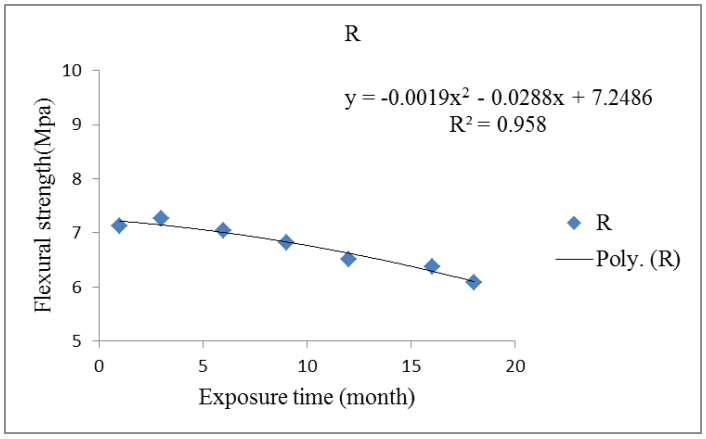
R
y = -0.0019x² - 0.0288x + 7.2486
R² = 0.958
Flexural strength(Mpa)
Exposure time (month)
R
Poly. (R)

(a)

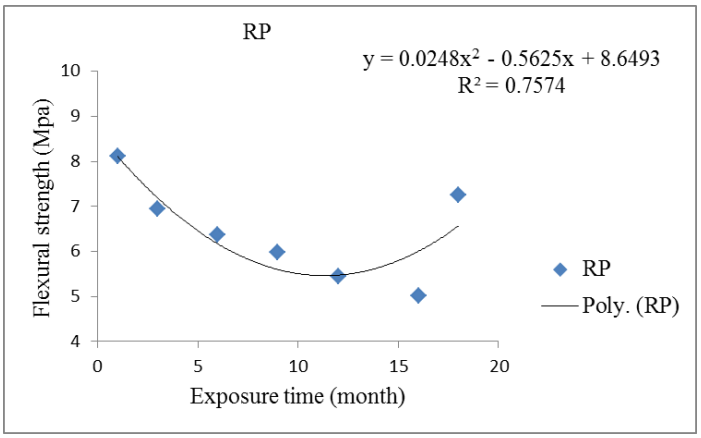
RP
y = 0.0248x² - 0.5625x + 8.6493
R² = 0.7574
Flexural strength (Mpa)
Exposure time (month)
RP
Poly. (RP)

(b)

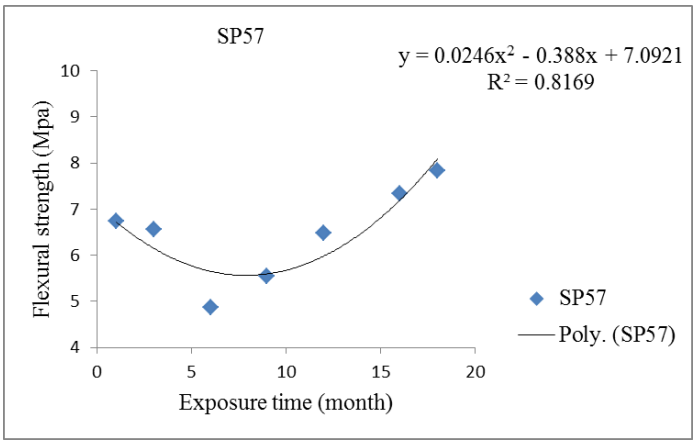
SP57
y = 0.0246x² - 0.388x + 7.0921
R² = 0.8169
Flexural strength (Mpa)
Exposure time (month)
SP57
Poly. (SP57)

(c)

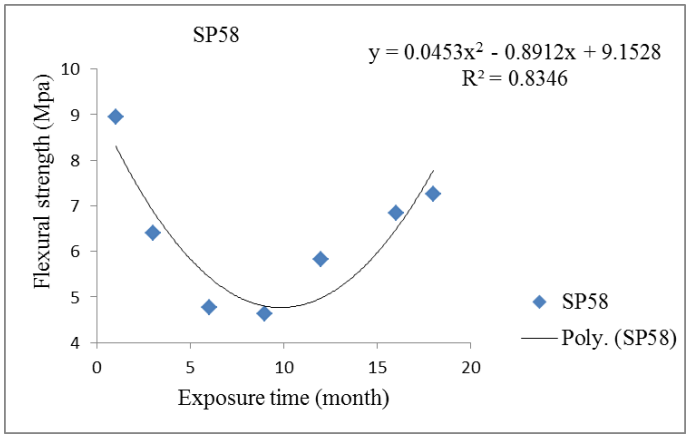

(d)

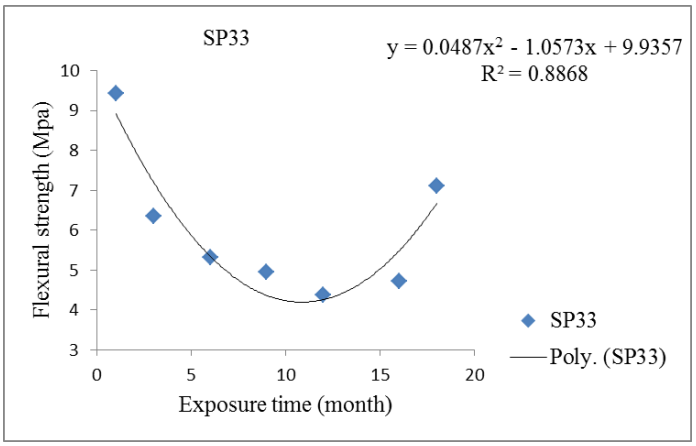

(e)

Figure 9-6 Fitting curves of flexural strength versus outdoor exposure time of control (a), nutrients only(b), SP57self-healing mortar(c), SP58self-healing mortar(d) and SP33self-healing mortar(e)

9.3.2.3 Correlation of outdoor exposure and accelerated experimental results

9.3.2.3.1 Correlation based on compressive strength results

To establish s possible correlation between the effect of outdoor exposure and accelerated exposure (wet-dry and freeze-thaw) on the compressive strength of bacterial self-healing mortar, a new set of equations have been derived from non-linear regression analysis of the relative compressive strength versus the time of outdoor exposure for 5 different mortar mixture (Appendix B, Figure B-1 (a-e)). These equations are listed in the Table 9-5 and 9-7. These equations have been applied on the accelerated experimental results. The relative compressive strength values of all mortar samples subjected to 3, 10 and 30 of Freeze-Thaw cycles are also listed in the same table.

Before drawing conclusions concerning the possible correlation that might exist between the changes in compressive strength property of self-healing mortar during the accelerated and outdoor exposure tests performed, some basic concept must be clarified. These are "correlation", the degree to which the data obtained in the accelerated exposure test agree with those obtained outdoors, and "acceleration", the measure of how fast the test can be conducted using an accelerated exposure compared with outdoor testing. The usefulness of the accelerated exposure tests may be characterised by the two parameters. The estimation of the acceleration factor of an accelerated test is valid only if an agreement or correlation between the results of outdoor and accelerated test exists. The acceleration factor is the time to change in a property under an outdoor exposure divided by the time to change in an accelerated test, both evaluated by the same technique. However, in this study, it is not applicable to calculate the accelerated factor because the accelerated exposure test was evaluated via number of cycles, while in the outdoor exposure, the evaluation was via time of exposure (months).

It has been found from the data presented in Table 9-6 that, for bacterial self-healing mortar, there is no correlations observed between the data obtained from F-T cycles exposure and the results of the outdoor exposure. This means that the results of F-T are not in good agreement with outdoor results. This is because the clear difference in the compressive strength trend of the bacterial mortar between the two exposure types. The compressive strengths of bacterial mortar were decreasing with increasing the F-T cycles number, while, an increase in compressive strength values of bacterial mortars were observed with the time of outdoor exposure as discussed in the previous chapters.

The data for non-bacterial mortar could be used for revealing a correlation between the F-T and outdoor exposure. For control (R) mortar, the drop of compressive strength occurred after 3, 10 and 30 freeze-thaw cycles was corresponding to the compressive strength decreasing happened after 13.25, 22.4 and 25 months of outdoor exposure. RP samples exposing to 3, 10 and 30 cycles of freeze-thaw showed the same compressive strength reduction as for those exposed to 16.7, 22.5 and 23.5 months of outdoor weathering.

Table 9-5 Correlation of compressive test results of outdoor and the accelerated (Freeze-Thaw cycles) exposure

Mix	Number of Freeze-Thaw cycles						Outdoor Exposure formula
	3		10		30		
	Relative compressive strength (%)*	Time (months)	Relative compressive strength (%)*	Time (months)	Relative compressive strength (%)*	Time (months)	
R	96.0	13.25	73.0	22.4	63.6	25	Fc = -0.0967t2 + 0.9113t + 101
RP	92.0	16.7	69.6	22.5	64.4	23.5	Fc = -0.1543t2 + 2.1376t + 99.404
SP57	89.7	NA	82.0	NA	78.9	NA	Fc= -0.003t2 + 1.9904t + 100.22
SP58	89.0	NA	83.5	NA	81.6	NA	Fc= -0.0001t2 + 1.0763t + 99.527
SP33	93.0	NA	84.0	NA	80.6	NA	Fc= 0.0515t2 + 0.6874t + 99.764

*the change in compressive strength due to exposer divided by the original compressive strength before exposing.

Table 9-6 displays the relative compressive strength values of all mortar samples subjected to 3, 10 and 30 of Wet-Dry cycles. From the data presented in this table, a reasonable correlation between the results of wet-dry cycle test of bacterial self-healing mortar and those obtained under outdoor exposure has been found. After exposing to 3, 10 and 30 cycles of wetting and drying, SP57 mortar samples show similar compressive strength enhancement to that produced by 15, 3.1 and 2.9 months of outdoor exposure. For SP58, the improvement in compressive strength occurred after 30 cycles of wet-dry was equivalent to that obtained after 12.3 months outdoor exposure. The enhancement in compressive strength values of SP33 samples subjecting to 3 and 30 wet-dry cycles were comparable to those exposing to 7.5 and 18.5 month of outdoor weathering. For non-bacterial mortar samples, no reliable correlations can be obtained between outdoor and wet-dry exposure test results. As the results of compressive strength tests of bacterial self-healing mortar specimens agree with some of the data obtained in the wet-dry accelerated tests, following the same trend, then predictions for the outdoor long term of the bacterial formulations might be done.

Table 9-6 Correlation of compressive test results of outdoor and the accelerated (Wet-Dry cycles) exposure

Mix	Number of Wet-Dry cycles						Outdoor Exposure formula
	3		10		30		
	Relative compressive strength (%)	Time (months)	Relative compressive strength (%)	Time (months)	Relative compressive strength (%)	Time (months)	
R	114.5	NA	140.2	NA	162.0	NA	Fc = -0.0967t2 + 0.9113t + 101
RP	126.0	NA	131.0	NA	171.7	NA	Fc = -0.1543t2 + 2.1376t + 99.404
SP57	129.4	15	106.3	3.1	105.9	2.9	Fc= -0.003t2 + 1.9904t + 100.22
SP58	80.1	NA	94.7	NA	112.7	12.3	Fc= -0.0001t2 + 1.0763t + 99.527
SP33	107.8	7.5	94.4	NA	130.0	18.5	Fc= 0.0515t2 + 0.6874t + 99.764

9.3.2.3.2 Correlation based on flexural strength results

Polynomial equations have been derived from non-linear regression analysis of the relative flexural strength versus the time of outdoor exposure for 5 different mortar mixtures (Appendix B, Figure B-2 (a-e)). These equations were used to check the possibility of correlation between the effect of outdoor exposure and accelerated exposure (wet-dry and freeze-thaw) on flexural strength of bacterial self-healing mortar. The relative flexural strength values of all mortar samples subjected to 3, 10 and 30 of Freeze-Thaw cycles are also listed in Table 9-7. Generally, flexural strengths results of accelerated and outdoor weathering exhibited better correlation than the compressive strength. From this table, it can be seen that some relative flexural strengths results for accelerated test correlated to the strength test results of outdoor exposure at one age and not at the other. As can be seen from SP57 samples, there is no correlations detected between the data obtained after subjecting to 10 and 30 F-T cycles exposure and the results of the outdoor exposure. This behaviour could be because of the fact that SP57 mortar suffered more flexural strength reduction under high number of freeze-thaw cycles compared to outdoor exposure. The flexural strengths of bacterial mortar were decreasing with increasing the F-T cycles number and the outdoor

exposure time, except for SP 59 which retain some of its flexural strength after subjecting to 18 months of outdoor exposure as discussed in the previous chapters. Subjecting SP58 bacterial mortar to 3, 10 and 30 freeze-thaw cycles resulted in flexural strength reduction equivalent to that subjected to 19.5, 14.8 and 12.6 months of outdoor exposure, respectively. SP33 experience flexural deterioration after 3, 10 and 30 F-T cycles comparable to that occurred after 21, 18.7 and 17 months of outdoor exposure, respectively. Control (R) samples suffered slower flexural deterioration under outdoor weathering than F-T accelerated exposure. The deterioration happened after 3, 10 and 30 F-T cycles can be seen after 31.7, 32.8 and 37.4 months of outdoor weathering, respectively. This could be because of the fact that the freeze-thaw cycles applied in this study do not represent the true components of outdoor environment as these were applied mainly to simulate severe exposure conditions.

Table 9-7 Correlation of flexural test results of outdoor and the accelerated (Freeze-Thaw cycles) exposure

Mix	Number of Freeze-Thaw cycles						Outdoor Exposure formula
	3		10		30		
	Relative flexural strength (%)*	Time (months)	Relative flexural strength (%)*	Time (months)	Relative flexural strength (%)*	Time (months)	
R	61.6	31.7	59.2	32.8	48.7	37.4	Ff = -0.0272t2 - 0.4045t + 101.81
RP	72.6	15.5	67.3	NA	61.0	NA	Ff = 0.3059t2 - 6.9359t + 106.65
SP57	89.4	12.2	69.0	NA	64.8	NA	Ff = 0.3651t2 - 5.7521t + 105.15
SP58	100	19.5	65.8	14.8	57.0	12.6	Ff = 0.5057t2 - 9.9524t + 102.21
SP33	97.2	21	76.0	18.7	63.7	17	Ff = 0.5157t2 - 11.2t + 105.25

*the change in flexural strength due to exposer divided by the original flexural strength before exposing.

Table 9-8 displays the relative flexural strength values of all mortar samples subjected to 3, 10 and 30 of Wet-Dry cycles. From the data presented in this table, a reasonable correlation between the results of wet-dry cycle test of bacterial self-healing mortar and those obtained under outdoor exposure has been found. SP57 experienced improvement in flexural behaviour after 3 W-D cycles comparable to that subjected to outdoor exposure for 16.6 months. A decrease in flexural strength can be noticed after 10 cycles which is equivalent to the reduction happened after 10.8 months outdoor exposure. Similar relative flexural strength of 12 months of outdoor exposure was achieved by subjecting SP57 mortar sample to 30 W-D cycles. SP58 mortar samples have an identical trend to the other bacterial samples when subjected to W-D cycles. This mean that the flexural strength start to increase with the first W-D- cycles followed by a reduction, then increasing in flexural property. After 17.5 and 19.2 months of outdoor exposure, 10 and 30 W-D cycles, respectively, need to be applied to achieve the same relative flexural strength. More time of outdoor exposure (about 20 months) required to obtain the same flexural strength after subjecting to 10 and 30 cycles of W-D.

Table 9-8 Correlation of flexural test results of outdoor and the accelerated (Wet-Dry cycles) exposure

Mix	Number of Wet-Dry cycles						Outdoor Exposure formula
	3		10		30		
	Relative flexural strength (%)	Time (months)	Relative flexural strength (%)	Time (months)	Relative flexural strength (%)	Time (months)	
R	152.3	NA	65.6	29.8	142.0	NA	Ff = -0.0272t2 - 0.4045t + 101.81
RP	65.4	NA	123.0	24.8	103.5	22.2	Ff = 0.3059t2 - 6.9359t + 106.65
SP57	110.5	16.6	85.7	10.8	88.7	12	Ff = 0.3651t2 - 5.7521t + 105.15
SP58	121.5	21.5	82.6	17.5	97.8	19.2	Ff = 0.5057t2 - 9.9524t + 102.21
SP33	167.0	26.3	88.6	20, 1.6	92.8	20.5	Ff = 0.5157t2 - 11.2t + 105.25

Regarding the correlation between the results of the accelerated exposure and those obtained under the outdoor exposure, on the basis of 18 months' time scale, it was found that the former test accelerated the changes in the compressive and flexural strength properties of the bacterial self-healing mortar compared with that in the latter one. Predictions of the long-term behaviour of bacterial mortar under outdoor conditions can be attempted. Since the major deleterious effects of weathering are confined to external layers of the material, another point that should be realised is the fact that the degree of damage depends on the size of structural elements. It is not reasonable to expect that a large element made of bacterial mortar will lose the same fraction of its strength as a standard prismatic specimen.

9.3.3 **Effect of outdoor weathering on the microstructure**

9.3.3.1 Non- bacterial mortar

When exposed to outdoor weathering for up to 18 months, the control (non-bacterial) cement mortar suffered more surface deterioration than other bacterial mortars. The cracks in the matrix of control specimens were visible due to severe exposure conditions. Looking closer at the cracking behaviour of control and specimen contain nutrients after three months of exposure, it appears that cracking goes through the C-S-H and at the interface between the C-S-H and the other hydration products (Figures 9-7(a) and (b) and Figure 9-8(a) and (b), respectively). The cracks were found in different directions and were empty. The appearance of micro-cracks on the surface fracture of both samples suggested that non-bacterial mortar experienced oxidative degradation upon outdoor natural weathering.

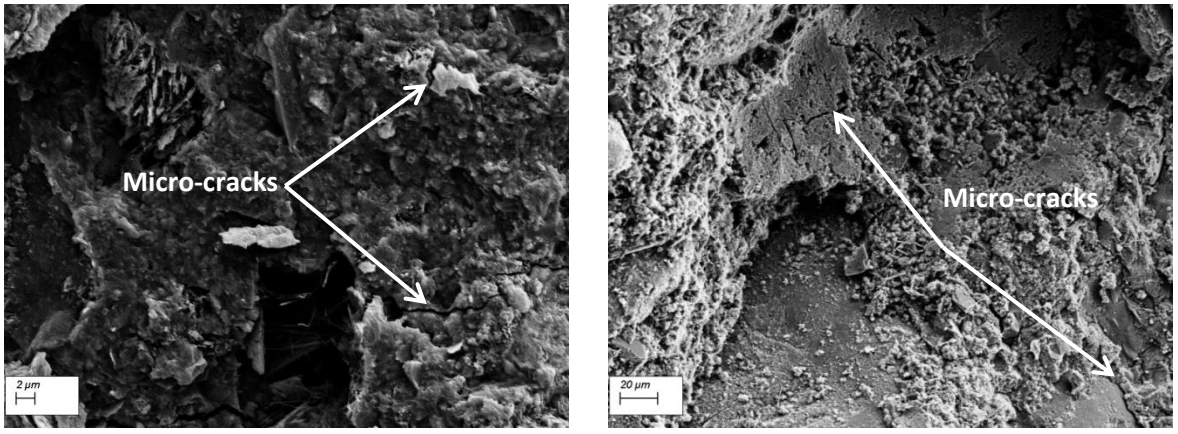

(a) (b)

Figure 9-7 SEM images of control specimen (R) after exposing to three months of outdoor environment at (a) 5000x magnification and (b) 1000x magnification

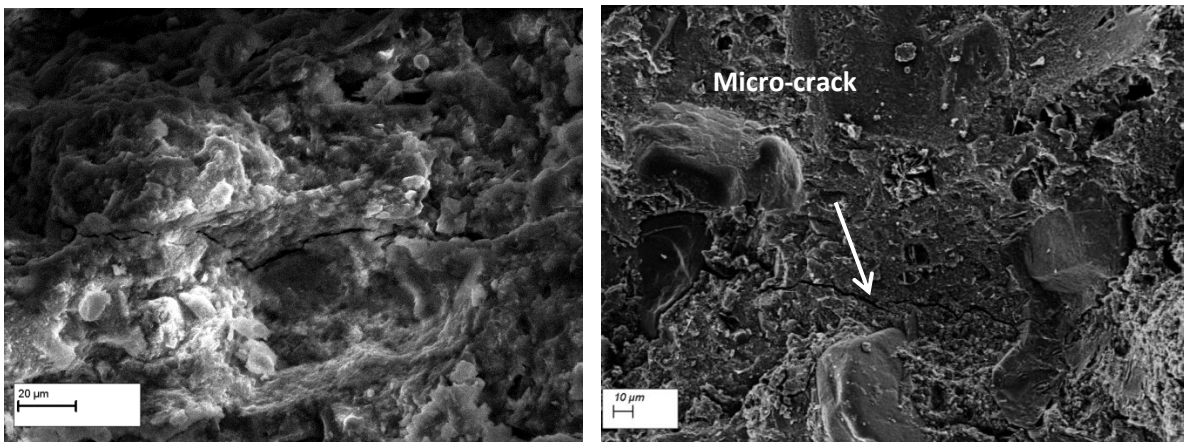

Figure 9-8 SEM images of nutrients only specimen (RP) after exposing to three months of outdoor exposure at (a) 500x and (b) at 1000x magnification

Figure 9-9 also shows the surface fractures of control cement mortar exposed to six months outdoor weathering. The main distinguishing feature in the SEM images of this mortar is the small needles and platy crystals of ettringite and portlandite, respectively and the ettringite needles were totally or partially filling the air-voids.

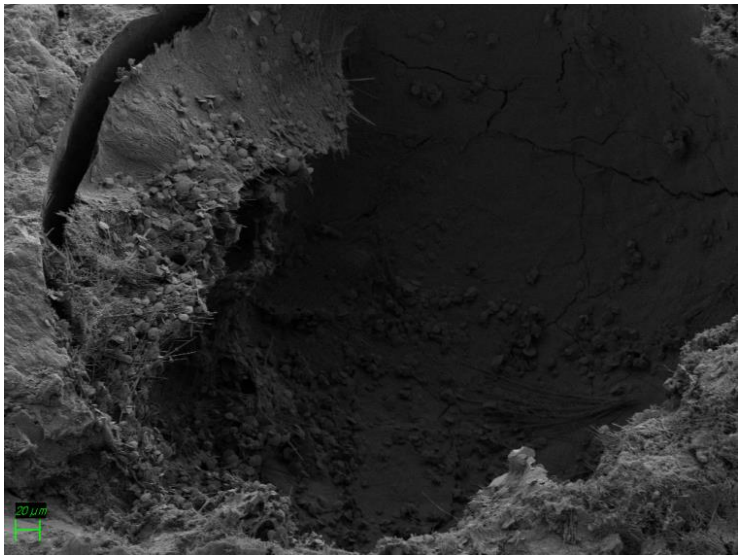

Figure 9-9 SEM image of control specimen (R) after exposing to six months of outdoor environment (Mag=500X)

Figure 9-10 displays the microstructure of the nutrients only mortar after six months of outdoor exposing. It was observed that the hydration products dispersed in the matrix consist of small and large hexagonal plate-like crystals of CH which results in a denser and more compact micro-structure comparing to control specimen. However, gelling hydration products are absent in the microstructure of this sample. This may be attributed to the carbonation process, in which, the CO2 from the environment reacts with the cement hydration products producing the non-gelling calcium silicates or carbonates. In addition to that, the microstructure of RP is more homogeneous than R due to the chemical influence of the nutrients (Calcium acetate, Urea and Yeast extract) added to the cement mortar. Nutrients also work as retarder to delay the setting time and reduce porosity of the matrix.

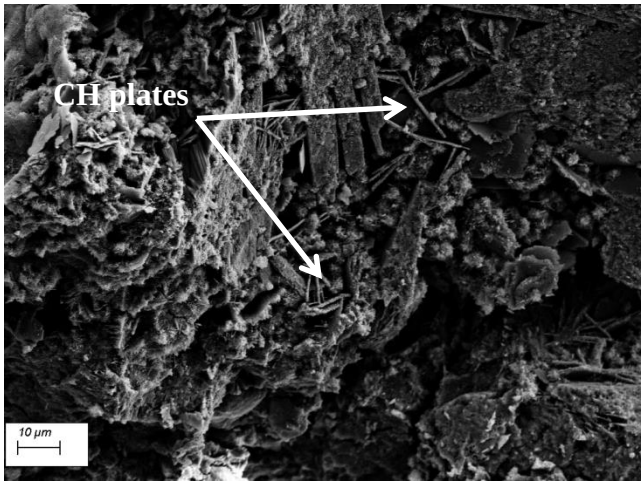

Figure 9-10 Nutrients only specimen (RP) after exposing to six months of outdoor environment (Mag=2000X)

The microstructure of control cement mortar exposing to outdoor environment for nine months was characterised by distribution of C-S-H gel in a form of tiny fibres which gathers to make a mesh, known as "honeycomb" (Figure 9-11). The formation of honeycomb-type C-S-H gel in control specimen after exposing to nine months of outdoor environment may have been the reason for the lower gain in strength. On the other hand, the formation of honeycomb C-S-H gel leads to produce high porous structure.

Figure 9-11 Control specimen (R) after exposing to nine months of outdoor environment (Transformations of needle forms of C-S-H into "honeycomb" structure) (Mag=1000X)

9.3.3.2 Bacterial mortar

Variations in microstructure are observed in the bacterial mortars after exposing to outdoor weathering. As the bacterial cement mortar is weathered, the microstructure seems to be less

porous then that on non-bacterial as the pores are progressively occupied by calcium carbonate precipitation.

The microstructure of Bacillus Megaterium 33 and distribution of bacterial mortar was slightly different from that on control specimen (Figure 9-7 and Figure 9-12(a) and (b)). It has been observed that the structure has fewer microcracks and was denser than the control mortar. Figures 9-12, 9-13, 9-12, 9-16 and 9-17 present the microstructure of the SP33 samples after 3, 6, 9, 12 and 18 months of outdoor weathering exposure, respectively. It can be seen that the microstructure of SP33 exposed to 3, 6, and 9, respectively, was characterised by a lot of platy-shape crystals and fewer ettringite with messy distribution (Fig 9.12, 9.13and 9.14). It was also obvious that narrow strands of filler are almost completely filling the pores.

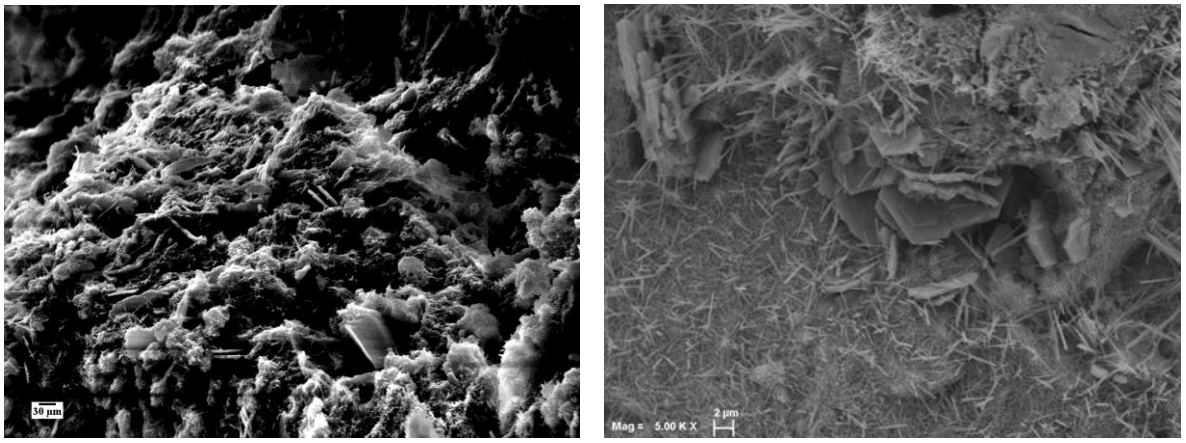

(a) (b)

Figure 9-12 SEM of SP 33 after 3 month of outdoor exposure at (a) 4000x and (a) 5000x magnification

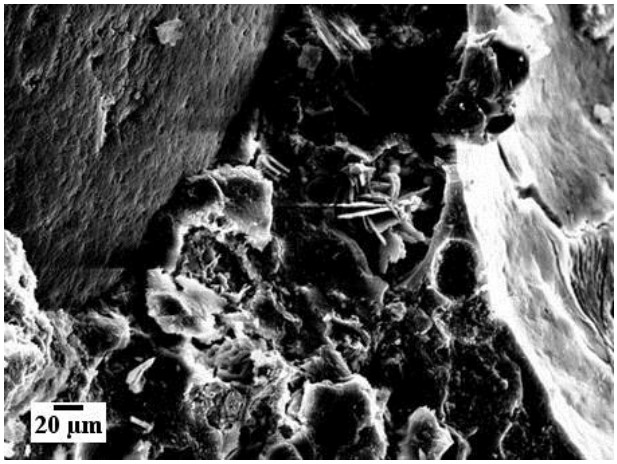

Figure 9-13 SP 33 after 6 months exposure under 2000x magnification

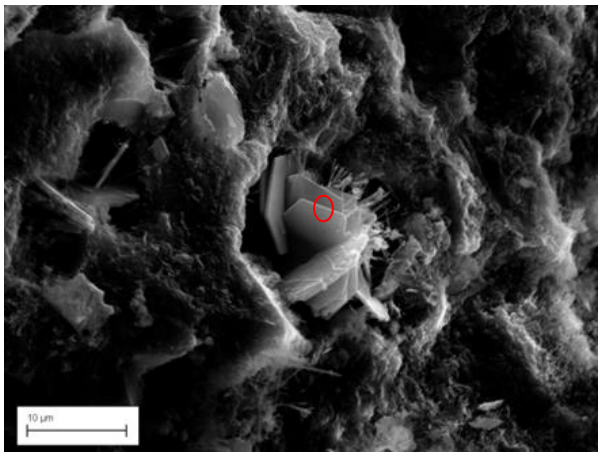

Figure 9-14 SP 33 after 9 months exposure under 5000x magnification

Additionally, the energy-dispersive spectroscopy (EDAX) analysis was conducted to determine the elemental composition of SP 33 mortar sample after 9 months outdoor exposure as shown in Figure 9.15. The area in the red circle indicated in the Figure 9.14 was scanned to examine the main elements of the platy-shape crystals. The classification of the platy-shape crystal can be inferred based on these key elements. Based on the element compositions presented in Table 9-9 ,the platy-shape crystal could be calcium hydroxide (portlandite).

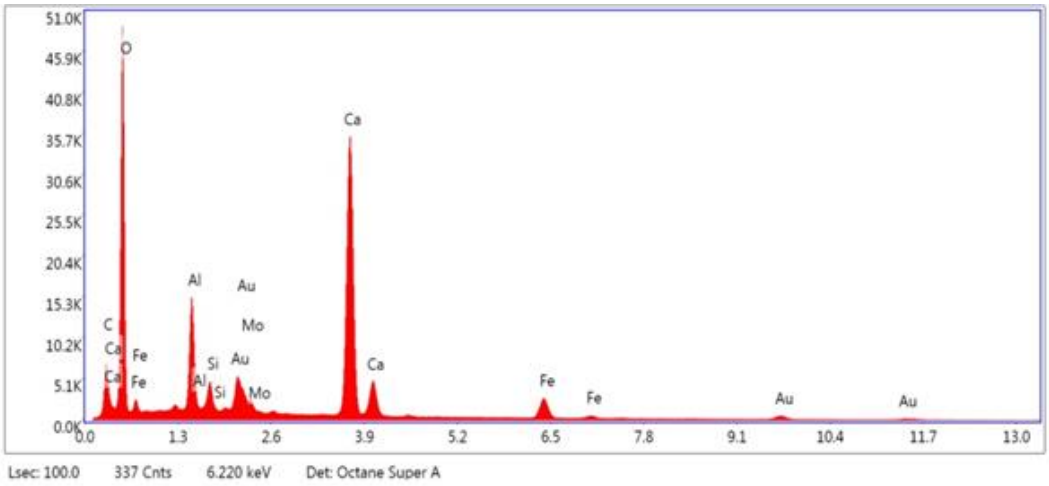

Figure 9-15 EDAX analysis of SP 33 after 9 months exposure

Table 9-9 Results of EDAX analysis of SP33 after 9 months of exposing

Element	Weight %
C K	3.83
O K	53.39
AlK	5.63
SiK	1.37
MoL	1.29
CaK	24.44
FeK	3.88
AuL	6.17

Extraordinarily, after 12 and 18 months of exposure, many regular platy-shape calcite crystals got together to fill almost all the surface (Figure 9.16 and 9.17). The synergy effect of needle-like etterngite (late etterngite formation) and plate-shape CaCO3 on the microstructure of bacterial cement mortar can be clearly seen. The role of etteringite was the crack bridging in cement paste, whereas the plate-shape CaCO3 crystals were played the micro-cracks crossing role to strengthen the microstructure of the mortar. The plate-shape calcite crystals have the same function as the steel rebar in concrete. Thus, the strength of the bacterial cement mortar was significantly improved.

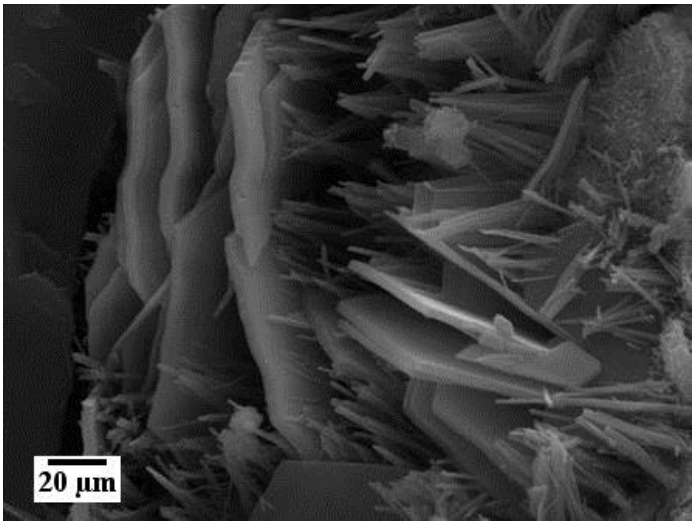

Figure 9-16 SP 33 after 12 months exposure under 1000x magnification

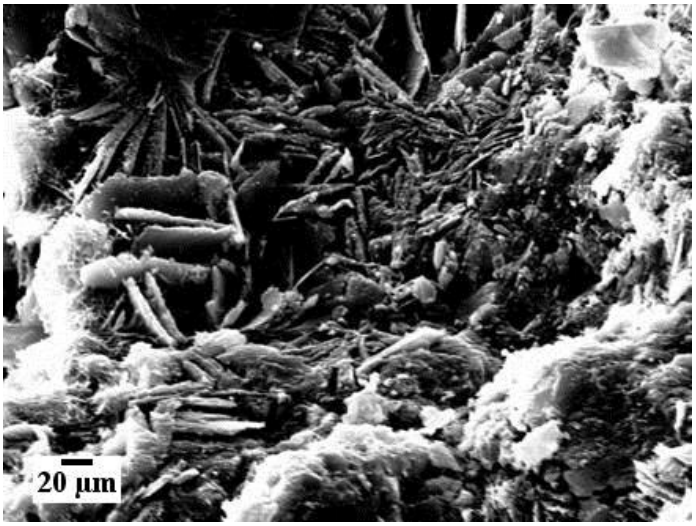

Figure 9-17 SP 33 after 18 months exposure under 5000x magnification

Examining the microstructure of SP 57 showed that after 3 month exposure, there were just a few white precipitates and calcite crystals dispersed among the cement hydration products which were usually in a plate-shape (Figure 9.18). It is also clear that the interior structure of this bacterial sample has developed.

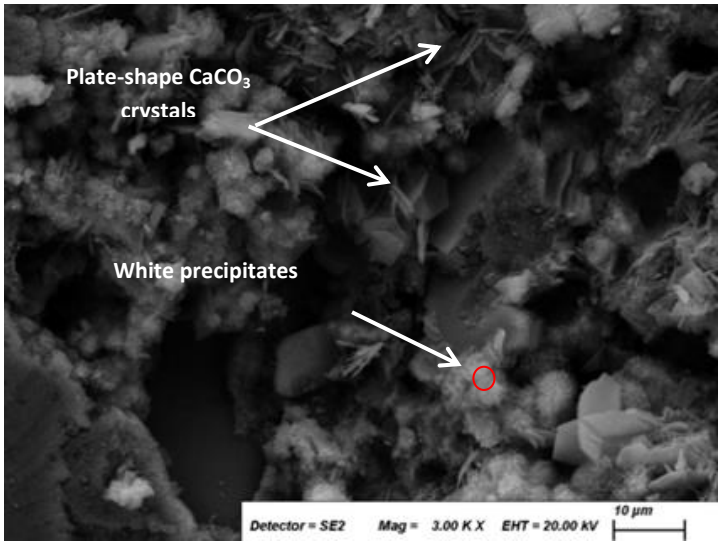

Figure 9-18 SP 57 after 3 months exposure under 3000x magnification

The main elements presented in the EDAX analysis of the white precipitates (Figure 9.19 and Table 9.10) are C, Ca and O in addition to negligible traces of Al, Si, S, Cl and Fe. These elements refer to the calcium carbonate formation due to the presence of Bacillus Sphaericus 57, which induced calcite precipitation.

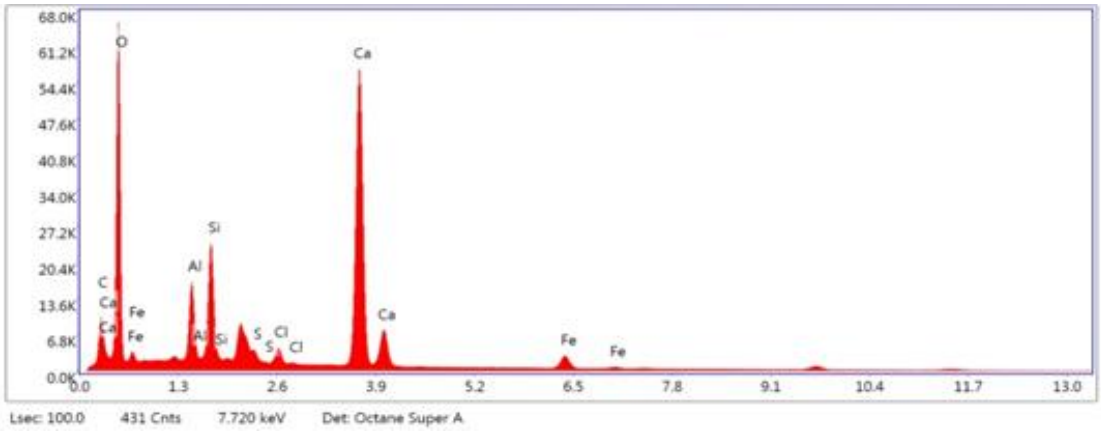

Figure 9-19 EDAX analysis of SP 57 after 3 months of exposure

Table 9-10 Results of EDAX analysis of SP 57 after 3 months of exposure

Element	Weight %
C K	4.05
O K	54.63
AlK	3.98
SiK	5.21
S K	2.98
ClK	0.98
CaK	25.75
FeK	2.41

In some places of the surface fracture of the SP57 after six months exposing to outdoor weathering, pores are partly infilled with needle-fibre calcite (Figure 9.20).

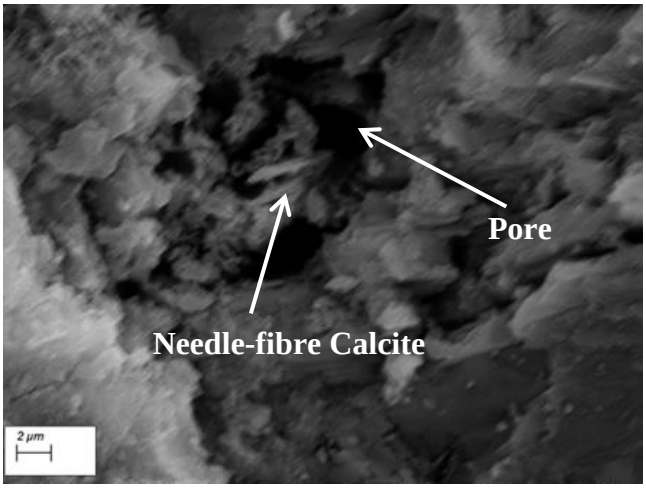

Figure 9-20 SP 57 after 6 months exposure under 8000x magnification

The calcite crystals were totally filled the air-voids after 9 and 12 months of outdoor exposure (Figures 9.21 and Figure 9.22(a) and (b)). The calcium carbonate crystals were well developed inside the pores and close to the surface of cracks. The crystals were fully grown as indicated by the distinct and sharp edges.

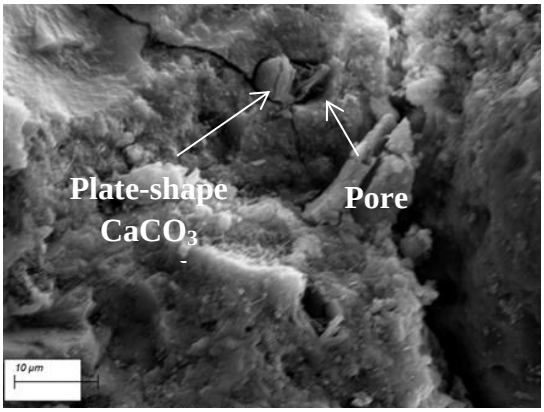

Figure 9-21 SP 57 after 9 months exposure under 5000x magnification

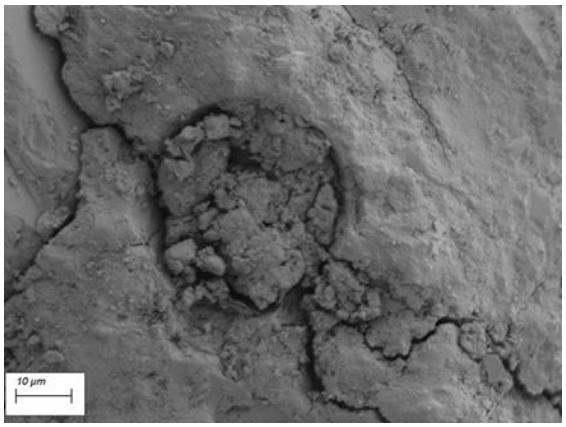

Figure 9-22 SEM images of SP 57 after 12 months of outdoor exposure at (a) 5000x and (b) 3000x magnification

After exposing to 18 months of outdoor weathering, the surface of SP57 mortars was covered by a layer of calcium carbonate crystals (Figure 9.23). This layer on the surface fracture could be a result of carbonation reaction and microbially induced calcium carbonate precipitation (MICI). Carbonation reaction occurs when the atmospheric carbon dioxide (CO2) reacts with hydrating cement.

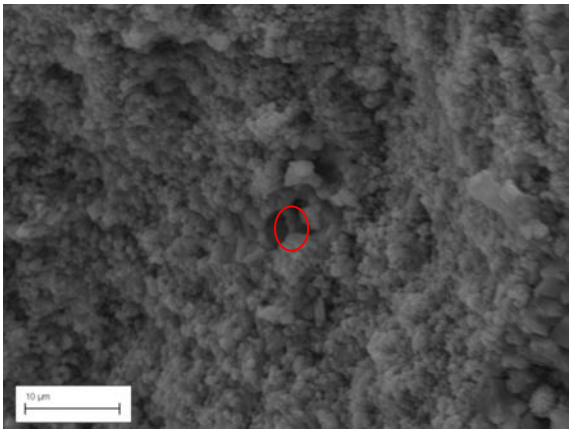

Figure 9-23 SP 57 after 18 months exposure under 5000x magnification

The chemical compositions of the selected area on the surface fracture of SP 57 exposed to 18 months of natural weathering were analysed using EDAX, which slowed the existence of Ca, C and O and the absence of the other elements of hydrating cement (Figure 9-24). Although there is no other element, such as Si or Al, in the analysis results other than the Ca, C and O, it still not clear if the precipitates were calcium carbonate crystal or not. Because the differences between the actual and theoretical values of the composition of calcium carbonate is relatively high. Therefore, the precipitates could be either a non-pure calcium carbonate or other hydration products. The presence of Au element was present in the EDAX analysis because the sample was gold coated in the preparation process. This could also affect the accuracy of elemental analysis.

(Table 9-11). The Au element presents in the analysis result was from the sputter gold coating of the sample.

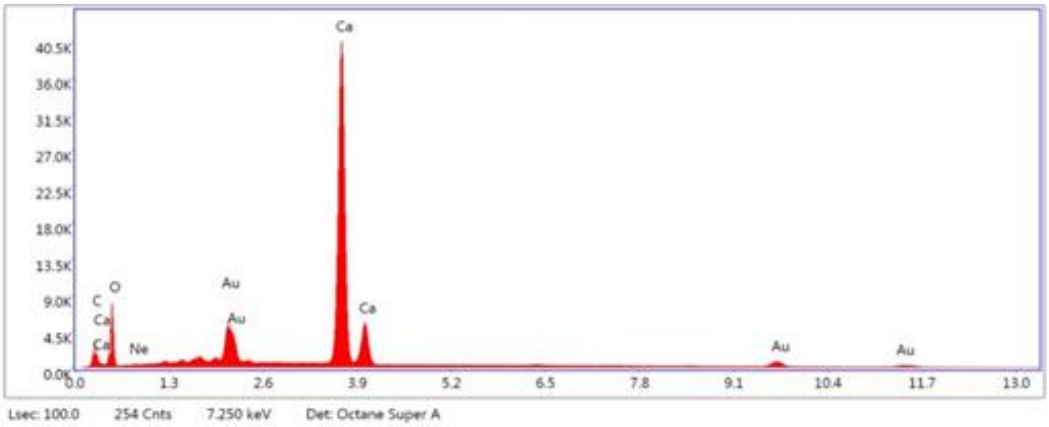

Figure 9-24 EDAX analysis of SP 57 after 18 months of exposure

Table 9-11 Results of EDAX analysis of SP57 after 18 months of exposure

Element	Weight %
C K	4.13
O K	27.68
NeK	0.00
CaK	52.54
AuL	15.64

A close look at the microstructure of SP58 specimen after 3 months of weathering exposure reveals that the continuous cement hydration along with natural carbonation during the weathering exposure led to the decrease in matrix pores. After 3 months of exposure, the small pores of SP58 mortar specimens as shown in Figure 9-25 are filled by etterngite during natural carbonation, while the calcium carbonate crystals from MICP filled the large pores (Figure 9.26).

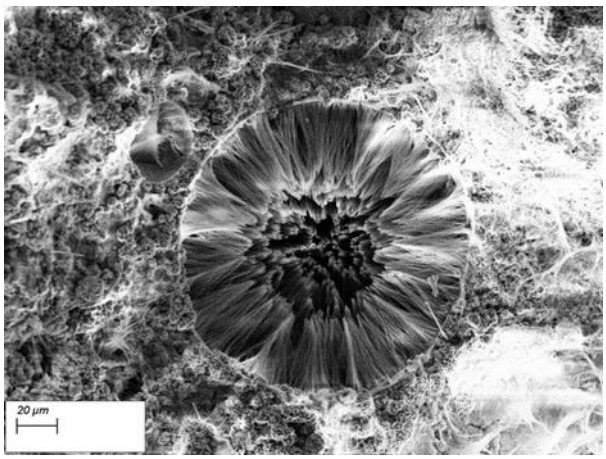

Figure 9-25 SP58 after 3 month exposure showing the overall growth of ettringite crystals (Ettringite is filling the pores)

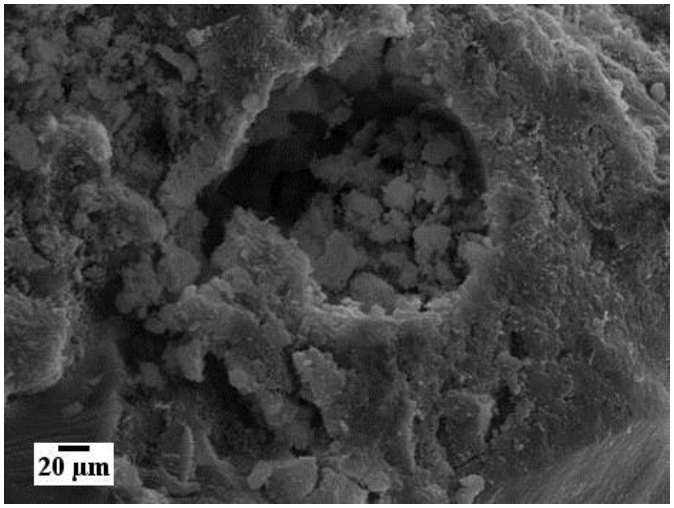

Figure 9-26 SP 58 after 3 month exposure under 4000x magnification

The surface fracture of the SP58 sample after six and nine months exposure was covered by small ettringite needles, but not much ettringite needles was observed in the cracks (Figure 9.27(a) and (b)). Figure 9.28 shows a similar ettringite deposit filling a crack across the cement mortar after six months of exposure. The ettringite crystals appear in these micrographs are mainly small and fibrous. The additional ettringite formation along with the calcium carbonate precipitated by bacteria may have caused the clear increase in compressive strength of SP58 after weathering exposure.

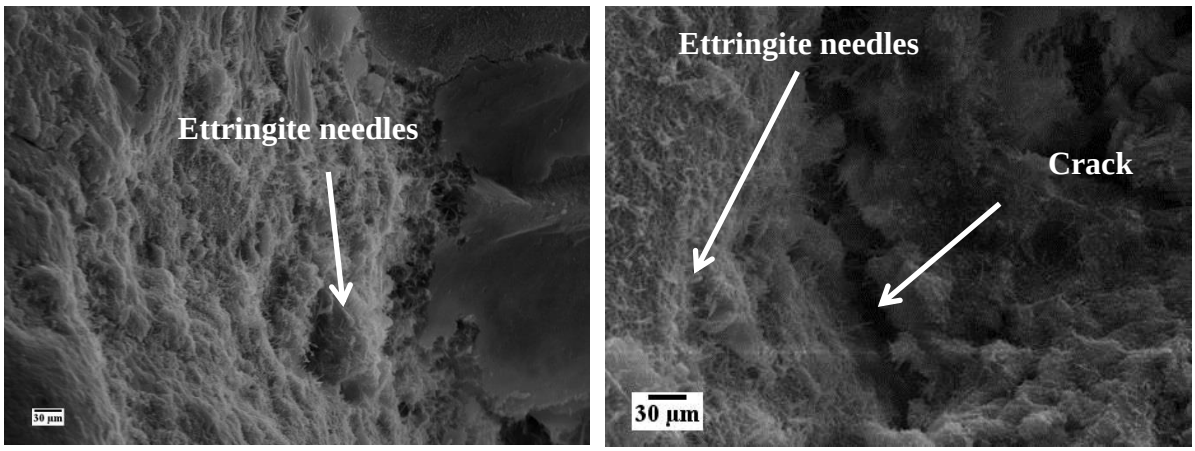

(a) (b)

Figure 9-27 SEM images of SP 58 after 6 months of outdoor exposure at 4000x magnification, (a) ettringite needles coverd the surface fracture (b) few ettringite needles in the crack

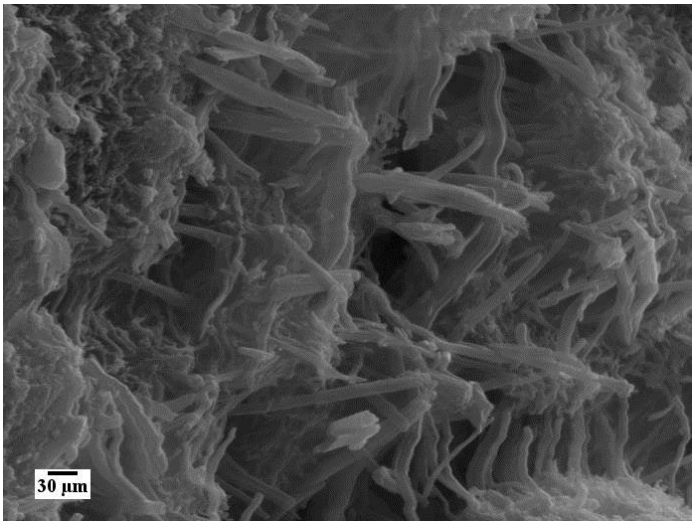

Figure 9-28 SP 58 after 9 months exposure under 4000x magnification

After 12 and 18 months of weathering, irregular shaped calcite crystals and portlandite were replaced the ettrigite and the other cement hydration products (Figures 9.29 and 9.30). It was not clear if these calcium carbonate crystals were formed by biomineralization process or natural carbonation of portlandite. Carbonation of portlandite results in a net increase of volume and precipitation of calcium carbonate in the pore network.

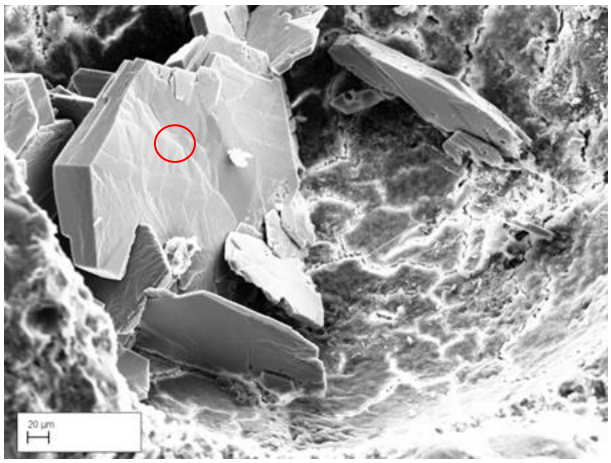

Figure 9-29 SP 58 after 12 months exposure under 525x magnification

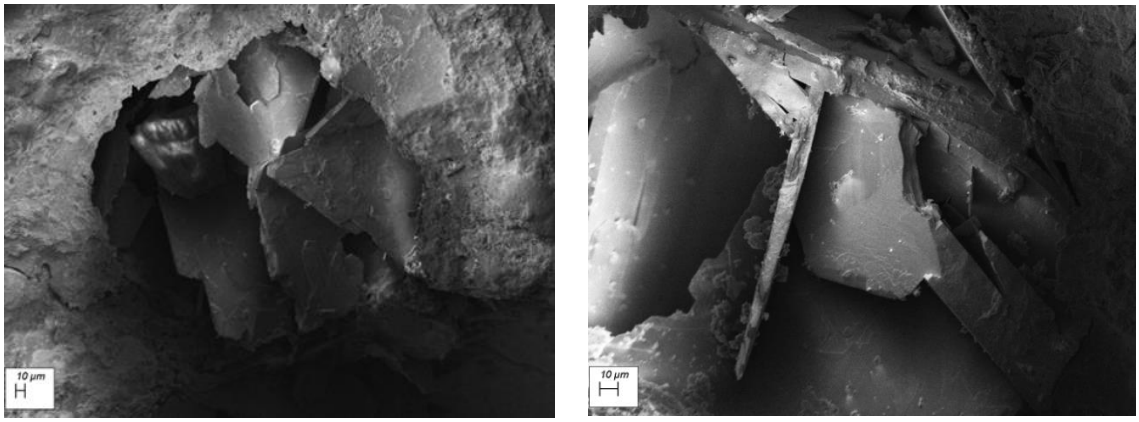

(a) (b)

Figure 9-30 SEM images of SP 58 after 18 months of outdoor exposure at (a) 500x and (b) 1000x magnification

Figure 9-31 depicts the EDAX spectra into the surface fracture of SP58 specimen after 12 months of exposure showing the higher percentages of calcium, carbon and oxygen. However, because of the differences between the actual and theoretical values of the composition of calcium carbonate, the area analysed in Figure 9-29 could be either a non-pure calcium carbonate or calcium hydroxide plate. The presence of Au element was present in the EDAX analysis because the sample was gold coated in the preparation process. This could also affect the accuracy of elemental analysis.

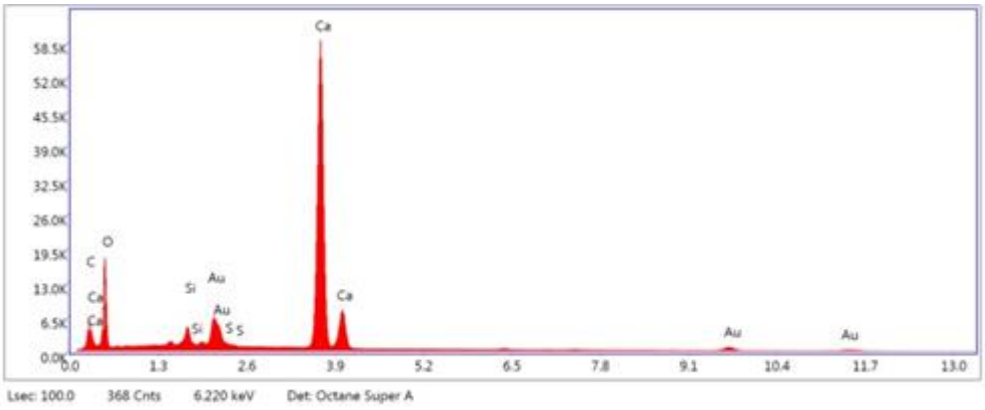

Figure 9-31 EDAX analysis of Sp58 after 12 months of exposure

Table 9-12 Results of EDAX analysis of SP58 after 12 months of exposure

Element	Weight %
C K	2.56
O K	37.60
SiK	1.32
S K	0.30
CaK	48.11
AuL	10.11

Carbonation in concrete takes place when carbon dioxide gas from the atmosphere diffuses into concrete voids or directly penetrates with rain water and dissolves into carbonic acid. Dissolution of hydrated in cement paste, mainly portlandite, leads to medium change by reducing the pH from 13.5 to less than 8.5. Calcium ions Ca+2 are also released in this solution and react with carbonate ions CO3-2 to form calcium carbonate CaCO3. Different parameters affect the carbonation reaction; portlandite content and the porosity of the medium are two main factors influencing this reaction. The strength and density of the cement paste of the carbonised concrete may be attributed to the large molecules and low solubility of carbonates comparing to hydroxides.

9.4 Interim conclusions

The purpose of this experimental work was to present the assessment of the self-healing processes in bacterial mortar that were subjected to outdoor weathering for 18 months. Over the course of the investigation, it has been focused on the task by taking the mechanical properties and microstructural observations into account. As a result of the experiments presented in the previous sections, a number of conclusions were determined as follows:

1) Under the same environmental conditions, the compressive strength of all bacterial mortar samples increased with the increase of exposure time. The highest compressive strength was achieved by SP33: the compressive strength value reached 53.5 MPa after 18 months of exposure with improvement of 85% comparing to control.

2) With time, the bacterial mortar placed outdoor underwent some kind of post cure process, which led to an increased flexural strength after six and twelve months of weathering.
3) The flexural strength of bacteria were enhanced as a result of calcium carbonate crystals formation during MICP process and carbonation process leading to blocking the mortar pores and reducing the mortar's internal porosity , hence improving mortar density and strength.
4) The correlation coefficient between compressive strength and exposure time of SP57, SP58 and SP33 are 0.968, 0.971and0.983, respectively, demonstrating that the compressive strength and exposure time are still well positively correlated under environmental effects for long period of time.
5) For bacterial mortar, the regression curve of the flexural strength and outdoor exposure time were less accurate than that of compressive strength. However, based on the shape of the regression curves, it could be stated that the flexural strength continue to increase and reach a point of highest development after subjecting to 18 months of outdoor exposure.
6) Concerning the correlation between the results of the accelerated exposure and those obtained under the outdoor exposure, on the basis of 18 months' time scale, it was found that the former exposure accelerated the changes in the compressive and flexural strength properties of the bacterial self-healing mortar compared with that in the latter one. Predictions of the long-term behaviour of bacterial mortar under outdoor exposure can be attempted.
7) There are no accurate results obtained from EDAX analysis of the bacterial samples subjected to outdoor environment, in spite of the enhancements in the compressive strength behaviour of bacterial self-healing mortar.

Chapter 10: Final Appraisals

10.1 Conclusions

1) Based on the phenotypic characteristics, such as its cell morphology and biochemical properties, the isolates were found to be Bacilli as they all gram positive and had short to long rod shape. They were all able to grow under aerobic conditions at 30oC. Almost half of the strains were able to sporulate when exposed to adverse environmental conditions (starvation). Oxidase and catalse test were also performed as part of biochemical identification. Genotypic characteristics revealed that six isolates were recognized as Bacillus Megaterium. A very fast urease activity was noticed with Bacillus Sphaericus 57 and 58 taken from Brunel University microbiological bank for comparison. Bacillus Megaterium 33 started its urease activity after 16 h, whereas the other Megaterium isolates showed very slow or negative activity. Bacillus Sphaericus 57 and 58 and Bacillus Megaterium 33 grew well in the environmental surroundings around pH 6-10. These three isolates were therefore selected for further application in self-healing concrete to evaluate their ability to precipitate calcium carbonate crystal in this study.
2) Regarding the urease activity of the urease positive bacterial species such as Bacillus Sphaericus 57 and 58, both species displayed very fast urease activity. The difference in this activity could be attributed to different capabilities of these species to provide varied types of urease enzymes and the difference in the level of urease enzyme among these strains.
3) Considerable work was undertaken to prepare a calcium alginate-clay beads to encapsulate B. sphaericus spores and evaluate beads ability to preserve B. sphaericus viability. The beads were prepared by mixing sodium alginate and Pyrophyllite (Pyrax) clay solution and then cross-linked them with CaCl2 solution. The characterization of calcium alginate-clay beads encapsulated with B. sphaericus was thoroughly examined. FTIR analysis results showed that the functional group of pyrophyllite and alginate has strong interaction with each other. The surface and cross section characteristics of Ca-alginate-Pyrophyllite beads shown by the SEM micrographs have supported this conclusion. It appears from thermogravimetric analysis that pyrophyllite was well dispersed in alginate matrix; therefore, the Ca-alginate-pyrophyllite beads structure was stable and firm compared with alginate

beads. Furthermore, the matrix was suitable for B.sphaericus encapsulation and preservation of spore's viability over time.

4) It has been found that the optimum quantity of beads must be added to cement mortar mixture was found to be 3% without adversely affecting the strength properties of cement mortar. It has also been indicated that 3% is the optimum amount of reagent can be used not only to avoid the deterioration effect of nutrient, but to enhance the strength properties. The highest increment of compressive strength was 20.28% when 3% nutrient was added.
5) Mechanical properties of self-healing mortar with directly added spores were higher than that with encapsulated spores. In addition to that, 3% calcium alginate-clay bead concentration has a low density, and positioned on the surface of the specimens. Non uniform distribution of beads in mortar matrix could result in difficulty in delivering bacterial spores into matrix. Therefore, the spores have been added directly in the preparation of mortar in the subsequent chapters (Chapter 7, 8 and 9).
6) Bacterial based self-healing mortar endures freezing and thawing action better than control cement mortar. After exposing to 30 F-T cycles, the compressive strengths of SP33, SP58 and SP57 have been reduced by 19.4%, 18.37% and 21%, respectively, while the reduction in compressive strength of control mortar was 36.4% percent of the initial strength. This could be attributed to the dense microstructure of the bacterial specimens.
7) A decrease in flexural strength with increase the number of the cycles has been noticed with the three different types of bacterial spores. The osmotic and swelling pressures cause by water movement leading to a gradual decomposing of calcium carbonate crystal which result in the reduction of flexural strength under freezing and thawing action. Two factors involved in the deterioration processes operating in cement mortars exposed to FT cycles: the hydraulic pressure from osmotic phenomena and water crystallisation.
8) Bacterial self-healing mortar samples exhibited lower compressive strength than the control After 30 cycles of wetting and drying. It has been detected that a reduction of 21% was found in compressive strength for SP57, whereas for SP58 and SP33 strength dropped by 18.3% and 9.4%, respectively. This behaviour could be attributed primarily to the reduction in the bacterial metabolic activities which responsible for precipitation of calcium carbonate as the temperature increased to 55 ^{o}C during the drying time of the cycle.

9) SP33 samples show the highest increase during the 1st, 3rd, 10th and 30th W-D cycle. The flexural strength of specimens containing SP58, SP57 and RP subjected to three wet-dry cycles was increased by 7.3, 0.5 and 5.4%, respectively compared to control specimen.
10) The self-healing of micro-cracks in bacterial mortar was expected to overcome the problem of cracking in cementitious materials for structures exposed to wetting and drying environmental conditions. Thus self-healing should maintain strength and durability even when subjected to these conditions. Outdoor exposure studies should be conducted to confirm this expectation in bacterial mortars exposed to natural environments.
11) Under the same environmental conditions, the compressive strength of all bacterial mortar samples increased with the increase of exposure time. The highest compressive strength was achieved by SP33: the compressive strength value reached 53.5 MPa after 18 months of exposure with improvement of 85% comparing to control.
12) The flexural strength of bacteria were enhanced as a result of calcium carbonate crystals formation during MICP process and carbonation process leading to blocking the mortar pores and reducing the mortar's internal porosity , hence improving mortar density and strength.
13) The correlation coefficient between compressive strength and exposure time of SP57, SP58 and SP33 are 0.968, 0.971and0.983, respectively, demonstrating that the compressive strength and exposure time are still well positively correlated under environmental effects for long period of time.
14) For bacterial mortar, the regression curve of the flexural strength and outdoor exposure time were less accurate than that of compressive strength. However, based on the shape of the regression curves, it could be stated that the flexural strength continue to increase and reach a point of highest development after subjecting to 18 months of outdoor exposure.
15) Regarding the correlation between the results of the accelerated exposure and those obtained under the outdoor exposure, on the basis of 18 months' time scale, it was found that the former exposure accelerated the changes in the compressive and flexural strength properties of the bacterial self-healing mortar compared with that in the latter one. Predictions of the long-term behaviour of bacterial mortar under outdoor exposure can be attempted.

16) There are no accurate results obtained from EDAX analysis of the bacterial samples subjected to outdoor environment, in spite of the enhancements in the compressive strength behaviour of bacterial self-healing mortar.
17) Table 10-1 and 10-2 summarise the relative compressive and flexural strength of the non-bacterial mortar and the bacterial self-healing mortar subjected to outdoor weathering exposure and accelerated exposure (freeze-thaw and wet-dry cycles). Based on the result of the relative compressive strength, it has been found the bacterial self-healing mortar perform better under outdoor exposure.
18) In term of flexural behaviour, bacterial self-healing mortar performed better in wet-dry exposure. Generally, the wet-dry action exhibited the optimum mechanical recovery among different accelerated exposure conditions. It can be assumed that, the additional water has been evaporated during the drying period leading to increase the ions concentrations in the water remaining in the cracks. Significant amounts of reactant were concentrated; in this case, for further reactions and the through-solution reactions were also available in the presence of adequate amount of water. Furthermore, the additional precipitation of $CaCO_3$ due to carbon dioxide penetration into the crack during the drying time would be beneficial for crack closing.

Table 10-1 the relative compressive strength of bacterial and non-bacterial mortar subjected to outdoor weathering exposure and accelerated exposure (freeze-thaw and wet-dry cycles).

Mix	Relative compressive strength (%)											
	Type of exposure											
	Number of Freeze-Thaw cycles			Number of Wet-Dry cycles			Outdoor exposure time(month)					
	3	10	30	3	10	30	3	6	9	12	16	18
R	96.1	72.9	63.6	114.5	140.2	162.0	103.6	106.9	99.8	96.0	90.6	87.1
RP	92.1	69.6	64.4	126.0	131.0	171.7	104.7	110.5	104.6	100.3	95.6	87.8
SP57	89.7	82.1	78.9	129.4	106.3	105.9	107.8	116.8	112.3	124.5	131.8	135.1
SP58	89.3	83.5	81.6	80.1	94.7	112.7	102.9	106.4	110.8	111.6	113.8	121.1
SP33	93.2	84.1	80.6	107.8	94.4	130.0	102.1	106.4	111.9	114.7	120.3	131.6

Table 10-2 the relative flexural strength of bacterial and non-bacterial mortar subjected to outdoor weathering exposure and accelerated exposure (freeze-thaw and wet-dry cycles).

Mix	Relative flexural strength (%)											
	Type of exposure											
	Number of Freeze-Thaw cycles			Number of Wet-Dry cycles			Outdoor exposure time(month)					
	3	10	30	3	10	30	3	6	9	12	16	18
R	61.6	59.2	48.7	152.3	65.6	142.0	102.1	98.9	95.8	91.4	89.6	85.4
RP	72.6	67.3	61.0	65.4	123.0	103.5	85.7	78.4	73.7	67.1	61.8	89.4
SP57	89.4	69.0	64.8	110.5	85.7	88.7	97.3	72.3	82.2	96.2	108.8	116.1
SP58	100	65.8	57.0	121.5	82.6	97.8	71.4	53.3	51.7	65.0	76.3	81.0
SP33	97.2	76.0	63.7	167.0	88.6	92.8	67.2	56.4	52.5	46.3	49.9	75.3

10.2 Limitation of the research and Recommendations

10.2.1 Limitation

1. The relation between number of bacteria and the amount of calcium carbonate produced has not been studied as Bacillus are still under research are still under research.

3. There is little evidence in the literature about the negative effects of self-healing agent (precursor and nutrients) on early-age and the fresh properties of cementitious materials and the limitation of self-healing agent, which does not affect the physical and mechanical properties of cementitious materials.

4. The ability of these bacterial species to germinate spores and precipitate calcite at conditions near ideal as demonstrated by previous studies, which is often somewhere between 25 and 35°C for alkaliphilic microorganisms. Nevertheless, the ability of bacterial species to germinate and produce calcite at various ranges of temperature still needs to be confirmed.

10.2.2 Recommendations

The findings of this research explain the performance of bacteria based self-healing concrete under harsh environment. Beyond the chosen experimental programme, some additional improvements may be carried out, including:

1) Using calcium-gluconate instead of calcium chloride as gelling agents for sodium alginate to enhance the survival of encapsulated spores.
2) Studying the effect of the initial concentrations of bacterial spores on the viability to find out the optimum spores concertation for better survival.
3) Studying the effect of chemical attack on the properties of bacteria based self-healing mortar.
4) More fundamental and more focused studies are needed on specific loading mechanisms/exposure in combination with the environmental loading such as flexural loading.
5) It is necessary to use other techniques to study the deterioration mechanisms such as dynamic elastic modulus, expansion and mass change.
6) Study the influence of different calcium sources such as calcium nitrate, calcium acetate, calcium glutamate, calcium chloride etc. on bacteria based self-healing cementitious composites as the type of source of calcium compound may greatly influence the rate of formation, morphology, crystalline nature and chemical composition of the mineral precipitation.
7) Conduct more detailed self-healing behavior study on bacteria incorporated BBCC specimens giving emphasis on durability properties such as gas permeability, water permeability, RCPT, sorptivity etc.

References

Abo-El-Enein, S., Ali, A., Talkhan, F.N. and Abdel-Gawwad, H. (2013) 'Application of microbial biocementation to improve the physico-mechanical properties of cement mortar', HBRC Journal, 9(1), pp. 36-40.

Abo-El-Enein, S., Ali, A., Talkhan, F.N. and Abdel-Gawwad, H. (2012) 'Utilization of microbial induced calcite precipitation for sand consolidation and mortar crack remediation', HBRC Journal, 8(3), pp. 185-192.

Achal, V., Mukherjee, A., Basu, P. and Reddy, M.S. (2009) 'Strain improvement of Sporosarcina pasteurii for enhanced urease and calcite production', Journal of industrial microbiology & biotechnology, 36(7), pp. 981-988.

Achal, V., Mukerjee, A. and Reddy, M.S. (2013a) 'Biogenic treatment improves the durability and remediates the cracks of concrete structures', Construction and Building Materials, 48, pp. 1-5.

Achal, V., Mukherjee, A. and Reddy, M.S. (2011) 'Effect of calcifying bacteria on permeation properties of concrete structures', Journal of industrial microbiology & biotechnology, 38(9), pp. 1229-1234.

Achal, V., Mukherjee, A. and Reddy, M.S. (2010a) 'Microbial concrete: way to enhance the durability of building structures', Journal of Materials in Civil Engineering, 23(6), pp. 730-734.

Achal, V., Mukerjee, A. and Reddy, M. (2013b) 'Biogenic treatment improves the durability and remediates the cracks of concrete structures', Construction and Building Materials, 48, pp. 1-5.

Achal, V., Mukherjee, A. and Reddy, M.S. (2010b) 'Microbial concrete: A way to enhance durability of building structures', in, pp. 23-28.

Achal, V., Pan, X. and Özyurt, N. (2011) 'Improved strength and durability of fly ash-amended concrete by microbial calcite precipitation', Ecological Engineering, 37(4), pp. 554-559.

Adzmi, F., Meon, S., Musa, M.H. and Yusuf, N.A. (2012) 'Preparation, characterisation and viability of encapsulated Trichoderma harzianum UPM40 in alginate-montmorillonite clay', Journal of microencapsulation, 29(3), pp. 205-210.

Afifudin, H., Hamidah, M.S., Noor Hana, H. and Kamaruddin, K. (2011) 'Microorganism precipitation in enhancing concrete properties', Applied Mechanics and Materials. Trans Tech Publ, 1157-1165.

Al-Akhras, N.M. (2012) 'Performance of glass concrete subjected to freeze-thaw cycling', Open construction and building technology journal, 6, pp. 392-397.

Aldea, C., Song, W., Popovics, J.S. and Shah, S.P. (2000) 'Extent of healing of cracked normal strength concrete', Journal of Materials in Civil Engineering, 12(1), pp. 92-96.

Al-Thawadi, S. and Cord-Ruwisch, R. (2012) 'Calcium carbonate crystals formation by ureolytic bacteria isolated from Australian soil and sludge', J.Adv.Sci.Eng.Res, 2(1).

Andalib, R., MAJID, M.Z.A., Keyvanfar, A., Talaiekhozan, A., Hussin, M.W., Shafaghat, A., Zin, R.M., Lee, C.T., Fulazzaky, M.A. and Ismail, H.H. (2014) 'Durability improvement assessment in different high strength bacterial structural concrete grades against different types of acids', Sadhana, 39(6), pp. 1509-1522.

Andalib, R., Majid, M.Z.A., Hussin, M.W., Ponraj, M., Keyvanfar, A., Mirza, J. and Lee, H. (2016) 'Optimum concentration of Bacillus megaterium for strengthening structural concrete', Construction and Building Materials, 118, pp. 180-193.

Aono, R., Ito, M. and Machida, T. (1999) 'Contribution of the cell wall component teichuronopeptide to pH homeostasis and alkaliphily in the alkaliphile Bacillus lentus C-125', Journal of Bacteriology, 181(21), pp. 6600-6606.

Arias, J.L. and Fernández, M.S. (2008) 'Polysaccharides and proteoglycans in calcium carbonate-based biomineralization', Chemical reviews, 108(11), pp. 4475-4482.

Ash, C., Farrow, J., Wallbanks, S. and Collins, M. (1991) 'Phylogenetic heterogeneity of the genus Bacillus revealed by comparative analysis of small□subunit□ribosomal RNA sequences', Letters in applied microbiology, 13(4), pp. 202-206.

Bååth, E. and Arnebrant, K. (1994) 'Growth rate and response of bacterial communities to pH in limed and ash treated forest soils', Soil Biology and Biochemistry, 26(8), pp. 995-1001.

Badwan, A., Abumalooh, A., Sallam, E., Abukalaf, A. and Jawan, O. (1985) 'A sustained release drug delivery system using calcium alginate beads', Drug development and industrial pharmacy, 11(2-3), pp. 239-256.

Baeuerlein, E. (2004) Biomineralization: Progress in biology, molecular biology and application. John Wiley & Sons.

Bang, S.S., Galinat, J.K. and Ramakrishnan, V. (2001) 'Calcite precipitation induced by polyurethane-immobilized Bacillus pasteurii', Enzyme and microbial technology, 28(4), pp. 404-409.

Barabesi, C., Galizzi, A., Mastromei, G., Rossi, M., Tamburini, E. and Perito, B. (2007) 'Bacillus subtilis gene cluster involved in calcium carbonate biomineralization', Journal of Bacteriology, 189(1), pp. 228-235.

Barreca, S., Orecchio, S. and Pace, A. (2014) 'The effect of montmorillonite clay in alginate gel beads for polychlorinated biphenyl adsorption: Isothermal and kinetic studies', Applied Clay Science, 99, pp. 220-228.

BARTHOLOMEW, J.W. and FINKELSTEIN, H. (1958) 'Relationship of cell wall staining to gram differentiation', Journal of Bacteriology, 75(1), pp. 77-84.

Basheer, L., Kropp, J. and Cleland, D.J. (2001) 'Assessment of the durability of concrete from its permeation properties: a review', Construction and Building Materials, 15(2), pp. 93-103.

Batic, O.R., Milanesi, C.A., Maiza, P.J. and Marfil, S.A. (2000) 'Secondary ettringite formation in concrete subjected to different curing conditions', Cement and Concrete Research, 30(9), pp. 1407-1412.

Bäuerlein, E. (2003) 'Biomineralization of unicellular organisms: an unusual membrane biochemistry for the production of inorganic nano□and microstructures', Angewandte Chemie International Edition, 42(6), pp. 614-641.

Bayramoglu, G., Denizli, A., Bektas, S. and Arica, M.Y. (2002) 'Entrapment of Lentinus sajor-caju into Ca-alginate gel beads for removal of Cd (II) ions from aqueous solution: preparation and biosorption kinetics analysis', Microchemical Journal, 72(1), pp. 63-76.

Bazylinski, D.A., Frankel, R.B. and Konhauser, K.O. (2007) 'Modes of biomineralization of magnetite by microbes', Geomicrobiology Journal, 24(6), pp. 465-475.

Ben Omar, N., Arias, J.M. and Gonzalez-Munoz, M.T. (1997) 'Extracellular bacterial mineralization within the context of geomicrobiology', Microbiologia (Madrid, Spain), 13(2), pp. 161-172.

Beveridge, T.J. (2001) 'Use of the Gram stain in microbiology', Biotechnic & Histochemistry, 76(3), pp. 111-118.

Binici, H., Shah, T., Aksogan, O. and Kaplan, H. (2008) 'Durability of concrete made with granite and marble as recycle aggregates', Journal of Materials Processing Technology, 208(1-3), pp. 299-308.

Bolobova, A. and Kondrashchenko, V. (2000) 'Use of yeast fermentation waste as a biomodifier of concrete', Applied Biochemistry and Microbiology, 36(3), pp. 205-214.

Boquet, E., Boronat, A. and Ramos-Cormenzana, A. (1973) 'Production of calcite (calcium carbonate) crystals by soil bacteria is a general phenomenon', .

Bosak, T. (2011) 'Calcite precipitation, microbially induced', in Encyclopedia of Geobiology. Springer, pp. 223-227.

Bowser, J.D., Krause, G.L. and Tadros, M.K. (1996) 'Freeze-thaw durability of high-performance concrete masonry units', Materials Journal, 93(4), pp. 386-394.

Braude, A.I. and Berkowitz, H. (1961) 'Detection of urinary catalase by disk flotation', The Journal of laboratory and clinical medicine, 57(3), pp. 490-494.

Bregni, C., Degrossi, J., Garcia, R., Lamas, M., Firenstein, R. and D'aquino, M. (2000) 'Alginate microspheres of Bacillus subtilis', .

Brennan, S.T., Lowenstein, T.K. and Horita, J. (2004) 'Seawater chemistry and the advent of biocalcification', Geology, 32(6), pp. 473-476.

Brink, B. (2010) 'Urease test protocol', .

BS EN 196-1: 2016 (2016) 'Methods of testing cement. Part 1: Determination of strength', .

BSI (2005) 'BS EN 196-1: 2005: Methods of testing cement. Determination of strength', .

Bundur, Z.B., Kirisits, M.J. and Ferron, R.D. (2015) 'Biomineralized cement-based materials: Impact of inoculating vegetative bacterial cells on hydration and strength', Cement and Concrete Research, 67, pp. 237-245.

Burbank, M.B., Weaver, T.J., Green, T.L., Williams, B.C. and Crawford, R.L. (2011) 'Precipitation of calcite by indigenous microorganisms to strengthen liquefiable soils', Geomicrobiology Journal, 28(4), pp. 301-312.

Cacchio, P., Ercole, C., Cappuccio, G. and Lepidi, A. (2003) 'Calcium carbonate precipitation by bacterial strains isolated from a limestone cave and from a loamy soil', Geomicrobiology Journal, 20(2), pp. 85-98.

Cailleux, E. and Pollet, V. (2009) 'Investigations on the development of self-healing properties in protective coatings for concrete and repair mortars', Proceedings of the 2nd International Conference on Self-Healing Materials, Chicago, IL, USA.

Cao, Q., Gao, Q., Gao, R. and Jia, J. (2018) 'Chloride penetration resistance and frost resistance of fiber reinforced expansive self-consolidating concrete', Construction and Building Materials, 158, pp. 719-727.

Castanier, S., Le Métayer-Levrel, G. and Perthuisot, J. (1999) 'Ca-carbonates precipitation and limestone genesis—the microbiogeologist point of view', Sedimentary Geology, 126(1), pp. 9-23.

Cavallaro, G., Gianguzza, A., Lazzara, G., Milioto, S. and Piazzese, D. (2013) 'Alginate gel beads filled with halloysite nanotubes', Applied Clay Science, 72, pp. 132-137.

Chafetz, H.S. and Folk, R.L. (1984) 'Travertines: depositional morphology and the bacterially constructed constituents', Journal of Sedimentary Research, 54(1).

Chahal, N., Siddique, R. and Rajor, A. (2012a) 'Influence of bacteria on the compressive strength, water absorption and rapid chloride permeability of concrete incorporating silica fume', Construction and Building Materials, 37, pp. 645-651.

Chahal, N., Siddique, R. and Rajor, A. (2012b) 'Influence of bacteria on the compressive strength, water absorption and rapid chloride permeability of fly ash concrete', Construction and Building Materials, 28(1), pp. 351-356.

Choi, S., Wang, K. and Chu, J. (2016) 'Properties of biocemented, fiber reinforced sand', Construction and Building Materials, 120, pp. 623-629.

Cizer, Ö, Rodriguez-Navarro, C., Ruiz-Agudo, E., Elsen, J., Van Gemert, D. and Van Balen, K. (2012) 'Phase and morphology evolution of calcium carbonate precipitated by carbonation of hydrated lime', Journal of Materials Science, 47(16), pp. 6151-6165.

Claus, D. and Berkeley, R. (1986) 'Genus pseudomonas', Bergey's Manual of Systematic Bacteriology, 1, pp. 140-219.

Clear, C. (1985) The effects of autogenous healing upon the leakage of water through cracks in concrete, .

Cruickshank, R. (1968) '11th (ed) Medical microbiology: a guide to diagnosis and control of infection', Edinburghand London: E&S.Livingston Ltd, 888.

Cultrone, G., Sebastian, E. and Huertas, M.O. (2005) 'Forced and natural carbonation of lime-based mortars with and without additives: Mineralogical and textural changes', Cement and Concrete Research, 35(12), pp. 2278-2289.

Da Silva, F.B., De Belie, N., Boon, N. and Verstraete, W. (2015) 'Production of non-axenic ureolytic spores for self-healing concrete applications', Construction and Building Materials, 93, pp. 1034-1041.

Daemi, H. and Barikani, M. (2012) 'Synthesis and characterization of calcium alginate nanoparticles, sodium homopolymannuronate salt and its calcium nanoparticles', Scientia Iranica, 19(6), pp. 2023-2028.

Davidsohn, I., Henry, J.B. and Todd, J.C. (1969) 'Todd-Sanford clinical diagnosis by laboratory methods', .

De Belie, N. and Wang, J. (2016) 'Bacteria-based repair and self-healing of concrete', Journal of Sustainable Cement-Based Materials, 5(1-2), pp. 35-56.

De Muynck, W., Debrouwer, D., De Belie, N. and Verstraete, W. (2008) 'Bacterial carbonate precipitation improves the durability of cementitious materials', Cement and Concrete Research, 38(7), pp. 1005-1014.

De Muynck, W., Cox, K., Belie, N.D. and Verstraete, W. (2008b) 'Bacterial carbonate precipitation as an alternative surface treatment for concrete', Construction and Building Materials, 22(5), pp. 875-885.

De Muynck, W., Verbeken, K., De Belie, N. and Verstraete, W. (2013) 'Influence of temperature on the effectiveness of a biogenic carbonate surface treatment for limestone conservation', Applied Microbiology and Biotechnology, 97(3), pp. 1335-1347.

De Muynck, W., Verbeken, K., De Belie, N. and Verstraete, W. (2010) 'Influence of urea and calcium dosage on the effectiveness of bacterially induced carbonate precipitation on limestone', Ecological Engineering, 36(2), pp. 99-111.

de Rooij, M., Van Tittelboom, K., De Belie, N. and Schlangen, E. (2013) Self-healing phenomena in cement-Based materials: state-of-the-art report of RILEM technical committee 221-SHC: self-Healing phenomena in cement-Based materials. Springer.

De Yoreo, J.J. and Vekilov, P.G. (2003) 'Principles of crystal nucleation and growth', Reviews in mineralogy and geochemistry, 54(1), pp. 57-93.

DeJong, J.T., Mortensen, B.M., Martinez, B.C. and Nelson, D.C. (2010) 'Bio-mediated soil improvement', Ecological Engineering, 36(2), pp. 197-210.

Dejonghe, P., De Belie, N., Steuperaert, S., Snoeck, D. and Dubruel, P. (2011) 'The behaviour of suberabsorbing polymers as a sealing agent in concrete: absorption kinetics, degradation and water permeability', 3rd International conference on Self-Healing Materials (ICSHM 2011). , 123-124.

Dhami, N.K., Reddy, M.S. and Mukherjee, A. (2013) 'Biomineralization of calcium carbonates and their engineered applications: a review', Frontiers in microbiology, 4.

Dhami, N.K., Mukherjee, A. and Reddy, S.M. (2012) Biofilm and microbial applications in biomineralized concrete. INTECH Open Access Publisher.

Dhami, N.K., Reddy, M.S. and Mukherjee, A. (2014) 'Synergistic role of bacterial urease and carbonic anhydrase in carbonate mineralization', Applied Biochemistry and Biotechnology, 172(5), pp. 2552-2561.

Dhami, N.K., Reddy, M.S. and Mukherjee, A. (2012) 'Improvement in strength properties of ash bricks by bacterial calcite', Ecological Engineering, 39, pp. 31-35.

Diamond, S. (2004) 'The microstructure of cement paste and concrete—a visual primer', Cement and Concrete Composites, 26(8), pp. 919-933.

Dick, J., De Windt, W., De Graef, B., Saveyn, H., Van der Meeren, P., De Belie, N. and Verstraete, W. (2006) 'Bio-deposition of a calcium carbonate layer on degraded limestone by Bacillus species', Biodegradation, 17(4), pp. 357-367.

Dong, B., Han, N., Zhang, M., Wang, X., Cui, H. and Xing, F. (2013) 'A microcapsule technology based self-healing system for concrete structures', Journal of Earthquake and Tsunami, 7(03), pp. 1350014.

Dry, C.M. (2001) 'Design of self-growing, self-sensing, and self-repairing materials for engineering applications', Smart Materials. International Society for Optics and Photonics, 23-30.

Dry, C.M. (1999) 'Repair and prevention of damage due to transverse shrinkage cracks in bridge decks', Smart Structures and Materials 1999: Smart Systems for Bridges, Structures, and Highways. International Society for Optics and Photonics, 253-257.

Dry, C.M. (1998) 'Release of smart chemicals for the in-service repair of bridges and roadways', 1996 Symposium on Smart Materials, Structures, and MEMS. International Society for Optics and Photonics, 140-145.

Dry, C.M. (1996) 'Smart earthquake-resistant materials: using time-released adhesives for damping, stiffening, and deflection control', 3rd International Conference on Intelligent Materials and 3rd European Conference on Smart Structures and Materials. International Society for Optics and Photonics, 958-968.

Dry, C. and Corsaw, M. (2003) 'A comparison of bending strength between adhesive and steel reinforced concrete with steel only reinforced concrete', Cement and Concrete Research, 33(11), pp. 1723-1727.

Dry, C., Corsaw, M. and Bayer, E. (2003) 'A comparison of internal self-repair with resin injection in repair of concrete', Journal of Adhesion Science and Technology, 17(1), pp. 79-89.

Dry, C. (2000) 'Three designs for the internal release of sealants, adhesives, and waterproofing chemicals into concrete to reduce permeability', Cement and Concrete Research, 30(12), pp. 1969-1977.

Dubey, R. and Maheshwari, D. (2012) Practical microbiology. S. Chand Pvt. Limited.

Ducasse-Lapeyrusse, J., Gagné, R., Lors, C. and Damidot, D. (2017) 'Effect of calcium gluconate, calcium lactate, and urea on the kinetics of self-healing in mortars', Construction and Building Materials, 157, pp. 489-497.

Edvardsen, C. (1999) 'Water permeability and autogenous healing of cracks in concrete', ACI Materials Journal, 96(4).

El-Didamony, H., Amer, A., Heikal, M. and Shoaib, M. (1999) 'Effect of calcium acetate as accelerator and water reducer on the properties of silica fume blended cement', CERAMICS SILIKATY, 43, pp. 29-33.

Emberger, O. (1970) 'Cultivation methods for the detection of aerobic sporeforming bacteria', Zentralblatt fur Bakteriologie, Parasitenkunde, Infektionskrankheiten und Hygiene.Zweite naturwissenschaftliche Abt.: Allgemeine, landwirtschaftliche und technische Mikrobiologie, 125(6), pp. 555-565.

EN, B. '206-1: 2000 (2001)', Concrete-Part 1: Specification, performance, production and conformity, .

Erşan, Y.Ç, Gruyaert, E., Louis, G., Lors, C., De Belie, N. and Boon, N. (2015a) 'Self-protected nitrate reducing culture for intrinsic repair of concrete cracks', Frontiers in microbiology, 6, pp. 1228.

Erşan, Y.Ç, Da Silva, F.B., Boon, N., Verstraete, W. and De Belie, N. (2015b) 'Screening of bacteria and concrete compatible protection materials', Construction and Building Materials, 88, pp. 196-203.

Erşan, Y.Ç, De Belie, N. and Boon, N. (2015) 'Microbially induced CaCO3 precipitation through denitrification: an optimization study in minimal nutrient environment', Biochemical engineering journal, 101, pp. 108-118.

Erşan, Y.Ç, Hernandez-Sanabria, E., Boon, N. and De Belie, N. (2016) 'Enhanced crack closure performance of microbial mortar through nitrate reduction', Cement and Concrete Composites, 70, pp. 159-170.

Evans Jr, D.J., Evans, D.G., Kirkpatrick, S.S. and Graham, D.Y. (1991) 'Characterization of the Helicobacter pylori urease and purification of its subunits', Microbial pathogenesis, 10(1), pp. 15-26.

Farmer, V.C. (1974) The infrared spectra of minerals. London: Mineralogical Society.

Fenice, M., Selbman, L., Federici, F. and Vassilev, N. (2000) 'Application of encapsulated Penicillium variabile P16 in solubilization of rock phosphate', Bioresource technology, 73(2), pp. 157-162.

Ferrer, M.R., Quevedo-Sarmiento, J., Rivadeneyra, M.A., Bejar, V., Delgado, R. and Ramos-Cormenzana, A. (1988a) 'Calcium carbonate precipitation by two groups of moderately halophilic microorganisms at different temperatures and salt concentrations', Current microbiology, 17(4), pp. 221-227.

Ferrer, M., Quevedo□Sarmiento, J., Bejar, V., Delgado, R., Ramos□Cormenzana, A. and Rivadeneyra, M. (1988b) 'Calcium carbonate formation by Deleya halophila: effect of salt concentration and incubation temperature', Geomicrobiology Journal, 6(1), pp. 49-57.

Ferris, F., Phoenix, V., Fujita, Y. and Smith, R. (2004) 'Kinetics of calcite precipitation induced by ureolytic bacteria at 10 to 20 C in artificial groundwater', Geochimica et Cosmochimica Acta, 68(8), pp. 1701-1710.

Florea, M. and Brouwers, H. (2014) 'Modelling of chloride binding related to hydration products in slag-blended cements', Construction and Building Materials, 64, pp. 421-430.

Florea, M. and Brouwers, H. (2012) 'Chloride binding related to hydration products: Part I: Ordinary Portland Cement', Cement and Concrete Research, 42(2), pp. 282-290.

Frankel, R.B. and Bazylinski, D.A. (2003) 'Biologically induced mineralization by bacteria', Reviews in mineralogy and geochemistry, 54(1), pp. 95-114.

Fravel, D., Marois, J., Lumsden, R. and Connick Jr, W. (1985) 'Encapsulation of potential biocontrol agents in an alginate-clay matrix', Phytopathology, 75(7), pp. 774-777.

Ghosh, P., Mandal, S., Chattopadhyay, B. and Pal, S. (2005) 'Use of microorganism to improve the strength of cement mortar', Cement and Concrete Research, 35(10), pp. 1980-1983.

Girskas, G. and Skripkiūnas, G. (2017) 'The effect of synthetic zeolite on hardened cement paste microstructure and freeze-thaw durability of concrete', Construction and Building Materials, 142, pp. 117-127.

Gollapudi, U., Knutson, C., Bang, S. and Islam, M. (1995) 'A new method for controlling leaching through permeable channels', Chemosphere, 30(4), pp. 695-705.

Gorospe, C.M., Han, S., Kim, S., Park, J., Kang, C., Jeong, J. and So, J. (2013) 'Effects of different calcium salts on calcium carbonate crystal formation by Sporosarcina pasteurii KCTC 3558', Biotechnology and bioprocess engineering, 18(5), pp. 903-908.

Granger, S., Loukili, A., Pijaudier-Cabot, G. and Chanvillard, G. (2007) 'Experimental characterization of the self-healing of cracks in an ultra high performance cementitious material: Mechanical tests and acoustic emission analysis', Cement and Concrete Research, 37(4), pp. 519-527.

Greenwood, N.N. (2007) Spectroscopic properties of inorganic and organometallic compounds. Royal Society of Chemistry.

Gurbuz, A., Sari, Y.D., Yuksekdag, Z.N. and Cinar, B. (2013) 'Cementation in a matrix of loose sandy soil using biological treatment method', African Journal of Biotechnology, 10(38), pp. 7432-7440.

Hamilton, W. (2003) 'Microbially influenced corrosion as a model system for the study of metal microbe interactions: a unifying electron transfer hypothesis', Biofouling, 19(1), pp. 65-76.

Hammes, F. and Verstraete, W. (2002) 'Key roles of pH and calcium metabolism in microbial carbonate precipitation', Reviews in environmental science and biotechnology, 1(1), pp. 3-7.

Hammes, F., Boon, N., de Villiers, J., Verstraete, W. and Siciliano, S.D. (2003) 'Strain-specific ureolytic microbial calcium carbonate precipitation', Applied and Environmental Microbiology, 69(8), pp. 4901-4909.

Hasan, H. (2000) 'Ureolytic microorganisms and soil fertility: A review', Communications in Soil Science and Plant Analysis, 31(15-16), pp. 2565-2589.

Hassan, M., Milla, J., Rupnow, T. and Soysal, A. (2019) 'Self-Healing Concrete using Encapsulated Bacterial Spores in a Simulated Hot Subtropical Climate', .

Homma, D., Mihashi, H. and Nishiwaki, T. (2009) 'Self-healing capability of fibre reinforced cementitious composites', Journal of Advanced Concrete Technology, 7(2), pp. 217-228.

Horikoshi, K. (1999) 'Alkaliphiles: some applications of their products for biotechnology', Microbiology and molecular biology reviews : MMBR, 63(4), pp. 735-50, table of contents.

Huang, H. and Ye, G. (2013) 'Possibility of self-healing by using capsules and vascular system to provide water in cementitious materials', ICSHM 2013: Proceedings of the 4th International Conference on Self-Healing Materials, Ghent, Belgium, 16-20 June 2013. Magnel Laboratory for Concrete Research.

Huang, H. and Ye, G. (2015) 'Self-healing of cracks in cement paste affected by additional Ca2 ions in the healing agent', Journal of Intelligent Material Systems and Structures, 26(3), pp. 309-320.

Huang, H., Ye, G., Leung, C. and Wan, K. (2011) 'Application of sodium silicate solution as self-healing agent in cementitious materials', International RILEM conference on advances in construction materials through science and engineering. RILEM Publications SARL: Hong Kong, China, 530-536.

Iliescu, R.I., Andronescu, E., Daniela, C., Ghiţulică, D.B. and Ficai, A. (2011) 'Montmorillonite-alginate nanocomposite beads as drug carrier for oral administration of carboplatin–preparation and characterization', UPB Scientific Bulletin, Series B, 73(3).

Jacobsen, S., Marchand, J. and Hornain, H. (1995) 'SEM observations of the microstructure of frost deteriorated and self-healed concretes', Cement and Concrete Research, 25(8), pp. 1781-1790.

Jagadeesha B G Kumar, R Prabhakara and H Pushpa (2013) 'BIO MINERALISATION OF CALCIUM CARBONATE BY DIFFERENT BACTERIAL STRAINS AND THEIR APPLICATION IN CONCRETE CRACK REMEDIATION', International Journal of Advances in Engineering & Technology, 6(1), pp. 202-213.

Jagadeesha Kumar, B., Prabhakara, R. and Pushpa, H. (2013) 'Effect of bacterial calcite precipitation on compressive strength of mortar cubes', Int J Eng Adv Technol (IJEAT), 2.

Jana, D. (2006) 'Sample preparation techniques in petrographic examinations of construction materials: A state-of-the-art review', Proceedings of the twenty-eighth Conference on Cement Microscopy. , 48.

Janssen, D. (2011) 'Water encapsulation to initiate self-healing in cementitious materials', Master's Thesis, Delft University, Delft, .

Jonkers, H.M. (2007) 'Self healing concrete: a biological approach', in Self Healing Materials. Springer, pp. 195-204.

Jonkers, H.M. and Thijssen, A. (2010) 'Bacteria mediated remediation of concrete structures', Proceedings of 2nd International Symposium on Service Life Design for Infrastructure, Delft, The Netherlands. , 4-6.

Jonkers, H.M., Thijssen, A., Muyzer, G., Copuroglu, O. and Schlangen, E. (2010) 'Application of bacteria as self-healing agent for the development of sustainable concrete', Ecological Engineering, 36(2), pp. 230-235.

Jonkers, H.M. and Schlangen, E. (2007) 'Self-healing of cracked concrete: A bacterial approach', in, pp. 1821-1826.

Jonkers, H.M. and Schlangen, E. (2009) 'A two component bacteria-based self-healing concrete', in, pp. 119-120.

Kantha D.Arunachalam, K.S. Sathyanarayanan, B.S. Darshan and R.Balaji Raja (2010) 'Studies on the characterisation of Biosealant properties of Bacillus sphaericus', International Journal of Engineering Science and Technology, 2, pp. 270-277.

Karagöl, F., Demirboğa, R., Kaygusuz, M.A., Yadollahi, M.M. and Polat, R. (2013) 'The influence of calcium nitrate as antifreeze admixture on the compressive strength of concrete exposed to low temperatures', Cold Regions Science and Technology, 89, pp. 30-35.

Karahan, O. and Atiş, C.D. (2011) 'The durability properties of polypropylene fiber reinforced fly ash concrete', Materials & Design, 32(2), pp. 1044-1049.

Kawaguchi, T. and Decho, A.W. (2002) 'A laboratory investigation of cyanobacterial extracellular polymeric secretions (EPS) in influencing CaCO3 polymorphism', Journal of Crystal Growth, 240(1-2), pp. 230-235.

Khan, M. (2003) 'Isoresponses for strength, permeability and porosity of high performance mortar', Building and Environment, 38(8), pp. 1051-1056.

Kim, D., Ryu, H., Shin, S. and Park, W. (2016) 'Properties of calcium acetate manufactured with etching waste solution and limestone sludge as a cementitious high-early-strength admixture', Advances in Materials Science and Engineering, 2016.

Kim, G., Kim, J. and Youn, H. (2018) 'Effect of Temperature, pH, and Reaction Duration on Microbially Induced Calcite Precipitation', Applied Sciences, 8(8), pp. 1277.

Kittinaovarat, S., Kansomwan, P. and Jiratumnukul, N. (2010) 'Chitosan/modified montmorillonite beads and adsorption Reactive Red 120', Applied Clay Science, 48(1-2), pp. 87-91.

Kırca, Ö (2018) 'Ancient binding materials, mortars and concrete technology: history and durability aspects', Structural Analysis of Historical Constructions-2 Volume Set: Possibilities of Numerical and Experimental Techniques-Proceedings of the IVth Int. Seminar on Structural Analysis of Historical Constructions, 10-13 November 2004, Padova, Italy. CRC Press, 87.

Kjellsen, K.O. and Jennings, H.M. (1996) 'Observations of microcracking in cement paste upon drying and rewetting by environmental scanning electron microscopy', Advanced Cement Based Materials, 3(1), pp. 14-19.

Klement, Z., Rudolph, K. and Sands, D. (1990) Methods in phytobacteriology. Akademiai Kiado.

Kloprogge, J.T. and Frost, R.L. (1999) 'An infrared emission spectroscopic study of synthetic and natural pyrophyllite', Neues Jahrbuch fur Mineralogie, Monatshefte, 2, pp. 62-74.

Kloprogge, J.T., Ruan, H. and Frost, R.L. (2000) 'Near-infrared spectroscopic study of synthetic and natural pyrophyllite', Neues Jahrbuch fur Mineralogie, Monatshefte, 8, pp. 337-347.

Knoll, A.H. (2003) 'Biomineralization and evolutionary history', Reviews in mineralogy and geochemistry, 54(1), pp. 329-356.

Knorre, H.v. and Krumbein, W.E. (2000) 'Bacterial calcification', in Microbial sediments. Springer, pp. 25-31.

Kong, J.S., Ababneh, A.N., Frangopol, D.M. and Xi, Y. (2002) 'Reliability analysis of chloride penetration in saturated concrete', Probabilistic Engineering Mechanics, 17(3), pp. 305-315.

Koransky, J.R., Allen, S.D. and Dowell, V.R.,Jr (1978) 'Use of ethanol for selective isolation of sporeforming microorganisms', Applied and Environmental Microbiology, 35(4), pp. 762-765.

Korb, J. (2007) 'Microstructure and texture of cementitious porous materials', Magnetic resonance imaging, 25(4), pp. 466-469.

Krishnapriya, S. and Babu, D.V. (2015) 'Isolation and identification of bacteria to improve the strength of concrete', Microbiological research, 174, pp. 48-55.

Krumbein, W. and Giele, C. (1979) 'Calcification in a coccoid cyanobacterium associated with the formation of desert stromatolites', Sedimentology, 26(4), pp. 593-604.

Krumbein, W.E. (1979) 'Photolithotropic and chemoorganotrophic activity of bacteria and algae as related to beachrock formation and degradation (Gulf of Aqaba, Sinai)', Geomicrobiology Journal, 1(2), pp. 139-203.

Kuang, Y. and Ou, J. (2008) 'Passive smart self-repairing concrete beams by using shape memory alloy wires and fibers containing adhesives', Journal of Central South University of Technology, 15(3), pp. 411-417.

Kunal, K. and Killemsetty, N. (2014) 'Study on control of cracks in a Structure through Visual Identification & Inspection', Volume, 11, pp. 64-72.

Kureel, M., Geed, S., Giri, B., Rai, B. and Singh, R. (2017) 'Biodegradation and kinetic study of benzene in bioreactor packed with PUF and alginate beads and immobilized with Bacillus sp. M3', Bioresource technology, 242, pp. 92-100.

Laurienzo, P., Malinconico, M., Motta, A. and Vicinanza, A. (2005) 'Synthesis and characterization of a novel alginate–poly (ethylene glycol) graft copolymer', Carbohydrate Polymers, 62(3), pp. 274-282.

Leal, D., Matsuhiro, B., Rossi, M. and Caruso, F. (2008) 'FT-IR spectra of alginic acid block fractions in three species of brown seaweeds', Carbohydrate research, 343(2), pp. 308-316.

Lederberg, J. (1956) 'Bacterial Protoplasts Induced by Penicillin', Proceedings of the National Academy of Sciences of the United States of America, 42(9), pp. 574-577.

Lee, H., Wong, H. and Buenfeld, N. (2018) 'Effect of alkalinity and calcium concentration of pore solution on the swelling and ionic exchange of superabsorbent polymers in cement paste', Cement and Concrete Composites, 88, pp. 150-164.

Lee, H., Wong, H. and Buenfeld, N. (2016) 'Self-sealing of cracks in concrete using superabsorbent polymers', Cement and Concrete Research, 79, pp. 194-208.

Lee, H., Wong, H. and Buenfeld, N. (2010) 'Potential of superabsorbent polymer for self-sealing cracks in concrete', Advances in Applied Ceramics, 109(5), pp. 296-302.

Leszczyńska, A., Njuguna, J., Pielichowski, K. and Banerjee, J. (2007) 'Polymer/montmorillonite nanocomposites with improved thermal properties: Part I. Factors influencing thermal stability and mechanisms of thermal stability improvement', Thermochimica Acta, 453(2), pp. 75-96.

Levinson, S.A. and MacFate, R.P. (1969) Clinical laboratory diagnosis. Lea & Febiger.

Li, G., Zeng, J., Luo, J., Liu, M., Jiang, T. and Qiu, G. (2014) 'Thermal transformation of pyrophyllite and alkali dissolution behavior of silicon', Applied Clay Science, 99, pp. 282-288.

Li, V.C., Lim, Y.M. and Chan, Y. (1998) 'Feasibility study of a passive smart self-healing cementitious composite', Composites Part B: Engineering, 29(6), pp. 819-827.

Li, Y., Wang, R. and Zhao, Y. (2017) 'Effect of coupled deterioration by freeze-thaw cycle and carbonation on concrete produced with coarse recycled concrete aggregates', Journal of the Ceramic Society of Japan, 125(1), pp. 36-45.

Li, M., Gustchina, A., Glesner, J., Wunschmann, S., Vailes, L.D., Chapman, M.D., Pomes, A. and Wlodawer, A. (2011) 'Carbohydrates contribute to the interactions between cockroach allergen Bla g 2 and a monoclonal antibody', Journal of immunology (Baltimore, Md.: 1950), 186(1), pp. 333-340.

Lian, B., Hu, Q., Chen, J., Ji, J. and Teng, H.H. (2006) 'Carbonate biomineralization induced by soil bacterium Bacillus megaterium', Geochimica et Cosmochimica Acta, 70(22), pp. 5522-5535.

Liu, L., Wu, F., Ju, X., Xie, R., Wang, W., Niu, C.H. and Chu, L. (2013) 'Preparation of monodisperse calcium alginate microcapsules via internal gelation in microfluidic-generated double emulsions', Journal of colloid and interface science, 404, pp. 85-90.

López-García, P., Kazmierczak, J., Benzerara, K., Kempe, S., Guyot, F. and Moreira, D. (2005) 'Bacterial diversity and carbonate precipitation in the giant microbialites from the highly alkaline Lake Van, Turkey', Extremophiles, 9(4), pp. 263-274.

Lowenstein, H. and Weiner, S. (1989) 'On BiomineralizationOxford University Press', .

Luo, Q., Liu, D., Qiao, P., Feng, Q. and Sun, L. (2017) 'Microstructural damage characterization of concrete under freeze-thaw action', International Journal of Damage Mechanics, , pp. 1056789517736573.

Madejová, J. (2003) FTIR techniques in clay mineral studies.

Makul, N. and Sua-iam, G. (2018) 'Effect of granular urea on the properties of self-consolidating concrete incorporating untreated rice husk ash: Flowability, compressive strength and temperature rise', Construction and Building Materials, 162, pp. 489-502.

Mangat, P. and Limbachiya, M. (1995) 'Repair material properties which influence long-term performance of concrete structures', Construction and Building Materials, 9(2), pp. 81-90.

Marusin, S.L. (1995) 'Sample preparation—the key to SEM studies of failed concrete', Cement and Concrete Composites, 17(4), pp. 311-318.

Maruyama, I. and Sasano, H. (2014) 'Strain and crack distribution in concrete during drying', Materials and Structures, 47(3), pp. 517-532.

McClure, W.F. and Stanfield, D.L. (2002) 'Near□Infrared Spectroscopy of Biomaterials', Handbook of vibrational spectroscopy, .

McConnaughey, T. and Whelan, J. (1997) 'Calcification generates protons for nutrient and bicarbonate uptake', Earth-Science Reviews, 42(1-2), pp. 95-117.

Mehta, P.K. and Monteiro, P.J. (2017) 'CONCRETE Microstructure, Properties and Materials', .

Meiron, O.E., Bar□David, E., Aflalo, E.D., Shechter, A., Stepensky, D., Berman, A. and Sagi, A. (2011) 'Solubility and bioavailability of stabilized amorphous calcium carbonate', Journal of Bone and Mineral Research, 26(2), pp. 364-372.

Melnyczuk, J.M. and Palchoudhury, S. (2018) 'Introduction to Bio-Inspired Hydrogel and Their Application: Hydrogels', in Biomedical Engineering: Concepts, Methodologies, Tools, and Applications. IGI Global, pp. 1255-1281.

Meurens, M. and Yan, S.H. (2002) 'Applications of vibrational spectroscopy in brewing', Handbook of Vibrational Spectroscopy, .

Micaelo, R., Al-Mansoori, T. and Garcia, A. (2016) 'Study of the mechanical properties and self-healing ability of asphalt mixture containing calcium-alginate capsules', Construction and Building Materials, 123, pp. 734-744.

Mihashi, H., KANEKO, Y., Nishiwaki, T. and Otsuka, K. (2001) 'Fundamental study on development of intelligent concrete characterized by self-healing capability for strength', Transactions of the Japan Concrete Institute, 22, pp. 441-450.

Mitchell, A.C. and Ferris, F.G. (2005) 'The coprecipitation of Sr into calcite precipitates induced by bacterial ureolysis in artificial groundwater: temperature and kinetic dependence', Geochimica et Cosmochimica Acta, 69(17), pp. 4199-4210.

Mobley, H.L. and Hausinger, R.P. (1989) 'Microbial ureases: significance, regulation, and molecular characterization', Microbiological reviews, 53(1), pp. 85-108.

Mohr, P., Hansen, W., Jensen, E. and Pane, I. (2000) 'Transport properties of concrete pavements with excellent long-term in-service performance', Cement and Concrete Research, 30(12), pp. 1903-1910.

Mondal, S. and Ghosh, A.D. (2018) 'Investigation into the optimal bacterial concentration for compressive strength enhancement of microbial concrete', Construction and Building Materials, 183, pp. 202-214.

Montgomerie, J.Z., Kalmanson, G.M. and Guze, L.B. (1966) 'The use of the catalase test to detect significant bacteriuria', The American Journal of the Medical Sciences, 251(2), pp. 184-187.

Morita, R.Y. (1980) 'Calcite precipitation by marine bacteria', Geomicrobiology Journal, 2(1), pp. 63-82.

Mwaluwinga, S., Ayano, T. and Sakata, K. (1997) 'Influence of urea in concrete', Cement and Concrete Research, 27(5), pp. 733-745.

Nadeem, U. and Datta, M.D. (2014) 'ADSORPTION STUDIES OF ZINC (II) IONS ON BIOPOLYMER COMPOSITE BEADS OF ALGINATE-FLY ASH', European Chemical Bulletin, 3(7), pp. 682-691.

Neves, R., Branco, F. and De Brito, J. (2013) 'Field assessment of the relationship between natural and accelerated concrete carbonation resistance', Cement and Concrete Composites, 41, pp. 9-15.

Ng, W., Lee, M. and Hii, S. (2012) 'An overview of the factors affecting microbial-induced calcite precipitation and its potential application in soil improvement', World Academy of Science, Engineering and Technology, 62, pp. 723-729.

Nikolić, S., Mojović, L., Pejin, D., Rakin, M. and Vukašinović, M. (2010) 'Production of bioethanol from corn meal hydrolyzates by free and immobilized cells of Saccharomyces cerevisiae var. ellipsoideus', Biomass and Bioenergy, 34(10), pp. 1449-1456.

Nishiwaki, T., Koda, M., Yamada, M., Mihashi, H. and Kikuta, T. (2012) 'Experimental study on self-healing capability of FRCC using different types of synthetic fibers', Journal of Advanced Concrete Technology, 10(6), pp. 195-206.

Nonakaran, S.H., Pazhouhandeh, M., Keyvani, A., Abdollahipour, F.Z. and Shirzad, A. (2015) 'Isolation and identification of Pseudomonas azotoformans for induced calcite precipitation', World Journal of Microbiology and Biotechnology, 31(12), pp. 1993-2001.

Novitsky, J.A. (1981) 'Calcium carbonate precipitation by marine bacteria', Geomicrobiology Journal, 2(4), pp. 375-388.

Ohadi, M., Amir-Heidari, B., Moshafi, M.H., Mirparizi, A., Basir, M. and Dehghan-Noudeh, G. (2014) 'Encapsulation of Biosurfactant-Producing Bacillus licheniformis (PTCC 1320) in Alginate Beads', Biotechnology, 13(5), pp. 239.

Okwadha, G.D. and Li, J. (2010) 'Optimum conditions for microbial carbonate precipitation', Chemosphere, 81(9), pp. 1143-1148.

Østnor, T. and Justnes, H. (2011) 'Anodic corrosion inhibitors against chloride induced corrosion of concrete rebars', Advances in applied ceramics, 110(3), pp. 131-136.

Pacheco-Torgal, F. and Labrincha, J.A. (2013) 'Biotech cementitious materials: Some aspects of an innovative approach for concrete with enhanced durability', Construction and Building Materials, 40, pp. 1136-1141.

Pade, C. and Guimaraes, M. (2007) 'The CO2 uptake of concrete in a 100 year perspective', Cement and Concrete Research, 37(9), pp. 1348-1356.

Paine, K. (2016) 'Bacteria-based self-healing concrete: Effects of environment, exposure and crack size', .

Palin, D., Wiktor, V. and Jonkers, H. (2015) 'Bacteria-based agent for self-healing marine concrete', Proc. 5th Int. Conf. on Self-Healing Materials (Durham, USA). , 2-6.

Papadakis, V.G., Vayenas, C.G. and Fardis, M.N. (1991) 'Physical and chemical characteristics affecting the durability of concrete', Materials Journal, 88(2), pp. 186-196.

Pareek, S. and Oohira, A. (2011) 'A fundamental study on regain of flexural strength of mortars by using a self-repair network system', Proceedings of the 3rd International Conference on Self Healing Materials, Bath, UK.

Parikh, A. and Madamwar, D. (2006) 'Partial characterization of extracellular polysaccharides from cyanobacteria', Bioresource technology, 97(15), pp. 1822-1827.

Park, J. and Chang, H. (2000) 'Microencapsulation of microbial cells', Biotechnology Advances, 18(4), pp. 303-319.

Park, S. (2010) 'Calcite-forming bacteria for compressive strength improvement in mortar', Research and reviews: journal of microbiology and biotechnology, 20(4), pp. 782; 782-788; 788.

Park, S.J., Park, J.M., Kim, W.J. and Ghim, S.Y. (2012) 'Application of Bacillus subtilis 168 as a multifunctional agent for improvement of the durability of cement mortar', Journal of microbiology and biotechnology, 22(11), pp. 1568-1574.

Patil, K.R., Waghere, B., Salve, R., Ahire, B., Patel, K., Bhoir, P. and Thakare, A. 'Effect of bacteria calcite precipitation on compressive strength of general concrete cubes', .

Peckmann, J., Paul, J. and Thiel, V. (1999) 'Bacterially mediated formation of diagenetic aragonite and native sulfur in Zechstein carbonates (Upper Permian, Central Germany)', Sedimentary Geology, 126(1-4), pp. 205-222.

Pelletier, M., Brown, R., Shukla, A. and Bose, A. 'Self-Healing Concrete with a Microencapsulated Healing Agent, 2011', Kingston, USA, .

Pigeon, M. (1994) 'Frost resistance, a critical look', Special Publication, 144, pp. 141-158.

Poon, C., Wong, Y. and Lam, L. (1997) 'The influence of different curing conditions onthe pore structure and related properties of fly-ash cement pastes and mortars', Construction and Building Materials, 11(7), pp. 383-393.

Portland Cement Association (2001) Ettringite formation and the performance of concrete. Portland Cement Association.

Powers, T.C. and Helmuth, R. (1953) 'Theory of volume changes in hardened portland-cement paste during freezing', Highway research board proceedings.

Powers, T.C. (1955) 'Basic considerations pertaining to freezing-and-thawing tests', ASTM Proceedings.

Qian, S., Zhou, J. and Schlangen, E. (2010) 'Influence of curing condition and precracking time on the self-healing behavior of engineered cementitious composites', Cement and concrete composites, 32(9), pp. 686-693.

Rahim, S.N.A., Sulaiman, A., Hamzah, F., Hamid, K.H.K., Rodhi, M.N.M., Musa, M. and Edama, N.A. (2013) 'Enzymes encapsulation within calcium alginate-clay beads: Characterization and application for cassava slurry saccharification', Procedia Engineering, 68, pp. 411-417.

Ramachandran, S.K., Ramakrishnan, V. and Bang, S.S. (2001) 'Remediation of concrete using micro-organisms', ACI Materials Journal-American Concrete Institute, 98(1), pp. 3-9.

Ramakrishnan, V., Bang, S. and Deo, K. (1998) 'A novel technique for repairing cracks in high performance concrete using bacteria', Proc. of the Int. Conf. on HPHSC. , 597-618.

Ramakrishnan, V., Panchalan, R.K., Bang, S.S. and City, R. (2005) 'Improvement of concrete durability by bacterial mineral precipitation', Proceedings of 11th International Conference on Fracture. , 20-25.

Ramakrishnan, V., Ramesh, K. and Bang, S. (2001) 'Bacterial concrete', Smart Materials. International Society for Optics and Photonics, 168-177.

Rao, M., Reddy, V.S., Hafsa, M., Veena, P. and Anusha, P. (2013) 'Bioengineered concrete-a sustainable self-healing construction material', Research journal of engineering sciences ISSN, 2278, pp. 9472.

Reddy, T.C.S. and Ravitheja, A. (2018) 'Macro mechanical properties of self healing concrete with crystalline admixture under different environments', Ain Shams Engineering Journal, .

Reinhardt, H. and Jooss, M. (2003) 'Permeability and self-healing of cracked concrete as a function of temperature and crack width', Cement and Concrete Research, 33(7), pp. 981-985.

Rendevski, S.J. and Andonovski, A.N. (2005) 'Reaggregation of sodium alginate microgel structures after shear-induced deaggregation at filtering', Polymer Bulletin, 54(1-2), pp. 93-100.

Rivadeneyra, M., Delgado, R., Delgado, G., Moral, A.D., Ferrer, M. and Ramos Cormenzana, A. (1993) 'Precipitation of carbonates by Bacillus sp. isolated from saline soils', Geomicrobiology Journal, 11(3-4), pp. 175-184.

Rivadeneyra, M.A., Delgado, R., del Moral, A., Ferrer, M.R. and Ramos-Cormenzana, A. (1994) 'Precipatation of calcium carbonate by Vibrio spp. from an inland saltern', FEMS microbiology ecology, 13(3), pp. 197-204.

Rivadeneyra, M.A., Párraga, J., Delgado, R., Ramos-Cormenzana, A. and Delgado, G. (2004) 'Biomineralization of carbonates by Halobacillus trueperi in solid and liquid media with different salinities', FEMS microbiology ecology, 48(1), pp. 39-46.

Robertson, R. (1973) 'Industrial uses of clay minerals', Silic.Ind, 38, pp. 33-43.

Rodriguez-Navarro, C., Rodriguez-Gallego, M., Ben Chekroun, K. and Gonzalez-Munoz, M.T. (2003) 'Conservation of ornamental stone by Myxococcus xanthus-induced carbonate biomineralization', Applied and Environmental Microbiology, 69(4), pp. 2182-2193.

Roger, S., Talbot, D. and Bee, A. (2006) 'Preparation and effect of Ca2 on water solubility, particle release and swelling properties of magnetic alginate films', Journal of Magnetism and Magnetic Materials, 305(1), pp. 221-227.

Sagripanti, J.L. and Bonifacino, A. (1996) 'Comparative sporicidal effects of liquid chemical agents', Applied and Environmental Microbiology, 62(2), pp. 545-551.

Sánchez-Soto, P.J., Justo, A., Pérez-Rodríguez, J.L. and Morillo, E. (1994) 'Structural alteration of pyrophyllite by dry grinding as studied by IR spectroscopy', Journal of Materials Science Letters, 13(12), pp. 915-918.

Sangadji, S. and Schlangen, E. (2012) 'Self Healing of Concrete Structures-Novel approach using porous network concrete', Journal of Advanced Concrete Technology, 10(5), pp. 185-194.

Sangadji, S. and Schlangen, E. (2011) 'Porous network concrete: A new approach to make concrete structures self-healing using prefabricated porous layer', Third international conference self-healing materials, Bath, United Kingdom. Citeseer, 291-292.

Santhosh, K., Ramakrishnan, V., Duke, E. and Bang, S. (2000) 'SEM Investigation of Microbial Calcite Precipitation in Cement', PROCEEDINGS OF THE INTERNATIONAL CONFERENCE ON CEMENT MICROSCOPY. INTERNATIONAL CEMENT MICROSCOPY ASSOCIATION, 293-305.

Sarda, D., Choonia, H.S., Sarode, D. and Lele, S. (2009) 'Biocalcification by Bacillus pasteurii urease: a novel application', Journal of industrial microbiology & biotechnology, 36(8), pp. 1111-1115.

Sarkar, M., Chowdhury, T., Chattopadhyay, B., Gachhui, R. and Mandal, S. (2014) 'Autonomous bioremediation of a microbial protein (bioremediase) in Pozzolana cementitious composite', Journal of Materials Science, 49(13), pp. 4461-4468.

Scherer, G.W. (1999) 'Crystallization in pores', Cement and Concrete Research, 29(8), pp. 1347-1358.

Schlangen, H., Jonkers, H., Qian, S. and Garcia, A. (2010) 'Recent advances on self healing of concrete', FraMCos-7: Proceedings of the 7th International Conference on Fracture Mechanics of Concrete and Concrete Structures, Jeju Island, Korea, 23-28 May 2010.

Schlegel, H.G. and Zaborosch, C. (1993) General microbiology. Cambridge university press.

Schwantes-Cezario, N., Peres, Maria Vânia Nogueira do Nascimento, Fruet, T.K., Nogueira, G.S.F., Toralles, B.M. and Cezario, D.D.S. (2018) 'Crack filling in concrete by addition of Bacillus subtilis spores-Preliminary study', Dyna, 85(205), pp. 132-139.

Segale, L., Giovannelli, L., Mannina, P. and Pattarino, F. (2016) 'Calcium alginate and calcium alginate-chitosan beads containing celecoxib solubilized in a self-emulsifying phase', Scientifica, 2016.

Seltmann, G. and Holst, O. (2013) The bacterial cell wall. Springer Science & Business Media.

Setina, J., Gabrene, A. and Juhnevica, I. (2013) 'Effect of pozzolanic additives on structure and chemical durability of concrete', Procedia Engineering, 57, pp. 1005-1012.

Setlow, P. (1994) 'Mechanisms which contribute to the long□term survival of spores of Bacillus species', Journal of applied microbiology, 76(S23).

Shang, H. (2013) 'Triaxial T–C–C behavior of air-entrained concrete after freeze–thaw cycles', Cold Regions Science and Technology, 89, pp. 1-6.

Shang, H.S. and Yi, T.H. (2013) 'Freeze-thaw durability of air-entrained concrete', TheScientificWorldJournal, 2013, pp. 650791.

Sharma, T., Alazhari, M., Heath, A., Paine, K. and Cooper, R. (2017) 'Alkaliphilic Bacillus species show potential application in concrete crack repair by virtue of rapid spore production and germination then extracellular calcite formation', Journal of applied microbiology, 122(5), pp. 1233-1244.

Shen, Y., Buick, R. and Canfield, D.E. (2001) 'Isotopic evidence for microbial sulphate reduction in the early Archaean era', Nature, 410(6824), pp. 77-81.

Shilpa, A., Agrawal, S. and Ray, A.R. (2003) 'Controlled delivery of drugs from alginate matrix', Journal of Macromolecular Science, Part C: Polymer Reviews, 43(2), pp. 187-221.

Siddique, R. and Chahal, N.K. (2011) 'Effect of ureolytic bacteria on concrete properties', Construction and Building Materials, 25(10), pp. 3791-3801.

Siline, M., Ghorbel, E. and Bibi, M. (2017) 'Effect of freeze–Thaw cycles on the physicomechanical properties of a pozzolanic mortar', Construction and Building Materials, 134, pp. 32-38.

Singh, B., Sharma, D., Kumar, R. and Gupta, A. (2009) 'Controlled release of the fungicide thiram from starch–alginate–clay based formulation', Applied Clay Science, 45(1-2), pp. 76-82.

Sisomphon, K. and Copuroglu, O. (2011) 'Self healing mortars by using different cementitious materials', Proceedings of International Conference on advances in construction materials through science and engineering, Hong Kong, China.

Sisomphon, K., Copuroglu, O. and Koenders, E.A.B. (2013) 'Effect of exposure conditions on self healing behavior of strain hardening cementitious composites incorporating various cementitious materials', Construction and Building Materials, 42, pp. 217-224.

Sloan, W., Quince, C. and Curtis, T. (2008) 'The uncountables. Pg 35− 54. Chapter 3 in Accessing Uncultivated Microorganisms, from the Environment to Organisms and Genomes and Back. K. Zengler ed', .

Sneath, P.H., Mair, N.S., Sharpe, M.E. and Holt, J.G. (1986) Bergey's manual of systematic bacteriology. Volume 2. Williams & Wilkins.

Snoeck, D. and De Belie, N. (2016) 'Effect of sample age on the self-healing properties of cementitious mateials with superabsorbent polymers', Fourth International Conference on Sustainable Construction Materials and Technologies (SCMT4). , 1324-1333.

Snoeck, D. and De Belie, N. (2012) 'Mechanical and self-healing properties of cementitious composites reinforced with flax and cottonised flax, and compared with polyvinyl alcohol fibres', biosystems engineering, 111(4), pp. 325-335.

Snoeck, D., Steuperaert, S., Van Tittelboom, K., Dubruel, P. and De Belie, N. (2012) 'Visualization of water penetration in cementitious materials with superabsorbent polymers by means of neutron radiography', Cement and Concrete Research, 42(8), pp. 1113-1121.

Snoeck, D., Van Tittelboom, K., Steuperaert, S., Dubruel, P. and De Belie, N. (2014) 'Self-healing cementitious materials by the combination of microfibres and superabsorbent polymers', Journal of Intelligent Material Systems and Structures, 25(1), pp. 13-24.

Stark, J. and Bollmann, K. (2000) 'Delayed ettringite formation in concrete', NORDIC CONCRETE RESEARCH-PUBLICATIONS-, 23, pp. 4-28.

Stocks-Fischer, S., Galinat, J.K. and Bang, S.S. (1999) 'Microbiological precipitation of CaCO3', Soil Biology and Biochemistry, 31(11), pp. 1563-1571.

Stuart, C.A., Van Stratum, E. and Rustigian, R. (1945) 'Further Studies on Urease Production by Proteus and Related Organisms', Journal of Bacteriology, 49(5), pp. 437-444.

Su, Y., Qi, Y. and Cai, L. (2012) 'Induction of sporulation in plant pathogenic fungi', Mycology, 3(3), pp. 195-200.

Sukhotskaya, S., Mazhorova, V. and Terekhin, Y.N. (1983) 'Effect of autogenous healing of concrete subjected to periodic freeze-thaw cycles', Power Technology and Engineering (formerly Hydrotechnical Construction), 17(6), pp. 294-296.

Sumbali, G. and Mehrotra, R. (2009) Principles of microbiology. Tata McGraw-Hill New Delhi, India.

Sun, W., Mu, R., Luo, X. and Miao, C. (2002) 'Effect of chloride salt, freeze–thaw cycling and externally applied load on the performance of the concrete', Cement and Concrete Research, 32(12), pp. 1859-1864.

Tal, Y., Van Rijn, J. and Nussinovitch, A. (1997) 'Improvement of Structural and Mechanical Properties of Denitrifying Alginate Beads by Freeze□Drying', Biotechnology progress, 13(6), pp. 788-793.

Tanaka, K. and Kurumisawa, K. (2002) 'Development of technique for observing pores in hardened cement paste', Cement and Concrete Research, 32(9), pp. 1435-1441.

Taylor, W.I. and Achanzar, D. (1972) 'Catalase test as an aid to the identification of Enterobacteriaceae', Applied Microbiology, 24(1), pp. 58-61.

Teall, O. (2016) Crack closure and enhanced autogenous healing of structural concrete using shape memory polymers, .

Ter Heide, N. (2005) 'Crack healing in hydrating concrete', Delft University of Technology, Delft, .

ter Heide, N. and Schlangen, E. (2007) 'Self-healing of early age cracks in concrete', Proceedings of 1st International Conference on Self Healing Materials, Noordwijk aan Zee, The Netherlands. , 18-20.

Termkhajornkit, P., Nawa, T., Yamashiro, Y. and Saito, T. (2009) 'Self-healing ability of fly ash–cement systems', Cement and Concrete composites, 31(3), pp. 195-203.

Thomas, M. and Ramlochan, T. (2004) 'Field cases of delayed ettringite formation', International RILEM Workshop on Internal Sulfate Attack and Delayed Ettringite Formation. RILEM Publications SARL, 85-97.

Thomas, P., Sekhar, A.C., Upreti, R., Mujawar, M.M. and Pasha, S.S. (2015) 'Optimization of single plate-serial dilution spotting (SP-SDS) with sample anchoring as an assured method for bacterial and yeast cfu enumeration and single colony isolation from diverse samples', Biotechnology Reports, 8, pp. 45-55.

Thompson, J. and Ferris, F. (1990) 'Cyanobacterial precipitation of gypsum, calcite, and magnesite from natural alkaline lake water', Geology, 18(10), pp. 995-998.

Todak, H.N., Tsui, M., Ley, M.T. and Weiss, W.J. (2017) 'Evaluating freeze-thaw damage in concrete with acoustic emissions and ultrasonics', in Advances in Acoustic Emission Technology. Springer, pp. 175-189.

Toohey, K.S., Sottos, N.R., Lewis, J.A., Moore, J.S. and White, S.R. (2007) 'Self-healing materials with microvascular networks', Nature materials, 6(8), pp. 581.

Toth, E.M., Borsodi, A.K., Felföldi, T., Vajna, B., Sipos, R., Romsics, C., Makk, J., Jáger, K., Palatinszky, M. and Ács, É (2013) 'Practical microbiology', Microbiological Laboratoriumi Gyakorlatok, .

Truong, P., Kishi, T. and Kayondo, M. (2013) 'Crack self-healing effect on performance of reinforced concrete members subjected to water supply and cyclic loading', .

Tziviloglou, E., Wiktor, V., Jonkers, H. and Schlangen, E. (2016a) 'Bacteria-based self-healing concrete to increase liquid tightness of cracks', Construction and Building Materials, 122, pp. 118-125.

Tziviloglou, E., Van Tittelboom, K., Palin, D., Wang, J., Sierra-Beltrán, M.G., Erşan, Y.Ç, Mors, R., Wiktor, V., Jonkers, H.M. and Schlangen, E. (2016b) 'Bio-based self-healing concrete: from research to field application', in Self-healing Materials. Springer, pp. 345-385.

Urzi, C., Garcia-Valles, M., Vendrell, M. and Pernice, A. (1999) 'Biomineralization processes on rock and monument surfaces observed in field and in laboratory conditions', Geomicrobiology Journal, 16(1), pp. 39-54.

Van Balen, K. (2005) 'Carbonation reaction of lime, kinetics at ambient temperature', Cement and Concrete Research, 35(4), pp. 647-657.

Van Breugel, K. (2007) 'Is there a market for self-healing cement-based materials', Proceedings of the First International Conference on Self-Healing Materials, Noordwijk, The Netherlands. , 18-20.

Van Paassen, L.A. (2009) Biogrout, ground improvement by microbial induced carbonate precipitation, .

Van Tittelboom, K. and De Belie, N. (2010) 'Self-healing concrete: suitability of different healing agents', International Journal of 3R's, 1(1), pp. 12-21.

Van Tittelboom, K., Adesanya, K., Dubruel, P., Van Puyvelde, P. and De Belie, N. (2011a) 'Methyl methacrylate as a healing agent for self-healing cementitious materials', Smart Materials and Structures, 20(12), pp. 125016.

Van Tittelboom, K. and De Belie, N. (2013) 'Self-healing in cementitious materials—A review', Materials, 6(6), pp. 2182-2217.

Van Tittelboom, K., De Belie, N., De Muynck, W. and Verstraete, W. (2010) 'Use of bacteria to repair cracks in concrete', Cement and Concrete Research, 40(1), pp. 157-166.

Van Tittelboom, K., De Belie, N., Van Loo, D. and Jacobs, P. (2011b) 'Self-healing efficiency of cementitious materials containing tubular capsules filled with healing agent', Cement and Concrete Composites, 33(4), pp. 497-505.

Van Tittelboom, K., De Belie, N., Zhang, P. and Wittmann, F. (2011c) 'Self-healing of cracks in concrete', International workshop (ASMES) 2011: basic research on concrete and applications. , 303-314.

Van Tittelboom, K., Gruyaert, E., Rahier, H. and De Belie, N. (2012) 'Influence of mix composition on the extent of autogenous crack healing by continued hydration or calcium carbonate formation', Construction and Building Materials, 37, pp. 349-359.

Verma, R.K., Chaurasia, L., Bisht, V. and Thakur, M. (2015) 'Biomineralization and bacterial carbonate precipitation in mortar and concrete', Biosci Bioeng, 1, pp. 5-11.

Verma, S.K., Bhadauria, S.S. and Akhtar, S. (2015) 'Determination of carbonation depth through In-situ testing of concrete structures', Revista Româna de Materiale-Romanian Journal of Materials, 45(3), pp. 226-231.

Virta, R.L. (2005) 'Talc and pyrophyllite', Am.Ceram.Soc.Bull, 84(8), pp. 25-26.

Wang, J., Jonkers, H.M., Boon, N. and De Belie, N. (2017) 'Bacillus sphaericus LMG 22257 is physiologically suitable for self-healing concrete', Applied Microbiology and Biotechnology, 101(12), pp. 5101-5114.

Wang, J., Mignon, A., Snoeck, D., Wiktor, V., Van Vliergerghe, S., Boon, N. and De Belie, N. (2015) 'Application of modified-alginate encapsulated carbonate producing bacteria in concrete: a promising strategy for crack self-healing', Frontiers in microbiology, 6, pp. 1088.

Wang, J., Van Tittelboom, K., De Belie, N. and Verstraete, W. (2012) 'Use of silica gel or polyurethane immobilized bacteria for self-healing concrete', Construction and Building Materials, 26(1), pp. 532-540.

Wang, J., De Belie, N. and Verstraete, W. (2012) 'Diatomaceous earth as a protective vehicle for bacteria applied for self-healing concrete', Journal of industrial microbiology & biotechnology, 39(4), pp. 567-577.

Wang, J., Snoeck, D., Van Vlierberghe, S., Verstraete, W. and De Belie, N. (2014a) 'Application of hydrogel encapsulated carbonate precipitating bacteria for approaching a realistic self-healing in concrete', Construction and Building Materials, 68, pp. 110-119.

Wang, J., Soens, H., Verstraete, W. and De Belie, N. (2014b) 'Self-healing concrete by use of microencapsulated bacterial spores', Cement and Concrete Research, 56, pp. 139-152.

Wang, J., Dewanckele, J., Cnudde, V., Van Vlierberghe, S., Verstraete, W. and De Belie, N. (2014c) 'X-ray computed tomography proof of bacterial-based self-healing in concrete', Cement & Concrete Composites, 53, pp. 289-304.

Wang, J., Soens, H., Verstraete, W. and De Belie, N. (2014g) 'Self-healing concrete by use of microencapsulated bacterial spores', Cement and Concrete Research, 56, pp. 139-152.

Wang, X., Xing, F., Zhang, M., Han, N. and Qian, Z. (2013) 'Experimental study on cementitious composites embedded with organic microcapsules', Materials, 6(9), pp. 4064-4081.

Warth, A.D. (1978) 'Relationship between the heat resistance of spores and the optimum and maximum growth temperatures of Bacillus species', Journal of Bacteriology, 134(3), pp. 699-705.

Warthmann, R., Van Lith, Y., Vasconcelos, C., McKenzie, J.A. and Karpoff, A.M. (2000) 'Bacterially induced dolomite precipitation in anoxic culture experiments', Geology, 28(12), pp. 1091-1094.

WEIBULL, C. (1953) 'The isolation of protoplasts from Bacillus megaterium by controlled treatment with lysozyme', Journal of Bacteriology, 66(6), pp. 688-695.

Weidel, W. and Pelzer, H. (1964) 'Bagshaped macromolecules—a new outlook on bacterial cell walls', Advances in Enzymology and Related Areas of Molecular Biology, , pp. 193-232.

Whiffin, V.S. (2004a) Microbial $CaCO_3$ precipitation for the production of biocement, .

White, S.R., Sottos, N.R., Geubelle, P.H., Moore, J.S., Kessler, M., Sriram, S., Brown, E. and Viswanathan, S. (2001) 'Autonomic healing of polymer composites', Nature, 409(6822), pp. 794.

Wiktor, V. and Jonkers, H.M. (2011a) 'Quantification of crack-healing in novel bacteria-based self-healing concrete', Cement and Concrete Composites, 33(7), pp. 763-770.

Witter, L. (1996) 'Immobilized microbial cells', Physical chemistry of food processes, 2, pp. 475-486.

Wong, L.S. (2015) 'Microbial cementation of ureolytic bacteria from the genus Bacillus: A review of the bacterial application on cement-based materials for cleaner production', Journal of Cleaner Production, .

Wu, Z., Wong, H. and Buenfeld, N. (2015) 'Influence of drying-induced microcracking and related size effects on mass transport properties of concrete', Cement and Concrete Research, 68, pp. 35-48.

Wu, M., Johannesson, B. and Geiker, M. (2012) 'A review: Self-healing in cementitious materials and engineered cementitious composite as a self-healing material', Construction and Building Materials, 28(1), pp. 571-583.

Xing, F., Ni, Z., Han, N., Dong, B., Du, X., Huang, Z. and Zhang, M. (2008) 'Self-healing mechanism of a novel cementitious composite using microcapsules', Proceedings of the International Conference on Durability of Concrete Structures, Hangzhou, China.

Xu, J., Du, Y., Jiang, Z. and She, A. (2015) 'Effects of calcium source on biochemical properties of microbial CaCO3 precipitation', Frontiers in microbiology, 6, pp. 1366.

Xu, S., Tabaković, A., Liu, X. and Schlangen, E. (2018) 'Calcium alginate capsules encapsulating rejuvenator as healing system for asphalt mastic', Construction and Building Materials, 169, pp. 379-387.

Yang, Y., Lepech, M.D., Yang, E. and Li, V.C. (2009) 'Autogenous healing of engineered cementitious composites under wet–dry cycles', Cement and Concrete Research, 39(5), pp. 382-390.

Yang, Y., Yang, E. and Li, V.C. (2011) 'Autogenous healing of engineered cementitious composites at early age', Cement and Concrete Research, 41(2), pp. 176-183.

Yang, Z., Hollar, J., He, X. and Shi, X. (2011) 'A self-healing cementitious composite using oil core/silica gel shell microcapsules', Cement and Concrete Composites, 33(4), pp. 506-512.

Yang, Z., Hollar, J., He, X. and Shi, X. (2010) 'Laboratory assessment of a self-healing cementitious composite', Transportation Research Record, 2142(1), pp. 9-17.

Yeung, T.W., Üçok, E.F., Tiani, K.A., McClements, D.J. and Sela, D.A. (2016) 'Microencapsulation in alginate and chitosan microgels to enhance viability of Bifidobacterium longum for oral delivery', Frontiers in microbiology, 7, pp. 494.

Young, C.C., Rekha, P.D., Lai, W.A. and Arun, A.B. (2006) 'Encapsulation of plant growth-promoting bacteria in alginate beads enriched with humic acid', Biotechnology and bioengineering, 95(1), pp. 76-83.

Yuan, Y.C., Rong, M.Z., Zhang, M.Q., Chen, J., Yang, G.C. and Li, X.M. (2008) 'Self-healing polymeric materials using epoxy/mercaptan as the healant', Macromolecules, 41(14), pp. 5197-5202.

Yun, Y. and Wu, Y. (2011) 'Durability of CFRP–concrete joints under freeze–thaw cycling', Cold Regions Science and Technology, 65(3), pp. 401-412.

Zhang, J., Wang, Q., Xie, X., Li, X. and Wang, A. (2010) 'Preparation and swelling properties of pH□sensitive sodium alginate/layered double hydroxides hybrid beads for controlled release of diclofenac sodium', Journal of Biomedical Materials Research Part B: Applied Biomaterials, 92(1), pp. 205-214.

Zhang, L., Liu, Q., Li, H., Norambuena-Contreras, J., Wu, S., Bao, S. and Shu, B. (2019) 'Synthesis and characterization of multi-cavity Ca-alginate capsules used for self-healing in asphalt mixtures', Construction and Building Materials, 211, pp. 298-307.

Zhang, Y., Guo, H. and Cheng, X. (2015) 'Role of calcium sources in the strength and microstructure of microbial mortar', Construction and Building Materials, 77, pp. 160-167.

Zhang, Y., Guo, H. and Cheng, X. (2014) 'Influences of calcium sources on microbially induced carbonate precipitation in porous media', Materials Research Innovations, 18(sup2), pp. S2-79-S2-84.

Zhao, Y., Wang, L., Lei, Z., Han, X. and Shi, J. (2018) 'Study on bending damage and failure of basalt fiber reinforced concrete under freeze-thaw cycles', Construction and Building Materials, 163, pp. 460-470.

Zhong, L. and Islam, M. (1995) 'A new microbial plugging process and its impact on fracture remediation', SPE Annual Technical Conference and Exhibition. Society of Petroleum Engineers.

Zhu, C., Niu, J., Li, J., Wan, C. and Peng, J. (2017) 'Effect of aggregate saturation degree on the freeze–thaw resistance of high performance polypropylene fiber lightweight aggregate concrete', Construction and Building Materials, 145, pp. 367-375.

Zhu, F., Ma, Z. and Zhao, T. (2016) 'Influence of freeze-thaw damage on the steel corrosion and bond-slip behavior in the reinforced concrete', Advances in Materials Science and Engineering, 2016.

Živica, V. (1997) 'Relationship between pore structure and permeability of hardened cement mortars: on the choice of effective pore structure parameter', Cement and Concrete Research, 27(8), pp. 1225-1235.

Zohar□Perez, C., Ritte, E., Chernin, L., Chet, I. and Nussinovitch, A. (2002) 'Preservation of Chitinolytic Pantoae agglomerans in a Viable Form by Cellular Dried Alginate□Based Carriers', Biotechnology progress, 18(6), pp. 1133-1140.

Zohar-Perez, C., Chet, I. and Nussinovitch, A. (2004) 'Irregular textural features of dried alginate–filler beads', Food Hydrocolloids, 18(2), pp. 249-258.

Appendix A Prediction of compressive strength under outdoor exposure

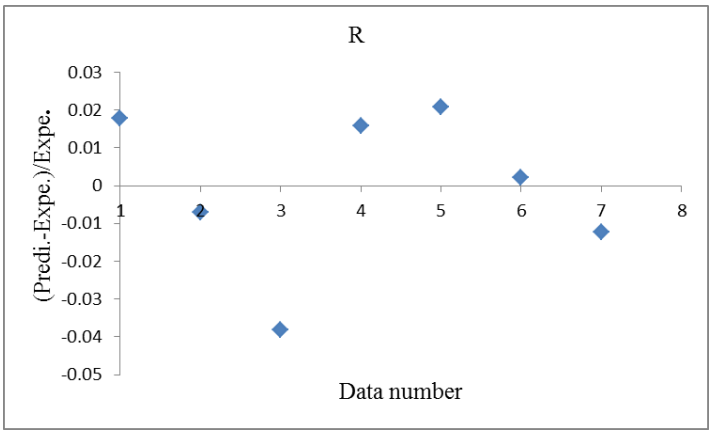

(a)

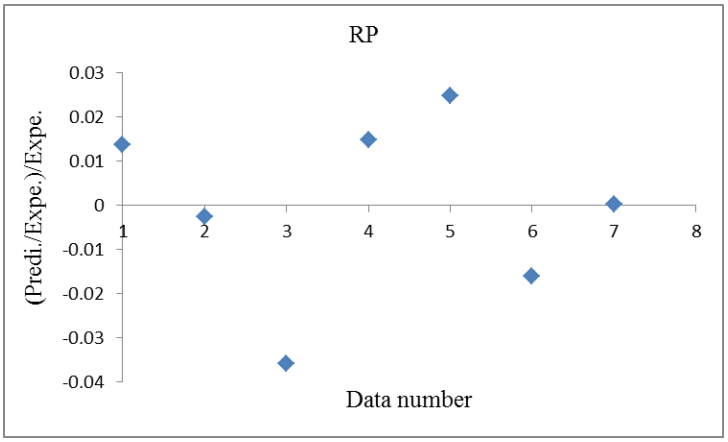

(b)


SP57
(Predi./Expe.)/Expe.
0.06
0.05
0.04
0.03
0.02
0.01
0
-0.01
-0.02
-0.03
-0.04
-0.05
1
2
3
4
5
6
7
8
Data number

(c)

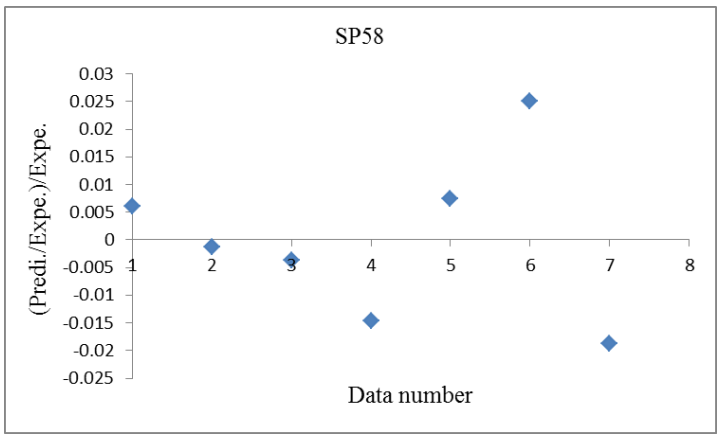
SP58
(Predi./Expe.)/Expe.
0.03
0.025
0.02
0.015
0.01
0.005
0
-0.005
-0.01
-0.015
-0.02
-0.025
1
2
3
4
5
6
7
8
Data number

(d)

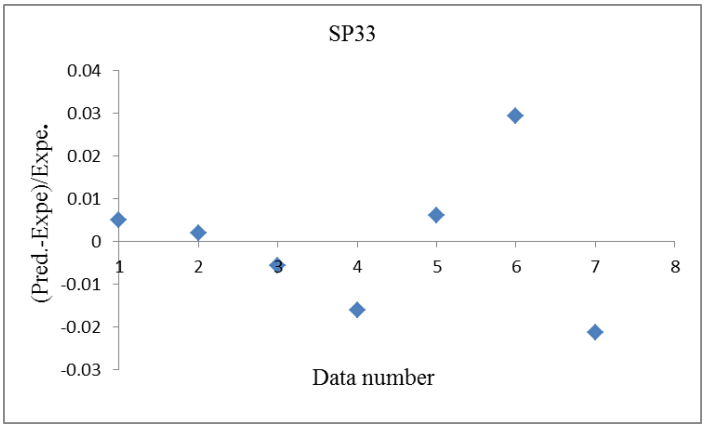

(e)

Figure A-0-1 Errors between experimental and predicted values of compressive strength of control (a), nutrients only(b), SP57self-healing mortar(c), SP58self-healing mortar(d) and SP33self-healing mortar(e)

Appendix B Correlation of outdoor exposure and accelerated experimental results

B-1 Correlation of outdoor exposure and accelerated experimental results based on relative compressive strength result

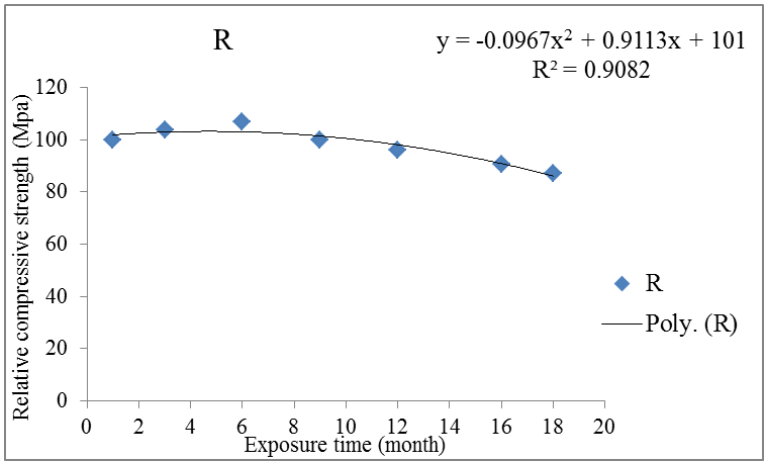

(a)

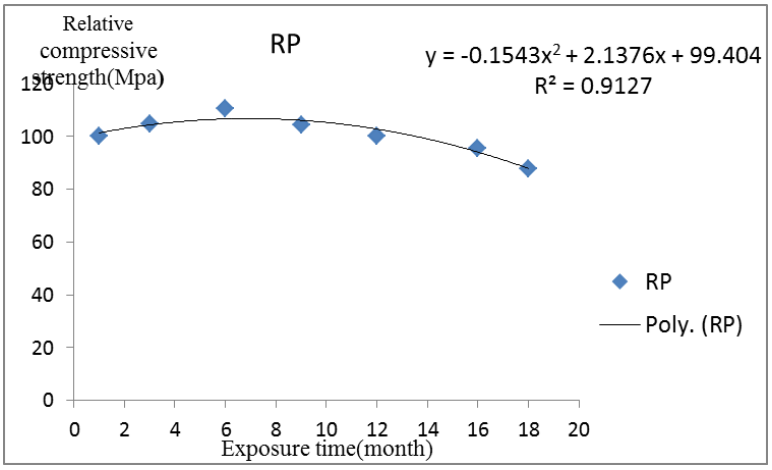

(b)

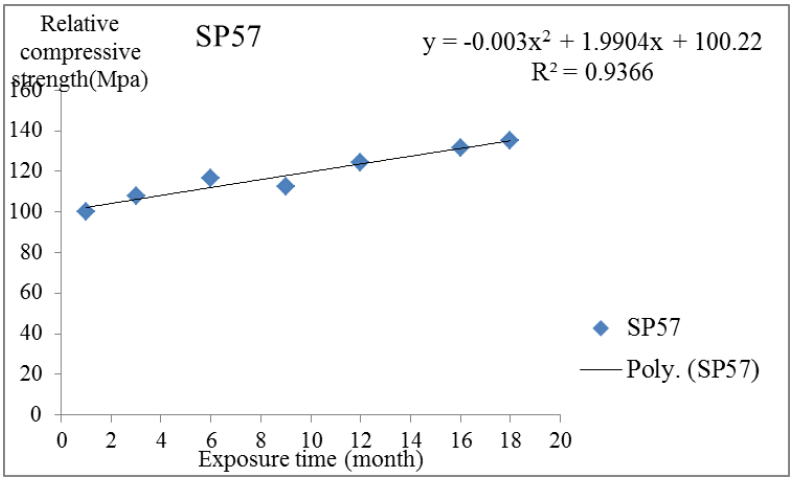

(c)

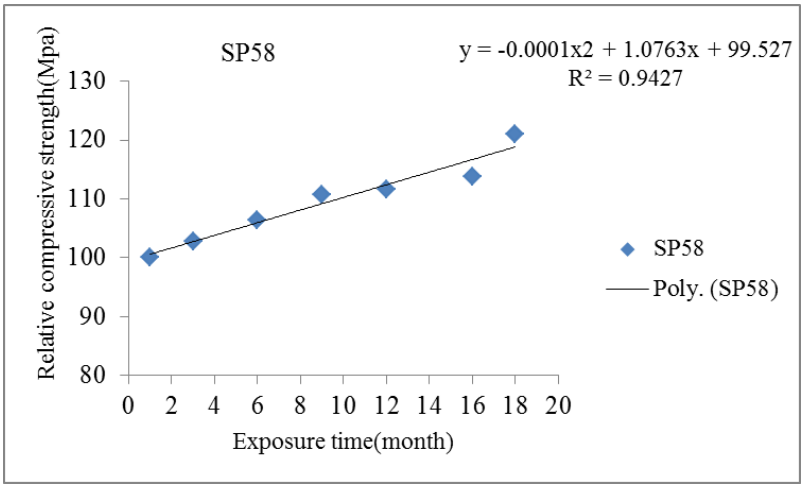

(d)

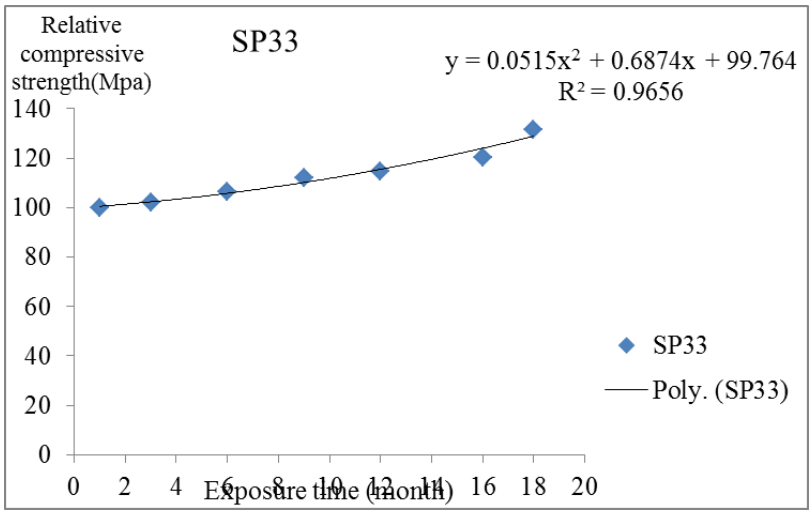

(e)

Figure B-1 Fitting curves of relative compressive strength versus outdoor exposure time of control (a), nutrients only (b), SP57self-healing mortar(c), SP58self-healing mortar(d) and SP33self-healing mortar(e)

B-2 Correlation of outdoor exposure and accelerated experimental results based on relative flexural strength result

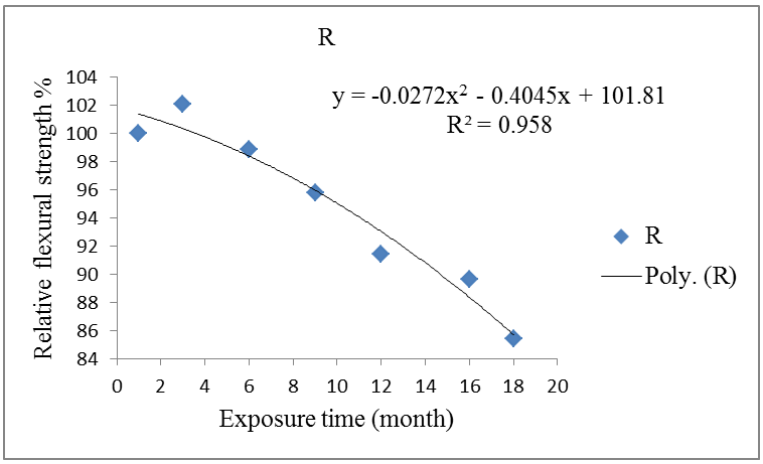

(a)

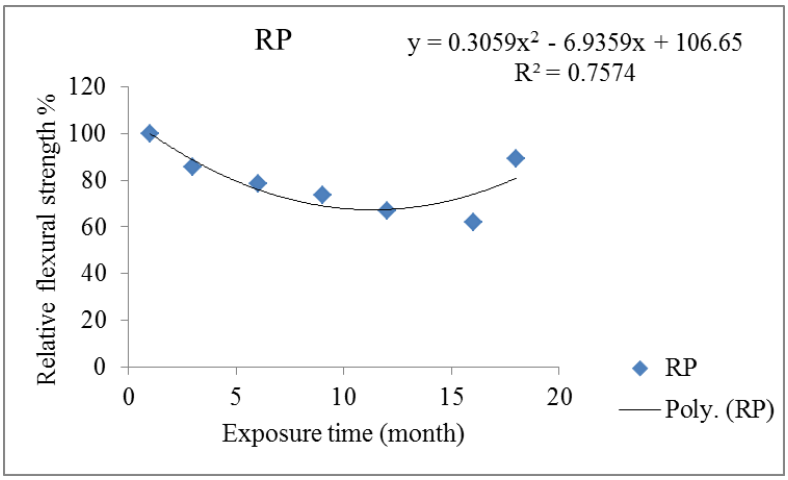

(b)

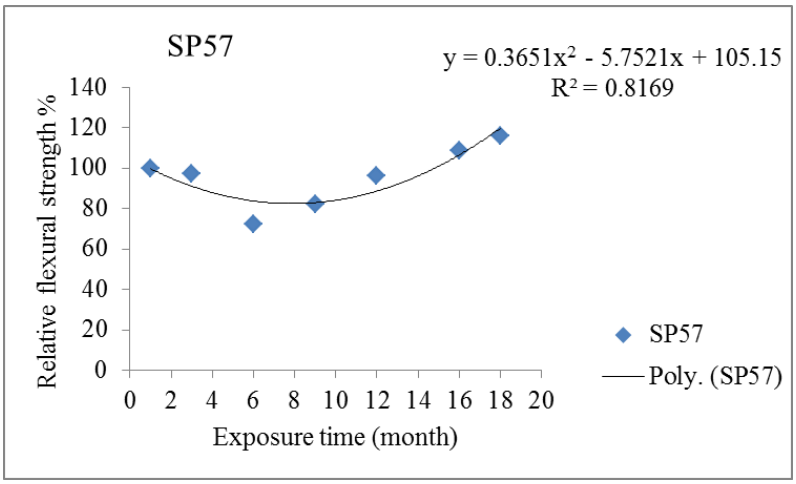

(c)

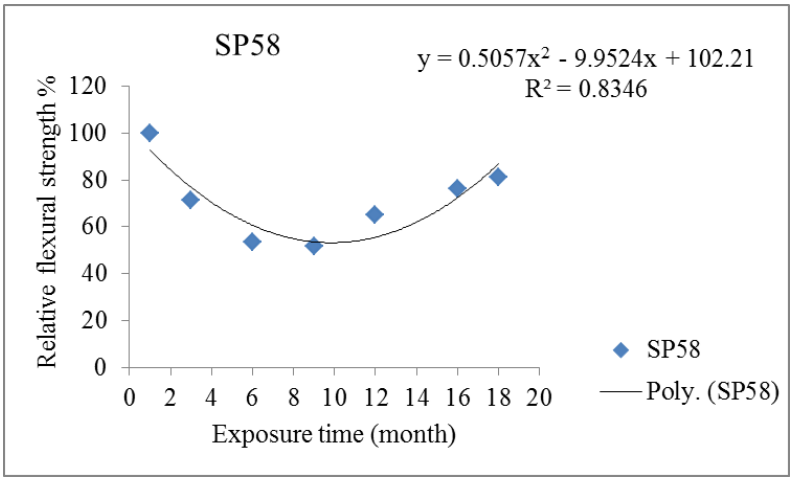

(d)

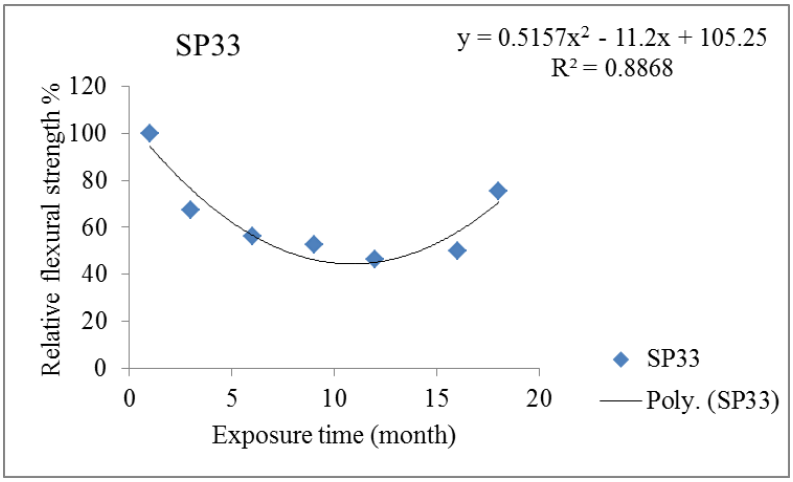

(e)

Figure B-0-2 Fitting curves of relative flexural strength versus outdoor exposure time of control (a), nutrients only (b), SP57self-healing mortar(c), SP58self-healing mortar(d) and SP33self-healing mortar(e)